Continuous sensory-motor transformations and their electrophysiological signatures

Maciej J. Szul

A thesis presented for the degree of
Doctor of Philosophy

School of Psychology
Cardiff University
Wales
30 September 2019

Contents

Summary

Perceptual decisions require efficient transformation of sensory information to motor responses. Most laboratory-based research on decision-making considered discrete and over-simplified actions. This thesis focused on human performance and electrophysiological signatures of continuous actions in response to decisions from three aspects. First, a systematic comparison between joystick movements and key presses showed that behavioural performance and underlying cognitive processes are not affected by response modality, establishing the validity and consistency of using joystick trajectories to measure decision responses. Second, a behavioural paradigm was developed to integrate continuous circular joystick movements with perceptual decisions of coherent motion. The signal-to-noise ratio of sensory inputs has been shown to affect the accuracy and response time of ongoing actions, but its influence on movement speed diminished after substantial training. Multivariate pattern analysis on magnetoecephalography (MEG) data recorded during the experiment identified stable information representations that sensitive to the quality of sensory information as well as the direction of periodic kinematics of circular movements. Furthermore, pattern information of complex actions was observed prior to movement onset, indicating the encoding of abstract preparatory action plans. Third, this thesis investigated the MEG signatures of circular joystick movements initiated via voluntary choices, instead of external sensory inputs. In a novel oddball paradigm, voluntarily choosing a continuous action built up an expectation of the statistical regularity of subsequent sensory inputs. Violating that expectation via incongruent sensory information resulted in significant multivariate representation in MEG activity of the mismatch event. Overall results presented in this thesis highlighted how ongoing actions

can be influenced by, and impact on, the continuous processing of sensory inputs in the human brain.

Acknowledgements

In the first place, I would like to thank my PhD supervisor, Dr Jiaxiang Zhang, for the support, endless amount of patience and guidance throughout the past four years. I have learned a lot from You.

I would like to thank my second supervisor Prof Petroc Sumner, the Cardiff University School of Psychology for the funding and institutional support, that enabled me to embark on this difficult journey.

I would like to thank Dr Aline Bompas for always refreshing evaluations that helped me to refine the understanding of the theoretical basis and implications of my research.

I would like to thank the amazing community in CUBRIC for creating an environment that greatly facilitated the scientific and social exchange.

I would like to thank present and past members of the Cognition and Computational Brain Lab: Aysegul, Beth, Dominik, Esin, and Wojtek for stimulating discussions and any help along the way.

I would like to thank my closest friends: Loukia Tzavella, Nick Gethin, Andrew Pavey, and Ana Silva who made difficult times more bearable and moments of joy even more enjoyable.

Last but not least, I would like to thank my family, my parents: Piotr and Urszula, and my siblings: Nina and Jakub, who were always there for me. I truly could not have done this without you.

Preface

The research presented in the Chapter 3 has been published as an article in *Behavior Research Methods* journal.

Szul, M. J., Bompas, A., Sumner, P., & Zhang, J. (2019). The validity and consistency of continuous joystick response in perceptual decision-making. Behavior Research Methods. https://doi.org/10.3758/s13428-019-01269-3

Results from Chapter 4 have been presented on Festival of Neuroscience conference organised by the British Neuroscience Association (BNA). Birmingham, 2017

Results from Chapter 5 have been presented on Annual Meeting organised by the Organisation for Human Brain Mapping (OHBM). Singapore, 2018

Chapter 1

Introduction

1.1 What is decision-making?

Decision-making is a process of choosing an appropriate action in response to the environmental requirements (Wolpert and Landy, 2012). A successful survival of an animal depends on its ability to interact with the environment. It means performing the appropriate actions based on incoming noisy sensory inputs. For example, to avoid a predator, a mouse has to be aware of the dark spot in the sky and direct their movement to avoid detection. Conversely, an eagle has to detect a mouse among the vegetation and follow the movement until the prey is caught (Chittka et al., 2009).

Humans, like other animals, constantly perform actions based on noisy sensory inputs. When living in a complex environment, we need to navigate it efficiently. Walking through a busy intersection requires to extract key clues from a cluttered scene, e.g. missing a red light could lead to an accident. Similar action-decision cycles are especially important in sports that require making rapid decisions based on noisy sensory inputs and under extreme time pressure. A rally driver has to negotiate a narrow, twisty, gravel road maintaining up to 130 km/h. Expertly controlling a car requires a continuous, reliable processing of the sensory input, visual and proprioceptive among others, to cope with the situation: determining the surface lies ahead, the current levels of grip, or the load of suspension.

Not only animals with complex nervous system are capable of some level of interaction with the environment. Simple non-neuronal organisms are capable of actions incorporating multiple sources of information (Reid et al., 2015). Slime moulds (*Physarum polycephalum*) have bodies around 10 to 10000 times bigger than *E. coli* bacteria. Moulds use differences in nutrient gradients across the body to provide the direction for growth. With such ability, slime moulds are capable of performing similar irrational patterns of decisions in a gambling task, similar to more complex organisms like bees, birds or humans (Reid et al., 2016). *E. coli* bacteria like a mould, cannot plan strategic foraging. However, their ability to move helps to explore the surroundings. *E. coli* can retain the information about the nutrient concentration in the current environment, which is then used to decide the direction of movement (Reid et al., 2015).

However interesting examples of the simple organisms reacting to the changing environment, they do not represent the wide range of actions and flexibility of more complex organisms (Reid et al., 2016, 2015; Perkins and Swain, 2009). The action selection is a complex, active, and dynamic process. It is characterised by a continuous loop of information fed forward to perform an action, and fed back to inform about the result of the action (Wolpert and Landy, 2012). A great example of the flexibility in response selection is the speed-accuracy trade-off (SAT), a relation heavily examined in human (Zhang and Rowe, 2014; Wickelgren, 1977; Rae et al., 2014a; Heitz, 2014) and animal cognition (Chittka et al., 2009). SAT refers to the trade-off between responding fast and inaccurate or slow and accurate. For example, low light conditions require longer inspection times to obtain sufficient visual information. Thus e.g. nocturnal bees and wasps trade off the speed for the accuracy of the flight to accurately navigate the environment (Chittka et al., 2009). The other, longer lasting example are male guppies. The ones grown in tanks with more predators took longer to make decisions in a maze, compared to guppies grown in less threatening environment (Chittka et al., 2009). We can observe that the the SAT can be solved according to various internal goals as well as environmental pressures.

We make decisions and pick actions almost all the time, using wide range of information to make our choices. The decision-making process became a proxy for studying many aspects of cognition. For example, the psychophysical paradigms were commonly used to investigate the basic principles of perception. It was done by greatly simplifying the range of possible actions (e.g. a simple button press) and introducing controlled changes in the properties of sensory inputs (visual, auditory, tactile etc.) (Gold and Shadlen, 2007). Computational principles realised as mathematical functions allowed to describe, and predict the transition of information between sensory input and subjective experience expressed by the action. This was enabled by the precise control of the sensory input (the environment) and obtaining the probabilities of the simple responses (a button press) (Krueger, 1989). Early psychophysical studies were mostly designed to examine the sensitivity of sensory systems to basic features like e.g., contrast or motion. Observers had to report their subjective experience over many trials and experimental conditions, from which their behavioural responses could be summarised. E.g., participants were instructed to indicate the presence or the absence of the target stimulus. The proportion of the responses (choice probability) was useful in quantifying the representation of the sensory input which led to a particular choice. In addition, the latency between stimulus onset and response was added. It quantified the time needed to gather enough information prior to a choice (i.e., reaction time - RT). Choice probability and RT are the two fundamental behavioural measures in decision-making research, which will also be the focus of this thesis (Gold and Shadlen, 2007).

Perceptual decision-making based on random-dot motion (RDM) is a classical psychophysical paradigm, in which the observer has to determine the global motion direction of noisy dot patterns. The dot pattern is consisting of signal dots, moving coherently in a certain direction and noise dots, moving randomly. The proportion of the signal dots to the noise dots is effectively the signal to noise ratio, which can be controlled by the experimenter (Lappin and Bell, 1976; Watamaniuk et al., 1989; Pilly and Seitz, 2009). Newsome and Pare (1988) used the RDM to examine the role of MT/V5 area in macaque during perceptual decisions. A chemical lesion of MT/V5 caused a decrease in motion detection performance, while contrast detection performance remained intact, suggesting the causal role of MT/V5 in perceptual decisions based on motion information (Newsome et al., 1989).

Decisions are made not only using an ongoing stream of the sensory information, but also information stored in memory. A methodology used in basic perceptual decision-making was used to probe memory processes. Ratcliff in his seminal paper (1978) used a simple forced choice tasks to establish a model of memory retrieval that takes into account reaction time and choice accuracy. Participants were asked to make a decision based on the information retained from the learning phase, whether or not the visual information currently presented were shown before. The model was based on an assumption that the noisy information was sequentially sampled from the memory. Information is accumulated until a certain threshold, after which a response is made.

Another example of harnessing the simplicity of the experimental decision-making to probe the cognitive processes is a case of response inhibition. Sometimes the appropriate action is to maintain the current action or to not act at all. In humans, the stop-signal task is commonly used to study response inhibition. The particpant's task is to rapidly respond to the a stimulus with occasional cues to withhold a response (Logan et al., 1984; de Jong et al., 1990). Successful inhibition of a response involves primarily a monitoring for relevant cues and then cancelling the immediate response. This process can be thought of as a decision between responding and withholding a response. These aspects of action selection are often impaired in cases of e.g. addiction or obsessive compulsive disorder (OCD) (Verbruggen and Logan, 2008). The methodology developed studying basic perceptual decision-process allowed to characterise the impairments of the decision process in such instances.

The experimental procedures derived from decision making studies were used to a wide range of questions about the cognition. However informative, the simplified, compared to real life situations, experimental settings have their disadvantages as well. The discrete response like e.g. a button press, can limit the understanding of the dynamic processes underlying the cognition (Spivey and Dale, 2006; Freeman et al., 2011; Song and Nakayama, 2009). However, if the decision process is framed as the selection of the appropriate action, augmenting the common decision-making methodology with more complex responses could give rise to more ecologically valid experimental designs. The ultimate goal is to expand our tool set to understand the cognition (Freeman et al., 2011).

The source of the methodological tools to appropriately characterise the action can be found in the field of motor control. The focus of motor control research is finding principles guiding motor actions across the range of output modalities (e.g.: reach, grasp (Brinkman et al., 2016), locomotion (Wagner et al., 2016) etc.). More precisely, the main research question of motor control is to reconcile the high degrees of freedom of the movement afforded by the human body, with efficiently achieving the goals demanded by the task. Even in constrained experimental setting, the motor outputs were highly variable across trials, still reliably achieving the same goals. On top of that a certain degree of external perturbation unravelled levels of adaptations that allow to maintain the efficiency in performing the action (Todorov and Jordan, 2002). Complex motor responses in research briefly mentioned above are in a sharp contrast with the simple, discrete, categorical choices in the experimental paradigms for simple decisions (Freeman et al., 2011). Motor control unfolds in space and time, and as such carry a larger amount of information, e.g. velocity, acceleration and force, which could be useful in probing cognitive processes (de Lange and Fritsche, 2017). The use of complex responses has been successful in unravelling the aspects of decision-making otherwise inaccessible to a conventional methodology utilising a simple button press (Burk et al., 2014; Resulaj et al., 2009; Hagura et al., 2017).

1.2 Outline of the thesis

The aim of this thesis is to bridge two lines of research, perceptual decision-making and motor control during continuous actions, which allows to extend the current decision-making framework with a richer and more ecologically valid response modality. The thesis focused on how we make decisions about continuous action, and how continuous actions may affect subsequent decisions and perception. Throughout the thesis, I used a well established experimental paradigm for decision (i.e., RDM-based motion discrimination) and a joystick for recording continuous actions. Below I present a brief summary of each chapter.

In Chapter 2, I reviewed a range of theoretical and empirical accounts of the research on decision-making. I presented the evolution of ideas that led to the currently used cognitive models. Then, the commonly observed behavioural effects were characterised and linked to the brain activity. The evidence from animal electrophysiology and human neuroimaging has been reviewed in the context of substantial advances it brought to our understanding of the decision-making process. Furthermore, I described several motor control theories to connect the conventional decision making process with novel approaches using continuous response measures to improve our understanding of decision-making process dynamics. Finally, I reviewed the methods and analyses applied to the magnetoencephalography (MEG) data in Chapters 5 and 6.

In Chapter 3, I presented research which served as a basis for the subsequent studies presented in this thesis. A key press, the conventional way of responding in the decision making studies, was compared with simple linear response using joystick. I used a well established random dot motion (RDM) task and Drift-diffusion model (DDM) to establish the validity of using a joystick as the response instrument. Results showed that the initial stage of the joystick trajectory was comparable in behavioural performance and underlying cognitive processes to a conventional button press, thus establishing a continuous response as a valid way to conduct decision-making research. Furthermore, it enabled the use of more complex movements in a broader context of decision-making.

In Chapter 4, I presented a novel task that combined continuous movements and perceptual decisions. Participants were indicating the direction of the RDM stimuli with clockwise or anti-clockwise movement. The direction and quality of the stimuli were changing in the 75% of the trials, which forced participants to adjust the action while the previous action was still ongoing. Across four experiments, I consistently observed behavioural performance akin to conventional decision-making studies. The noisy stimulus caused participants to became slower and less accurate in their continuous movements. The movement speed was also affected by the stimulus quality.

In Chapter 5, the novel continuous decision-making task was used concurrently with MEG recording. The goal was to examine the brain states elicited by the experimental procedure, and how the continuous movement is represented in the brain. The univariate analysis did not show any differences in oscillatory power and event related fields (ERFs) across experimental conditions. Multivariate pattern analysis (MVPA) showed that the choice of action can be decoded up to 0.5 s prior to the onset of the movement. Furthermore, the stable movement did not form an abstract and widely generalisable pattern but reflected the movement kinematics. Moreover, MVPA was only able to distinguish the stimulus strength when the participants maintained the action direction throughout the trial.

In chapter 6, I described a newly developed Action-Perception Congruency (APC) task. The task aimed to establish a causal expectation between continuous movements in the action stage and subsequent visual stimulus in the observation stage, and evaluate MEG signals that were sensitive to the violation of the causal expectation. Using MVPA, I identified action-perception expectation associated with changes in multivariate data patterns in MEG signal. Furthermore, I found MEG representations of participant's voluntary choices of continuous movements prior to action onset, and the multivariate pattern of continuous movements replicated the results in Chapter 5.

Chapter 7 summarised the results and contributions presented in the thesis. I further discussed the limitation of the presented research and possible future directions.

Chapter 2

Literature review

2.1 The computational principles and the neurobiology of decision-making

In Chapter 1 I have briefly outlined the decision-making as the ubiquitous phenomenon in humans and animals. It is a research topic of a broad variety and scale of investigations. For example, in political science, the involvement in political decision-making has been shown to shape further participation in democratic processes (Morrell, 2005). Moreover, the sources of information that lead to the success or failure in an elections could be tracked by monitoring the social media (Buhl, 2011). In organisational decision-making, the quality of decisions within organisational units plays a crucial role in achieving goals (Csaszar and Eggers, 2013). Decision making process in courtrooms has been extensively studied (Heise, 2002; Devine et al., 2001), e.g. the jury decision-making process could be more influenced by personal ideologies than the law and presented evidence (Gillman, 2001; Devine et al., 2001). In emergency medicine, the cognitive load and the time pressure heavily affect the decisions about the medical procedure which can save or cost human lives (Laxmisan et al., 2007).

2.1.1 Simple decision-making as a statistical inference problem

The decision process can be formulated as a problem of a statistical inference (Bogacz et al., 2006; Gold and Shadlen, 2007). This view of decision-making assumes that the representation of the momentary sensory information affects the choice behaviour. The decision variable (DV) combines all the available information to render a choice. Given the evidence e obtained from sensory inputs and two alternatives A and B as a binary decision, within the signal detection theory (SDT) framework, a DV can be described as a ratio of two likelihoods (Bogacz et al., 2006; Gold and Shadlen, 2007).

$$DV = \frac{P(e|A)}{P(e|B)}, \tag{2.1}$$

$P(e|A)$ represents the probability of observing e when A is the correct choice, and $P(e|B)$ represents the probability of observing e when B is the correct choice. Here, one can apply a threshold to the DV to reach a decision. Although the DV in Equation 2.1 can be used for binary decisions, the time required to make a choice is not accounted for.

This issue can be addressed using a sequential analysis, a direct extension of the SDT. Assuming the evidence for decision comprised of multiple observations at time step $t = 1, 2, 3, ..., n$, then the DV (Equation 2.1) can be represented as the likelihood ratio of all the pieces of evidence:

$$DV = \frac{P(e_1, e_2, e_3, ..., e_n|A)}{P(e_1, e_2, e_3, ..., e_n|B)}. \tag{2.2}$$

If we further assume that the stream of evidence $e_1, e_2, ..., e_n$ is independently sampled over time, we could take the logarithm of the DV, then convert the joint probability into a summation of samples of evidence.

$$\log DV = \log \frac{P(e_1, e_2, e_3, ..., e_n|A)}{P(e_1, e_2, e_3, ..., e_n|B)} = \sum_{t=1}^{n} \log \frac{P(e_t|A)}{P(e_t|B)} \tag{2.3}$$

The logarithmic DV in Equation 2.3 can be used in a sequential probability ratio test (SPRT) to represent a decision outcome (Bogacz et al., 2006; Gold and Shadlen, 2007). At the every time step t, a new piece of evidence e_t is sampled and the log-likelihood ratio of e_t is added to the $\log DV$. Which is accumulated until the last time point. In SPRT, if the $\log DV$ is larger than a decision threshold T_A, then option A is chosen. Alternatively, if the $\log DV$ is smaller than alternative threshold $T_B (T_B <= T_A)$, the option B is chosen. If $T_B < \log DV < T_A$, there is insufficient information for a decision and the test assumes that one should continue sampling and accumulating new evidence. The number of time steps to reach a decision threshold is equivalent to the decision time.

2.1.2 Sequential sampling models of decision-making

The essence of the sequential analysis like SPRT is that a decision is rendered via accumulation of evidence samples. From a statistical perspective, evidence accumulation reduces the noise in momentary evidence and hereby affords more accurate decisions. For example, it has been shown that SPRT is the optimal procedure to achieve a given decision accuracy with the minimum number of evidence samples (Bogacz et al., 2006; Gold and Shadlen, 2007).

This evidence accumulation framework underpins a large family of cognitive models for decision making: sequential sampling models (Gold and Shadlen, 2007; Bogacz et al., 2006; Ratcliff and Smith, 2004). These models build upon decades of psychophysical research on the statistical relations between sensory information and behaviour (Gold and Shadlen, 2007; Bogacz et al., 2006). They provide biologically plausible accounts of electrophysiological and neuroimaging results in decision-making studies (Shadlen and Kiani, 2013; Gold and Shadlen, 2007). Furthermore, as formal computational models of a cognitive process, sequential sampling models have the ability to formalise the hypotheses into numerical predictions and simulate the behavioural outcomes (Kriegeskorte and Douglas, 2018; Forstmann et al., 2016; Mulder et al., 2014). In the context of David Marr's three levels of analysis of information-processing systems (Marr and Poggio, 1976; Marr et al., 1979; McClamrock, 1991; Kriegeskorte and Douglas, 2018), sequential sampling models can be classified as an algorithmic interpretation of the decision process. However, their detailed neural implementation is also under active investigation (e.g.

Wang, 2008).

The drift-diffusion model is a classical sequential sampling model, initially proposed by Roger Ratcliff (1978; 1981; 1985; 1988) to account for the reaction time and accuracy in memory retrial tasks (Ratcliff, 1978, 1981). The DDM has later been applied to many other tasks with RT measures, including perceptual decisions (Ratcliff and McKoon, 2008), lexical decisions (White et al., 2010) and value-based decisions (Fontanesi et al., 2019). In the section 2.1.2, I introduced the DDM in more detail as it was used in the Chapter 3.

In two-alternative forced choice (TAFC) tasks, observers need to respond to (or discriminate) a certain stimulus quality (e.g. a motion direction) with two choice alternatives. In the DDM, the noisy evidence is accumulated continuously over time, until a decision threshold is reached. Apart from the DDM, there exists a plethora of different models that can account for the accuracy and RT in a TAFC task, and the implementation of evidence accumulation varies among the models (Bogacz et al., 2006).

For example, the Ornstein-Uhlenbeck model (Busemeyer and Townsend, 1993) also describes the decision process as a diffusion process The main difference between this model and the DDM is the addition of a linear term, specifying that the accumulation rate increases or decreases as the accumulated evidence approaching one of the two decision boundaries. A similar model behaviour can be implemented in an extended version of DDM with thresholds varying in time (Bogacz et al., 2006).

Other, more complex, sequential sampling models use simple networks of computational units to describe the decision process, including input units and decision units. The input units encode the incoming evidence (i.e. leftward or rightward visual motion) to the decision units that integrate it over time. For example, the Leaky Competing Accumulator model for TAFC contains two input units feeding to the two decision units which also inhibit each other. The decision units accumulate the information with a stable continuous loss of previously accumulated evidence (i.e., the integration is leaky). The decision is reached when the activity of one decision unit reaches a certain threshold. The feed-forward inhibition model assumes that decision units integrate the information without the leakage (Shadlen and Newsome, 2001). However, they integrate excitatory signal from the corresponding input unit and inhibitory activity from the input unit responsible for the alternative response. The pooled inhibition model is more biophysically realistic (Wong et al., 2007; Wong and Wang, 2006). It introduced an additional inhibitory unit that inhibits the activities of decision units, mimicking the functionality of inhibitory interneurons. Bogacz et al. (2006) compared the families of models mentioned above against the DDM. The aim was to explore to what extent the models can implement optimal decisions in terms of behavioural performance. Simulations and empirical results have shown that for simple TAFC tasks, most models can be reduced to the DDM within certain parameter spaces. However, in practice, it has been shown that the DDM provides a better fit to behavioural data than other competing models (Ratcliff and Smith, 2004).

The drift-diffusion model is used often as an analytic tool to describe in more detail the behavioural results (RT and accuracy) obtained from rapid decision-making studies (Smith and Ratcliff, 2004; Voss et al., 2004; O'Connell et al., 2018; Forstmann et al., 2016). It was used with various stimuli and tasks. For example, the DDM was useful in accounting for performance differences in basic brightness discrimination task (Ratcliff, 2002). Pairing a simple choice task with the DDM was used to highlight the speed-accuracy trade-off in a lexical decision task (Wagenmakers et al., 2008b). A go/no-go task with the DDM showed that the responses and non-responses engage the evidence accumulation but vary in the non-decision processes (Gomez et al., 2007). Similar tasks paired with the cognitive models found use in psychiatric research. The model parameters help to more precisely describe the differences in performance found across the groups and interventions and link cognitive models with the models of the disease. The DDM was used to distinguish patients with different levels of anxiety as a trait, in a lexical decision task with emotionally loaded words (White et al., 2010). The flanker task, commonly used to test the response inhibition, was applied in conjunction with the DDM to uncover the mechanisms behind contradictory results between healthy and depressed individuals. The results pointed towards the delayed but not poor executive function in people suffering from depression (Dillon et al., 2015).

Most sequential sampling models assume that different samples of sensory evidence are independent, i.e., the previous sample is not predictive of subsequent ones (Bogacz et al., 2006). This assumption may not be true in all experimental paradigms. The urgency-gating model was developed as an alternative theory to address this issue (Cisek et al., 2009). In the case when information samples are not independent, the urgency-gating model proposed that a subsequent sample should be ignored if it can be predicted from a prior sample, and only novel samples should be used to drive the decision. Instead of continuous accumulation of evidence, the decision process was implemented as a step function in the urgency-gating model, which also includes a motor urgency signal with ramping up activity prior to response. The convolution of the step-wise decision function and the motor urgency signal gives rise to the neuronal activity observed in decision-making experiments, and hence takes into account the non-stationary and dependent information samples. Nevertheless, when the information samples are independent and provide stable evidence for an alternative, the model behaves similar to an accumulation model (Cisek et al., 2009).

The random dot motion (RDM) stimulus used in this thesis provide constant, independent samples of information about the direction of coherent motion (see: Section 3.2.3 for a detailed technical description and Section 2.1.4 for an overview of decision-making research using the RDM stimulus). As such, all experiments presented here are appropriate to be considered within the sequential sampling framework.

The drift-diffusion model (DDM)

Sequential sampling models differ in the distribution of evidence (e.g., discrete vs continuous), the nature of time sampling (e.g., discrete vs continuous), as well as the model structure (e.g., the number of accumulators) (Smith, 1995; Busemeyer and Townsend, 1993). For example, the Poisson counter model assumes discrete evidence to be accumulated in discrete time steps (Rammsayer and Ulrich, 2001). If one assumes that the evidence accumulation process is continuous both in (evidence) space and in time (of evidence samples), the SPRT in Equation 2.3 can be extended into a drift-diffusion model (DDM), in

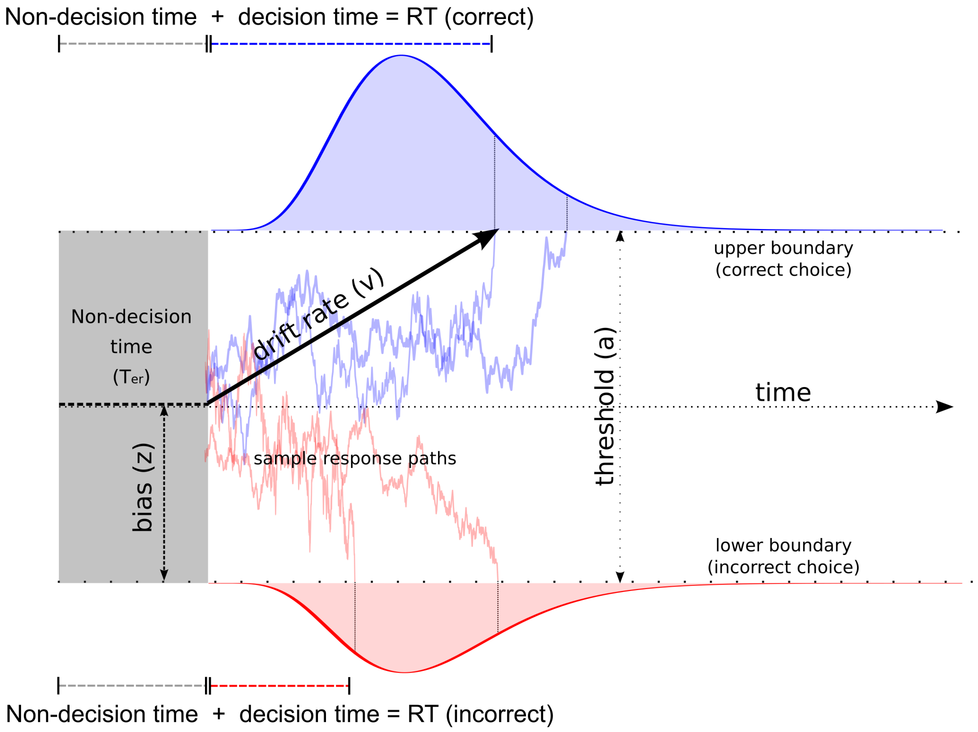

Figure 2.1: The drift-diffusion model and examples of evidence accumulation trajectories. A positive drift rate (μ) indicates that, on average, the accumulation of sensory evidence is towards the correct decision threshold (blue paths). The non-decision time is illustrated as a gray shaded area before the evidence accumulation starts. The RT is a sum of the non-decision time (a duration of sensory encoding and motor function) and a decision time (a duration of the sensory evidence accumulation)

which the dynamic of the accumulated evidence $dx(t)$ at time t is:

$$dx(t) = \mu \cdot dt + \sigma \cdot dW \tag{2.4}$$

The DDM can be applied to a binary decision problem between a correct and an incorrect choice. For simplicity, we can denote positive evidence ($dx(t) > 0$) to support the correct choice, and negative evidence ($dx(t) < 0$) to support the incorrect choice. The momentary evidence is noisy, as represented by the second term in Equation 2.4, a Gaussian random process with mean 0 and variance σ^2. The drift rate (μ) represents the average speed of evidence accumulation and its magnitude is determined by the strength (i.e., the signal-to-noise ratio) of the evidence. Figure 2.1 illustrated several time courses of decisions predicted by the DDM. The parameter (a) indicates the distance between the correct and incorrect decision thresholds, and it can be interpreted as the amount of evidence needed to trigger a decision. The starting point (z) represents the response bias towards one of the two thresholds before the start of the accumulation process (i.e., $x(0) = z$. The non-decision time (T_{er}) represents the latencies of non-decision processes like stimulus encoding and motor function. The diffusion process starts at the starting point (z) until the accumulated evidence reaches one of the two thresholds. If the accumulated evidence reaches the correct (upper) threshold (blue trajectories), the model predicts a correct response. Because of noise, the accumulated evidence may reach the incorrect (lower) threshold (red trajectories) and the model predicts an incorrect response. The predicted single-trial RT is the sum of the duration of the evidence accumulation (decision time) and the non-decision time T_{er}.

2.1.3 Behavioural characteristics of decision-making processes

This section reviewed main behavioural characteristics of decision-making and their interpretations in the framework of sequential sampling models.

Speed-accuracy trade-off

As mentioned in Chapter 1, the speed-accuracy trade-off (SAT) demonstrates the adaptability of the decision process to changing motivational and environmental requirements. In humans, the experimental manipulations of the SAT usually are delivered by explicit instructions. Participants are asked to respond in a task as fast as possible, or as accurate as possible, which explicitely affects the outcome of the SAT. The speed emphasis usually leads to shorter RT at the cost lower accuracy, and accuracy emphasis leads to longer RT which allows for higher accuracy (e.g. Zhang and Rowe, 2014; Wickelgren, 1977; Rae et al., 2014a; Bogacz et al., 2010; Heitz, 2014). Moreover, the rapid motor decisions (e.g. reach or grasp) are subject to the SAT. Movements under the speed emphasis condition, compared to the accuracy emphasis condition, are faster, less accurate and more variable in both action velocity and action trajectory (Newell, 1980; Wobbrock et al., 2008; Hancock and Newell, 1985; Plamondon and Alimi, 1997; Battaglia and Schrater, 2007). This relation is not only limited to simple perceptual or action decisions, but can also be observed in complex decision-making processes, such as decisions made by a group in the social setting of the teamwork (De Dreu et al., 2008).

The change of the RT and accuracy under varied SAT instructions are robust (Heitz, 2014; Heitz and Schall, 2012). Theoretical (Ratcliff and Rouder, 1998; Usher and McClelland, 2001; Brown and Heathcote, 2008) and empirical (e.g. Ratcliff and Rouder, 1998; Forstmann et al., 2010b; Palmer et al., 2005; van Veen et al., 2008; Ratcliff, 2002) accounts of the SAT suggested that sequential sampling models are ”selectively sensitive” to the SAT. Only the decision threshold, the amount of evidence needed, was changing with the SAT instruction. Emphasising the speed of response would decrease the decision threshold, which resulted in faster and more error-prone responses. However, manipulations of the SAT instructions in various rapid decision tasks have shown that both the threshold and the drift rate was affected (Rae et al., 2014a; Zhang and Rowe, 2014). In the speed emphasis condition, the decision boundary separation was decreased accompanied by the increase in the drift rate. This means that SAT modulates not only the amount of evidence needed to make a decision, but also the nature of the information processing (Rae et al., 2014a; Starns and Ratcliff, 2014; Wagenmakers et al., 2008b). However, in case of the perceptual learning the sensitivity of drift rate to SAT conditions was observed only in the initial phase. Over the course of the learning process only the threshold remained sensitive to the SAT conditions (Zhang and Rowe, 2014), suggesting that the effect of SAT instructions on other model parameters is learning-dependent.

Evidence strength

A common finding in many studies is that increasing evidence strength (or signal-to-noise ratio) resulted in reduced RT and increased accuracy (Fine and Jacobs, 2002). Across various experiments, the quality or the strength of the incoming evidence was reflected in the drift rate of DDM, which links directly to the sensitivity index d'. The more noisy, or less visible the stimulus, the lower the drift rate (e.g. Voss et al., 2004; Ratcliff et al., 2009; Zhang and Rowe, 2014; Palmer et al., 2005; Szul et al., 2019). For example, in perceptual decisions with random-dot motion (RDM, for technical details see Section 3.2.3), the stimulus strength is explicitly manipulated by the changing motion coherence (i.e., the proportion of the signal dots to the noise dots) (e.g. Fredericksen et al., 1994; Lappin and Bell, 1976; Pilly and Seitz, 2009; Ramachandran and Anstis, 1983; Watamaniuk et al., 1989). During the learning of a motion discrimination task using RDM, as the information processing became more efficient over repeated sessions, the drift-rate reflected the improvement in behavioural performance (Eckhoff et al., 2008).

Multiple alternatives

Most experimental studies focused on binary decisions as most of the models and theories were based on such methodology. However, in some have been considered decisions between more than two alternatives. A comparison between a RDM-based perceptual decision task with two and four choices has shown longer RT and lower accuracy with more choice alternatives (Churchland et al., 2008). The original version of the DDM was intended for binary decision problems, and other models of evidence accumulation can be used for multi-alternative decisions (Tsetsos et al., 2011; Ditterich, 2010; McMillen and Behseta, 2009).

An extended version of the DDM has been proposed to account for behavioural performance in a four-alternative decisions (Churchland et al., 2008). The model has been converted to acommodate four-alternative decisions by dividing them into two stages of binary decisions. In the first stage, the choice between two orthogonal axes was made, and in the second stage, the choice within the axis was made. The extended DDM reproduced the RT distribution and the lower response chance level in four-alternative decisions (25% instead of 50% in binary decisions). In a recent study (Maanen et al., 2012), the authors manipulated the number of alternatives (up to 9) and the similarity among the alternative options in a RDM-based decision-making task. An accumulation model fitted to the behavioural data showed a dissociation between the similarity and the number of alternatives. Lower discriminability between alternatives was associated with reduced drift rate, while increasing the number of choice alternatives was associated with reduced starting point (Maanen et al., 2012). These results suggest that the same evidence accumulation framework can be extended to complex decision problems with multiple alternatives.

Other contextual factors

The decision process is affected by many contextual factors. These modulators originate from external environment, or from internal factors such as goals or bodily states (Doya, 2008). Earlier in this section, I have reviewed that external instruction of SAT can effectively modulate the decision threshold (Heitz, 2014). There is a growing body of evidence that the history of previous decisions or related actions biases subsequent decisions (Urai et al., 2018; Braun et al., 2018; Pape and Siegel, 2016; Pape et al., 2017). Hagura et al. (2017) showed that the physical cost of actions (i.e., the amount of energy spent) biases the responses in perceptual decisions. Increasing the force resistance caused participants to bias their decisions towards a choice requiring less effort. Moreover, this bias persisted when the response was changed to verbal. Modelling analysis using the DDM showed that the starting point was sensitive to the motor cost, suggesting that humans have the tendency to incorporate action costs into the decision prior to accumulation of the evidence.

In addition to action cost, prior decisions themselves can also bias the subsequent evidence accumulation process (Urai et al., 2018). Participants making simple decisions were likely to alter their responses based on the decision made previously. This phenomenon has been associated with the action inhibition regarding recently made responses (Pape and Siegel, 2016). Within the sequential sampling framework, the history of decisions has affected the starting point parameter of the DDM (Larsen and Bogacz, 2010). Thus, as shown in Hagura et al. (2017) the biases tend to affect the decision process prior to obtaining new evidence.

2.1.4 Neural characteristics of decision-making processes

In this section I reviewed the neural systems involved in perceptual decision processes based on RDM.

Neural representations of sensory evidence

The sequential sampling models discussed above were developed as mathematically formal ways to describe the cognitive processes of decision-making (Ratcliff, 1979; Luce, 1986). A parallel line of research considers the neural systems and their computational functions during decision process. Neurons in area MT/V5 have shown to be sensitive to motion direction (Dubner and Zeki, 1971). Therefore, area MT is thought to be mediating the perceptual decision tasks with RDM.

Results from non-human primates supported this hypothesis. In one previous study (Newsome and Pare, 1988), macaque monkeys were trained in two different tasks, one to decide the coherent motion direction of RDM stimuli and the other to discriminate orientation of stationary gratings with varied contrasts. The animals rendered their decisions with saccadic eye movements towards a corresponding target. When the area MT/V5 was pharmacologically disabled, the animals' behavioural performance in the RDM-based motion discrimination task was impaired, while their performance in the orientation discrimination task remained intact. Electric stimulation of MT neurons unravelled that one can causally influence the decision outcome in a multiple alternative RDM task. Stimulating a sub-region of area MT/V5 selectively responsive to a specific motion direction biased behavioural choices towards that alternative (Salzman and Newsome, 1994). These results showed the role of MT/V5 in motion perceptual decisions is to encode momentary sensory evidence (Figure 2.2A) (Britten et al., 1992).

Representations of decisions in the primate brain

Although area MT/V5 encodes sensory information, neural activity in area MT only weakly correlated with the decision outcome (i.e., responses) (Brit-

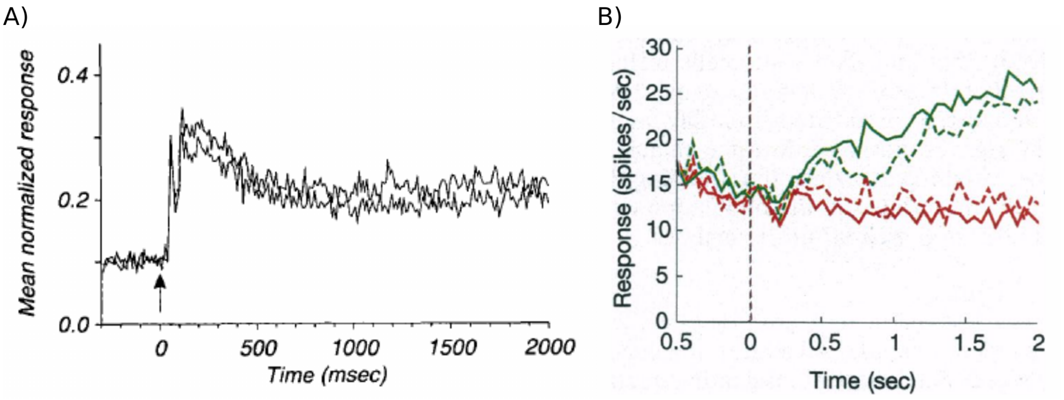

Figure 2.2: **A)** Mean normalised neural responses of MT neurons under the RDM stimulus with different motion direction. Adapted from (Britten et al., 1996); **B)** Mean responses (spiking rate) of 47 neurons recorded from area LIP. Solid line denotes a correct choice, and dashed line denotes an incorrect choice. Colours denote the direction of the target the saccade was made towards, green - left, red- right. Adapted from (Shadlen and Newsome, 1996)

ten et al., 1992; Shadlen et al., 1996), indicating that the evidence accumulation process, as assumed by the sequential sampling models, is implemented elsewhere.

Converging evidence from a series of monkey electrophysiological studies suggested that the lateral intraparietal area (LIP) is essential for evidence accumulation during perceptual decisions (Shadlen and Newsome, 2001; Roitman and Shadlen, 2002). The LIP receives inputs from MT/V5 neurons and and projects its outputs to eye-movement related areas such as superior colliculus (Paré and Wurtz, 1997), and thus the LIP is able to link sensory information with actions (here: saccades). When recording from the LIP neurons with their receptive fields covering the saccadic targets, the neuronal firing rates are predictive of behavioural responses irrespective of the accuracy (Figure 2.2 B). The spiking rate of the LIP neurons exhibited a characteristic ramping up pattern after stimulus onset, reflecting the dynamics of the decision process by which the appropriate action is being selected (Shadlen and Newsome, 1996). The slope of the ramping up activity in LIP reflected the quality of the visual input. The higher the stimulus strength, the steeper the slope. Moreover, the signal related to the movement execution was consistent across the conditions (Roitman and Shadlen, 2002).

The MT-LIP circuit can implement the evidence accumulation computation as described by the DDM (Ratcliff et al., 2016). Assuming the task is to decide between one of two possible coherent motion directions of the RDM stimulus (e.g., left vs. right). The sensory information is represented in two pools of MT neurons responding to the two opposite motion directions (Shadlen and Newsome, 1996; Shadlen et al., 1996). LIP neurons integrate the magnitude of the difference between the two representations of sensory information. The accumulation of the sensory information is terminated when the firing rate of the LIP neurons reaches a certain threshold (Shadlen and Newsome, 2001).

Further evidence supporting the hypothesis that area LIP integrates sensory evidence during the RDM task is available from direct behavioural and neural intervention. Behaviourally, during the formation of a perceptual decision, a brief pulse of motion information is added to the visual stimulus to perturb the coherent motion. Such a brief pulse had persistent effects on the activity of LIP neurons up to 800 ms and affected animals' decision (Huk and Shadlen, 2005). Furthermore, microstimulation of the LIP neurons leads to faster (when making choices towards the response fields of simulated neurons) or slower (when making choices away from the response fields of simulated neurons) responses (Hanks et al., 2006). These results suggest that LIP neurons are essential in implementing the evidence accumulation process during perceptual decisions.

Other frontal regions such as the frontal eye field (FEF) and the dorsolateral prefrontal cortex (DLPFC) show a similar pattern of ramping up activity as the LIP during perceptual decisions (Gold and Shadlen, 2000; Kim and Shadlen, 1999). Furthermore, after the neural activity reached a threshold and motor output had been executed, the trace activity was maintained in FEF (Ding and Gold, 2012). This could suggest the retention of the decision information in the frontal cortex to be used e.g. to evaluate or monitor the action as well as to alter the response (Resulaj et al., 2009).

Rodents as a simple animal model of decision making

Recently, rodents emerged as a viable model to investigate the decision-making (Carandini and Churchland, 2013). To test the effect of the noise on the decision-making process, a new experiment design was developed with auditory clicks played towards rats' left and right ears (Brunton et al., 2013). The auditory clicks were considered as the sensory evidence. The rats were trained to indicate with nose pokes which side had received more clicks. The DDM has been shown to account for the behavioural performance in rats. The inference from the model parameters suggested that the auditory information at the different temporal locations within a trial, equally contributed to the final decision (i.e., no primacy or recency effect). Replication of the same task with optogenetic control brought new evidence on the role of parietal and frontal regions in decision-making in rodents (Hanks et al., 2015). The parietal cortices were taking part in the accumulation of the evidence unlike the frontal cortex. The frontal cortex was involved in transforming the accumulated evidence into a categorical choice.

2.1.5 Evidence from human neuroimaging

In humans, non-invasive neuroimaging enables to examine the neural implementation of decision processes across the whole brain. Functional magnetic resonance imaging (fMRI) offers a good spatial resolution to localise the decision-making network. Electroencephalography (EEG) and magnetoencephalography (MEG) (for more technical details see: Section 2.3) record electrical and magnetic activity of neuronal populations with a millisecond temporal resolution (Heekeren et al., 2008; Keuken et al., 2014; Kelly and O'Connell, 2015).

Sensory evidence

The early fMRI studies examined the representation of evidence for decisions in early sensory cortices. In a visual target detection task, the BOLD (blood-oxygen-level dependent) response in early visual cortices (V1, V2, V3) is influenced by both bottom-up sensory information, as well as top-down post-decision signals (Ress and Heeger, 2003). In the RDM task with multiple alternatives, a multivariate pattern classification was able to distinguish the direction of coherent motion in the signal from early visual cortices (V1-V5/MT).

The classification accuracy increased when the attention was directed towards the stimulus. Results showed a role of attention in enhancing the brain representation of sensory evidence for decisions (Kamitani and Tong, 2006).

Evidence accumulation

The prefrontal cortex has been suggested as the putative region for evidence accumulation during the decision-making. The early study by Heekeren et al. (2004) examined the role of the DLPFC in perceptual decision-making in humans. The participants had to determine whether a noisy picture is a house or a face. The pictures were scrambled and contained both types of images in a different proportions. The choice of categories was dictated by the fact that they share basic visual features but a different meaning and a pattern of brain activity. Activations in the face-selective (fusiform face area, FFA) and house-selective (parahippocampal area, PPA) regions encoded the category-specific information in the visual stimulus. The BOLD response in the left DLPFC correlated with the behavioural performance. Higher the task difficulty, the higher the activation in the left DLPFC. Moreover, the difference between activity in category specific regions (FFA and PPA) was positively correlated with the activity found in left DLPFC. These findings are in line with sequential sampling framework of decision process.

Similar patterns of DLPFC activation were found during decisions based on the tactile inputs (Pleger et al., 2006). Using the RDM task with two response modalities (eye movement and button press), a fMRI study showed a motor-agnostic pattern of activity reflecting the quality of the evidence. A further conjunction analysis indicated that the DLPFC was involved in evaluating sensory evidence across response modalities (Heekeren et al., 2006). These results suggested a generalised accumulation-to-threshold process in the DLPFC for the decision-making process, regardless of stimulus or response context.

Investigating the dynamic representation of decision forming requires better temporal resolution than fMRI. An EEG study used the same face/house stimului as in Heekeren et al. (2004) for a categorisation decision task and a colour discrimination task, aiming to capture the time course of forming a decision (Philiastides et al., 2006; Philiastides and Sajda, 2006). EEG analysis and the DDM fitting to behavioural data unravelled three event related potentials (ERPs) related to the decision process ($\sim$170ms, $\sim$220ms and $\sim$300ms). The earliest ERP component was selective to the coherence of the face stimulus. The second ERP component appearing $\sim$220ms after stimulus onset was related to the task difficulty in the faces/houses categorisation task but absent in the colour discrimination task. The late component ($\sim$300ms) reflected the behavioural performance in both tasks, with its latency associated with the RT and its amplitude associated with the drift rate of the DDM fitted to corresponding behavioural data.

Subsequent studies using a concurrent EEG-fMRI recording localised the potential sources of the decision-related ERP components (Philiastides and Sajda, 2007). The early component, related to an early sensory processing, was linked to the BOLD responses in FFA and other visual areas. The ERP component related to task difficulty, was associated with increased BOLD responses in DLPFC and error monitoring areas such as anterior insula (AI) and anterior cingulate cortex (ACC). The late component, reflecting evidence accumulation and the final decision stage, covaried with the BOLD responses in the right ventromedial prefrontal cortex (vmPFC). The activity pattern was interpreted as reflecting the effort to maintain the accumulated information to select the right response (Philiastides and Sajda, 2007; Williams et al., 2007). The decision process is characterised not only by visual inputs, but also by associated motor outputs. The previously described house vs face discrimination task was adapted in this study to test the results of choosing a different effector to response in the task. The participants were instructed to respond either with a saccade or with an arm-reaching action towards a target. The two distinct ways of responding allowed to outline the pattern of activity reflecting a pure decision process, regardless of the effector used to respond. A prefrontal network consisting of VLPFC, DLPFC, AI and ACC was found to be associated with the task difficulty, regardless of the way of responding. The behavioural outcomes of the decisions like a direction of the movement and latency were reflected in motor planning regions specific to the way of respondong (FEF for eye movement or motor cortices for hand movements) (Tosoni et al., 2008).

The association of the anterior insular (AI) cortex with the task difficulty has been one of the common points of the studies highlighted above. However, this association was found in early decision-making research. The AI was deemed as a domain general locus of activation associated with the performance across the visual, auditory, semantic and non-semantic rapid decisions (Binder et al., 2004). Later studies augmenting neuroimaging data with model-based inference showed that the AI is involved in evidence accumulation during decision making across range of cognitive domains (Ho et al., 2009; Liu and Pleskac, 2011).

MEG and EEG have been used to directly examine the dynamic of evidence accumulation during decisions. In a MEG study with the RDM task (Donner et al., 2009), the beta- and gamma-band activities in the motor and pre-motor cortex were predictive of the choices. The predictability of the choices arises over time, suggesting a gradual formation of decisions (Figure 2.3). Those results suggested the ramping up was predictive of the motor action, which in the conventional understanding of the decision process occurs after the accumulation of the evidence (Ratcliff et al., 2016). Vugt et al. and colleagues (2012) conducted an EEG study with the RDM task. Ramping of theta-band oscillatory power was observed over the course of a trial in superior parietal channels, and the slope of the change was associated with the DDM drift rate estimated from individual participants' behavioural data. This result is at odds with the MEG study (Donner et al., 2009), which beta-band activity was observed just before the response and displayed weak associations with model parameters. There are few factors that may be underlying this discrepancy. First, it may stem from the fundamental difference between imaging modalities. High-frequency signal may be attenuated by the skull for scalp EEG, but less affected for MEG (da Silva (2013), see the overview of the neuronal source of MEG in Section 2.3.1), and differences in pre-processing steps may also render some frequency bands to be attenuated (Vugt et al., 2012; van Vugt et al., 2007). Second, the delayed response task used in the MEG study (Donner et al., 2009), to a certain extent, dissociated information accumulation from motor responses and allowed participants to make slower decisions. As such, beta-band activity may become salient due intentionally inhibiting and/or delaying an action (see the overview of frequency-specific MEG activities in Section 2.3.3).

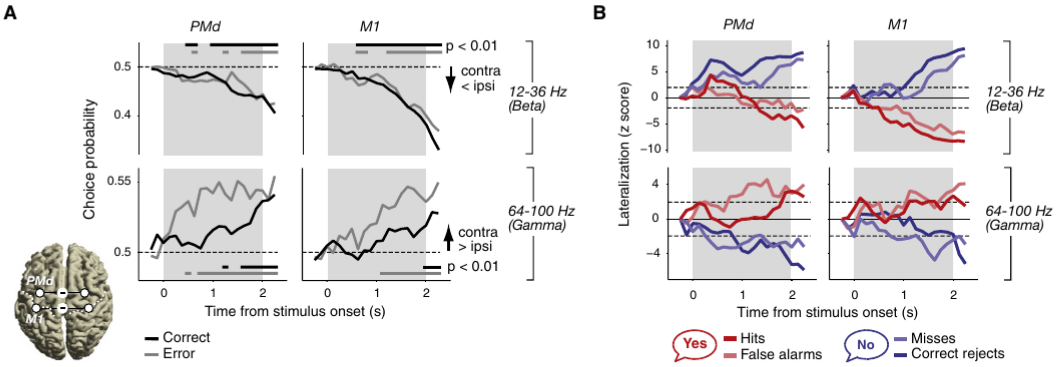

Figure 2.3: **Buildup of choice predictive activity during the stimulus presentation. A** The time courses of the frequency-specific signal localised in dorsal pre-motor cortex (PMd) and primary motor cortex (M1) within beta and gamma frequency bands. Activity indicates the lateralised choice responses. **B** Lateralisation of the choice predictability. Adapted from Donner et al. (2009)

Speed-accuracy trade-off

The combination of neuroimaging and sequential sampling models helped to confirm the involvement of the striatum in modulating the SAT (Bogacz et al., 2010). In a fMRI study with the RDM task (Forstmann et al., 2008), the participants were instructed to trade response speed for accuracy, or vice versa. After fitting an accumulator model to behavioural data, a caution score was derived as the ratio between drift rate and decision threshold. The caution score was negatively correlated with the BOLD response in the striatum and pre-supplementary motor area (pre-SMA). Furthermore, the caution score was also positively correlated with the strength of the structural connectivity between pre-SMA and striatum, measured by diffusion MRI and probabilistic tractography (Forstmann et al., 2010a). These results associated striatum with releasing the inhibition when the fast responding is needed (Ivanoff et al., 2008; van Veen et al., 2008).

In sum, human brain imaging studies offered considerable insights into the complex nature of the decision-making process. The decision variable proposed by the sequential sampling models is likely represented by a distributed neural activity across the fronto-parietal, motor and striatal networks. It reflects a wide variety of influences that the decision process can be subjected to (Heekeren et al., 2008; Keuken et al., 2014; Kelly and O'Connell, 2015).

2.2 Continuous motor outputs

2.2.1 Embodied cognition and the affordance competition hypothesis

Historically, cognitive science was mainly focused on the representation of the external information but not the computations underlying those processes (Engel et al., 2013). With cognition to be considered as a set of sequential, mostly unidirectional processes, actions are often simplified as an end product of cognitive processing (Sternberg, 1969; Donders, 1969; Padoa-Schioppa, 2011). Although this line of research has advanced our understanding of basic cognitive processes, the embodied cognition account took an different approach with a more action-oriented focus. Instead of creating an inner representation of the external world, one essential function of cognition is to help an agent generate action plans and interact effectively with the environment (Clark, 1999; O'Regan and Noë, 2001). This approach assumes action plans and their executions to have a continuous and afferent influence on cognitive processes, and hence the dynamic interplay between actions, sensory inputs and the wider context of actions needs to be considered (Clark, 1999, 2013; Shepard, 1984).

The embodied cognition theory views behaviour as a result of an ongoing process of action selection constrained by the affordances, referring to the perceived variety of possible actions constrained by the environment (Shepard, 1984). The affordance competition hypothesis (ACH, Figure 2.4), which stems from the embodied cognition theory, has been proposed to account for experimental results from animal and human studies of motor control and decision-making (Cisek, 2007). The ACH assumes that the brain provides a platform to interact with the environment and behaviour emerges on the basis of a constant competition between action plans (Cisek, 2007; Cisek and Kalaska, 2010; Cisek, 2012).

According to the ACH (Cisek and Kalaska, 2010), during perceptual decisions,

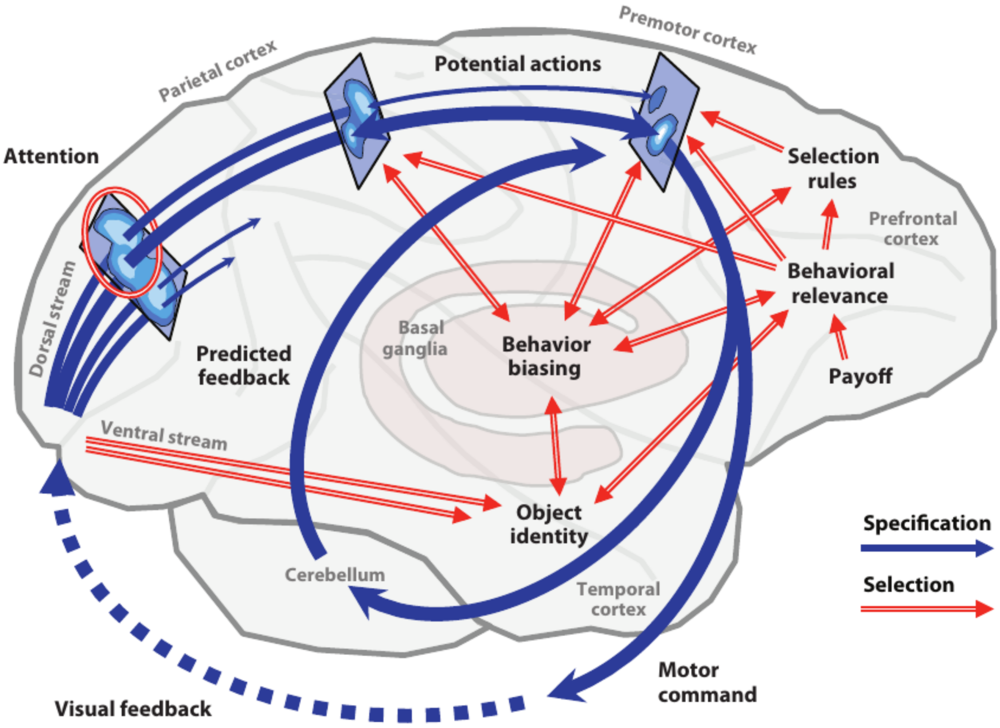

Figure 2.4: **The affordance competition hypothesis.** Proposed explanation of the movement directed by the visual input based on the primate brain. Adapted from Cisek and Kalaska (2010).

the dorsal visual stream provides spatial information that narrow down potential action plans to interact with the current environment (e.g. potential reach targets). The ventral visual stream provides specific information about which actions could be chosen. Action specific information is propagated to the basal ganglia that biases the action selection. The role of prefrontal cortex in high-level cognition makes it a suitable hub to integrate information across the brain and implement competitions among action plans. Specifically, the orbitofrontal cortex (OFC) integrates the affective- and the value-related information associated with action plans. The ventrolateral prefrontal cortex (VLPFC) compiles the motivational value with the sensory information, which is subsequently propagated to the DLPFC and pre-motor regions to modulate action selection (Cisek, 2012; Cisek and Kalaska, 2010; Cisek, 2007). The integration process across information domains was akin to the sequential sampling models.

The ACH implies parallel processing, with a constant impact from sensory and proprioceptive feedback upon ongoing actions and motor control, which enables a continuous interaction with a changing environment. Cisek and Kalaska (2010) argued that conventional experimental design is not suitable to unravel those dynamic processes, because the separation of task trials and discrete stages of stimulus with subsequent responses abolish the variability of those parallel processes, hence undermining their identifiability (Cisek and Kalaska, 2010).

A similar proposal was outlined in a seminal paper by Spivey and Dale (2004). Echoing the early work on embodied cognition, the authors expanded the proposition that the brain states or neural representations underlying cognitive functions are not static, but continuously changing in time. The use continuous response measures has been suggested as a way to unravel the dynamics of the cognitive processes (Spivey and Dale, 2006; Magnuson, 2005), which I will review in the rest of this section.

2.2.2 Motor control of discrete and continuous movements

In a contrast to the dominant use of the simple event logs for button presses in cognitive studies, a continuously measured movement trajectory has been the primary dependent variable in the field of motor control. One can define two types of movements based on their movement trajectories (Hogan and Sternad, 2007; Howard et al., 2011). A discrete movement can be characterised as the one with a single peak velocity between static periods. Examples of such movements include a point-to-point reach. On the other hand, when multiple peaks of velocity and periodic activity is observed, such movements can be classified as continuous movements.

Movement trajectories highlighted different computational and neural processes between discrete and continuous movement (Howard et al., 2011). Using state flow analysis of dynamic systems, computational modelling showed that discrete movements require a time keeping module to trigger the action, but maintaining continuous movements do not (Huys et al., 2008; Drew et al., 2004). Higher level cortical motor controllers influence the rhythmic activity by triggering and modulating spinal cord oscillation generators, as opposed to a direct cortical control in discrete movements (Dietz, 2003; Sasada et al., 2010; Marder and Bucher, 2001).

In a naturalistic setting, possible movements leading to the same outcome are highly variable, and control signals (sensory and proprioceptive) allow to counteract potential disturbances. Motor control can act in a stochastic manner, utilising variability and high degrees of freedom in a movement to approximate the optimal solution for the current environment. The optimal strategy under movement uncertainty is to minimise the variability relevant to the current action plan, while maintaining the variability in redundant (task-irrelevant) dimensions. This optimal feedback theory (Todorov and Jordan, 2002) provides a guidance for experimental designs in a laboratory setting. Instead of designing an experiment to reduce the variability in the data, one could leverage the variability from continuous recordings to characterise movements underpinned by action plans and noisy sensorimotor processes (Todorov and Jordan, 2002; Todorov, 2004; Scott et al., 2015; Scott, 2004; Tassinari et al., 2006; Trommershäuser et al., 2008; Wolpert and Landy, 2012).

2.2.3 Methodological advantages of continuous response measures

Joining the above ideas led to a wider use of continuous hand and upper limb movements as an experimental measure. The main advantage of tracking continuous movements over time is the richness of information in recordings, which suits especially to research questions on the dynamics of the cognitive process. For example, continuous movements allowed to examine and challenge the sequential models of the higher cognition (Spivey and Dale, 2006; Freeman et al., 2011; Song and Nakayama, 2009), and have been successfully applied in examining cognitive functions such as social interaction, language and memory (Spivey and Dale, 2006; Freeman, 2018; Freeman et al., 2011). Here I briefly reviewed a few key studies in perceptual decisions and actions selections with continuous responses.

Chapman et al. (2010) used a continuous reaching task to track the dynamics of action selection under multiple action plans. Prior to the onset of a reaching target, a cue was shown to indicate several possible locations of the target. Movement trajectories of participants' reaching behaviour was biased by the uncertainty of the target's spatial locations, suggesting that multiple action plans were formed (Gallivan and Chapman, 2014; Chapman et al., 2010). Furthermore, when the timing of the target cue presentation was manipulated (early vs late with respect to actions), movement trajectories showed evidence of an parallel specification of action plans. Early cue limited the ability to recover from the movement perturbation, and the uncertainty about target locations increased the movement variability and limited the effectiveness of the feedback. Late cue led to spatial averaging of the trajectories that is optimal for reaching the target. These results suggested that the brain maintains multiple action plans to reduce the costs of uncertain actions (Gallivan et al., 2016).

Another successful application of continuous response measures was used to examine the changes of mind. The competition between action plans driven by noisy information and can sometimes lead to an incorrect action. However, while performing an action, new evidence might arrive to adjust or alter the ongoing response. The changes of mind are difficult to capture using a discrete response measures like button presses. In a RDM task (Resulaj et al., 2009), participants were instructed to use a robotic arm to reach a target corresponding to the coherent motion direction. Most of the movement trajectories were optimal, i.e., close to the shortest path between the starting point and the target. However, some trajectories were longer and showed a deflection towards the direction opposite to the one chosen initially, suggesting occurrences of the change of mind. The DDM was extended to describe the underlying cognitive processes of the initial decision and the deflection of movement (Figure 2.5). The extended model proposed that, even after the decision being executed, the sequential sampling and accumulation processes were still ongoing, which could have changed the response later in a trial. The extended model included three decision thresholds, two for the initial binary decision as in the conventional DDM, and the third for the change of mind. If, after the initial decision, the accumulated evidence is towards the other alternative and reaches the threshold before a time limit, the change of mind occurs (Resulaj et al., 2009).

Berg et al., (2016) used a similar design to relate the change of mind with subjective ratings of confidence. Using a robotic arm, participants concurrently reported the choice and the associated confidence. The changes of mind more likely occurred when the confidence in the choice was low. The extended DDM showed that the time spent on deliberating was a strong predictor of the change of the mind. Further experiments showed that increasing the physical effort to change actions reduced the frequency of the change of mind, which can be explained by an increase in decision threshold in trials with high energy cost to alternate responses. Those results suggested that the decision process can indeed be dependent on the underlying actions as well as their energy costs (Burk et al., 2014; Moher and Song, 2014).

The studies reviewed above demonstrated how sequential sampling models can be extended to accommodate continuous movement measures. In either button presses or arm reaches, motor responses often have a clear beginning and the end point, from which conventional measures such as RT and decision ac-

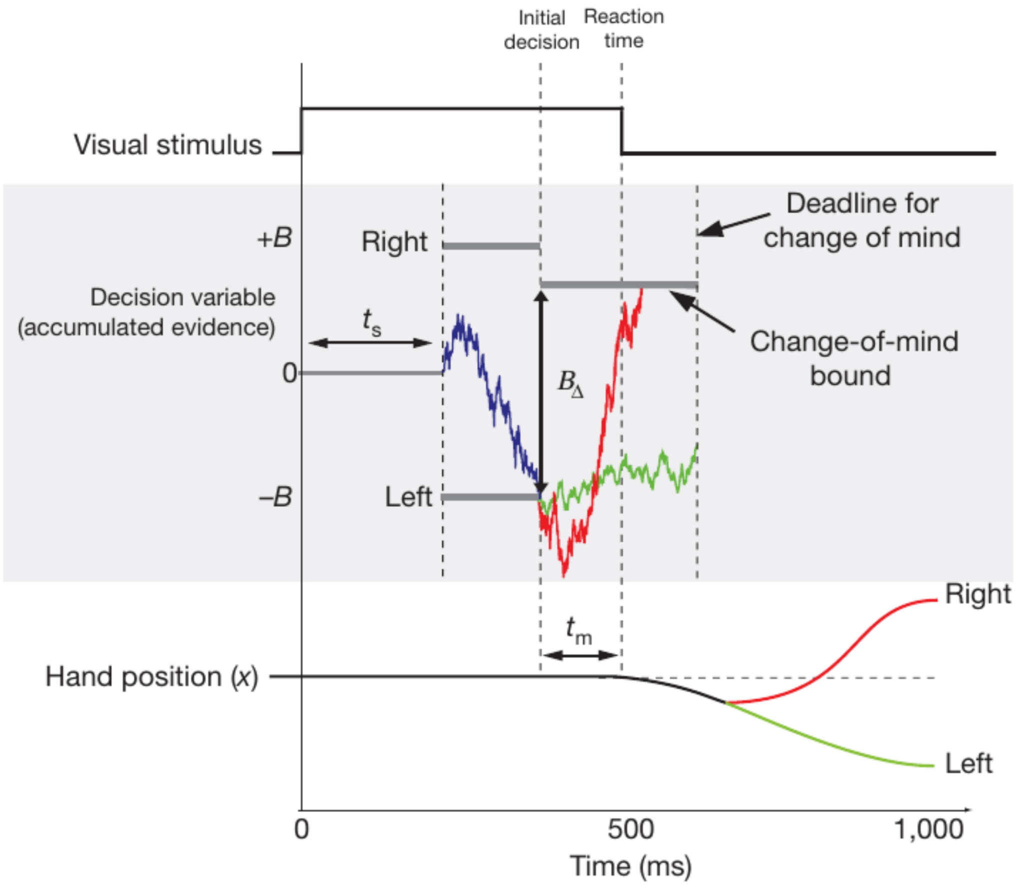

Figure 2.5: **A sequential sampling model extended to accommodate the change of mind.** The DDM (for more details see: Figure 2.1 was extended to take into account the observed trajectories (**Hand position**) and processes of change of mind. The red lines (the trace of accumulated evidence and hand position) represent the decision that was altered after the initial engagement in the action. The model assumes that the evidence accumulation still continues after the initial engagement. The subsequent processes have a temporal deadline and a different bound to the initial decision. As with the initial decision, when the accumulation trace reaches the **Change-of-mind bound**, the decision is altered, which is reflected in the deflection of the hand position. Conversely, the green trace which reaches the **Change-of-mind temporal deadline**, but does not reach the **Change-of-mind bound** represents a confirmed decision. There is no deflection in the **hand position** (green line). Adapted from Resulaj et al. (2009)

curacy can be derived. Therefore experimental results from discrete button presses are often generalizable to continuous movements, as demonstrated in Chapter 3. Continuous movements also have the potential to expand our current understanding of simple decisions. The joystick or similar devices allow to probe decision outputs in different ways and track how decision processes unfold in time. In Chapters 4-6, I demonstrated how continuous movements can be used in new decision-making experiments. To bring decision-making research closer to real life situations, a step further would be to merge continuous movements following motor control models (e.g. Wolpert and Landy, 2012) with continuous flow of non-stationary evidence (Cisek et al., 2009). In Section 7.2 I will outline future works that may challenge the current notion of decision process prescribed by the sequential sampling framework.

2.3 Magnetoencephalography (MEG)

Magnetoencephalography (MEG) is a non-invasive method to measure the magnetic fields generated by the electrical activity of neuronal populations (da Silva, 2010; Singh, 2006). MEG can sample macroscopic neural activity with a high temporal resolution (usually between 250 Hz and 1200 Hz and up to 30 kHz during recording) (Baillet, 2017) with an adequate spatial resolution ($\sim$1cm) (Goldman et al., 2002). Therefore, it is well suited to investigate the rapid dynamic changes of cognitive processes (Hari and Salmelin, 2012; Baillet et al., 2001; Aine, 2010) or impaired brain dynamics, e.g., in patients with epilepsy (Nakasatp et al., 1994). This section briefly reviewed theoretical background of MEG and analysis pipelines used in the later chapters (Chapters 5-6).

2.3.1 MEG signals

Neuronal sources of MEG signals

In the late 19th century, Polish physiologist Adolf Beck discovered the sensory evoked and spontaneous electrical activity on the scalp and the exposed cortex of the animals (Coenen et al., 2014). In the beginning of the 20th century Hans Berger made a first scalp electroencephalography (EEG) recordings in humans (Haas, 2003). Since then, the electrophysiology has become a popular tool in neuroscience, especially in examining cognitive functions (da Silva, 2013).

In this thesis, I used magnetoencephalography (MEG) to record electrophysiological activities in the brain. Both EEG and MEG signals originated from neural activity but from different sources. The main source of the signals measured in MEG are postsynaptic ionic currents in pyramidal neurons. Computational simulation suggested that synchronised activation from 50,000 pyramidal neurons is needed to obtain a noticeable difference in the MEG signal (Murakami and Okada, 2006), which limits the spatial resolution of the MEG signal (Baillet, 2017; Hari et al., 2010). The direction of the electric current determines the orientation of the accompanied magnetic field, which has to penetrate the skull to be measured by the MEG sensors. MEG is sensitive to magnetic fields oriented tangentially to the skull (see Figure 2.6) but less sensitive to radially oriented currents (towards or away from the scalp) (Singh, 2006; Crease, 1991; da Silva, 2013; da Silva, 2010; Malmivuo, 2012).

Although the EEG measurement is not independent, the recorded signal captures a different aspect of the same source. EEG measures the galvanic electrical activity using electrodes placed on the scalp. Due to the electrodes being placed directly on the scalp, the method can be sensitive to radial and tangential sources separately. EEG is more likely to pick up a deep sources, whereas the sensitivity of MEG decreases with distance from the sensor. Placement of the electrodes and obtained signal is more susceptible to the problem of volume conductance, the differences in conductivity across the brain tissues (e.g. cortex, dura matter, skull, skin). In contrast to EEG, MEG data does not need to be referenced as it is a measure of the actual physical values of the magnetic field strength (Malmivuo, 2012; da Silva, 2013; da Silva, 2010; Vrba, 2002; Vrba and Robinson, 2001).

MEG data acquisition

The magnetic field generated by brain activity is on the scale of femtoteslas ($10^{-15}T$), much weaker the the earth's magnetic field (2.5 to 6.5 $10^{-5}T$). As

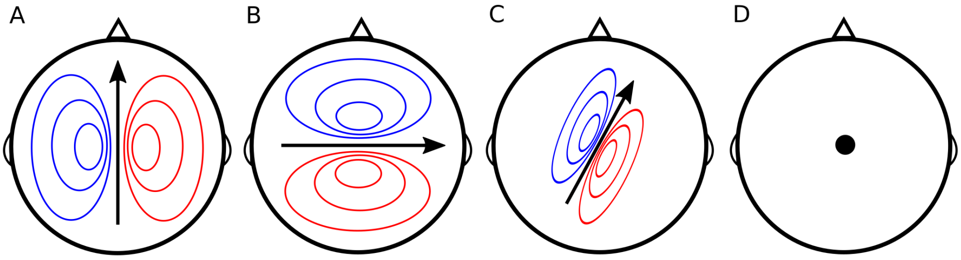

Figure 2.6: The orientation of the current direction and the visibility of the magnetic field to the MEG sensors. **(A)** the orientation of the magnetic field (red and blue pattern) when the direction of the current (black arrow) is aligned tangentially, along the anterior-posterior axis. **(B)** the orientation of the magnetic field when the direction of the current is aligned on the axis left-right. **(C)** the orientation of the magnetic field when the direction if the current is tilted, magnetic field still can be measured with MEG provided the source is close to the skull (Hillebrand and Barnes, 2002). **(D)** magnetic field is not visible by the MEG sensors as the direction of the current is oriented radially, along the ventral-dorsal line. Figure adapted from Singh (2006)

a result, MEG recording relies on very sensitive sensors (Baillet, 2017; Vrba, 2002; Vrba and Robinson, 2001) such as superconductive quantum interference devices (SQUIDs).

However, the high sensitivity of the SQUID sensors comes at a cost. The recording of the biomagnetic source (i.e. neuronal population) has to be guarded from much stronger, external fields. To mitigate that, the recordings are performed in magnetically shielded rooms. Magnetic walls were used to reduce the noise in 1-100 Hz range, relevant to recording of the biomagnetic signals. Use of copper and aluminium shells further allowed to tune out the high frequency noise (Hoenig et al., 1989).

Multiple SQUID (superconductive quantum interference device) sensors (up to around 300) are laid out in a array around participants' head. A helmet is used to separate participants' head from the SQUIDs immersed in liquid helium. With sensitive sensors, the muscular activity has a much stronger presence than the electrical brain activity, thus creating artifacts in the recorded signal. (Parkkonen, 2010; Baillet, 2017). Eye movement related muscular activity is often recorded using additional electrodes located directly around participants' eyes. Artifacts are needed to be removed during data pre-processing (Gramfort et al., 2013).

To reduce the electromagnetic noise in the signal recorded by the very sensitive SQUID sensors, multiple strategies are adopted. First, the MEG device is separated from the helium storage facilities and control room by locating it in the electromagnetically shielded chamber. Second strategy involves a special configuration of the pick-up coils. Magnetometers, the coils which are collecting the absolute value of the magnetic field strength are susceptible to the physiological (e.g. muscle activity) and remaining environmental noise. The addition of the gradiometers, the coils which are wound in the opposite direction to magnetometers, can cause the setup to be sensitive to the field patterns close to those of the neural origin. The combination of the gradiometers and the distances between the coils allow to fine tune the trade-off between the noise rejection and sensitivity to the deeper sources (Singh, 2006; Hari and Salmelin, 2012; Hoenig et al., 1989).

2.3.2 Common MEG pre-processing steps

This section summarised pre-processing steps commonly used in MEG research and this thesis. The origins of the recorded MEG signal are complex, containing neural signals as well as a wide range of environmental or physiological noise. Thus, appropriate pre-processing steps are necessary to remove artifacts from the MEG data and increase the signal to noise ratio. Many software packages are available to process the MEG data like e.g. Brainstorm (Tadel et al., 2011), Fieldtrip (Oostenveld et al., 2011), MNE-Python (Gramfort et al., 2014), SPM (Litvak et al., 2011). All the MEG data in this thesis were pre-processed and analysed using MNE-Python package (Gramfort et al., 2013, 2014).

Raw MEG recording is often acquired at > 500 Hz. The initial pre-processing steps are to apply frequency filters to limit the signal within a frequency band of interest (Parkkonen, 2010; Singh, 2006; Candès, 2006), and down-sample the data to reduce the computing load. and The sampling frequency limits the peak frequency of the data. According to the Nyquist-Shannon sampling theorem, for a peak frequency of (B), the sampling rate f_s has to be at least $2B$ to maintain all the information ($f_s > 2B$). If the power line frequency (50 or 60 Hz) and its harmonics are included within the frequency band, the common practice is to apply a notch filter to remove the mains interference (Parkkonen, 2010; Singh, 2006). It is important to manually inspect the filtered MEG data prior to further processing. The main purpose of this step is to identify noisy channels and sudden signal jumps in the recording. Depending on the experimental design, the affected data segments could be cut out if they contain too much noise.

Eye movements and cardiac artifacts are the main sources of noise in MEG data that contaminate the MEG recordings. There are many artifact correction methods available. The most basic one involves a manual inspection of the signal and removing all epochs containing e.g. muscle artifacts from eye movements. However, many visual paradigms involve stimuli of varied intensities that may cause involuntary blinks within a trial. As such, the statistical power of the experimental design may suffer if too many trials are to be rejected. In those scenarios, the removal of the contaminated epochs might not be feasible (Parkkonen, 2010; Singh, 2006; Gross et al., 2013).

Popular tool, aiding the artifact rejection strategy is the Independent Component Analysis (ICA), used to identify and remove noisy components. The ICA decomposes signals into statistically separate components, assuming the components of the observed signals are non-Gaussian and independent of each other. The properties of the ICA render this method especially suitable to separate brain signals from artifacts (Gonzalez-Moreno et al., 2014; Gramfort et al., 2014; Parkkonen, 2010). The ICA has been successfully applied to remove artifacts related to eye movements (Jung et al., 1998), cardiac activity (Jung et al., 1998) and cochlear implants stimulation (Gilley et al., 2006). To identify any noise components, the time courses of all independent components can be correlated with direct recordings of the activity of the interest (e.g. EOG or ECG). The ones with the highest correlation coefficients are often the noisy components to be removed (Gramfort et al., 2014). ICA was used to not only detect noises in the signal, but also to separate distinct brain networks across various imaging modalities (e.g. fMRI (Zuo et al., 2010), or MEG(Brookes et al., 2011)).

Another commonly used artifact rejection method is Signal Subspace Projection (SSP), which is based on a different way of signal decomposition - PCA. Unlike the ICA to find independent components, the PCA yields orthogonal components of the data that best explain the observed variance. SSP is incorporating the information about the the specific spatial patterns of noise components (physiological or external), which are different than the components reflecting neural signals. For example, the neural signals are usually confined to a small, linear subspace, while the noise components are more randomly distributed. By identifying and removing noisy components from the data, the effects of artefacts to MEG signals are reduced (Parkkonen, 2010; Gross et al., 2013; Gonzalez-Moreno et al., 2014; Gramfort et al., 2014).

2.3.3 MEG sensor-space analysis

Event-related fields

Evoked response fields (ERF) measures the magnetic field evoked by certain events (Singh, 2006), which could be triggered externally (e.g., stimulus onset) or voluntarily (e.g., response). To calculate ERFs, pre-processed MEG data is first segmented into epochs, which were then aligned to the timing of the events of interest. Usually, the short interval before stimulus onset was used for baseline correction, because it is assumed to be free from the evoked response to the event. Single-trial ERFs are often averaged across trials to improve the signal-to-noise-ratio. The assumption here is that the noise is random across trials and hence would be averaged out in the averaged ERFs, which reflects the central tendency of the evoked response. It is worth noting that, although the analysis pipeline for ERF (MEG) and EEG-based event-related potentials are to a certain degree equivalent, one has to be cautious when comparing ERP and ERF results, because of the difference between the modalities in signal sources and their sensitivity to the current orientation (Virtanen et al., 1998; Burra et al., 2017; Darvas et al., 2004).

The interpretation and the analysis of ERFs are based on the differences in their wave-forms (i.e., amplitude and latency) between conditions. Similar to the established ERP components from EEG data, ERF components have been identified as markers of of early sensory processing (N1 (Budd and Michie, 1994), Visual N1 (Wascher et al., 2009), P1 (Taylor, 2002)), attention allocation (Hopf et al., 2000), sensory mismatch (Näätänen et al., 2007), language processing (Van Petten and Luka, 2012) and memory (Friedman and Johnson, 2000).

Time-frequency data

Because MEG signal originates from synchronised activities of large neural populations, the synchronicity among neurons gives rise to rich frequency information in MEG recordings. MEG data in the time domain can be translated into the frequency domain using Fourier or wavelet transformation (Singh, 2006; Pfurtscheller and Lopes da Silva, 1999). As in ERFs, MEG oscillatory activity in different frequency bands can then be time-locked to stimulus onset or other events (e.g. motor response). Event Related Synchronisation (ERS) and Event Related Desynchronisation (ERD) refer to an increase or decrease in the oscillatory power of a frequency band (Pfurtscheller and Lopes da Silva, 1999; Pfurtscheller et al., 1996; Pfurtscheller, 1992). The ERSs/ERDs provide additional information over ERFs, since the decomposition of MEG data into a range of the frequencies allows to observe separately the frequency-specific changes over time (Singh, 2006).

The importance of frequency-specific information can be traced to functional roles of neuronal oscillation (Sejnowski and Paulsen, 2006). The innate oscillation of a neuronal population can retain or filter out incoming information (Buzsáki and Draguhn, 2004), and this selectivity has been shown to be able to amplify specific signals or coordinate information processing across populations (Uhlhaas et al., 2009). For example, cross-frequency coupling (CFC), the statistical dependency of between multiple regions at different frequency bands, plays a vital role in long-range information propagation across the brain during sensory, motor and learning processes (Canolty and Knight, 2010). More specifically, it has been proposed that the low frequency oscillations are the signatures of the long distance information transfer, which modulates the high frequency local processing (Canolty and Knight, 2010). CFC in phase was observed during learning and recall during sleep (Euston et al., 2007). Phase-amplitude CFC was found in hippocampal (Wulff et al., 2009) and basal ganglia activities (Tort et al., 2008) in rodents (Wulff et al., 2009) and during visual attention in humans (Osipova et al., 2008). Below I briefly overview the functional significance of different frequency bands.

The alpha-band

The alpha-band oscillation refers to the activity within the frequency range of 8 to 14 Hz, which is the dominant rhythm in EEG/MEG recordings when eyes are shut (Klimesch et al., 2007). During visual processing, strong alpha oscillations can often be localized in the midline of the posterior occipital cortex (Klimesch, 1999; Klimesch et al., 2007; Klimesch, 1999; Picazio et al., 2014). Evidence from the macaque intracranial recordings highlighted the functional distinction of alpha-band activity between the occipital and higher-level cortices. Consistently with the alpha being a signature of the attention, the ERD in the occipital cortex (V2, V4) was negatively correlated with behavioural performance (i.e., the higher the alpha power the longer RT). The inverse was true for the activity in higher level cortices (Bollimunta et al., 2008).

At the neuronal level, alpha-band activity is thought to relate to inhibition (synchronisation) and the withdrawal of inhibition (desynchronisation), more precisely to suppression and selective activation of the activity. This supports a functional role of alpha-band activity in cognition, which is likely to associate with the allocation and control of attention, suppressing areas not involved in current cognitive demands (e.g. Klimesch, 2012; Spaak et al., 2014; Foxe and Snyder, 2011; Snyder and Foxe, 2010; Thut et al., 2006). For example, spontaneous increase in alpha-band activity prior and during stimulus presentation reduces the detection rates (Mathewson et al., 2009), and a similar effect was observed when participants performed a working memory task with distractors (Hamidi et al., 2009). Alpha-band activity also depends on demands in tasks requiring a sustained attention (Klimesch, 1999; Klimesch et al., 2007; Klimesch, 1999; Jensen and Mazaheri, 2010). Moreover, the alpha-band activity is coupled with high frequency Gamma-band oscillations (Bonnefond and Jensen, 2015). The CFC between Alpha- and Beta-band activity was specifically linked to the distraction blocking (Bonnefond and Jensen, 2013).

The beta-band

Neural activity in the range of 12-30 Hz is categorised as the beta band. The sensorimotor and motor cortices are the predominant source of beta-band activity. During active movements, beta-band activity from the cortex exhibit a stereotypical pattern of desynchronisation, lasting as long as the duration of the movement (Engel and Fries, 2010; Kilavik et al., 2013; Khanna and Carmena, 2017). Beta-band desynchronisation is insensitive to the type of movements performed with the same part of the body (e.g. speed, direction, or ballistic vs. continuous).

Once the movement terminates, the beta-band activity shows a relative increase, known as "beta rebound" (e.g. Gaetz and Cheyne, 2006; Erbil and Ungan, 2007; Tan et al., 2016; Kilavik et al., 2013). It has been proposed that beta rebound relates to the inhibition of movement in the motor and premotor networks (Picazio et al., 2014), which facilitates information processing to guide subsequent actions (Tan et al., 2016).

An additional signature in the beta-band is the decrease of power prior to the movement, which has been attributed to motor preparation processes. For example, when participants voluntarily lowered the beta-band power though neurofeedback, subsequent movements were initiated faster (Savoie et al., 2019). Further, beta-band activity prior to the movement is predictive of the subsequent performance (Kilavik et al., 2013; Haegens et al., 2011; Grabot et al., 2019) and the certainty of the action plan (Tzagarakis et al., 2015).

Interestingly, muscle movement is not a prerequisite for beta-band desynchronisation, because it can occur during a motor imagery (Nakagawa et al., 2011), an observation of the movement (Meirovitch et al., 2015), tactile stimulation (Gaetz and Cheyne, 2006) or a passive movement (Keinrath et al., 2006). Recently, a neurofeedback study on macaque monkeys has shown that, when subjects were instructed to intentionally lower their beta-band oscillatory power. Subsequent reaching movements had faster onset time than when there was an increase in beta power (Khanna and Carmena, 2017). Therefore, beta-band desynchronisation during the movement is likely to be functionally tied to a general process of motor control rather than motor outputs (Kilavik et al., 2013).

The Gamma-band

The frequency range of 30-90Hz is categorised as the Gamma-band. The physiological origins of this signal spectrum are thought to come from temporary synchronous neuronal firing. Gamma-band activity obtained from local field recordings are mainly transient bursts with variable frequencies. The time window of 10 to 30 ms (i.e., gamma-band frequency) appeared to be optimal for neurons to respond to environmental changes. Neurons firing within this window can therefore form transient assemblies that are essential to the integration of inputs from multiple sources (Buzsáki and Wang, 2012).

On a macroscopic scale, in cognition, the Gamma-band activity is associated with binding task-relevant information. Activity in this power band was observed during conscious access to information (Melloni et al., 2007), speech perception (Kaiser et al., 2006) and memory encoding and retrieval (Jensen et al., 2007). All those tasks required integrating diverse sources of information into a coherent stream or conscious representation. During self-initiated movements, the increase of Gamma-band activity in the motor cortex (Muthukumaraswamy, 2010) was associated with the binding of the multi-sensory information (Cheyne et al., 2008) and the integration of the motor and proprioceptive signals (Pfurtscheller et al., 2003) that are crucial for motor control. It has been proposed that the synchrony of distant Gamma-band neuronal generators can be driven by fluctuations in lower frequency signals via cross frequency coupling (Buzsáki and Wang, 2012). For example, the integration and binding of visual information to ignore distractors was linked to the coupling between alpha and gamma bands. (Bonnefond and Jensen, 2013, 2015).

The delta- and theta-bands

The functional roles of delta-band (0.5-4 Hz) and theta-band (4-8 Hz) activity in human decision-making and action selection are relatively understudied. I have included those oscillatory spectra because they reflected the experimental conditions. In Chapter 5, I included the delta-band in the analysis because its frequency range overlaps with that of the continuous movements. In Chapter 6, I included a theta band in an analysis because its frequency range overlaps with that of the visual stimulus.

The delta-band activity was predominantly a focus of in sleep research (Amzica and Steriade, 1998; Dang-Vu et al., 2008). The delta waves are a distinct pattern during slow wave sleeps, which promotes the consolidation of information from recent awake periods (Rasch et al., 2007). Delta sleep activity is not a coherent wide-band oscillation, but rather a mix of cortical and thalamic oscillations that integrate activity across networks (Lu et al., 2007).

The delta band activity is also functionally relevant during awake. Ultra-low frequency (∼0.1 Hz) is associated with the modulation of global cortical excitability (Knyazev, 2012; Hamel-Thibault et al., 2018). Oscillatory power in the delta-band was correlated with the predictability of the cue in an auditory and a visual detection task (Ergen et al., 2008). The low frequency oscillations can potentially modulate faster rhythms to propagate the anticipatory information across the brain. For instance, the coupling between delta and gamma frequency was found during naturalistic scene viewing and visual detection (Händel and Haarmeier, 2009).

In animal studies, theta-band activity in the hippocampus has been linked with a wide range of cognitive functions including movement and exploration of the environment (Oddie and Bland, 1998; Bland, 1986), action selection (Oddie and Bland, 1998), spatial navigation (Hartley et al., 2014), memory retrieval and synaptic plasticity (Bland and Oddie, 2001). In humans, changes in the theta-band activity (Sauseng and Klimesch, 2008) were associated with the outcome evaluation, such as negative feedback (Cunillera et al., 2012) and conflict of information (Bernat et al., 2007; Hsiao et al., 2009; Harper et al., 2014). Recently, MEG and EEG theta-band activity has also been shown to be associated with information integration during decision-making (Vugt et al., 2012; Nácher et al., 2013) and continuous visually-guided movements (Grent-'t Jong et al., 2014; Cruikshank et al., 2012).

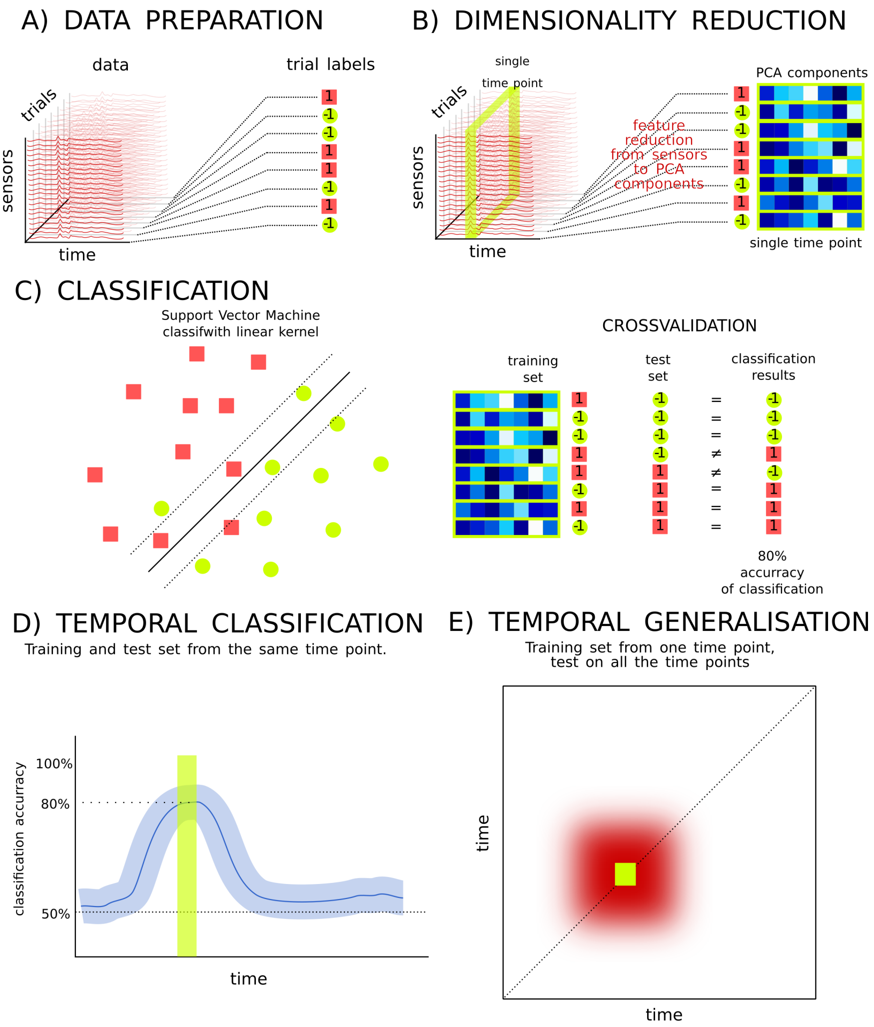

Figure 2.7: Overview of the typical steps in Multivariate Pattern Analysis (MVPA) of neuroimaging data. **A.** The labels are assigned for each observation (here: trial). Labels often reflect the different experimental conditions. Each observation contains features in multiple dimensions (e.g., signals from MEG sensors) **B.** To reduce the amount of features, PCA is applied to the data to extract the first few principal components. Here, instead of the signal from MEG sensors, selected principal components are used as features. Green highlight denotes a single time point. **C.** A classifier (e.g., Support-vector Machine (SVM) classifier) is used to train and test pattern separations in the observed data, using a cross-validation test to evaluate its performance and generalisability. The predicted labels are compared with the actual labels yielding the classification accuracy. **D.** Training and cross-validating at every single time point yields a time course of classification accuracy, representing the ability to distinguish between experimental conditions over time on the basis of multivariate patterns. **E.** Temporal generalisation (King and Dehaene, 2014). One can use a classifier trained at one time point to test the data from another time point. Significant classification would indicate that pattern information maintains and generalises across time.

2.3.4 Multivariate pattern analysis

Conventional univariate analyses make inferences on the basis of a single dependent variable, such as BOLD response in one voxel or one region, or MEG activity in one sensor or averaged from several sensors. Nevertheless, neuroimaging data is inherently multidimensional, and the information could be represented in multidimensional patterns instead of uni-dimensional activity. Multivariate Pattern Analysis (MVPA) refers to a range of methods to identify patterns of brain activity (Haxby, 2012). MVPA searches for information represented across high-dimensional data, which have been shown to be more sensitive than univariate analysis in localising complex information representation and computation in the brain (Kriegeskorte et al., 2006; Haynes and Rees, 2006; Haxby et al., 2001).

Figure 2.7 illustrates the typical steps of MVPA analysis for MEG data. The first step (Figure 2.7 A) is to prepare the data in an appropriate multidimensional format. Pre-processing steps can have an impact on the MVPA results (Poldrack et al., 2017). For example, an aggressive high-pass filter could introduce artifacts in MVPA results, and modest filtering is recommended (Driel et al., 2019; Tanner et al., 2016). Many machine learning models (e.g., support vector machines) performs better with standardised data, with zero-mean and unit variance in each dimension (Larsen and Marx, 2012). Each epoch (or trials) for MVPA is assigned with a label, referring to the experimental condition that is needed to be learnt.

The next step is dimensionality reduction (Figure 2.7 B). In most neuroimaging studies, the amount of data is limited due to constraints of scanning time, but the data often has large amount of dimensions. Here, data dimension refers to the number of features in each observation. For MEG data, it would be equivalent to the number of MEG sensors. In multivariate analyses, the complexity of the statistical model increases with the data dimension, which can lead to overfitting or poor results (Hastie et al., 2009). One solution is to reduce the data dimension prior to further analyses. Dimensionality reduction can be achieved by, for example, selecting a subset of features (Kriegeskorte et al., 2006) or applying PCA to the data and selecting a subset of principal components that explain most of the variance (Grootswagers et al., 2016).

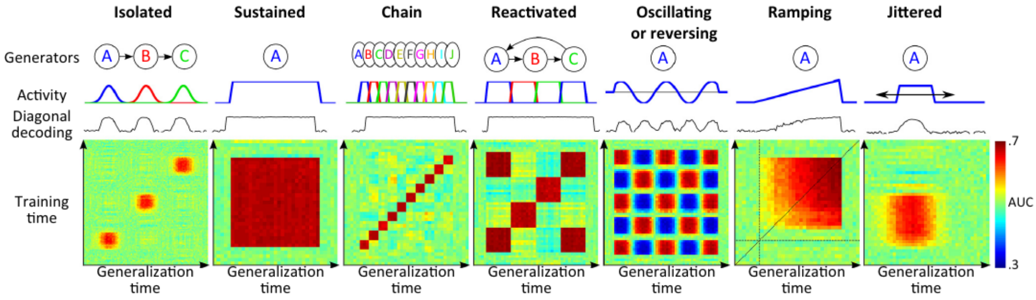

Figure 2.8: Temporal generalisation. The figure describes a theoretical guideline for the temporal generalisation results. The **diagonal decoding** and **temporal generalisation** depict possible MVPA classification results. The **diagonal decoding** highlights possible classification results when the training and testing data sets are pooled from the same time point across trials. The **temporal generalisation** shows the ability to generalise a statistical model that is trained on one time-point and classify data from all possible time points. The diagonal of the **temporal generalisation** matrix is equivalent to the **diagonal decoding**. Any significant classification performance off the diagonal indicates a generalisation of the multivariate pattern across time points. Adapted from King and Dehaene (2014).

The third step is to use a statistical learning model to learn and classify multivariate patterns in the data. In Chapters 5 and 6, I used linear support vector machines (SVM) for this purpose. The classification step involves fitting a chosen model to a observations. The linear SVM is a binary supervised classifier that fits a hyperplane to the multidimensional data space (see: Figure 2.7 C). The hyperplane divides the observations into one of two classes (i.e., labels). To evaluate classification performance, one can use a K-fold cross-validation procedure. That is, the dataset is divided into K parts. $K-1$ parts are used to train the SVM, and the remaining part is used to test the accuracy of the trained classifier. The procedure is repeated K times, with a different test set in each cross-validation. The classification accuracy is then averaged from all the K cross-validation folds. This validation scheme is used to evaluate whether the classifier enables to predict new data unseen during training (Hastie et al., 2009). If the classification accuracy is above chance level (50% for binary classification), the multivariate data contains substantial information to distinguish the two classes.

For MEG data, one can implement a previously described procedure (Figures

2.7A-C) at every time point of a trial, resulting in a time course of classification accuracy. This evaluates whether and when multivariate MEG data patterns can be distinguished between the two conditions (Figure 2.7D) (Kok et al., 2019; Lewis-Peacock and Postle, 2012). One could also train a classifier with data at time t and test its classification performance on data at a different time point t'. A significant cross-time classification would suggest that the multivariate representation can be generalised between the time points (Figure 2.7E). Recently, it has been proposed that the temporal generalisation pattern can reveal the underlying behaviour of the large scale brain signals sources (King and Dehaene, 2014; Grootswagers et al., 2016; Hebart and Baker, 2018) (Figure 2.8).

King and Dehaene (2014) proposed an approach to link the range of neuronal generator networks (Figure 2.8 **Generators**), the signal produced by the generator's activity (Figure 2.8 **Activity**) with the MVPA classification results (Figure 2.8 **Diagonal decoding** and **Temporal generalisation**). The particular generators produce distinct signal pattern of states and state occupancy duration. The classification results show that the activity can be accurately distinguished. However, the diagonal decoding results do not provide sufficient amount of information to distinguish across the signals coming from different generators. Diagonal decoding results are obtained by training and testing the statistical model on the same time point. As shown on the Figure 2.8, diagonal decoding produced equivalent results for generators producing chain of unrelated states (chain generator, Figure 2.8), for generators producing the repeating sequence of the states (reactivated generator, Figure 2.8), as well as for the state stable in time (sustained generator, Figure 2.8).

Only the temporal generalisation (Figure 2.8) unravelled the pattern of classification enabling the qualitative distinction between the generators. Temporal generalisation results are obtained by training the statistical model on one time point and testing the solution on all available time points. Resulting matrix shows how the model trained on one time point generalises over all the other time points. The diagonal decoding results are equal to the diagonal of the matrix. The chain of the unrelated states, has correctly shown no temporal generalisation. As the generator produced series of distinct states, the pattern of activity was not shared by any other time point. The temporal generalisation matrix accurately showed the common pattern of the repeated states produced by the reactivated generator. Stable generator produced signal generalisable across all the time points of the duration of the state. Despite the common diagonal decoding results, temporal generalisation allowed to distinguish those states.

It is worth highlighting a reversing/oscillating signal and associated classification results patterns. Significant, below the chance level performance is caused by the classifier reliably attributes opposite labels to the test set. It potentially mean that the signal is inversed. The temporal generalisation pattern shows the reactivation of the same pattern and the frequency of its occurrence.

Chapter 3

The validity and consistency of continuous joystick response in perceptual decision-making

3.1 Introduction

Discrete key presses on a keyboard or button box have been the long-standing response modality in computer-based experiments in psychology, from which on/off responses and response time (RT) are commonly measured. Developments in computers and electronics technology have improved the accessibility of other devices that are capable of recording continuous responses, e.g., joystick, computer mouse, motion sensor and robotic arm (Koop and Johnson, 2011; O'Hora et al., 2013). In addition to the standard behavioural measures available from key presses, continuous responses enable further inferences from movement trajectories. However, to utilise the full capacity of continuous response recording, we need to ensure that experimental results from these devices are consistent with, or generalisable to, the findings from conventional response modalities such as key presses. In the current chapter, I addressed this issue by comparing the behavioural performance between joystick movements and key presses in a perceptual decision-making task. Using computational modelling of behavioural data, the decision-making processes from the two response modalities were further compared.

3.1.1 Continuous and discrete responses in experimental psychology

As argued in the previous chapter the continuous responses can offer theoretical and practical advantages in experiments. First, although a discrete response is consistent with the assumption of sequential stages of cognition and motor outputs, a growing number of studies suggested a continuous and parallel flow of information between brain systems involved in sensory, cognitive and motor processes (Cisek, 2005; Spivey et al., 2005). Continuous responses can capture the dynamics of these multiple mental processes, as well as the transitions between them (Resulaj et al., 2009). The embodied approach to cognition, outlined in section 2.2.1 highlighted the action as a key aspect of cognition when interacting with the environment (Shepard, 1984). The use of the joystick or similar devices is offering more degrees of freedom, which brings them closer to day-to-day interactions with the surrounding than e.g. a button press (Freeman et al., 2011). Second, in experiments involving clinical populations, it can be difficult for patients to make discrete responses accurately on a keyboard, especially in patients with dementia or parkinsonism. Patients with motor function impairments (e.g., tremor, apraxia or loss of dexterity) often omit button presses, press the button too early or too late, press wrong buttons accidentally or are confused with response-button mapping. This limitation may result in a significant amount of experiment data being rejected in some studies (Wessel et al., 1994), while continuous response with natural movements can be well tolerated in patients (Limousin et al., 1997; Strafella et al., 2003).

The trajectories of continuous movements contain rich spatio-temporal information of the action, and provide unique insights into how cognitive processes unfold in time (Freeman et al., 2011; Song and Nakayama, 2009). In continuous reaching, movement trajectories showed that human participants can initiate a reaching action prior to when the target becomes fully available, and select from competing action plans at a later stage (e.g. Chapman et al., 2010; Gallivan and Chapman, 2014). In perceptual decision-making, movement trajectories from joysticks and other similar devices have been successfully used to investigate the cognitive processes underlying changes of mind (Resulaj et al., 2009), error correction (Acerbi et al., 2017) and subjective confidence (Berg et al., 2016) that are otherwise difficult to study with key presses.

3.1.2 A comparison between response modalities

To extend currently available experimental findings to other devices, it is necessary to assess the consistency of performance between response modalities. More importantly, characterising the consistency between response modalities may help us understand the interdependence of cognitive processes and motor systems. For example, in decision-making tasks, comparisons between saccadic eye movements and manual responses has suggested a domain general decision mechanism regardless of response modality (Ho et al., 2009; Gomez et al., 2015), and the apparent difference in response speed is accounted for by the neuroanatomical distinctions in saccadic and manual networks (Bompas et al., 2017).

The experiment described in the current chapter aimed to examine the validity and consistency of continuous joystick responses versus discrete button presses in perceptual decision-making. Participants performed a four-alternative motion discrimination task (Churchland et al., 2008) with two levels of perceptual difficulty. The task was to indicate the coherent motion direction from random dot kinematogram, a standard psychophysical stimulus for visual perceptual decision (Fredericksen et al., 1994; Lappin and Bell, 1976; Pilly and Seitz, 2009; Ramachandran and Anstis, 1983; Watamaniuk et al., 1989). In two counterbalanced sessions, the participants indicated their decisions with either joystick movements or key presses. The joystick response was to move the lever from its neutral position towards one of the four cardinal directions, aligned to the coherent motion direction, and the corresponding key press was one of the four arrow keys on the keyboard. The raw behavioural performance (decision accuracy and mean RT) was compared between the two response modalities and between the two levels of task difficulty. From continuous movement trajectories, I also examined whether joystick-specific measures were consistent between movement directions (i.e., trajectory length, peak velocity and acceleration time).

To assess whether the response modality affected the decision-making process, I fitted a drift-diffusion model (DDM) (Gold and Shadlen, 2007; Ratcliff et al., 2016) to individual participant's behavioural data and compared model parameters derived from the joystick and keyboard sessions. The DDM belongs to a family of sequential sampling models of reaction time. These models assume that the decision process is governed by the accumulation of noisy sensory evidence over time until a threshold is reached (Bogacz et al., 2006; Ratcliff and Smith, 2004), consistent with the electrophysiological (Britten et al., 1992; Churchland et al., 2008; Hanks et al., 2014; Huk and Shadlen, 2005; Shadlen and Newsome, 2001) and neuroimaging (Heekeren et al., 2008; Ho et al., 2009; Zhang, 2012) evidence on the identification of neural accumulators in the frontoparietal cortex.

The experiment described in the current chapter, I used the DDM to decompose the observed RT distributions and accuracy into three model components: decision threshold for the amount of evidence needed prior to a decision, drift rate for the speed of evidence accumulation, and non-decision time to account for the latencies of stimulus encoding and action initiation (Karahan et al., 2019; Zhang et al., 2012; Ratcliff and McKoon, 2008; Wagenmakers, 2009). The latter parameter is of interest in particular, because one may expect a difference in the latency distribution of action initiation between joystick movements and key presses.

Our findings demonstrated that when human participants used ballistic movements to respond with a joystick, their behavioural performance was modulated by task difficulty and similar to that from key presses during the same perceptual task. Further computational modelling analysis showed no evidence of a change in any model parameter when switching between response modalities. As such, it can be concluded that the joystick movement is a valid response modality for extending discrete actions to continuous behaviour in psychological experiments, although participants may exhibit differences in movement trajectory measures towards different directions.

3.2 Method

3.2.1 Participants

Twenty-one participants (7 males, aged range 18-24 years; M = 20.43 years, SD = 2.91 years) took part in the experiment following written informed consent. All but three were right-handed. All the participants had normal or corrected-to-normal vision, and none of them reported a history of motor impairments or neurological disorders. The experiment was approved by the Cardiff University School of Psychology Ethics Committee.

3.2.2 Apparatus

The experiment was conducted in a behavioural testing room with dimmed light. Stimuli were displayed on a 22-inch CRT monitor with 1600x1200 pixels resolution and 85 Hz refresh rate. A chin rest was used to maintain the viewing distance and position (for more details, see: Figure A.1 in the Appendix). A joystick (Extreme 3D Pro Precision, Logitech International S.A., Switzerland) was used to record movement trajectories at 85 Hz in the joystick session. The joystick handle could move nearly freely, with little resistance from its neutral position within the 20% movement radius. Beyond the 20% radius, the resistance during joystick movement was approximately constant. A standard PC keyboard was used to record key presses. The experiment was written using PsychoPy 1.85.4 library (Peirce, 2008).

3.2.3 Stimuli

In both the joystick and keyboard sessions, a random-dot kinematogram was displayed within a central invisible circular aperture of 14.22° diameter (visual angle). White dots were presented on a black background (100% contrast) with a dot density of 27.77 $dot/deg^2/s$ and a dot size of 0.14°. Similar to previous studies (Britten et al., 1992; Pilly and Seitz, 2009; Roitman and Shadlen, 2002; Shadlen and Newsome, 2001; Zhang and Rowe, 2014), the coherent motion in-

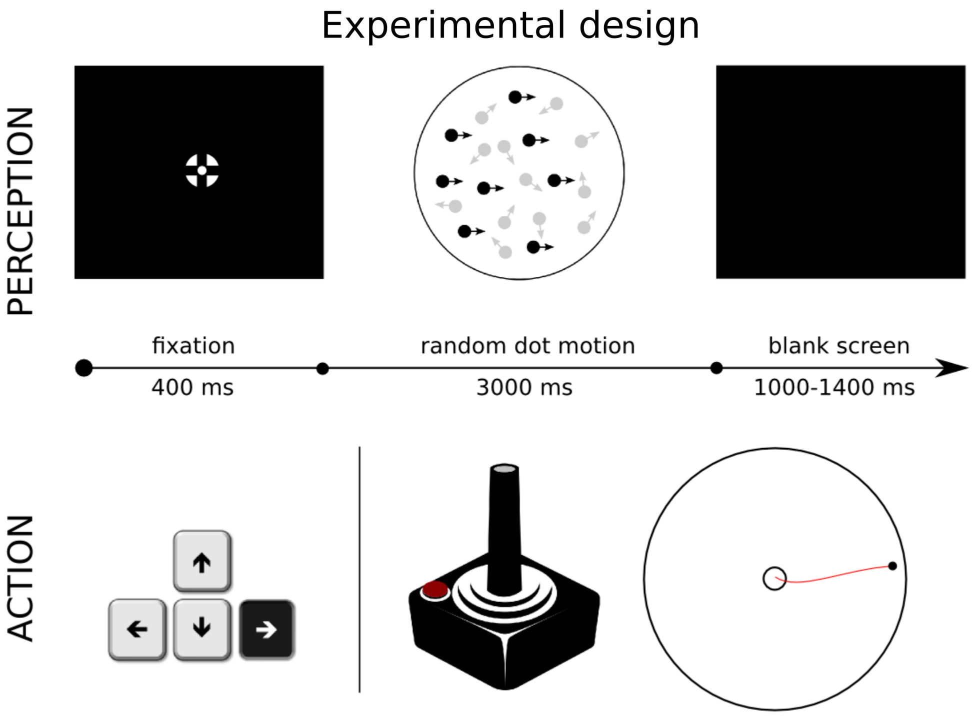

Figure 3.1: The structure of a single trial of the experiment. A fixation screen was presented for 400 ms, after which the random-dot kinematogram was presented for a maximum of 3000 ms or until response. The inter-trial interval was randomised between 1000 and 1400 ms. Participants were instructed to indicate the direction of the coherent motion direction (0°, 90°, 180° or 270°) using joystick or keyboard in two counterbalanced sessions.

formation was introduced by interleaving three uncorrelated sequences of dot positions across frames at 85 Hz. In each frame, a fixed proportion (i.e., the motion coherence) of dots was re-plotted at an appropriate spatial displacement in the direction of the coherent motion ($51.195°/s$ velocity), relative to their positions three frames earlier, and the rest of the dots were presented at random locations within the aperture. Signal dots had a maximum lifetime of three frames, after which they were reassigned to random positions. The coherent motion direction in each trial was set in one of the four cardinal directions (0°, 90°, 180° or 270°).

3.2.4 Task and procedure

Each participant took part in two experimental sessions using keyboard or joystick as a response modality. The order of response modality was counterbalanced across participants. In both sessions, participants performed a four-alternative motion discrimination task, indicating the coherent motion direction from four possible choices (0°, 90°, 180° or 270°). Each session comprised 960 trials, which were divided into 8 blocks of 120 trials. Each block had 15 repetitions of each of the four motion directions and two difficulty conditions. The motion coherence was set to 10% in the "Difficult" condition and 20% in the "Easy" condition. Feedback on the mean decision accuracy was provided after each block. The order of the conditions was pseudo-randomised across sessions and participants, ensuring that the same direction and difficulty condition did not occur in four consecutive trials. In the keyboard session, the participants responded with four arrow keys corresponding to the coherent motion direction (right - 0°, up - 90°, left - 180° and down - 270°). In the joystick session, the participants were instructed to indicate the motion direction with an appropriate joystick movement from the joystick's central position towards one of the four edges (right - 0°, up - 90°, left - 180° and down - 270°).

Every trial started with a 400 ms fixation period (Figure 1a). The random dot kinematogram appeared after the fixation period for a maximum of 3000 ms or until response. In the keyboard session, stimuli disappeared after a button press. In joystick condition, stimuli disappeared when the participants stopped joystick movement. The chosen stopping rule was when the joystick position did not change in the last four sampling points, and its position was outside of the 20% motion radius. After response, a blank screen was presented as the inter-trial interval, with a duration uniformly randomised between 1000 and 1400 ms.

The response time (RT) in the keyboard session was defined as the latency between the onset of random-dot kinematogram and the time of key press. In the joystick session, the RT was defined as the duration between the onset of the random-dot kinematogram and the first time when the joystick's position left the 20% movement radius from its neutral position. It coincided with the first noticeable increase in the velocity of the movement from the stimulus onset. Participants' choice in the joystick session was one of the four cardinal directions (i.e., 0°, 90°, 180° and 270°) closest to the last position of the joystick.

3.2.5 Drift-diffusion model (DDM) analysis

The DDM was fitted to each participant's response time distributions and accuracy. The DDM decomposes the behavioural data into four key model parameters (Ratcliff and McKoon, 2008). (1) The decision threshold (a) denotes the distance between the two decision boundaries. (2) The mean drift rate (v) denotes the strength of sensory information. (3) The starting point (z) denotes the response bias towards one of the two alternatives. (4) The non-decision time (T_{er}) denotes the latencies of stimulus encoding and response initiation. In addition, the DDM can be extended to include trial-by-trial variability in drift rate s_v and non-decision time s_t, which improves model fit to the data (Ratcliff and McKoon, 2008). The DDM predicts the decision time as the duration of the accumulation process and the observed RT as the sum of the decision time and T_{er} (Figure 3.1).

Similar to previous studies (Churchland et al., 2008), in this chapter the four-alternative forced choice task was simplified to a binary decision problem for model fitting. This was achieved by separately grouping trials with correct responses and trials with incorrect responses. The behavioural task was then reduced to a binary choice between a correct and an incorrect alternative. The hierarchical drift-diffusion model (HDDM) toolbox was used to fit the behavioural data (Wiecki et al., 2013). The HDDM implemented a hierarchical Bayesian model (Vandekerckhove et al., 2011) for estimating the DDM parameters, which assumes that the model parameters for individual participants are sampled from group-level distributions at a higher hierarchy. Given the observed experimental data, the HDDM used Markov chain Monte Carlo (MCMC) approaches to estimate the joint posterior distribution of all individual- and group-level parameters. The posterior parameter distributions can be used directly for Bayesian inference (Gelman et al., 2014), and this Bayesian approach has been shown to be robust in recovering model parameters when limited data are available (Ratcliff and Childers, 2015; Wiecki et al., 2013; Zhang et al., 2016).

Empirical results and simulations suggest that reducing the freely varying parameters led to improved model fit and increased reliability of obtained model parameters (Lerche and Voss, 2016). Applying those suggestions, following rules were applied to the model parameters. First, all the model parameters (a, v, T_{er}, s_v, and s_t) were allowed to vary between the two response modalities. Second, the mean drift rate v was further allowed to vary between task difficulties (easy, difficult) and correct directions (up, down, left and right). The intention of letting those parameters vary freely, was to assess the impact of basic experimental parameters like difficulty, visual motion direction and response modality. Third, the starting point parameter z indicates the proportion of distance of the starting point towards the two decision boundaries. Here, the experimental design and instructions did not introduce any *a priori* knowledge about the correct alternative at the beginning of each trial, and thus the starting point z was fixed at 0.5, assumption that there was no bias towards the two decision boundaries and the equal amount of evidence was required for a correct and incorrect decision (Voss et al., 2015). It is worth noting that when the two decision boundaries indicate two choice alternatives instead of correct and error alternatives, $z \neq 0.5$ would indicate the existence of a response bias towards one of the two alternatives.

The 15,000 samples were generated from the joint posterior distribution of all model parameters by using MCMC sampling (Gamerman and Lopes, 2006). The initial 7,000 samples were discarded as burn-in for stable posterior estimates. Geweke diagnostic (Cowles and Carlin, 1996) and auto-correlation were used to assess the convergence of the Markov chains in the last 8,000 samples. All parameter estimates were converged after 15,000 samples.

3.2.6 Data analysis

First, both the Bayesian and frequentist repeated-measures ANOVA were used to make inferences on behavioural measures (JASP Team, 2018). For frequentist ANOVAs, Greenhouse-Geisser correction was applied when the assumption of sphericity was violated. For Bayesian ANOVAs, the Cauchy distribution with median $m = 0$ and width $r = 0.707$ was used as a prior. The 50% of the values lie within -0.707 and 0.707. This particular parameter was used to reflect the belief about the expected effect sizes. With effect size of 0.2 considered small thus more likely and effect of 1.0 considered large and much less likely than 0.2. This choice meant that the unusually large effect sizes were deemed less probable than moderate, thus considered unreasonable to attach a larger prior weight (Rouder et al., 2009).

Also, the standard heuristic to characterise the strength of evidence based on the Bayes factor was followed (BF_{10}) (Wagenmakers et al., 2008a), which can provide evidence supporting either null ($\mathrm{BF}_{10}<1$) or alternative ($\mathrm{BF}_{10}>1$) hypotheses. A BF_{10} between [1, 3] (or [0, $^1/_3$]) suggests weak evidence for the alternative (or null) hypothesis. A BF_{10} between [3, 10] (or [$^1/_{10}$, $^1/_3$]) suggests moderate or compelling evidence for the alternative (or null) hypothesis. A BF_{10} larger than 10 (or smaller than $^1/_{10}$), suggests strong evidence for the alternative (or null) hypothesis.

Second, to quantify the difference of RT distributions between response modalities, the Kolmogorov-Smirnov test (Pratt and Gibbons, 1981) was used, a non-parametric statistical measure of difference between two one-dimensional empirical distributions.

Third, to compare a fitted DDM parameter between two conditions (e.g., between response modalities or between task difficulties), the Bayesian hypothesis testing (Bayarri and Berger, 2004; Gelman et al., 2014; Kruschke, 2015; Lindley, 1965) was used to make inferences from the posterior parameter distributions, under the null hypothesis that the parameter value is equal between the two conditions.

More specifically, the distribution of the parameter difference from the two MCMC chains of the two conditions was calculated, and the 95% highest density interval (HDI) of that difference distribution between the two conditions was obtained. A region of practical equivalence (ROPE) was set around the null value (i.e., 0 for the null hypothesis), which encloses the values of the posterior difference that are deemed to be negligible from the null value 0 (Kruschke, 2013). In each Bayesian inference, the ROPE was set empirically from the two MCMC chains of the two conditions under comparison. For each of the two conditions, the 95% HDI of the difference distribution between odd and even samples was calculated from that condition's MCMC chain. This 95% HDI from a single MCMC chain can be considered as negligible values around the null, because posterior samples from different portions of the same chain are representative values of the same parameter. That is, the null hypothesis is accepted as true when comparing the difference between odd and even samples from the same MCMC chain. The ROPE was then set to the widest boundaries of the two 95% HDIs of the two conditions.

From the 95% HDI of the difference distribution and the ROPE, a Bayesian P-value was calculated. To avoid confusion, p was used to refer to classical frequentist p values, and $P_{P|D}$ to refer to Bayesian P-values based on posterior parameter distributions. If ROPE is completely contained within 95% HDI, $P_{P|D} = 1$ and we accept the null hypothesis (i.e., the parameter values are equal between the two conditions). If ROPE is completely outside 95% HDI, $P_{P|D} = 0$ and we reject the null hypothesis (i.e., the parameter values differ between the two conditions). If ROPE and 95% HDI partially overlap, $P_{P|D}$ equals to the proportion of the 95% HDI that falls within the ROPE, which indicates the probability that the parameter value is practically equivalent between the two conditions (Kruschke and Liddell, 2018).

3.3 Results

3.3.1 Behavioural results

The behavioural performance of the four-alternative motion discrimination task was quantified by accuracy (proportion of correct responses, Figure 3.2A) and mean reaction time (RT, Figure 3.2B). The behavioural performance was compared between response modalities (joystick or keyboard), task difficulties (easy or difficult) and motion directions (up, down, left or right) using three-way Bayesian and frequentist repeated-measure ANOVAs. Across the two response modalities, participants showed decreased accuracy ($\text{BF}_{10} = 5.112 \times 10^{30}$; $F(1,20) = 292.709$, $p < 0.001$) and increased mean RT ($\text{BF}_{10} = 1.458 \times 10^{18}$; $F(1,20) = 63.163$, $p < 0.001$) in the more difficult condition. There was

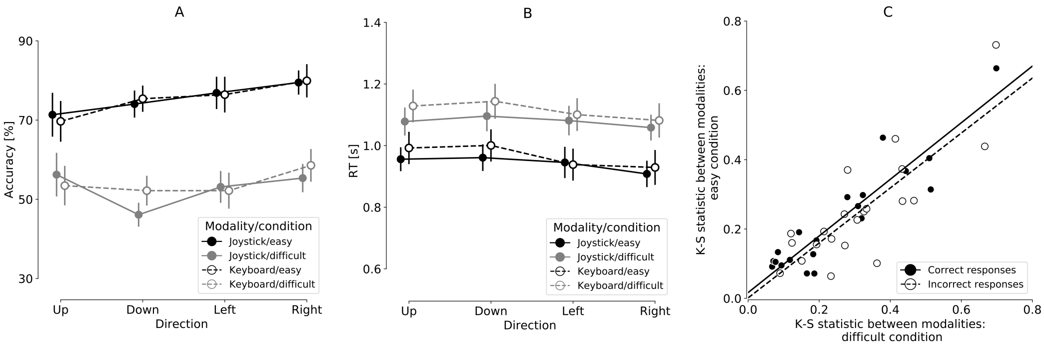

Figure 3.2: Behavioural results in joystick and keyboard sessions. (**A**) Average decision accuracy (proportion of correct) across participants. Error bars denote standard errors of the means. (**B**) Average mean RT across participants. Error bars denote standard errors of the means. (**C**) The Kolmogorov-Smirnov (K-S) statistics when comparing the RT distributions between response modalities. The scatter plot showed the K-S statistics in the difficult condition as a function of the that in the easy condition. Each data point represents the correct (filled data point) or incorrect (open data point) trials of one participant. Linear regression lines were illustrated for correct (solid line) and incorrect (dashed line) trials.

compelling evidence against the main effect of response modality on accuracy ($\mathrm{BF}_{10} = 0.124$; $F(1{,}20) = 0.083$, $p = 0.776$) and weak evidence against the main effect of response modality on mean RT ($\mathrm{BF}_{10} = 0.560$; $F(1{,}20) = 0.495$, $p = 0.490$). These results indicated similar behavioural performance between joystick and keyboard responses.

When comparing the behavioural performance between motion directions, there was compelling evidence against the main effect on accuracy ($\mathrm{BF}_{10} = 0.185$; $F(2.248,\ 44.961) = 0.107$, $p = 0.357$). On mean RT, the frequentist ANOVA suggested a significant main effect of motion direction ($F(2.853,\ 57.052) = 3.021$, $p = 0.039$), but this results was supported by neither post-hoc tests (p 0.139 in all post-hoc comparisons, Bonferroni corrected) or Bayesian ANOVA ($\mathrm{BF}_{10} = 0.305$). Furthermore, there was a significant interaction on accuracy between task difficulty and motion direction ($F(2.586,\ 51.718) = 6.317$, $p = 0.002$), although this was again not supported by Bayesian analysis ($\mathrm{BF}_{10} = 0.299$). There was evidence against all the other interactions on accuracy ($\mathrm{BF}_{10} = 0.179$; p = 0.228) and mean RT ($\mathrm{BF}_{10} = 0.199$; p = 0.083).

The results above suggested no systematic bias at the group level when comparing responses from a joystick and a keyboard. However, the consistency of behavioural performance between response modalities could vary between participants. For experiments with multiple response modalities, the researcher may want to confirm whether the consistency between response modalities is maintained across experimental conditions. This would allow, for example, a pre-screening procedure to identify participants with high response consistency to be recruited for further experiments. Here, the Kolmogorov-Smirnov (K-S) statistics was used to quantify the difference of individual participant's RT distributions between the joystick and keyboard sessions in each difficulty condition, separately for correct and incorrect trials. There was strong evidence of a positive correlation between the K-S statistics of the easy and difficult conditions (correct trials: $\mathrm{BF}_{10} = 3.647 \times 10^6$, $R = 0.92$, $p < 0.001$; incorrect trials: $\mathrm{BF}_{10} = 4526.00$, $R = 0.82$, $p < 0.001$) (Figure 3.2C). Therefore, the difference in behavioural performance between response modalities was consistent within participants across difficulty levels.

3.3.2 Hierarchical drift-diffusion model analyses

To compare the underlying decision-making process between joystick and keyboard responses, the four-alternative motion discrimination task was simplified to a binary decision task (Churchland et al., 2008, see also: "Drift-diffusion model" section) and fitted the drift-diffusion model (DDM) to the behavioural data using the hierarchical DDM (HDDM) toolbox (Wiecki et al., 2013). The DDM decomposed individual participant's behavioural data into model parameters of latent psychological processes, and the HDDM toolbox allowed to estimate the joint posterior estimates of model parameters using hierarchical Bayesian approaches. To evaluate the model fit, model predictions were generated by simulations with the posterior estimates of the model parameters. There was a good agreement between the observed data and the model simulations across response modalities, task difficulties and motion directions (Figure 3.3).

With no *a priori* knowledge on the effect of response modality on the decision-making process, all model parameters were allowed to vary between joystick

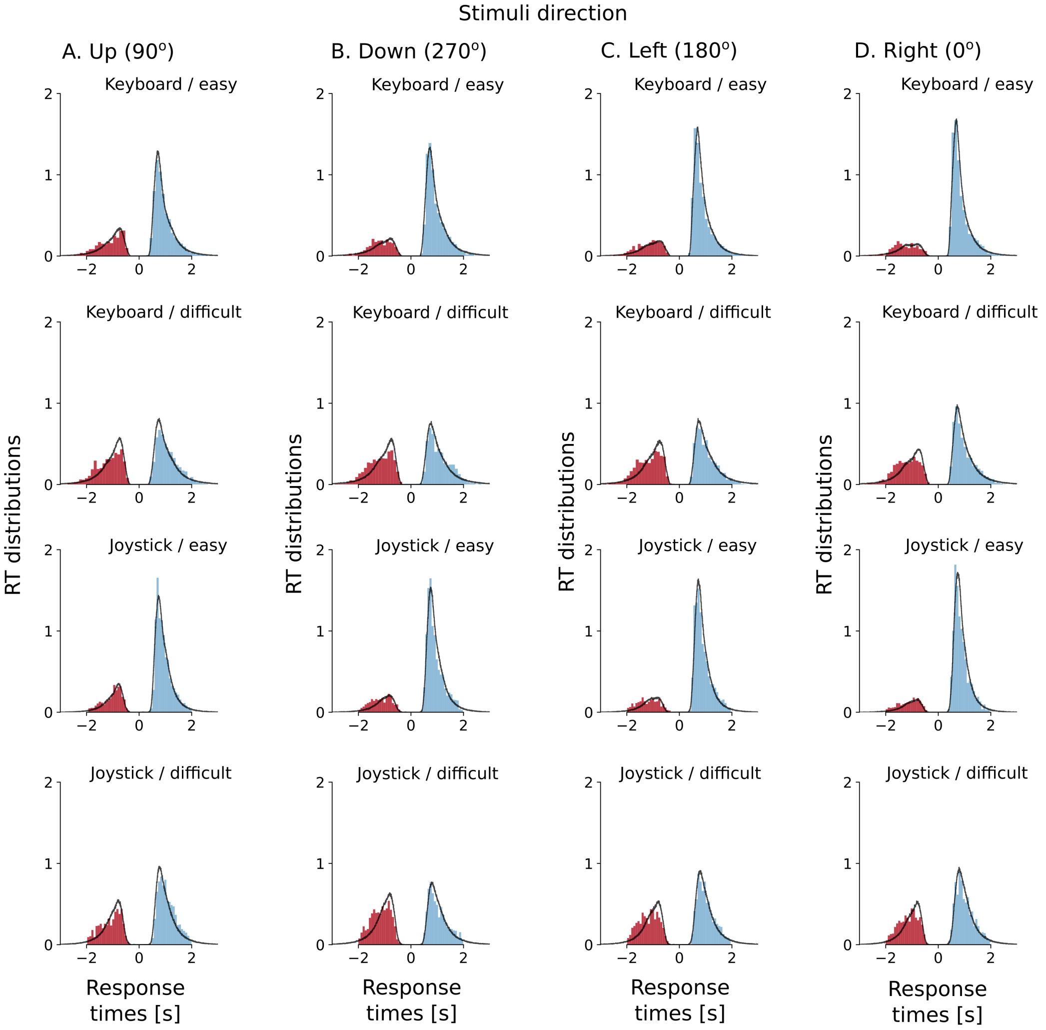

Figure 3.3: Posterior predictive RT distributions from the fitted DDM. Each panel shows the normalised histograms of the observed data (blue bars – correct responses, red bars – incorrect responses) and the model prediction (black lines) across participants. The RT distribution along the positive x-axis is from correct responses, and the areas under the curve on the positive x-axis corresponds to the observed and predicted accuracy. The RT distribution along the negative x-axis is from error responses, and the areas under the curve on the negative x-axis corresponds to the observed and predicted error. The posterior predictions of the model were generated by averaging 500 simulations of the same amount of model predicted data as observed in the experiment using posterior parameter estimates.

and keyboard responses: the boundary separation a, the mean drift rate v, the mean non-decision time T_{er}, the trial-by-trial variability of drift rate s_v, and the trial-by-trial variability of non-decision time s_t (Table 1). The mean drift rate was further allowed to vary between task difficulties and motion directions. Bayesian hypothesis testing was performed on the posterior parameter estimates between response modalities (Bayarri and Berger, 2004; Kruschke, 2015; Gelman et al., 2014; Lindley, 1965). This analysis yielded 95% HDI of the parameter difference between the joystick and keyboard sessions, as well as Bayesian P-values $P_{P|D}$ (see "Data analysis" section for details).

(a, v, T_{er}, s_v, and s_t)

Table 3.4: Posterior estimates of the hierarchical drift-diffusion model parameters (decision threshold a, mean drift rate v, non-decision time T_{er}, trial-by-trial drift rate variability s_v, trial-by trial non-decision time variability s_t). The first two data columns showed the posterior means and standard deviations of the parameters in the joystick and keyboard sessions. 95% HDI denoted the 95% highest density intervals for the parameter difference between the joystick and keyboard sessions. $P_{P|D}$ denoted the Bayesian P-value for the parameter difference being equal between response modalities.

			Joystick(mean ± sd)	**Keyboard**(mean ± sd)	**95% HDI**	$P_{P\|D}$
$\boldsymbol{a}$			1.508 ± 0.072	1.572 ± 0.073	[-0.270, 0.120]	0.872
$\boldsymbol{v}$	easy	up	1.694 ± 0.263	1.269 ± 0.260	[-0.300, 1.144]	0.720
		down	1.765 ± 0.264	1.454 ± 0.261	[-0.460, 0.999]	0.810
		left	2.169 ± 0.267	1.906 ± 0.260	[-0.450, 1.020]	0.789
		right	2.351 ± 0.267	2.187 ± 0.262	[-0.580, 0.880]	0.863
	difficult	up	0.477 ± 0.257	0.291 ± 0.263	[-0.526, 0.896]	0.866
		down	0.144 ± 0.262	0.202 ± 0.256	[-0.822, 0.603]	0.932
		left	0.441 ± 0.261	0.216 ± 0.257	[-0.529, 0.909]	0.854
		right	0.533 ± 0.263	0.597 ± 0.261	[-0.769, 0.685]	0.964
$\boldsymbol{T_{er}}$			0.613 ± 0.028	0.556 ± 0.028	[-0.025, 0.130]	0.658
$\boldsymbol{s_t}$			0.992 ± 0.047	0.916 ± 0.042	[-0.039, 0.203]	0.669
$\boldsymbol{s_v}$			0.268 ± 0.007	0.283 ± 0.007	[-0.035, 0.004]	0.641

For all the model parameters, we could not reject the null hypothesis that the posterior parameter estimates are practically equal between the joystick and keyboard sessions. The $P_{P|D}$, which quantifies the probability that the model parameter is practically equal between the two conditions, ranged from 0.641 to 0.964 (Table 3.4). Therefore, there was no evidence to support that switching from keyboard to joystick altered the decision-making process. Next, because the mean drift rate is often assumed to increase with decreased task difficulty (Ratcliff and McKoon, 2008), I compared the drift rate averaged from the joystick and keyboard sessions between easy and difficult conditions. As expected, the drift rate was larger in the easy compared with the difficult condition in all motion directions (up: 95% HDI = [0.589, 1.613], $P_{P|D} = 0$; down: 95% HDI = [0.930, 1.958], $P_{P|D} = 0$; left: 95% HDI = [1.204, 2.227], $P_{P|D} = 0$; right: 95% HDI = [1.185, 2.214], $P_{P|D} = 0$).

3.3.3 Additional measures from joystick trajectories

In the joystick session, the participants' movement trajectories were close to the four cardinal directions (Figure 3.5A). Continuous movements with the joystick enabled to acquire additional trial-by-trial behavioural measures beyond that possible from simple key presses. Three such measures were examined: peak velocity (Figure 3.5B), acceleration time (Figure 3.5C) and trajectory length (Figure 3.5D). These additional joystick measures were subsequent to accuracy and RT. In the current study, I did not expect them to have critical influence on the two primary behavioural measures. Hence our analyses were focused on the effects of movement direction and task difficulty on the trajectory measures. However, in experiments with more complex movement trajectories, decisions may be more directly coupled to continuous motor responses (Song and Nakayama, 2009).

The action velocity was calculated as the rate of changes of joystick position. There was a single peak of action velocity in each trial, consistent with the ballistic nature of the movement. There was strong evidence for the main effect of response direction on the peak velocity (Figure 3.5B, $BF_{10} = 3.900 \times 10^{24}$, F(2.000, 40.002) = 39.25, $p < 0.001$), moderate evidence for the main effect of difficulty ($BF_{10} = 4.612$, F(1,20) = 22.70, $p < 0.001$) and strong evidence for the interaction between direction and difficulty ($BF_{10} = 58.433$, F(2.841,56.813) = 30.58, $p < 0.001$). For post-hoc comparisons see Tables 3.8 and 3.9).

The acceleration time was calculated as the latency between the RT and the time of peak velocity (Figure 3.5C). There was strong evidence for the main effect of response direction ($BF_{10} = 1147.376$, F(2.253, 45.05) = 4.741, p = 0.011). We found moderate evidence against difficulty level ($BF_{10} = 0.172$,

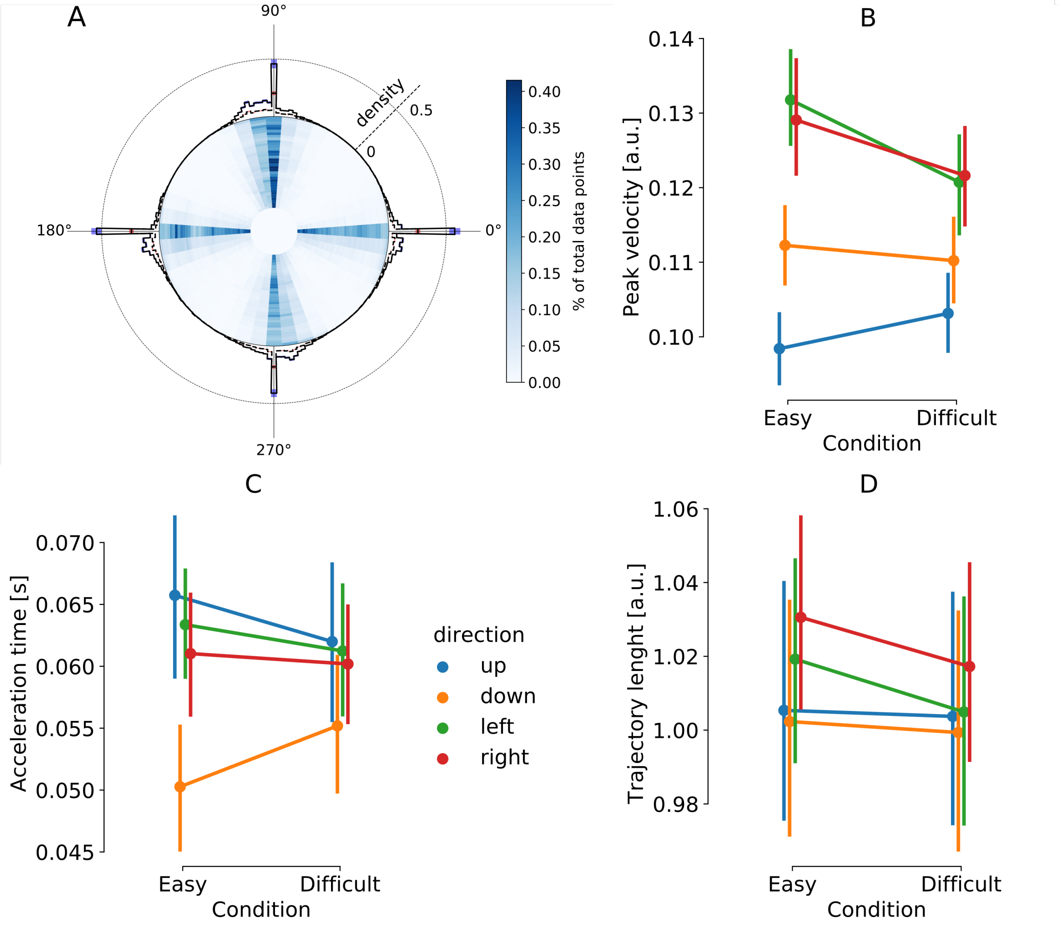

Figure 3.5: Measures from joystick trajectories. (A) The summary of movement trajectories and final positions. The heat map in the centre represents the proportion of the total joystick position across trials and participants. The histogram on the edge represents the distribution of final positions. (B) The peak velocity of joystick movements averaged across participants. (C) The mean acceleration time of joystick movements averaged across participants (D) The mean trajectory length averaged across participants. The error bars denote the standard errors of the means.

F(1,20) = 0.178, p = 0.677). Frequentist ANOVA showed a significant interaction between the response direction and difficulty levels (F(2.853, 57.053) = 4.470, p = 0.008), which was not supported by the Bayes factor (BF_{10} = 0.256). For post-hoc comparisons see Tables 3.6 and 3.7).

The trajectory length was calculated as the sum of the Euclidean distance between adjacent joystick positions in each trial (Figure 3.5D). There was no compelling evidence for the main effect of response direction on trajectory length (BF_{10} =1.759; F(3, 60) = 1.944, p = 0.151), nor the main effect of task difficulty (BF_{10} = 0.450, F(1, 20) = 3.171, p = 0.09). The evidence against the interaction between direction and difficulty was strong (BF_{10} = 0.090, F(3, 60) = 0.978, p = 0.409).

Table 3.6: Post Hoc Comparisons: Peak Action Velocity - Direction

		Mean Difference	SE	t	Cohen's d	p_{bonf}
Down	Left	-0.015	0.003	-5.575	-1.217	< .001
	Right	-0.014	0.003	-4.460	-0.973	0.001
	Up	0.010	0.002	5.922	1.292	< .001
Left	Right	8.991e-4	0.002	0.378	0.082	1.000
	Up	0.025	0.003	9.628	2.101	< .001
Right	Up	0.025	0.004	6.955	1.518	< .001

In summary, the peak action velocity of joystick movements was affected by both action direction and task difficulty, and acceleration time was affected only by trajectory direction. There was no compelling evidence to support that trajectory length was affected by action direction or task difficulty.

3.4 Discussion

In current chapter, I systematically compared the consistency between continuous and discrete responses during rapid decision-making. In a four-alternative motion discrimination task, joystick movements and key presses led to similar accuracy and mean RT. Further modelling analysis with hierarchical DDM showed no evidence in supporting a change of any model parameters between response modalities. Together, our findings provide evidence for the validity of using continuous joystick movement as a reliable response modality in behavioural experiments.

3.4.1 Behavioural measures

In both joystick and keyboard sessions, participants had lower accuracy and longer mean RT in the more difficult condition (i.e., lower motion coherence), in line with previous findings with similar tasks (Britten et al., 1992; Pilly and Seitz, 2009; Ramachandran and Anstis, 1983; Roitman and Shadlen, 2002). Using Bayesian statistics, there was evidence that response modality (joystick motion or key press) did not affect either accuracy or mean RT, confirming the validity of using joystick as a response device in decision-making tasks. Importantly, across participants, the difference in the RT distributions between response modalities was positively correlated between easy and difficult conditions. Therefore, participants with similar behavioural performance between response modalities maintained their consistency between experimental conditions.

Joystick positions estimated at a high sampling rate enabled additional behavioural measures beyond on/off key presses. In the current study, most of the movement trajectories were along the four cardinal directions (Figure 3.5A). The averaged trajectory length was close to 1 (Figure 3.5D), which was the shortest distance from the joystick's neutral position to the maximum range, suggesting that the participants were able to make accurate and ballistic movements following the task instruction. Nevertheless, it is worth noting that the movement direction affected the peak velocity and acceleration time. This may be due to the difference in upper limb muscle contractions when moving the joystick towards different directions (Oliver et al., 2011). Therefore, for future behavioural experiments relying on sensitive trajectories measures, I suggest extra cautious on the effects of ergonomics and human motor physiology, especially for rapid movements as in the current study. One potential solution would be to acquire baseline recordings of the movement to be expected during the experiment, which can then be used to compensate measurement biases.

3.4.2 Model-based measures

The DDM and other sequential sampling models (Bogacz et al., 2006; Smith and Ratcliff, 2004) are commonly used to investigate the cognitive processes underlying rapid decision-making (Bogacz et al., 2006; Smith and Ratcliff, 2004). In the current study, the mean drift rate increased in the easier task condition, consistent with previous modelling results (Ratcliff and McKoon, 2008). The combination of posterior parameter estimation and Bayesian inference allowed us to obtain the probability of the parameter being practically equal, a more informative measure than frequentist p-values (Kruschke, 2015). Although our results suggested that most parameter values had high probabilities to remain the same between response modalities (Table 3.4), the null hypothesis could not be accepted for certain (which requires $P_{P|D} = 1$) and need more data to confirm the inference.

It is worth to highlight two model parameters with low $P_{P|D}$ values, which indicate that, with additional observed data from future experiments, the posterior model parameters might be in favour of the alternative hypothesis (i.e., a difference between response modalities). First, when switching from key presses to joystick movements, there was a small increase in the mean non-decision time ($P_{P|D} = 0.658$). Second, responding with a joystick resulted in a slightly decreased decision threshold ($P_{P|D} = 0.872$). Several previous studies showed that instructing to respond faster or more accurately could efficiently modulate participants' behaviour (Beersma et al., 2003; Schouten and Bekker, 1967; Wickelgren, 1977). The decision threshold plays a substantial role under such speed-accuracy instructions (Mulder et al., 2013; Rae et al., 2014b; Starns and Ratcliff, 2014; Zhang and Rowe, 2014): a decrease of threshold is accompanied with faster reaction speed and lower accuracy. If participants do implicitly trade accuracy for speed when switching from keyboard to joystick movements, this cognitive discrepancy needs to be considered when conducting experiments involving continuous responses. One hypothesis for this potential behavioural change is that continuous joystick movements allow participants to change or correct their responses later in a trial (Albantakis and Deco, 2009; Gallivan and Chapman, 2014; Gallivan et al., 2016), and this response flexibility may lead to reduced deliberation in initial movements.

The trial-by-trial variabilities in drift rate and non-decision time also had $P_{P|D}$ values. Empirically, across-trial variability was introduced in DDM to improve the model fit to RT distributions (Ratcliff and McKoon, 2008), although the functional significance of these parameters to the decision process is still unclear. Across-trial variability in the drift rate produces different RT between correct and error trials (Ratcliff and Rouder, 1998), and across-trial variability in the non-decision time accounts for the large variability in trials with short RT across experimental conditions (Ratcliff, 2002). These model parameters allow the DDM to account for the subtle differences in the shape of RT distributions between response modalities. Future studies could apply formal model comparison to evaluate the need of trial-by-trial variability in modelling joystick responses.

3.4.3 The use of joystick and its validity

The current chapter aimed to establish the validity of joystick response in rapid decision-making tasks. More specifically, I examined whether response modality (joystick movements vs. key presses) alters the raw behavioural measures (RT and accuracy) and underlying cognitive processes. I found that both behavioural measures and model parameters from cognitive modelling did not differ significantly between response modalities. In other words, using joystick movements to indicate choices of perceptual decisions elicit behavioural and cognitive characteristics similar to those from conventional key presses.

Motion discrimination based on random dot kinematogram is a typical paradigm for simple decisions. The same computational mechanism of evidence accumulation has been suggested to account for the cognitive processes underlying a broad range of decision-making tasks, spanning across sensory modalities (O'Connell et al., 2012) and cognitive domains (Gold and Shadlen, 2007). Therefore, I expect that the validity of joystick response established in the current chapter can be extended to experimental paradigms in which participants make rapid choices with motor actions (Ratcliff and McKoon, 2008).

The joystick as a response modality has been successfully applied in ageing and clinical populations, in which conventional key presses may be error-prone due to impaired dexterity. Both older and young adults can operate joysticks in visuo-motor tasks with similar response patterns (Kramer et al., 1999). Previous studies showed that older adults can complete multiple hour-long cognitive training sessions with joystick responses, and the performance benefit persisted for 6 months after training (Anguera et al., 2013). In patients with neurodegenerative diseases, volitional joystick movements have been successfully used to examine the motor deficits and underlying neural abnormalities (Kew et al., 1993). This evidence suggested that the use of joystick can be well tolerated in older adults and patients.

In the current study, the participants did not report fatigue after joystick or keyboard sessions, which lasted approximately 45 minutes each. Other paradigms with longer experimental sessions and more intense joystick movements may impose a challenge to participants' stamina. Nevertheless, it is possible to use measures from the continuous joystick recording (Kahol et al., 2011) or concurrent physiological recording (Mascord and Heath, 1992) to identify the onset of fatigue prior to performance deterioration.

One may ask if joystick responses provide any additional value over conventional key presses. Here, I showed that, even in simple ballistic movements, joystick-specific measures (e.g. action velocity) can be affected by the task difficulty, providing additional information on behavioural performance in addition to RT and accuracy. It is yet to be determined whether continuous responses provide independent information from discrete responses (Freeman, 2018; Freeman and Ambady, 2010; Stillman et al., 2017). However, the capacity of recording continuous responses via joysticks enables new experimental designs to probe the continuous interplay between action, perception and cognition. For example, the ongoing locomotion can modify the sensory information flow (Ayaz et al., 2013; Souman et al., 2010).

In conclusion, our results validated the joystick as a reliable device for continuous responses during rapid decision-making. Compared with key presses, the additional complexity and continuity associated with joystick movements did not affect raw behavioural measures such as accuracy and mean RT, as well as underlying decision-making processes. However, I highlighted the effects of movement direction on continuous trajectory measures. Researchers should be cautious when adopting experimental designs that require complex movement trajectories.

Table 3.7: Post Hoc Comparisons:Peak Action Velocity - Coherence * Direction

		Mean Difference	SE	t	p_{bonf}
Easy, Down	Hard, Down	0.002	0.001	1.510	1.000
	Easy, Left	-0.020	0.003	-6.746	< .001
	Hard, Left	-0.008	0.003	-2.877	0.146
	Easy, Right	-0.017	0.003	-5.813	< .001
	Hard, Right	-0.009	0.003	-3.182	0.059
	Easy, Up	0.014	0.003	4.791	< .001
	Hard, Up	0.009	0.003	3.099	0.076
Hard, Down	Easy, Left	-0.022	0.003	-7.324	< .001
	Hard, Left	-0.011	0.003	-3.637	0.014
	Easy, Right	-0.019	0.003	-6.408	< .001
	Hard, Right	-0.011	0.003	-3.948	0.005
	Easy, Up	0.012	0.003	4.010	0.004
	Hard, Up	0.007	0.003	2.446	0.473
Easy, Left	Hard, Left	0.011	0.001	8.130	< .001
	Easy, Right	0.003	0.003	0.933	1.000
	Hard, Right	0.010	0.003	3.446	0.026
	Easy, Up	0.033	0.003	11.537	< .001
	Hard, Up	0.029	0.003	9.727	< .001
Hard, Left	Easy, Right	-0.008	0.003	-2.835	0.164
	Hard, Right	-8.984e-4	0.003	-0.311	1.000
	Easy, Up	0.022	0.003	7.583	< .001
	Hard, Up	0.018	0.003	6.083	< .001
Easy, Right	Hard, Right	0.007	0.001	5.483	< .001
	Easy, Up	0.031	0.003	10.604	< .001
	Hard, Up	0.026	0.003	8.810	< .001
Hard, Right	Easy, Up	0.023	0.003	7.888	< .001
	Hard, Up	0.018	0.003	6.394	< .001
Easy, Up	Hard, Up	-0.005	0.001	-3.484	0.023

Table 3.8: Post Hoc Comparisons: Acceleration Time - Direction

		Mean Difference	SE	t	Cohen's d	p_{bonf}
Down	Left	-0.010	0.003	-3.239	-0.707	0.025
	Right	-0.008	0.002	-3.218	-0.702	0.026
	Up	-0.011	0.003	-3.724	-0.813	0.008
Left	Right	0.002	0.003	0.542	0.118	1.000
	Up	-0.002	0.003	-0.477	-0.104	1.000
Right	Up	-0.003	0.004	-0.773	-0.169	1.000

Table 3.9: Post Hoc Comparisons: Acceleration Time - Coherence * Direction

		Mean Difference	SE	t	p_{bonf}
Easy, Down	Hard, Down	-0.005	0.002	-2.630	0.288
	Easy, Left	-0.013	0.003	-3.794	0.008
	Hard, Left	-0.011	0.003	-3.136	0.067
	Easy, Right	-0.011	0.003	-3.116	0.072
	Hard, Right	-0.010	0.003	-2.836	0.162
	Easy, Up	-0.015	0.003	-4.481	$< .001$
	Hard, Up	-0.012	0.003	-3.353	0.034
Hard, Down	Easy, Left	-0.008	0.003	-2.338	0.612
	Hard, Left	-0.006	0.003	-1.753	1.000
	Easy, Right	-0.006	0.003	-1.669	1.000
	Hard, Right	-0.005	0.003	-1.449	1.000
	Easy, Up	-0.011	0.003	-3.015	0.096
	Hard, Up	-0.007	0.003	-1.973	1.000
Easy, Left	Hard, Left	0.002	0.002	1.137	1.000
	Easy, Right	0.002	0.003	0.678	1.000
	Hard, Right	0.003	0.003	0.908	1.000
	Easy, Up	-0.002	0.003	-0.687	1.000
	Hard, Up	0.001	0.003	0.392	1.000
Hard, Left	Easy, Right	2.126e-4	0.003	0.061	1.000
	Hard, Right	0.001	0.003	0.304	1.000
	Easy, Up	-0.004	0.003	-1.286	1.000
	Hard, Up	-7.574e-4	0.003	-0.219	1.000
Easy, Right	Hard, Right	8.370e-4	0.002	0.448	1.000
	Easy, Up	-0.005	0.003	-1.365	1.000
	Hard, Up	-9.700e-4	0.003	-0.277	1.000
Hard, Right	Easy, Up	-0.006	0.003	-1.586	1.000
	Hard, Up	-0.002	0.003	-0.524	1.000
Easy, Up	Hard, Up	0.004	0.002	1.999	1.000

Chapter 4

Continuous movements during perceptual decision-making

4.1 Introduction

4.1.1 Background

In our daily lives, decisions and actions are intertwined in time. Constantly changing surroundings affect how we behave. In other words, the changes in sensory information require adjustments of motor outputs. Riding a bicycle on a foggy day is a good example of how environmental pressures require us to make decisions during ongoing actions. It forces us to process a stream of imperfect visual information to produce a specific series of movements. Riding on an empty park lane requires maintaining a continuous action (e.g., pedalling) with only sporadic adjustments with a handlebar. On the other hand, entering a busy street requires a decision among action plans, such as the right moment to join the traffic. To keep a safe position on the road, we need to adjust our continuous actions without stopping, e.g., to avoid jaywalking pedestrian or a pothole. Some aspects of those real-life scenarios could be found in studies using driving (Roenker et al., 2003) or flight simulators (Schriver et al., 2008). However, continuous responses are not commonly used in conventional lab-based experiments.

In Chapter 3, I assessed the use of a joystick as a response device. The behavioural performance as well as the underlying cognitive processes were not affected by the response modality (button press or joystick movement). Experimental design in Chapter 3 required participants to perform a simple ballistic movement to indicate their decisions, similarly to previous studies (Gallivan et al., 2016; Gallivan and Chapman, 2014; Gallivan et al., 2016; Resulaj et al., 2009; Burk et al., 2014; Berg et al., 2016; Freeman et al., 2011).

In this chapter, I aimed to investigate the performance of continuous, periodic movements in response to perceptual decisions. Here I outlined the rationale of this research.

First, ballistic joystick movements or rapid point-to-point reaching used in Chapter 3 are not strictly continuous actions from the point of view of motor control. As reviewed in Section 2.2, rapid ballistic movements are characterised by a single peak in velocity, which are in sharp contrast to rhythmic movements characterised by periodic trajectories or multiple peaks in velocity (Hogan and Sternad, 2007; Howard et al., 2011). Moreover, the distinction between discrete and continuous movement is non trivial from the standpoint of the motor control. Utilising a state flow analysis of dynamic systems, a computational model distinguished two ways of which the motor output is controlled. The simulation of the discrete movement required a module to monitor for a right time to trigger the action. The maintenance of the rhythmic movement did not rely on it (Huys et al., 2008).

The perceptual decision-making methodology has been useful in discovering and refining the understanding of the cognitive mechanisms mediating our interaction with the environment (Shadlen and Newsome, 2001; Cisek, 2007). The experimental designs based on random dot motion discrimination task were instrumental in linking a choice probability and a response time (RT) with the neuronal signals (Newsome and Pare, 1988; Newsome et al., 1989). As argued in Chapter 3, the continuous response measures can provide more detailed look on decision making process (Freeman et al., 2011; Song and Nakayama, 2009). Findings from my previous research (Chapter 3, Szul et al. (2019)) showed that a button press and responses made using joystick did not affect the behavioural performance in random dot motion discrimination task and underlying decision-making processes. Experiments utilising the continuous response measures (mouse (e.g. Spivey et al., 2005), motion tracking (e.g. Gallivan and Chapman, 2014), joystick (e.g. Resulaj et al., 2009)) and probing various aspects of decision processes, commonly use a simple directional movement towards an object or the alternative. Recent developments of the decision-making field reflected an expansion towards the exploration of various contextual factors affecting the processes of decision-making (de Lange and Fritsche, 2017; Shadlen and Kiani, 2013; Doya, 2008).

Second, our motor functions obey the same rules as found in research on perceptual decision-making, the speed-accuracy trade-off (SAT) (Plamondon and Alimi, 1997; Newell, 1980; Hancock and Newell, 1985; Battaglia and Schrater, 2007). In fact, the SAT in continuous movement is more robust to external perturbations than discrete movements (Guiard, 1997; Smits-Engelsman et al., 2006, and see Section 2.2.2). The existence of SAT in continuous movements suggests a information processing bottleneck similar to that in decision-making process. Wolpert and Landy (2012) suggested that continuous motor control and decision-making share a computational principle: the prior expectation being updated by ongoing sensory inputs. This implies that the judgement of the sensory evidence and motor execution could co-occur in parallel with continuous mutual influences (Selen et al., 2012; Cisek, 2007).

As I argued in the Chapter 3, the common ground between simple and more complex actions is the initial engagement. However, to find out how the contextual factors affect the decision process, one need to go beyond a simple response. The more complex the actions, the more opportunity for them to be affected by the environment (Doya, 2008; Hagura et al., 2017; Gallivan et al., 2016).

4.1.2 A new decision-making paradigm with continuous responses

As outlined in Chapter 2, the decision-making process can be influenced by a wide range of the contextual factors (Doya, 2008; Gold and Shadlen, 2007). The bodily state like arousal can affect the accumulation of information process (e.g. Honey et al., 2012; Urai et al., 2017). Not only internal states but also the environmental factors can modify the ongoing decision process. (e.g. Ossmy et al., 2013). The mutual influence of the action and perception occurs not only during the action-decision cycle (Selen et al., 2012; Cisek, 2007), but also extends over future cycles. The decision process can be biased by the events prior to the decision. It has been shown that the actions unrelated to choice can bias subsequent decision process (e.g. Pape et al., 2017). A phenomenon of the serial dependence, the stimulation and choice history affecting the subsequent decisions, highlighted the integration of the prior information and current state in the decision process (Fründ et al., 2014; Fischer and Whitney, 2014; John-Saaltink et al., 2016). The use of the cognitive models of the decision-making process unravelled that the prior decisions reduced the rate of evidence accumulation for the sensory input after the decision was made (Bronfman et al., 2015; Urai et al., 2018). This process is also mediated by the confidence in the prior choices (Braun et al., 2018).

I developed a two-alternative visual discrimination paradigm (Figure 4.1), which combined continuous flow of sensory inputs (RDM stimulus) and continuous motor outputs (clockwise or anti-clockwise joystick circular movement). Participants were instructed to continuously respond to the visual information over a few seconds, and adjust their actions if there was a change in the visual information.

A circular movement (clockwise or anti-clockwise) was used to continuously indicate the direction of the visual stimuli. Clockwise and anti-clockwise movement allowed to use the stable, stereotypic movement as the response measure in a simple perceptual discrimination task. The experimental design described in the current chapter, followed the experiment from the Chapter 3. The random dot motion stimuli were generated in the same way. Moreover, the initial engagement in the movement (clockwise or anti-clockwise) was uniform. To allow the comparison across the conditions, and ensure the interpretability of the movement initiation, participants were asked to start the continuous movement with the simple, directional upward movement (for detailed overview of the design see: Figure 3.1 and Methods section). The results from Chapter 3 showed that the initial engagement in the action is equivalent to a commonly used button press (Szul et al., 2019), and similar to linear trajectories used in other decision-making studies (e.g. Berg et al., 2016; Resulaj et al., 2009; Gallivan et al., 2016).

The complexity of the task and the relatively unusual way of responding required an intensive behavioural training. The current chapter included a set of four experiments. To facilitate the learning of stable circular movements, a self-guided practice session was introduced first (Sigrist et al., 2013) (see Section 4.2.4). In Experiment 1, participants were introduced to the trial structure. In Experiments 2-4, participants was trained with the RDM stimulus and continuous responses. In Experiments 3-4, a lower motion coherence was introduced in 50% of trials.

All the four experiments included two phases in each trial. In the first phase, a visual cue (arrows in Experiment 1 or RDM stimulus in Experiments 2-4) indicated a left or right direction, and the participants responded to the cue with continuous circular clockwise or anti-clockwise movements using a joystick. In the second phase, depending on the visual cue, the participants either maintained the ongoing movement in the same direction, or changed to the opposite circular direction.

The main goal of this chapter was to assess the validity of the new experimental task. The training procedure, which gradually introduced the complexity of the task, was expected to yield a stable behavioural performance across participants. This task was set to be further used in MEG (see Chapter 5). I expected that the participants will be able to adjust their continuous action to the change of visual information. This behavioural flexibility would be further influenced by the signal-to-noise ratio of the information (i.e., motion coherence), similar to previous perceptual decision-making studies using discrete responses (Fredericksen et al., 1994; Lappin and Bell, 1976; Pilly and Seitz, 2009; Ramachandran and Anstis, 1983; Watamaniuk et al., 1989; Szul et al., 2019; Zhang and Rowe, 2014).

The performance in the Experiments 3 and 4 was expected to be stable after training phase depicted in the Experiments 1 and 2. The engagement in action in the first phase of the trial should not be affected by the experimental manipulation as the directions of the stimuli are equally probable and the stimulus quality is constant. In the second phase of the trial, the adjustment in action

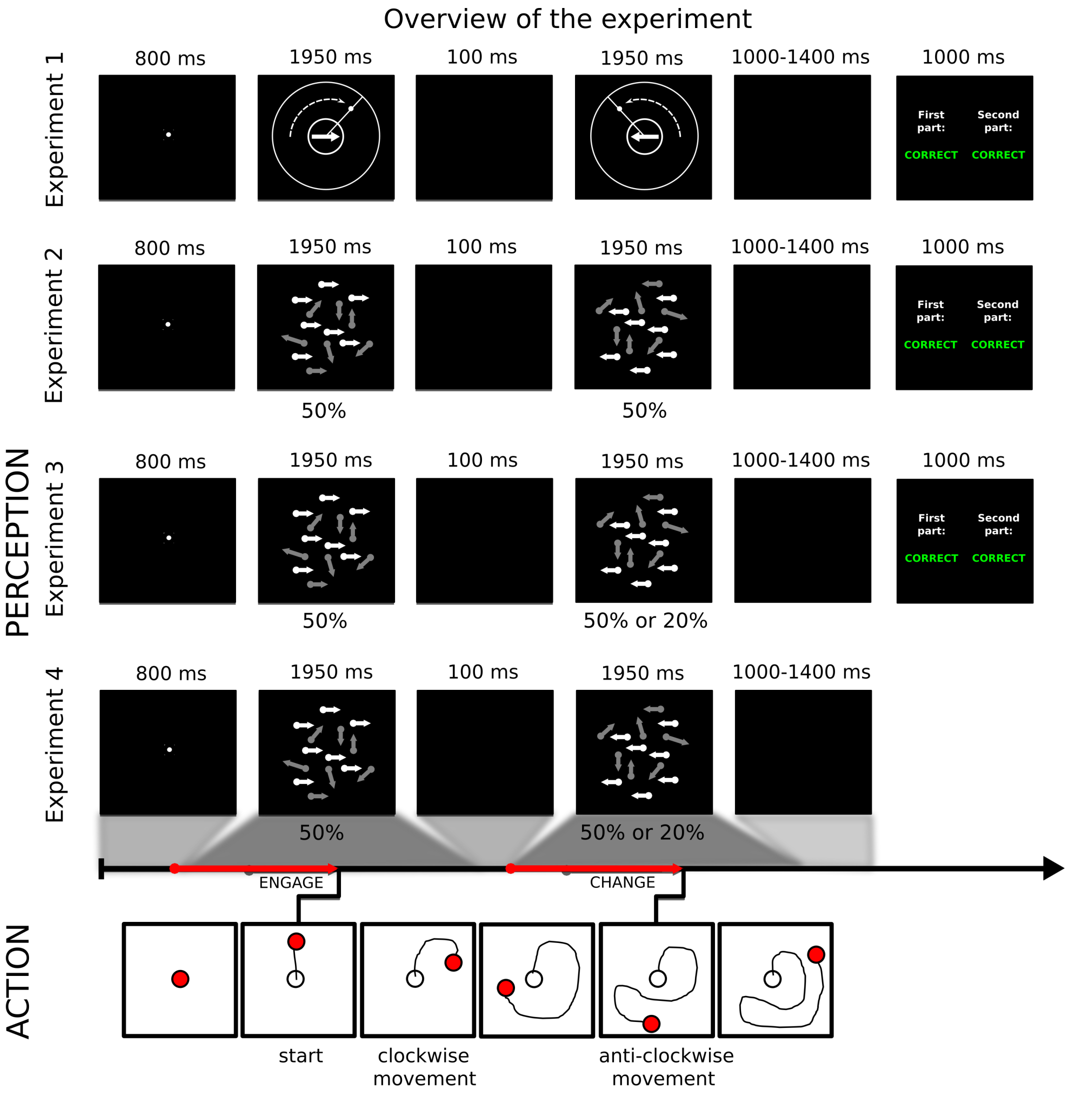

Figure 4.1: Structure of the trial across all experiments. In the Experiment 1, the direction of the arrow served as the visual cue for the action. A cursor (a circle), and a line provide a participant a visual feedback about the direction of their actions. In experiments 2-4, the coherent motion direction of RDM stimulus provided a cue for continuous movement. In experiments 1, 2, and 3 participants are receiving feedback information about the accuracy in each trial.

is expected to be affected by the quality of the visual stimulation. In cases of both maintenance and adjustment of the action, lower coherence would result in lower accuracy as there is more likely to produce a deflection in hand trajectories akin to changes in mind (Resulaj et al., 2009). The action adjustment should display a longer latency when the stimulus strength is lower.

Current chapter highlighted a multifaceted interaction between perceptual decision-making, action selection, and learning aspects of sensory-motor transformation. One of the goals of the study was to elicit states present in real life decision making, but infrequently addressed in the research. Building on the results from Chapter 3, I was able to evaluate the novel paradigm that linked continuous movements with perceptual decisions. Over the course of four experiments, participants successfully learned to perform the task. Experimental manipulation of the stimulus signal-to-noise ratio brought the effects in an expected direction. The learning effect was observed across all the experiments.

4.2 General methods

4.2.1 Participants

20 participants (5 males), aged between 19-26 (M = 21.1, SD = 1.83) took part in practice session and 4 experiments in exchange for the course credits. All participants were right-handed, with normal or corrected to normal vision. None of the participants reported motor impairments or neurological disorders. The study was approved by Cardiff University, School of Psychology Ethics Committee.

4.2.2 Apparatus

Experiments were conducted in a room with dimmed light. Stimuli were displayed on a CRT monitor with 1600x1200 pixels resolution and 100 Hz refresh rate. A Logitech 3D Pro Precision joystick (Logitech International S.A., Switzerland) was used to record the movement trajectories. The device was attached to the table using velcro straps to maintain the location and orientation during the experiment. The orientation of the device was adjusted for comfort of the participant before the session. A change of the joystick lever position was recorded with a time stamp (maximum polling rate of 125 Hz), in a process independent of the experiment. Within the 20% movement radius, joystick movement exhibited small amount of resistance. Beyond the 20% radius, the resistance during joystick movement was higher and approximately constant. PsychoPy 1.85.4 library (Peirce, 2008) was used to display the stimuli.

4.2.3 Experimental Design

Each experiment followed a similar trial structure (see Figure 4.1). Participants performed continuous circular movement using a joystick (clockwise or anti-clockwise) in responding to arrows (Experiment 1) or the coherent motion of RDM stimulus (Experiments 2-4), which indicating a left or right direction. Each participant was assigned to a stimulus-response mapping group (Group I: right - clockwise, left - anti-clockwise; Group II: right - anti-clockwise, left - clockwise). The group assignment was random and counterbalanced across participants.

Each trial was initiated with a 0.8 s fixation period (Thaler et al., 2013). In the first phase of the trial (1.95 s), participants initiated and maintained circular movements on a joystick from its neutral position. They were instructed to always initiate the movement with an upward action, followed by clockwise or anti-clockwise rotations. In the second phase of the trial (1.95 s), the visual cue changed its direction in 50% of the trials, in which participants had to adjust the direction of their circular movements accordingly and maintain the new movement direction until the end of the trial. Participants were instructed to keep a constant speed of circular movement and prioritise the accuracy over the speed when deciding to engage in movement or change movement direction.

4.2.4 Initial practice

Prior to the first experiment, participants familiarised themselves with the joystick and task instructions in a short practice session. To facilitate the early phases of learning, there was no trial structure or time pressure, present in experiments (Figure 4.1). Data from this session was not recorded.

Through verbal instructions, participants learned how to initiate an continuous action with a linear upward action followed by circular movement (clockwise or anti-clockwise). Various visual information displayed on the screen provided the feedback about the movement. A white disc (0.1 ° of visual angle) was indicating the position of the joystick handle. Two white circles, one at a 40% (4° diameter) and the other at a 100% (10° diameter) of the maximum movement radius, delineated the area where participants were instructed to keep the joystick positioned while performing a circular movement. Additionally, the line following the angle of the movement was displayed to provide better feedback about the speed of movement. To help with maintaining the movement within designated area, movement trajectory was displayed in real time.

4.2.5 Behavioural measures

Behavioural performance was quantified with four dependent measures (Table 4.2).

Reaction time

The results from Chapter 3 suggest that reaction time obtained using joystick is comparable to a button press, a widely used response method in perceptual decision making research. However, the direction of response had an impact on the velocity-derived measures of joystick movement. Taking those insights into account, participants were instructed to initiate continuous actions with a linear upward movement, irrespective of the direction of subsequent movement (i.e., clockwise or anti-clockwise). This design allowed to measure reaction time consistently across conditions.

Table 4.2: Summary of dependent measures.

Engage RT - Latency in a task engagement during the first phase of the trial. Time measured between the stimulus onset and leaving the area within 20% of the joystick range radius. Present in every trial.
Change RT - Latency in a change of direction. Time measured between the onset of the stimulus in the second phase of the trial and the moment when the direction of the movement changes. Only present in trials where the direction of the cue changed.
Accuracy - In the current series of experiments, term is used to describe the proportion of time spent performing correct movement with response to the visual cue, to a total duration of the phase of the trial.
Speed of movement - A measure of speed of circular movement. Rate of change in the angle of the joystick position.

Current experiments used the same joystick as in the experiment in Chapter 3. Thus, the same way of obtaining the engage RT could be used. The time was measured between the onset of the stimuli and leaving the area within the 20% of the joystick range radius. Latency in the change of direction (change RT) was measured between the onset of the second phase of the trial and the point when the movement speed is reduced to zero while switching to the opposite direction (see Figure 4.1).

Accuracy score

The response in current experiments involved maintaining a continuous movement in response to a visual cue. In this particular type of a continuous response, I defined the accuracy as the ratio between the time spent performing joystick rotation towards the correct direction, to the total duration of the phase of the trial. When the participants did not perform any action or performed an incorrect action, the accuracy is 0%. When the participants performed a circular movement with the joystick in the correct direction throughout a phase (e.g., in the second phase with no change of direction), the accuracy is 100%. The delay between the beginning of the trial and engaging in the action is considered an incorrect response due to lack of the action, thus the percentage of the accuracy is going to be lower than 100% in this phase of the trial. The same rule is applied to the trials when in the second phase the direction of the visual motion changes. When the participants are maintaining the opposite movement direction before the change, this part of the trial is considered incorrect, thus the percentage of the accuracy is going to be lower than 100%.

Other eventualities like e.g. momentary changes of direction or stopping of the movement due to hesitation were reflected in the accuracy score as well. In those instances the accuracy score was further lowered according to the time spent in that state, as with previously mentioned situations.

4.2.6 Analysis

Bayesian analysis for ANOVA designs (JASP Team, 2018) was used to make inferences on RTs and accuracy between conditions [1]. The mixed model method was used, that is, both random and fixed factors were specified in the Bayesian model. Random factors are included in the null model, which serves as a baseline for the model to estimate all fixed factors. Here, as in previous studies, between-subject variability was included in the null model as a random factor (Barr, 2013). In Experiments 1 and 2, the stimulus-to-response mapping was included as a fixed factor to examine the early stage of the skill acquisition. In Experiments 3 and 4, preliminary analysis showed that the fixed effect of stimulus-to-response mapping did not affect the accuracy ($BF_{10} = 0.913$) or RT ($BF_{10} = 0.991$) in the first phase of the trial. As a result, the stimulus-to-response mapping factor was included in the null model in the final statistical results, which helps to test the robustness of the experimental manipulation (Zhang, 2020).

The first phase and the second phase of the trial were analyzed separately, because the nature of movements and task designs differs between the two phases. The first phase of a trial established a context of the continuous

---

[1] In this chapter, all figures of accuracy and RT have a consistent colour scheme. The legend and the colour scheme are independent to the order of results in individual figures.

action, which was either maintained or changed in the second phase of the trial. The low perceptual difficulty of the first phase minimized the influence of action engagement on the second phase. In Experiments 3 and 4, analyses on accuracy and RT in the second phase were initially separated for trials with and without a motion direction change from the first phase. This was due to the fact that change RT was available only in trials with a change of direction. Furthermore, in the second phase, accuracy would be lower by default when there was a change of direction because participants needed to stop and reverse their continuous movements, which was confirmed in Sections 4.7.2 on the comparison between experiments.

To compare the time courses of the speed of motion (Figures 4.10, 4.11, 4.15 and 4.16), I used permutation tests with cluster-level correction for multiple comparisons (Maris and Oostenveld, 2007). A lenient cluster formation threshold ($F = 6.0$) was used to form an initial set of clusters. From the initial set of clusters, a permutation test was applied to obtain corrected p-values.

4.3 Experiment 1: Establishing the cue-movement mapping

Experiment 1 aimed to train participants to perform continuous circular movements with unambiguous direction cues (i.e., arrows) and real-time visual feedback about the ongoing movement (Figure 4.1).

4.3.1 Design

After a short practice session, participants were introduced to the trial structure with time pressure present, and a trial timing outlined on the Figure 4.1. In each trial, participants were instructed to perform continuous circular movements in response to the direction of an arrow presented at the centre of the screen. Experiment 1 contained a total of 120 trials. In the first phase, 60 trials had left arrows and the other 60 trials had right arrows. In the second phase, arrow changed to the opposite direction in half of the trials. Trials were presented in a pseudo-random order, with no more than four consecutive trials of the same condition.

The instructions emphasised the accuracy rather than response speed. Participants were asked to perform only one change of direction during a trial, and maintain their continuous movement even if the response was incorrect. After each trial, participants received a feedback (1000 ms) about the accuracy of their responses at each phase of the trial. At the end of the experiment, participants received a feedback of the percentage of correct trials (both phases of the trial correct), and the percentage of the trials in which participants stopped or performed more than one direction change.

4.3.2 Stimulus

Participants were shown a target area of movement on the screen, limited by two circles (as in the practice session, see Section 4.2.4). A white arrow (3° length) was placed within a smaller circle (4°). The visual feedback of the joystick movement was similar to the one used in the practice, except the trajectory of movement was not displayed.

4.3.3 Results

In the first phase of the trial, as expected, Engage RT ($BF_{10} = 0.060$) (Figure 4.3A) and accuracy ($BF_{10} = 0.055$) (Figure 4.4A) remained the same between trials with our without direction change in the second phase. The stimulus-response mapping also did not affect the Engage RT ($BF_{10} = 0.489$) or accuracy ($BF_{10} = 0.462$), although the evidence is inconclusive. There is no interaction between experimental conditions and stimulus-response mapping in engagement RT ($BF_{10} = 0.087$) and or ($BF_{10} = 0.069$).

In the second phase, Change RT ($BF_{10} = 0.286$) (Figure 4.3B) and accuracy ($BF_{10} = 0.250$) (Figure 4.4B) were not affected by stimulus-response mapping. Accuracy score was lower in trials with a change of movement direction ($BF_{10} = 6.607 \text{ x } 10^{84}$). There was no interaction in accuracy between stimulus-response mapping and the presence of direction change ($BF_{10} = 0.119$).

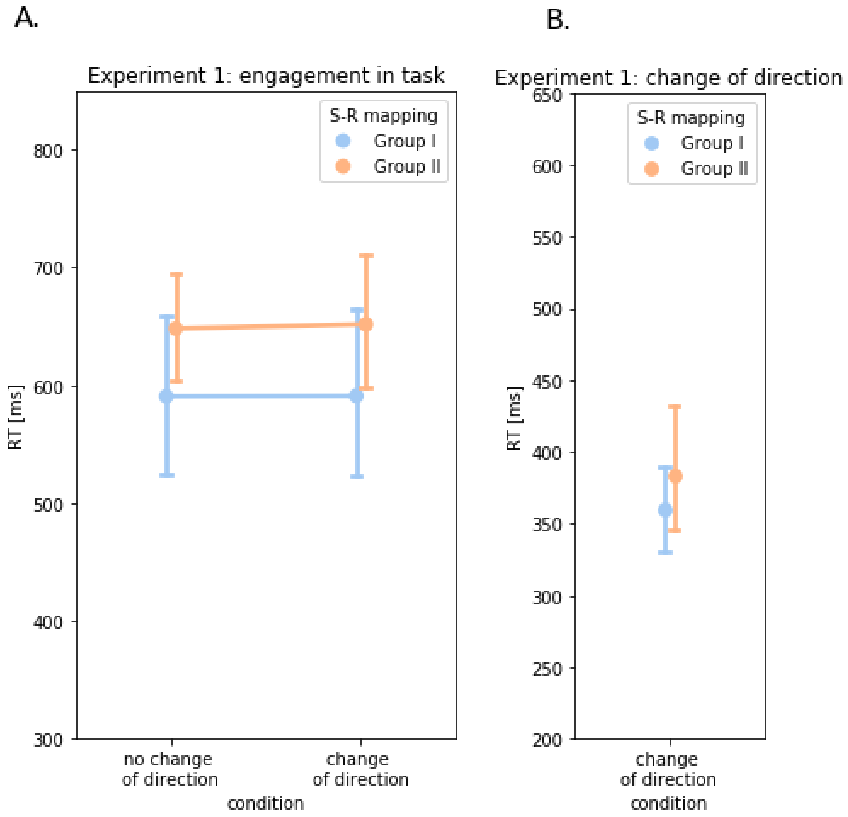

Figure 4.3: Reaction times in Experiment 1. Panel A shows the Engage RT in the first phase. Panel B shows the Change RT in the second phase when there was a change of movement direction. Data points represent the mean score and bars represent 95% bootstrapped confidence intervals. Line colour denotes the stimulus-response mapping group (Group I: right - clockwise, left - anti-clockwise; Group II: right - anti-clockwise, left - clockwise).

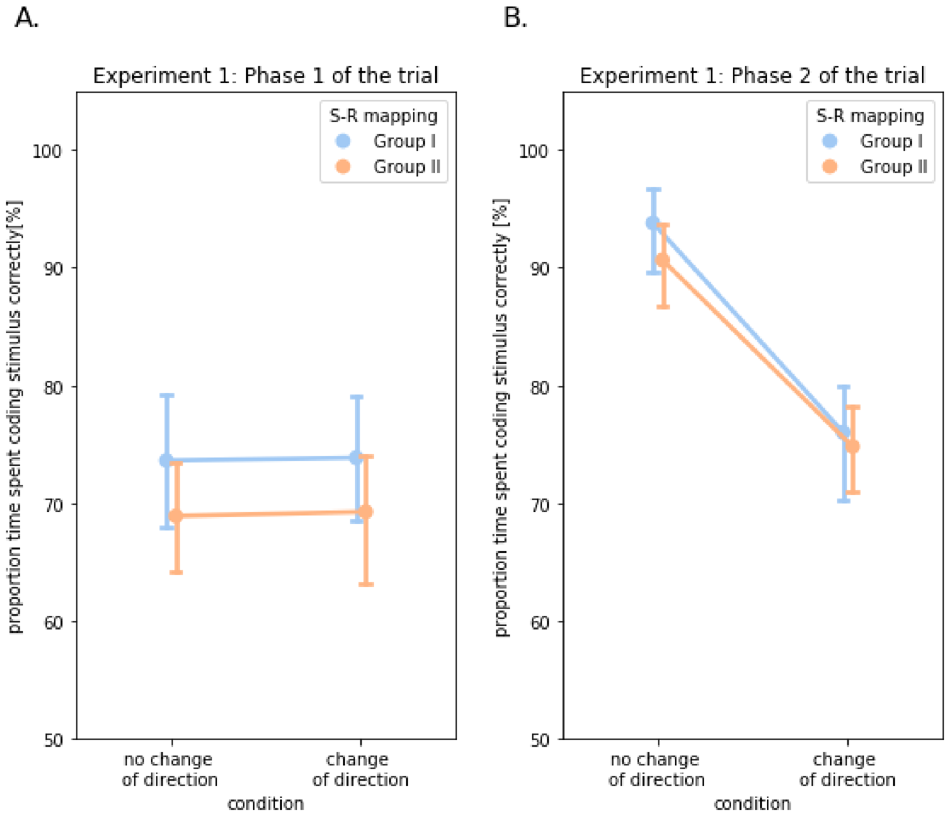

Figure 4.4: Experiment 1 accuracy scores (i.e., proportion of time spent in correct continuous movement to the overall duration of the phase) in the first (**A**) and second (**B**) phase. Data points represent the mean score and bars represent 95% bootstrapped confidence intervals. Line colour denotes the stimulus-response mapping group (Group I: right - clockwise, left - anti-clockwise; Group II: right - anti-clockwise, left - clockwise).

4.3.4 Conclusion

The results showed that the stimulus-response mapping did not affect any of the behavioural measures (accuracy score, Engage RT and Change RT). Participants were capable of performing the task at a satisfactory level. In the first phase of the trial, accuracy was well above 50% (Figure 4.4 A), indicating that the participants spent more than a half of the phase duration performing correct movements in response to the visual cue. In the second phase, accuracy score was over 90% in trials with no change of the direction of the visual cue, suggesting that the participants were able to maintain their ongoing actions without considerable delay or stopping. In trials with a change in the direction of the visual cue, participants adjusted their actions with an expected delay (Change RT). This was reflected in a lower accuracy in the second phase. Therefore, the participants can reliably perform continuous movements and change movement directions in response to visual cues.

4.4 Experiment 2: Continuous movement in response to noisy sensory information

Experiment 2 aims to examine continuous movements initiated and changed by perceptual decisions of noisy visual stimulus.

4.4.1 Design

Experiment 2 included 120 trials. The trial structure was the same as in Experiment 1 (Figure 4.1). Instead of a static arrow used in Experiment 1 participants were presented with the RDM stimulus with left- or rightward coherent motion. The participants were instructed to decide the direction of coherent motion and perform continuous clockwise or anti-clockwise joystick movements according to the stimulus-response mapping learnt in Experiment 1. There was no visual feedback of the joystick movement trajectory.

4.4.2 Stimulus

RDM stimulus were generated as in Chapter 3. Coherent motion was implemented by using three uncorrelated, interleaved sets of dot positions across frames at 100 Hz. White dots (0.14° diameter each) were presented on black background (100% contrast) within a centrally located aperture (15° diameter) with a 28.30 $dot/deg^2/s$ density. In each frame, 50% of signal dots were re-plotted at the appropriate displacement (velocity of $60.23°/s$) and direction (left - 0° or right - 180°) relative to the position three frames earlier, resulted in a motion coherence of 50%. Remaining dots were presented at random location within the aperture. Signal dots had lifetime of 5 frames, after which they were re-plotted in the random positions.

4.4.3 Results

In the first phase of the trial, there was anecdotal evidence for the stimulus-response mapping affecting the engagement RT ($BF_{10} = 2.843$) (Figure 4.5A) and moderate evidence for the accuracy ($BF_{10} = 3.578$) (Figure 4.6A). Participants responding to dots moving to the right with a clockwise motion were faster and with higher accuracy scores. Engagement RT ($BF_{10} = 0.052$) and accuracy ($BF_{10} = 0.051$) were not affected by the presence of direction change in the second phase. None of the main effects interact (Engage RT: ($BF_{10} = 0.129$), accuracy: ($BF_{10} = 0.074$))

In the second phase of the trial, stimulus-response mapping did not affect the Change RT ($BF_{10} = 0.319$, moderate evidence) (Figure 4.5B) or accuracy ($BF_{10} = 0.632$, inconclusive evidence) (Figure 4.6B). Change of motion direction reduced the accuracy ($BF_{10} = 9.884 \text{ x } 10^{136}$, strong evidence). There was no interaction in accuracy score between the presence of direction change and stimulus-response mapping ($BF_{10} = 0.273$).

I found moderate evidence for stimulus to response mapping affecting response latency and accuracy in the first phase of the trial, and inconclusive evidence against that effect in the second phase of the trial. In the second phase of the trial accuracy was lowered in the condition with the change of direction

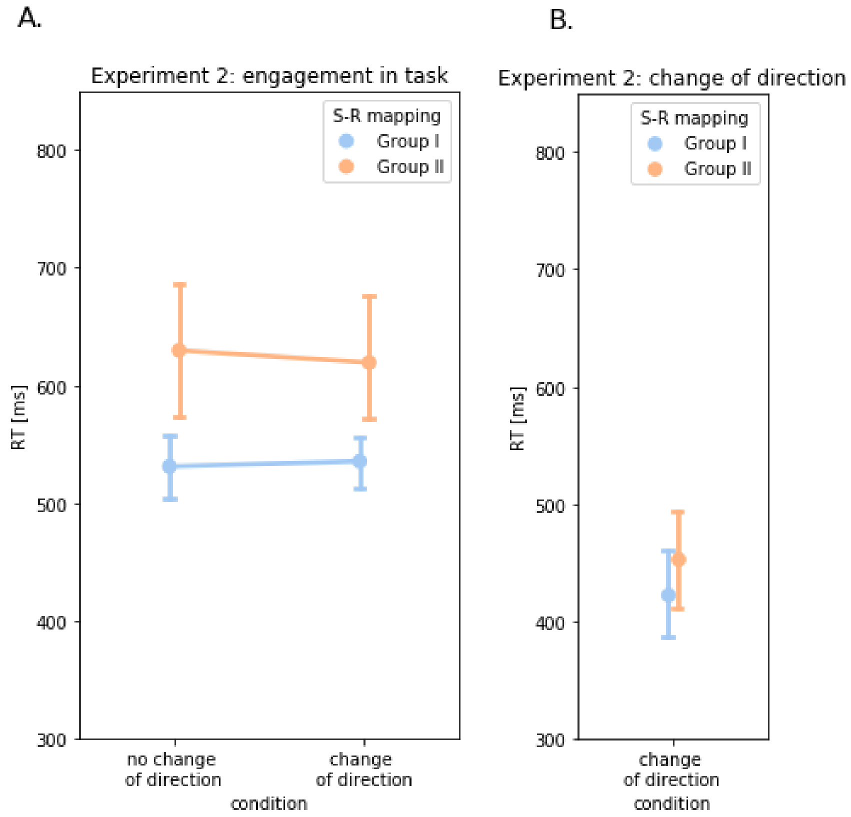

Figure 4.5: Reaction times in Experiment 2. Panel A shows the Engage RT in the first phase. Panel B shows the Change RT in the second phase in trials with a change of movement direction. Data points represent the mean score and bars represent 95% bootstrapped confidence intervals. Line colour denotes the stimulus-response mapping group (Group I: right - clockwise, left - anti-clockwise; Group II: right - anti-clockwise, left - clockwise)

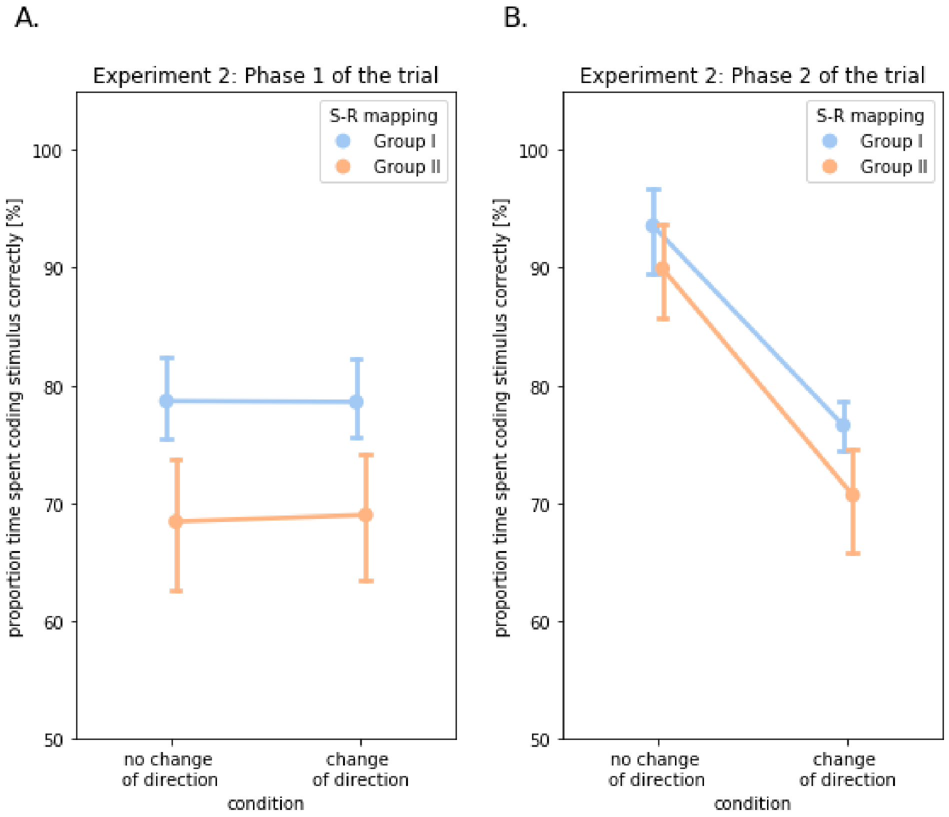

Figure 4.6: Experiment 2 accuracy scores in the first (**A**) and second (**B**) phase. Data points represent the mean score and bars represent 95% bootstrapped confidence intervals. Line colour denotes the stimulus-response mapping group (Group I: right - clockwise, left - anti-clockwise; Group II: right - anti-clockwise, left - clockwise).

4.4.4 Conclusion

The results showed that the stimulus-response mapping did not affect any of the behavioural measures (accuracy score, Engage RT and Change RT). Participants were capable of performing the task at a satisfactory level. In the first phase of the trial, accuracy was well above 50% (Figure 4.4 A), indicating that the participants spent more than a half of the phase duration performing correct movements in response to the visual cue. In the second phase, accuracy score was over 90% in trials with no change of the direction of the visual cue, suggesting that the participants were able to maintain their ongoing actions without considerable delay or stopping. In trials with a change in the direction of the visual cue, participants adjusted their actions with an expected delay (Change RT). This was reflected in a lower accuracy in the second phase. Therefore, the participants can reliably perform continuous movements and change movement directions in response to visual cues.

Experiment 2 introduced noisy sensory information (RDM stimulus) that the participants had to use to initiate and change their continuous actions. This design links perceptual decisions with continuous actions.

In the first phase of the trial, as in Experiment 1, the accuracy scores were above 50%. Therefore, despite the major change in visual information in comparison with Experiment 1, the participants were still able to perform the task at a satisfactory level. In the second phase of the trial, the change of coherent motion direction resulted in a lower accuracy score, while maintaining continuous movements without direction changes had high accuracy ($\sim$90%).

I found that the stimulus-response mapping affected the accuracy and the latency RT in the first phase of the trial in Experiment 2. Responding left motion with clockwise movement (and right motion with anti-clockwise movement) were slower and less accurate than the opposite S-R mapping. When there was a lack of visual feedback of the movement (cf. Experiment 1), at the early stages of the training this resulted in the difference in behavioural performance.

It is possible that humans have certain tendencies to perform rotation movements in response to a directional target (i.e., right direction - clockwise movement). These tendencies may be associated with factors like reading or writing. It has been observed that those daily activities have an impact on various aspects of cognition, including executive functions (Altemeier et al., 2008), visual attention (Siéroff et al., 2012), spatial perception (Román et al., 2013), and manual motor skills (Taguchi and Noma, 2005). Moreover, the influence of reading/writing patterns on cognition has been demonstrated in cross-cultural studies. Languages of mainly European origins, e.g. German, French or Polish have a left-to-right pattern of reading and writing. Languages with a right-to-left pattern are predominantly of Arabic origins like Arabic, Hebrew, Persian, and Urdu. While in east Asian languages such as Chinese, Japanese, and Korean, both left-to-right and right-to-left patterns have been used. Several studies have suggested that the directional patterns of writing and reading contribute to distinct patterns of motor actions (e.g. Taguchi and Noma, 2005; Taguchi, 2010; Kebbe and Vinter, 2013). Analysis of drawing patterns (e.g., the direction of the face, orientation of the vehicle, or the handle of the mug) showed that French participants (left-to-right pattern of reading or writing) exhibit a leftward bias in their direction of drawings. Conversely, Tunisian participants (right-to-left pattern of reading or writing) exhibit a rightward bias.

Probably directly relevant to the circular movements used in the experiments in Chapters 4, 5, and 6, it has been shown that Japanese participants are more likely to draw a circle in an anti-clockwise way, while German participants are more likely to use clockwise movements to draw a circle (Taguchi, 2010). Such cultural-dependent biases may underlie the behavioural difference between S-R mappings observed in the current study.

4.5 Experiment 3: Continuous movement in response to sensory information with different noise levels

Experiment 3 examined the effect of motion coherence on the performance of continuous movements.

4.5.1 Design and stimuli

Experiment 3 contained 5 runs and each run included 120 trials. Participants had a self-paced break between each two runs. The first phase of the trial had the same structure and RDM stimulus as in Experiment 2. In the second phase, there were four different types of stimulus:

1. motion direction and motion coherence remained unchanged,
2. motion direction remained unchanged and motion coherence was reduced from 50% to 20%,
3. motion change to the opposite direction and motion coherence remained unchanged,
4. motion change to the opposite direction and motion coherence reduced to 20%.

There were 30 trials of each of the four conditions in each run. The order of the conditions was randomised across runs. Participants received the same instructions and feedback about their performance as in previous experiments.

4.5.2 Results

RT and accuracy

In the first phase of the trial, Engage RT was different across runs (Figure 4.7A, $BF_{10} = 2.422 \text{ x } 10^{93}$, strong evidence). Post-hoc tests showed that RT decreased after each run (Table 4.9A). Engage RT was not affected by experimental conditions (change/no-change of direction/coherence, $BF_{10} = 1.699 \text{ x } 10^{-4}$, strong evidence), and there was no interaction between experimental conditions and runs ($BF_{10} = 2.111 \text{ x } 10^{-8}$, strong evidence). Accuracy differed across the runs (Figure 4.8A, $BF_{10} = 5.628 \text{ x } 10^{67}$, strong evidence). Post-hoc tests showed that the accuracy increased after the first run, and remained stable in later runs (Table 4.9B). Accuracy was not affected by experimental

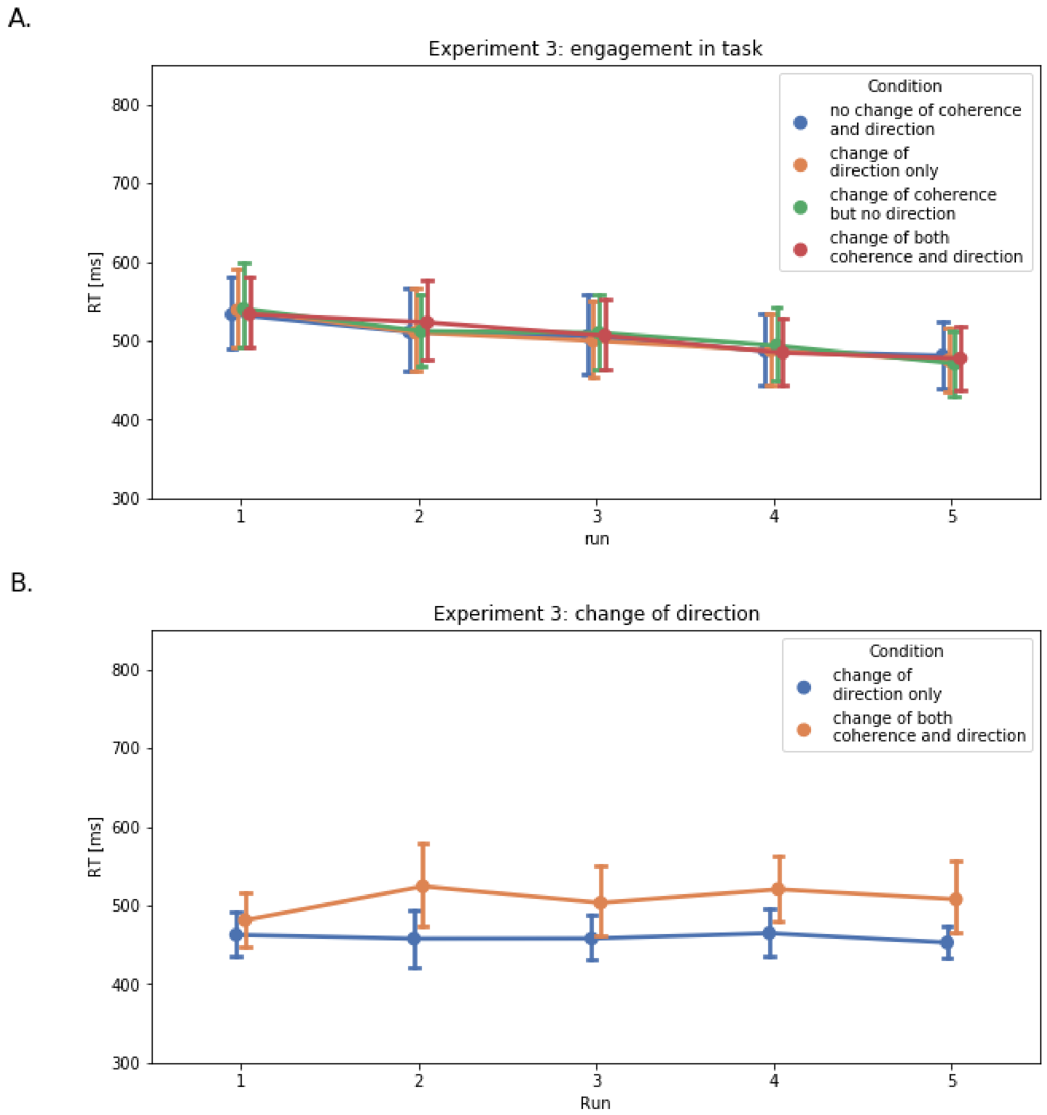

Figure 4.7: Reaction times in Experiment 3. (A) Engage RT in each run from the first phase of the trial. (B) Change RT in each run from the second phase of the trial. Data points represent the mean score and bars represent 95% bootstrapped confidence intervals.

conditions (BF_{10} = 3.444 x 10^{-4}, strong evidence), and there was no interaction between experimental conditions and runs (BF_{10} = 3.739 x 10^{-9}, strong evidence)

In the second phase, Change RT was measured in trials with a change of motion direction. Change RT was longer when the motion coherence was reduced (Figure 4.7B, BF_{10} = 3.548 x 10^{19}, strong effect), but it did not vary across runs (BF_{10} = 0.022, strong evidence). There was no interaction in Change RT between conditions and runs (BF_{10} = 0.003, strong evidence).

In conditions with a change of motion direction, accuracy scores decreased when the motion coherence was reduced (Figure 4.8B, BF_{10} = 3.479 x 10^{154}, strong evidence) and had no significant change across runs (BF_{10} = 1.785 x 10^{-4}, strong evidence). There was no interaction in Accuracy score between conditions and runs (BF_{10} = 0.002, strong evidence)

In conditions with no change of direction, there were strong evidence for the main effects of conditions (changed/unchanged coherence, BF_{10} = 7.463 x 10^{28}) and runs (BF_{10} = 1.562 x 10^{60}, strong evidence, see Table 4.9C for post-hoc tests). The interaction between experimental conditions and runs was inconclusive (BF_{10} = 1.181).

When comparing between the first and second phase, Change RT was longer than Engage RT (BF_{10} = 34.980, strong evidence), and accuracy was lower in the second phase than that in the first phase of the trial (BF_{10} = 559.163, strong evidence).

In sum, there was strong evidence for performance improvements across runs. Lowering motion coherence and Changing motion direction resulted in increased RT and decreased accuracy scores.

Movement speed

Using the continuous recording of the joystick, I could obtain a continuous measure of movement speed throughout the trial, time-locked to stimulus onset (Figure 4.10).

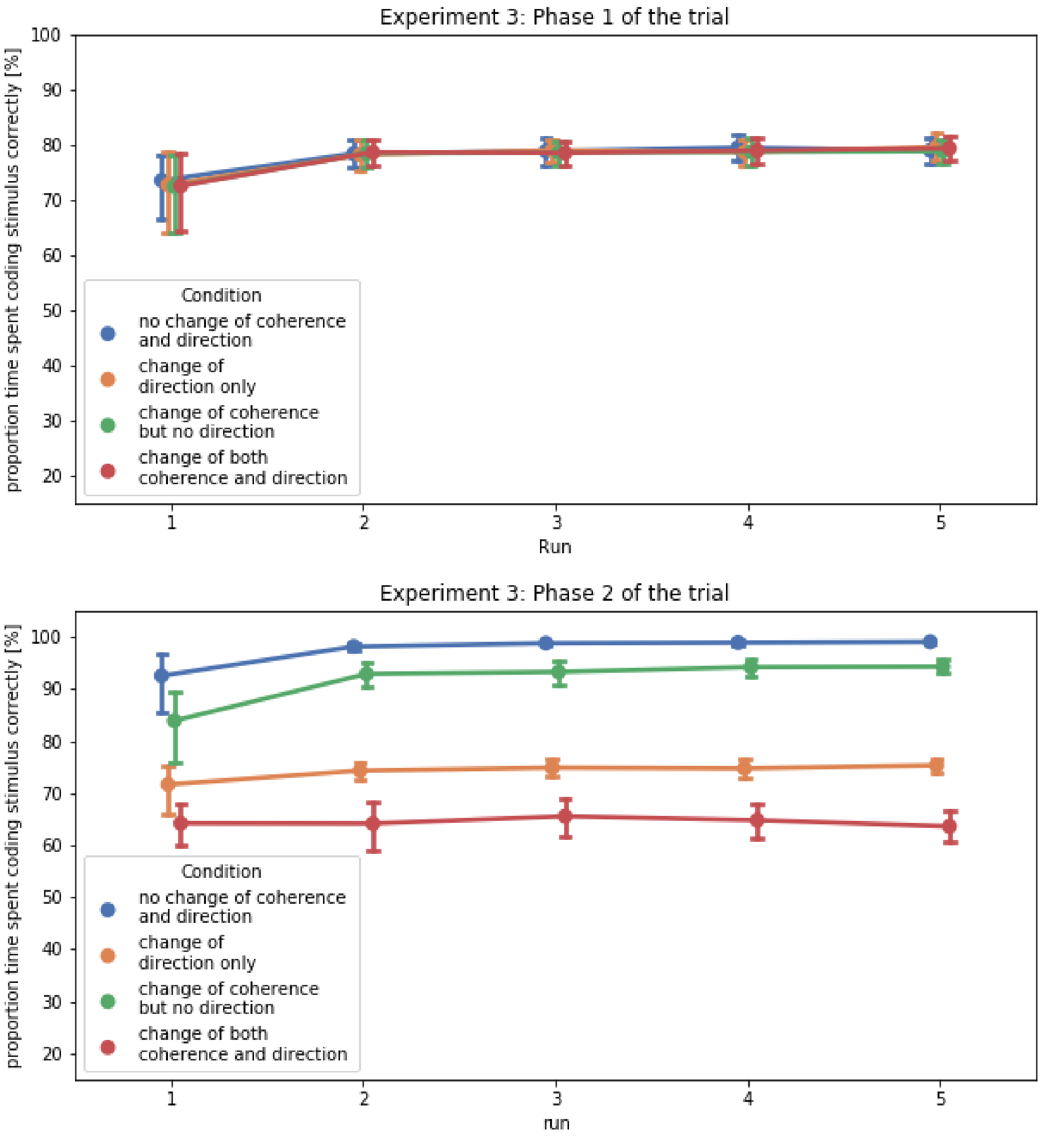

Figure 4.8: Accuracy scores in Experiment 3. (A) Accuracy scores in each run from the first phase of the trial. (B) Accuracy scores in each run from the second phase of the trial. Data points represent the mean score and bars represent 95% bootstrapped confidence intervals.

A. Response latency - phase 1

Run	1	2	3	4	5
1		4.796 x 10^{16}	1.670 x 10^{25}	9.783 x 10^{46}	2.115 x 10^{67}
2			0.049	1.311 x 10^{4}	5.168 x 10^{11}
3				5.411	1.683 x 10^{6}
4					0.267
5					

B. Accuracy - phase 1

Run	1	2	3	4	5
1		6.480 x 10^{18}	5.518 x 10^{23}	3.909 x 10^{26}	2.485 x 10^{31}
2			0.018	0.044	0.266
3				0.013	0.035
4					0.014
5					

C. Accuracy - phase 2 (no change of direction)

Run	1	2	3	4	5
1		1.067 x 10^{6}	2.029 x 10^{8}	1.181 x 10^{11}	4.553 x 10^{11}
2			0.022	0.086	0.130
3				0.023	0.029
4					0.015
5					

Table 4.9: Experiment 3. Posterior odds of post-hoc comparisons between runs. Cells highlighted in green indicate evidence for the difference in the comparison. Cells highlighted in red indicate evidence against the difference. Cells in white indicate inconclusive evidence.

In the first phase of the trial, there was no difference in movement speed between conditions. This was expected and confirmed the findings from the Engage RT and accuracy scores that experimental conditions did not introduce any bias in continuous movements. In the second phase, the participants showed signs of slowing down in the lower coherence conditions, regardless whether the motion direction changed (Figure 4.10, bottom panel) or not (Figure 4.10, top panel).

For trials with motion direction changes present, I aligned the movement speed to the Change RT (Figure 4.11, top panels). This showed the fact the participants slowed down before changing the direction (Change RT) and subsequently recovered the speed in the opposite direction. During a short interval

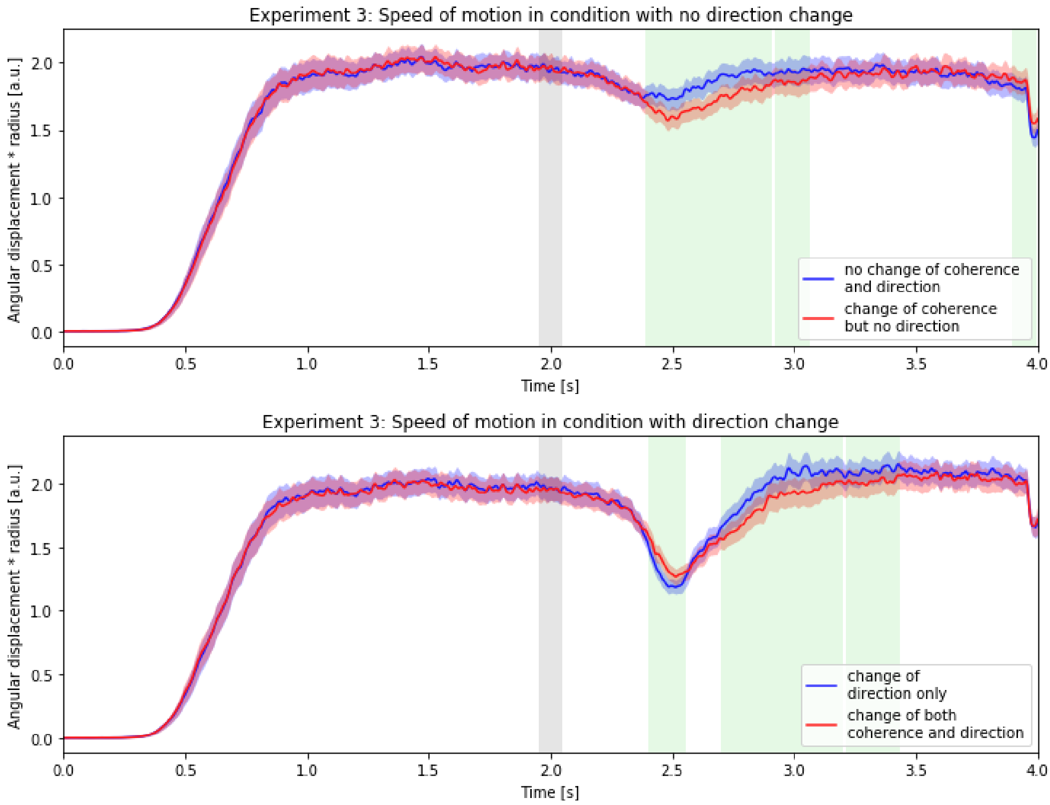

Figure 4.10: Movement speed in Experiment 3. Solid lines denote the mean movement speed, and shaded areas denote the standard error of the mean across participants. The differences between conditions are highlighted by green shading (cluster permutation test with cluster-level correction at $p < 0.05$). The grey shading around $t = 2s$ indicates the 100 ms gap between the two phases of the trial.

(0.25 s) after the Change RT, the movement speed was significantly slower in low coherent trials than that in high coherent trials.

Participants spent more time to accelerate after the direction change than to slow down before the change (Figure 4.11, middle panels). It might be due to the different processes guiding the maintenance of the action and adjusting the action after the decision is reached (e.g. forming a confidence judgement (Fleming et al., 2015)). Furthermore, the participants spent more time to reach a stable movement speed when engaging in an action, compared to adjusting an ongoing action to the opposite direction (Figure 4.11, bottom panels). All the evidence confirmed that participants engaged in the action according to the experimental instructions.

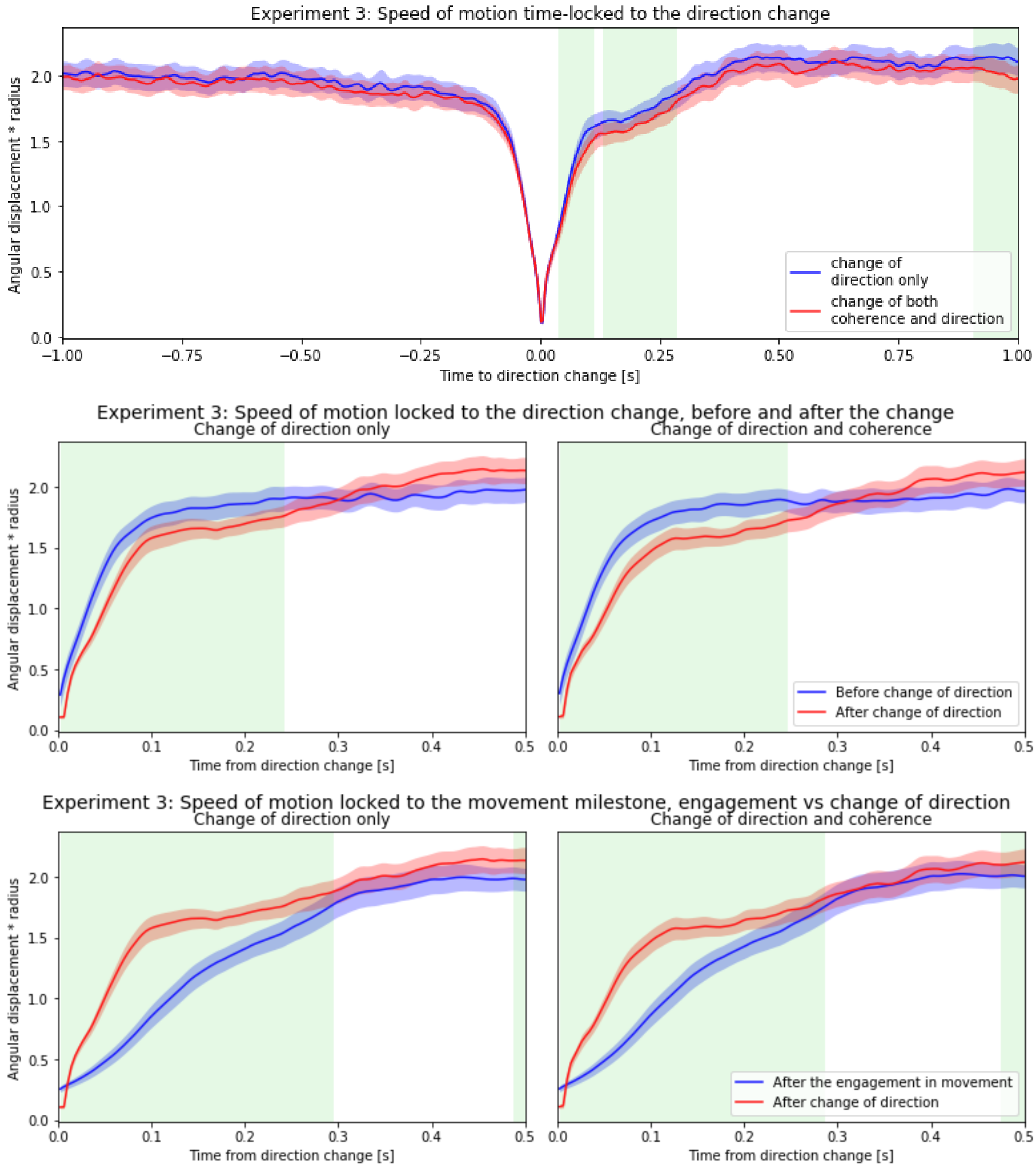

Figure 4.11: Experiment 3: movement speed time-locked to various movement milestones. Top panel: the time course of movement speed time-locked to Change RT. Middle panel: comparisons of movement speed before and after Change RT. Bottom panel: comparisons of movement speed from Engage RT (in the first phase) and Chagne RT (in the second phase). The differences between conditions are highlighted by green shading (cluster permutation test with cluster-level correction at $p < 0.05$).

4.5.3 Conclusion

The introduction of the change in RDM coherence was the main difference between Experiment 2 and Experiment 3 (Figure 4.1). Participants also completed five times more trials (5 runs x 120 trials) and exhibited training effects across runs. As with previous experiments, the first phase of the trial served as a baseline for the adjustment of action in the second phase.

In the second phase of the trial, when the direction of the RDM stimulus did not change, the accuracy was close to 90%. However, when the quality of the visual cue was lowered from 50% to 20%, participants were more likely to stop or slow down. Such behaviour decreased the time spent on performing their ongoing actions in response to the visual information in the first phase and resulted in lower accuracy scores and longer Change RT. The movement speed was also affected by the changes in the visual cue quality and the phase of the trial.

4.6 Experiment 4: Continuous responses to perceptual decisions without feedback

Experiment 4 aimed to evaluate the performance of continuous movements in response to perceptual decisions without trial-by-trial feedback.

4.6.1 Design and stimuli

Experiment 4 contained 5 runs and each run included 120 trials. Trial structure, instructions, experimental conditions and stimulus remained the same as in Experiment 3. However, participants only received a feedback about the performance after each run, and there was no feedback after each trial.

4.6.2 Results

RT and accuracy

In the first phase of the trial, Engage RT differed across runs (Figure 4.12A, BF_{10} = 1.605 x 10^{8}, strong evidence). Post-hoc test showed a decrease in Engage RT in first two runs, and the performance remained stable after (Table 4.14A). Engage RT did not differ between conditions (BF_{10} = 4.105 x 10^{-4}, strong evidence), and there was no interaction between experimental conditions and runs (BF_{10} = 4.105 x 10^{-4}, strong evidence). There was a strong evidence of a main effect of runs in accuracy scores (Figure 4.13A, BF_{10} = 2.010 x 10^{24}, strong evidence). Post-hoc tests showed that the accuracy increased after the first run and remained the same in subsequent runs (Table 4.14B). Accuracy did not differ between experimental conditions (BF_{10} = 1.873 x 10^{-4}, strong evidence), and there was no interaction between conditions and runs in accuracy (BF_{10} = 1.896 x 10^{-7}, strong evidence).

In the second phase, Change RT was longer in trials with lower motion coherence (Figure 4.12B, BF_{10} = 4.415 x 10^{20} ,strong evidence), but it did not differ across the runs (BF_{10} = 2.825 x 10^{-4}, strong evidence). There was no interaction in Change RT between conditions and runs (BF_{10} = 5.413 x 10^{-4}, strong effect).

Accuracy scores were lower in trials with lower motion coherence (Figure 4.13B, Change direction conditions: BF_{10} = 2.601 x 10^{75}; No-change direction conditions: BF_{10} = 3.268 x 10^{21}). There was a strong evidence against a main effect of runs (Change direction conditions: BF_{10} = 2.337 x 10^{-4}; No-change direction conditions: BF_{10} = 0.023) and against an interaction between runs and experimental conditions (Change direction conditions: BF_{10} = 0.004; No-change direction conditions: BF_{10} = 6.007 x 10^{-4}).

When comparing between the first and second phase, there was a moderate evidence supporting no difference between Engage RT and Change RT (BF_{10} = 0.273). Accuracy was lower in the second phase than that in the first phase of the trial (BF_{10} = 37600.699).

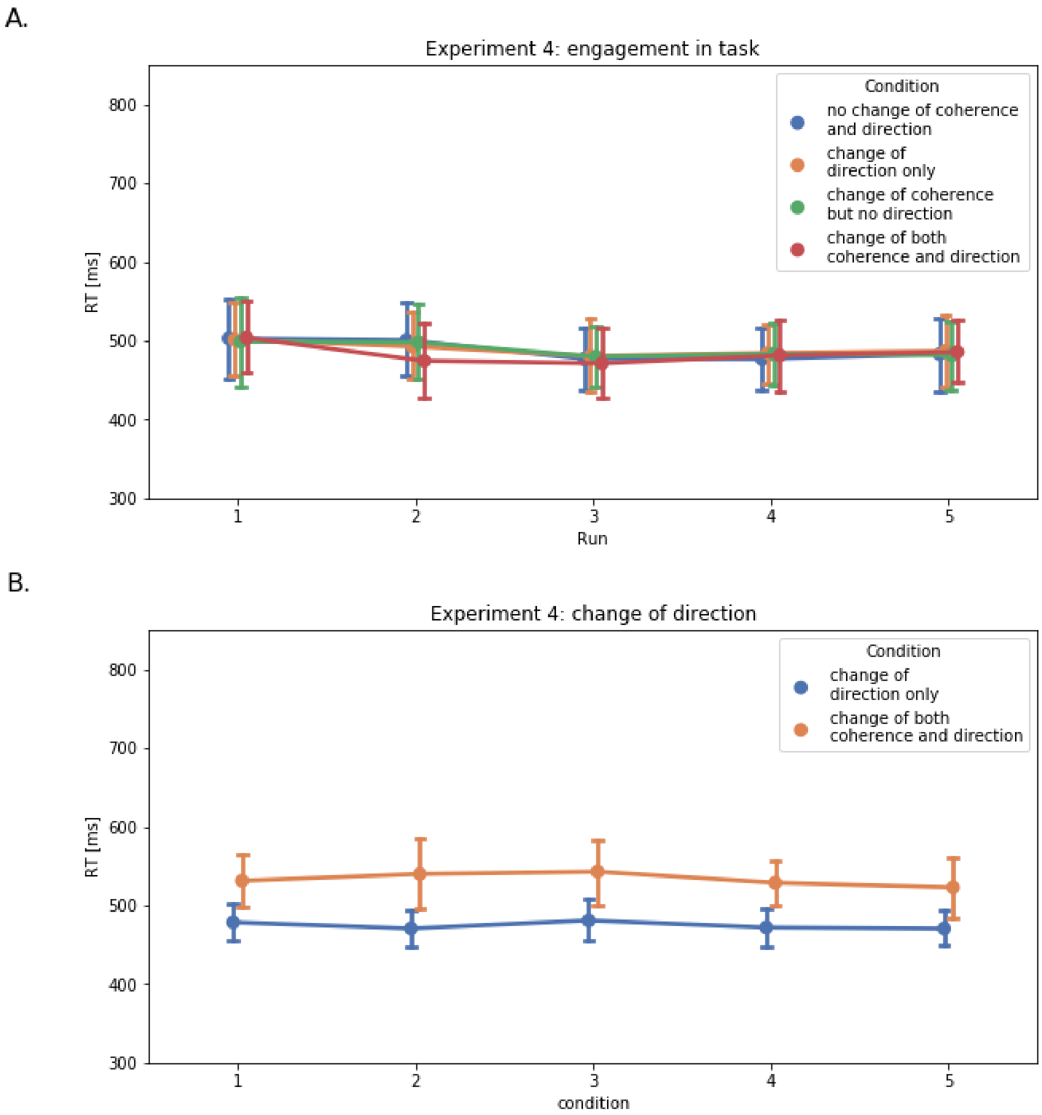

Figure 4.12: Reaction times in Experiment 4. (A) Engage RT in each run from the first phase of the trial. (B) Change RT in each run from the second phase of the trial. Data points represent the mean score and bars represent 95% bootstrapped confidence intervals.

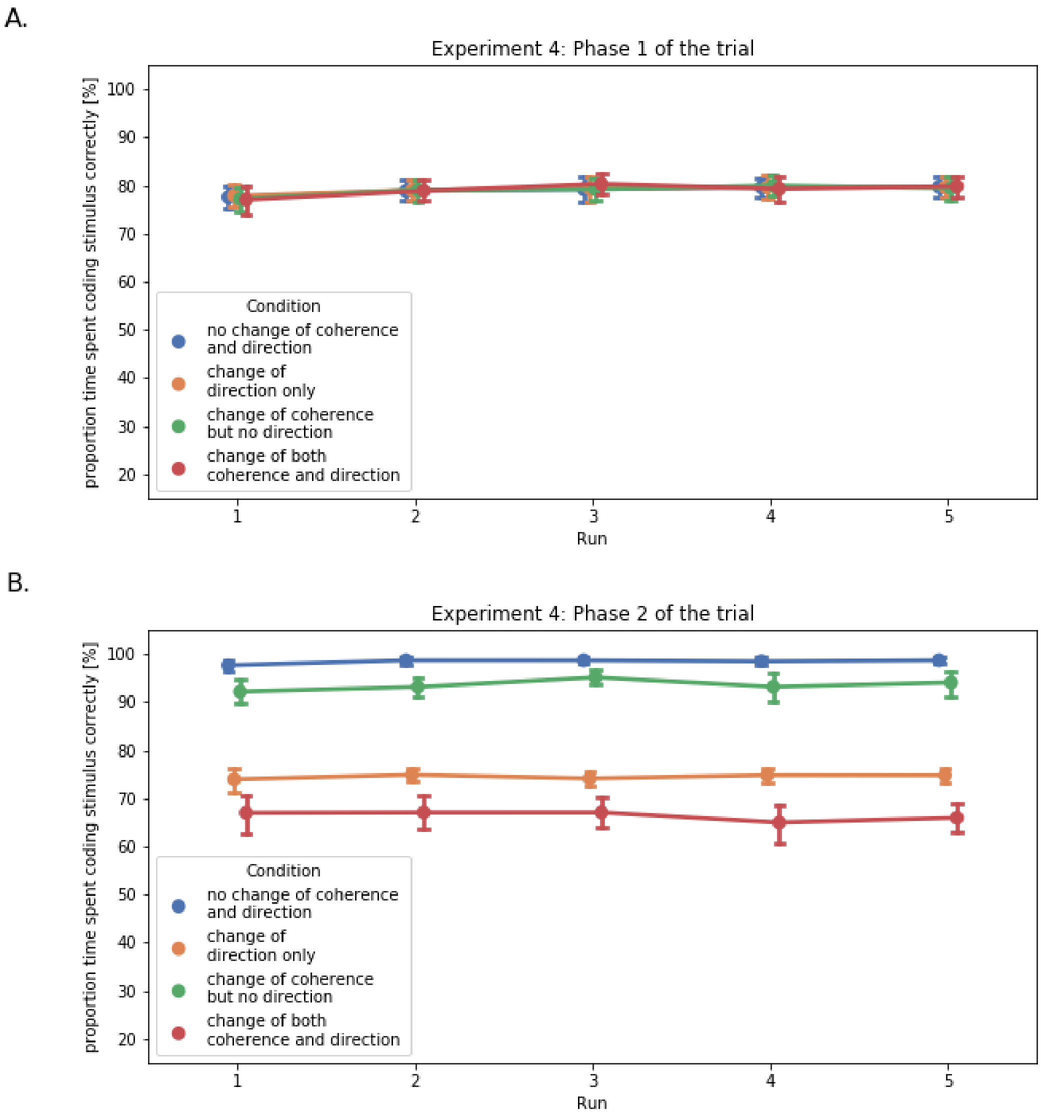

Figure 4.13: Accuracy scores in Experiment 4. (A) Accuracy scores in each run from the first phase of the trial. (B) Accuracy scores in each run from the second phase of the trial. Data points represent the mean score and bars represent 95% bootstrapped confidence intervals.

A. Response latency - phase 1

Run	1	2	3	4	5
1		1.537 x 10^{4}	1.146 x 10^{15}	6.193 x 10^{11}	5.618 x 10^{8}
2			14.193	.897	0.091
3				0.017	0.051
4					0.020
5					

B. Accuracy - phase 1

Run	1	2	3	4	5
1		1.266 x 10^{6}	6.122 x 10^{11}	6.276 x 10^{12}	1.766 x 10^{13}
2			0.161	0.302	0.386
3				0.014	0.014
4					0.013
5					

Table 4.14: Experiment 4. Posterior odds of post-hoc comparisons between runs. Cells highlighted in green indicate evidence for the difference in the comparison. Cells highlighted in red indicate evidence against the difference. Cells in white indicate inconclusive evidence.

Movement speed

I performed the same analysis on movement speed as in Experiment 3.

For the movement speed measure time-locked to stimulus onset 4.15, I observed similar effects as in experiment 3. In the first phase of the trial, participants were initiating movements uniformly across conditions. In the second phase of the trial, the movement speed slowed down in a short interval ∼0.5 s after low coherence stimulus was presented.

However, the movement speed time-locked to the Change RT showed no difference between high and low coherence trials (Figure 4.16, top panels), in contrast to the results Experiment 3. It is likely caused by the familiarity with the task, which as behavioural performance show, seemed to reach the saturation point. Other aspects of movement speed across different stages of the trial showed the same pattern as in Experiment 3. Participants took more time to regain movement speed after the direction change than to slow down before it (Figure 4.16, middle panel). Compared to the adjustment of ongoing actions, the participants took more time to reach a stable speed when initiating an

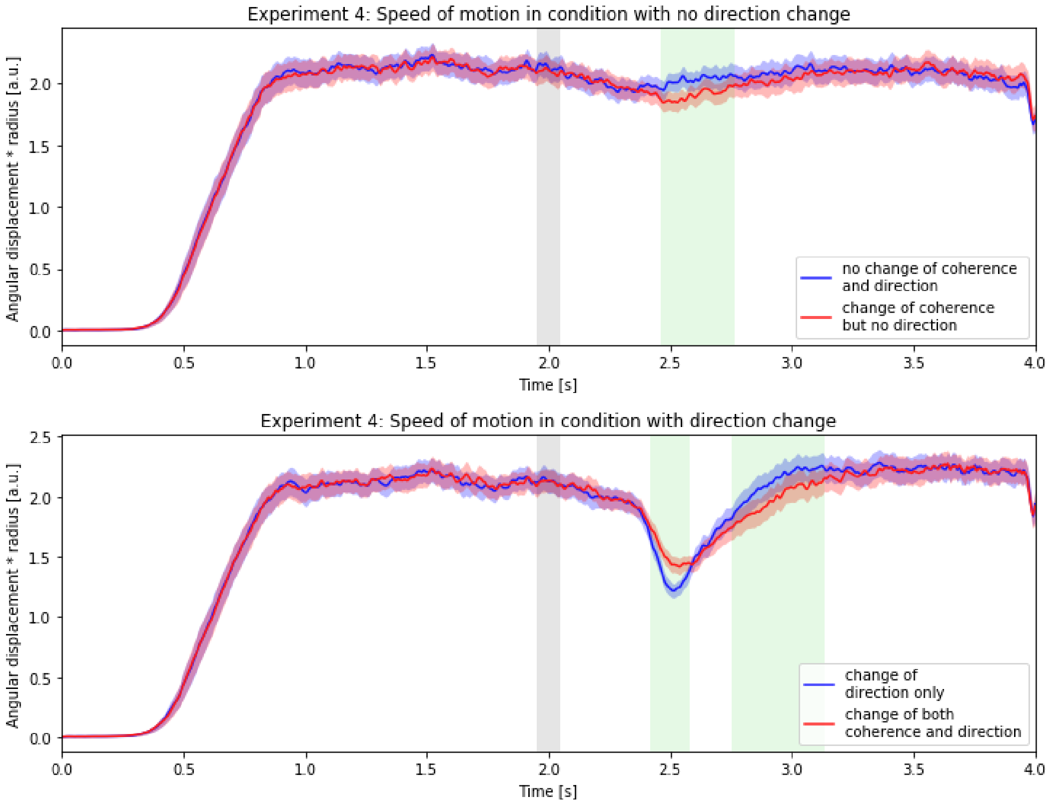

Figure 4.15: Movement speed in Experiment 4. Solid lines denote the mean movement speed, and shaded areas denote the standard error of the mean across participants. The differences between conditions are highlighted by green shading (cluster permutation test with cluster-level correction at $p < 0.05$). The grey shading around $t = 2s$ indicates the 100 ms gap between the two phases of the trial.

action (Figure 4.16, bottom panel).

4.6.3 Conclusion

The only difference between Experiment 4 and Experiment 3 was a lack of trial-by-trial feedback. Most of the behavioural results on accuracy, RT and movement speed reported in Experiment 3 were found in this experiment as well. Lowering the motion coherence and changing a motion direction resulted in increased RT and decreased accuracy scores. This occurred even after extensive training, suggesting the robustness of the behavioural effects I was looking for. The main difference between the two experiments was that, in Experiment

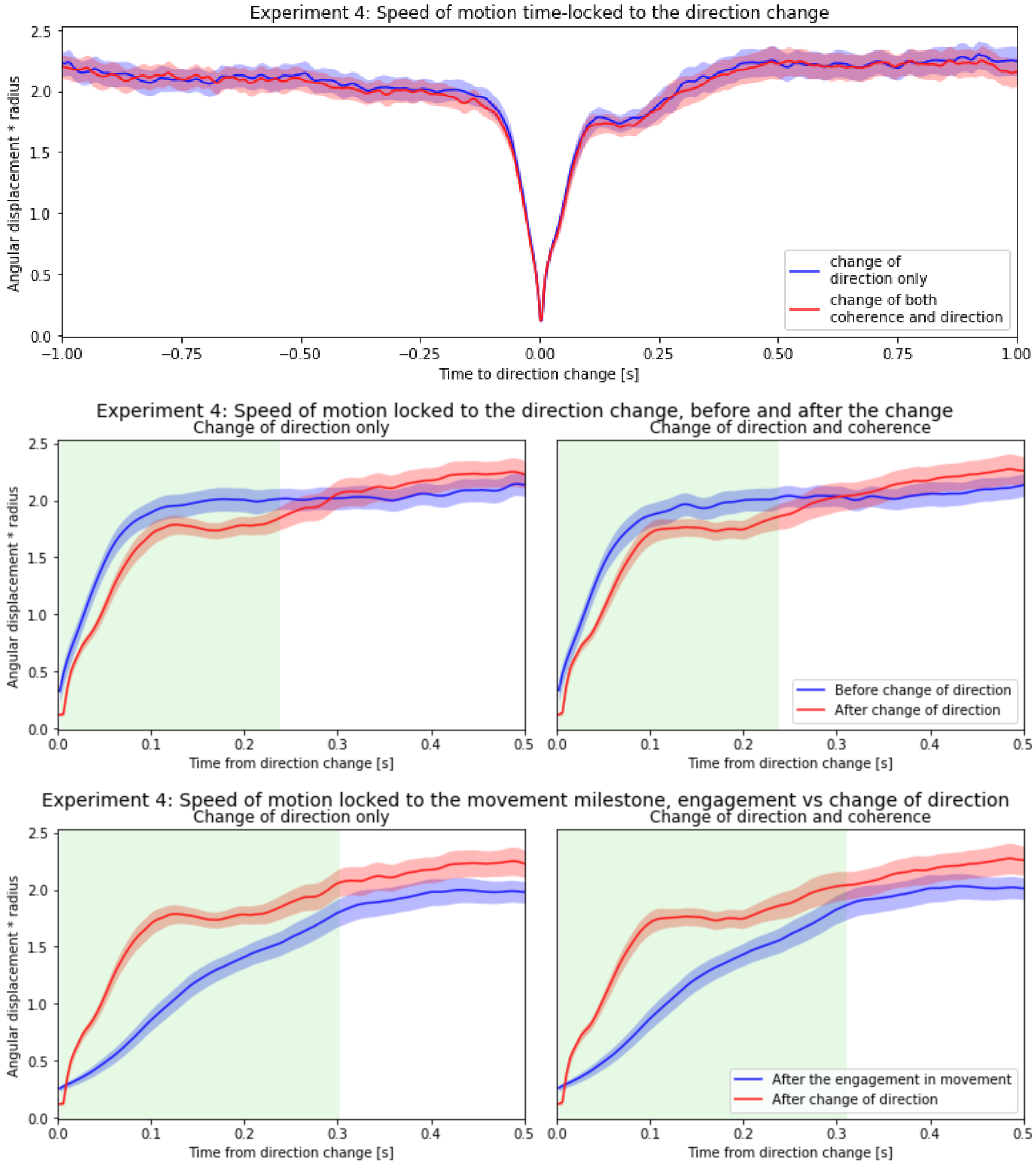

Figure 4.16: Experiment 4: movement speed time-locked to various movement milestones. Top panel: the time course of movement speed time-locked to Change RT. Middle panel: comparisons of movement speed before and after Change RT. Bottom panel: comparisons of movement speed from Engage RT (in the first phase) and Chagne RT (in the second phase). The differences between conditions are highlighted by green shading (cluster permutation test with cluster-level correction at $p < 0.05$).

4, I found no training effects across the runs on accuracy in the second phase.

4.7 Behavioural measures across experiments

This section compared the behavioural measures between Experiments 1-4 to evaluate the effects of training.

4.7.1 Experiment 1 vs. Experiment 2

The Engage RT was reduced from Experiment 1 to Experiment 2 (Figure 4.17A, BF_{10} = 4.329 x 10^8). There were strong evidence against a main effect of experimental conditions (BF_{10} = 0.038) or an interaction between conditions and experiments (BF_{10} = 0.067). The Change RT, however, was increased from Experiment 1 to Experiment 2 (Figure 4.17B, BF_{10} = 7.910 x 10^{17}).

The accuracy score increased from Experiment 1 to Experiment 2 in the first phase (Figure 4.17C, BF_{10} = 232.067), but decreased in the second phase, although the evidence for the latter was inconclusive (Figure 4.17D, BF_{10} = 0.656). There were strong evidence against the main effect of experimental conditions (first phase: BF_{10} = 0.041; second phase: BF_{10} = 2.045 x 10^{219}) or an interaction between conditions and experiments (first phase: BF_{10} = 0.051; second phase BF_{10} = 0.138).

In sum, over the first two experiments, the participants improved Engage RT and accuracy in the first phase but the performance decreased in the second phase. The increase of Change RT and the decrease of accuracy in the second phase were likely due to the introduction of the noisy RDM stimulus. Participants experienced a change of the direction which was not as apparent as in the Experiment 1.

4.7.2 Experiment 3 vs. Experiment 4

The Engage RT decreased from Experiment 3 to Experiment 4 (Figure 4.18A, BF_{10} = 2.423 x 10^{56}). There were strong evidence against a main effect of

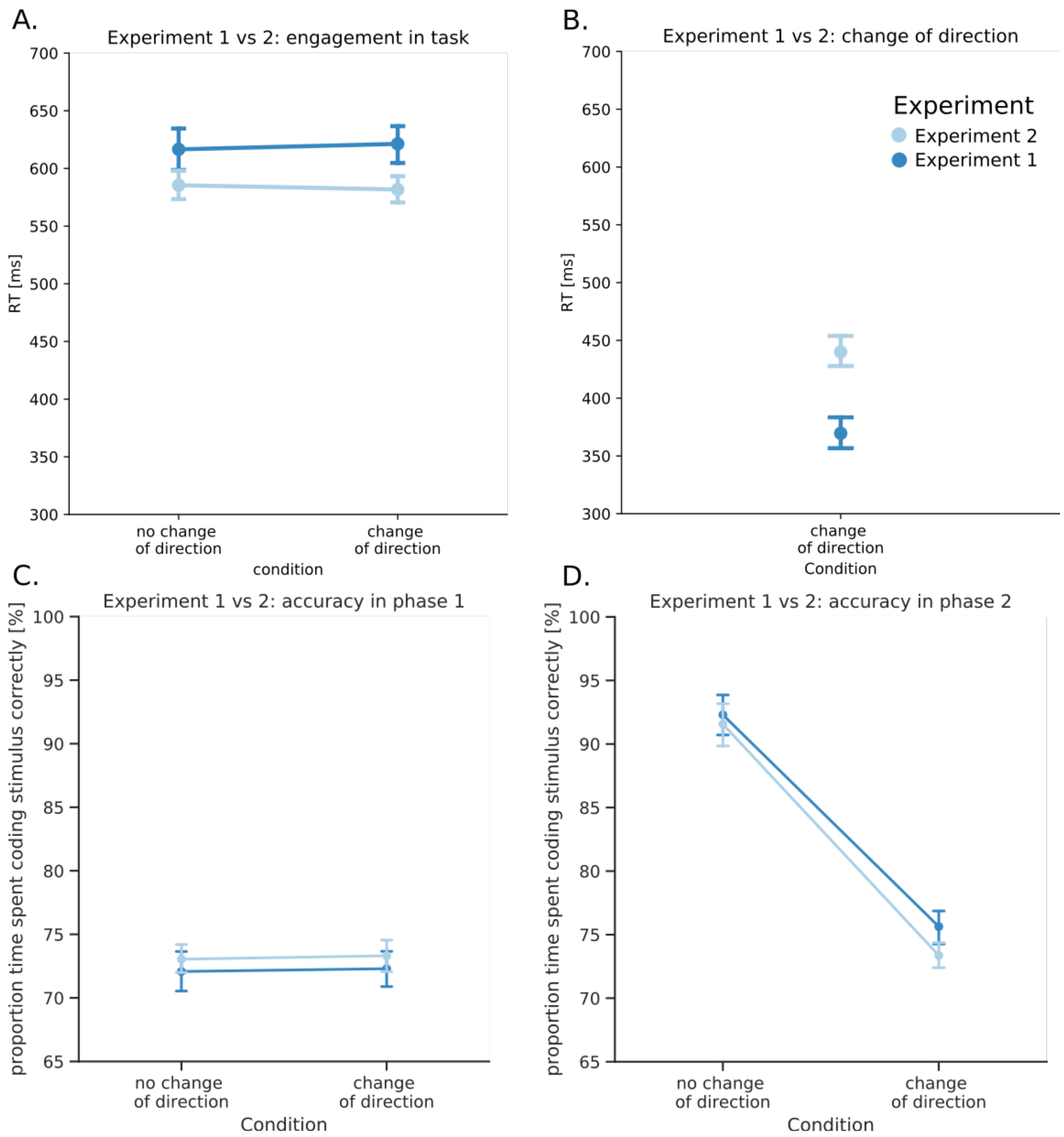

Figure 4.17: Summary of RT and accuracy in Experiments 1-2.

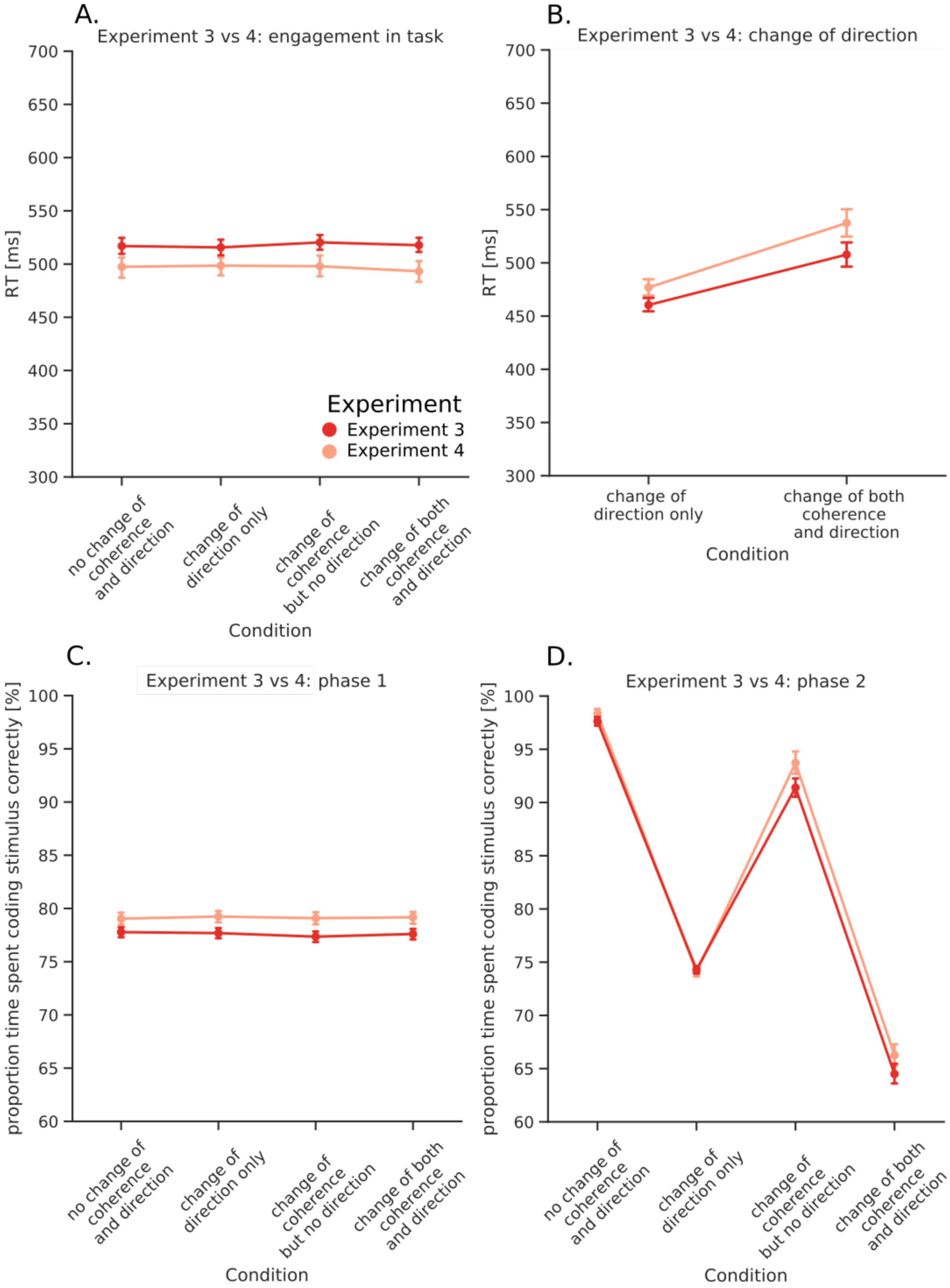

Figure 4.18: Summary of RT and accuracy in Experiments 3 and 4.

experimental conditions (i.e., change/no-change of direction and high/low coherence in the second phase) (BF_{10} = 7.905 x 10^{-5} or an interaction between conditions and experiments (BF_{10} = 2.645 x 10^{-4}. The Change RT from the second phase increased from Experiment 3 to 4 (Figure 4.17B, BF_{10} = 3.580). There was no effect in Change RT between experimental conditions (BF_{10} = 2.427 x 10^{39}) or interactions between conditions and experiments (BF_{10} = 0.111).

The accuracy score increased from Experiment 3 to Experiment 4 in the first phase (Figure 4.18C, BF_{10} = 2.193 x 10^{33}), and increased in the second phase over experiments (Figure 4.18D, BF_{10} = 8.565 x 10^{6}). In the first phase, there were strong evidence against the main effect of experimental conditions (BF_{10} = 1.187 x 10^{-4}) or an interaction between conditions and experiments (BF_{10} = 2.005 x 10^{-4}). In the second phase, I found strong evidence for the main effect of experimental condition ($BF_{10} > 9.999$ x 10^{100} and moderate evidence for the interaction of experimental conditions and experiments (BF_{10} = 3.583.

To sum up, the training without a feedback further improved the behavioural performance in the first run of Experiment 4. However in the second phase of the trial participants were slower but more accurate.

4.8 General discussion

This chapter highlighted a multifaceted interaction between perceptual decision-making, action selection and learning of sensory-motor transformation. Building on the results from Chapter 3, I was able to evaluate the novel paradigm that linked continuous movements with perceptual decisions. Over the course of four experiments, participants successfully learned to perform the task. Experimental manipulation of the stimulus signal-to-noise ratio led to results that were hypothesised. The learning effect in RT, accuracy and response speed was observed across all the experiments.

4.8.1 Initiation of continuous responses

Chapter 3 showed that movement speed and acceleration of joystick movements were affected by the movement direction. Incorporating this insight in the current set of experiments, a uniform way of engaging in the action was introduced. Participants initiated their movements in the same upward direction, regardless of the direction of the stimulus and stimulus-response mapping. This consistency during action initiation allowed to make comparisons of, e.g., Engage RT, across experiments. Previous studies using joysticks, often adopted linear trajectories as responses (e.g. Berg et al., 2016; Resulaj et al., 2009; Gallivan et al., 2016; Szul et al., 2019). Experiments in this chapter retained this feature at the action initiation stage, despite the departure with continuous movements later in a trial.

Because there was no manipulation of motion coherence in the first phase, I could use the behavioural measures in the first phase as a sanity check within and across experiments. Indeed, in most experiments, experimental conditions did not affect the accuracy score (Figures 4.4A, 4.6A, 4.8A, 4.13A), the Engage RT (Figures 4.3B, 4.5B, 4.7B, 4.12B) or movement speed (Figures 4.10, 4.15) in the first phase.

The only exception was observed in Experiment 2, in which the stimulus-response mapping affected RT and accuracy (Figure 4.6A). Such results might came from a compounded effect of the introduction of the noisy RDM stimulus which was more difficult than the arrow. Comparison between Experiments 1 and 2 (Figure 4.17A, C) supported this account. Participants were slower and less accurate when the noisy RDM stimulus was introduced in Experiment 2. On top of that, this new and challenging situation might have captured a bias towards a specific combination of the visual cue and action pattern. As argued in a Section 4.4.4 this tendency can have a cultural origin, more specifically being a reflection of the reading and writing patterns (e.g. Taguchi and Noma, 2005; Taguchi, 2010).

Across Experiments 3 and 4, I observed improvements in motion discrimination performance. Observed effects of low-level visual perceptual learning are consistent with results found in the literature (e.g. Zhang and Rowe, 2014;

Ratcliff et al., 2006; Seitz et al., 2006; Fine and Jacobs, 2002). During the Experiment 3, participants were consistently improving the speed and the accuracy of decisions throughout the runs (Figures 4.7A, 4.8A; Table 4.9A). In the Experiment 4, participants were overall faster and more accurate compared to the performance in the Experiment 3 (Figure 4.18A, C), but the performance stopped improving after the first run (Figures 4.12A, 4.13A; Table 4.14). Low-level, relatively salient stimuli, like the random dot motion, are subject to fairly rapid learning, reaching saturation in few sessions (e.g. Fine and Jacobs, 2002; Frisby and Clatworthy, 1975). Nevertheless, I cannot definitely rule out that the withdrawal of the feedback contributed to the lack of improvement across the runs in the Experiment 4 (Shiu and Pashler, 1992; Herzog and Fahle, 1997; Roelfsema et al., 2010). However important, resolving the reservations about the influence of learning and/or feedback are outside of the scope of the current design.

4.8.2 Changing and maintaining movements

A novel feature of this set of experiments was a combination of noisy visual inputs and continuous motor output. A decision of whether to maintain or change the direction of movement in the second phase was made while performing the action based on the previous decision in the first phase. In all experiments, participants were able to correctly respond to the demands of the task, and changed the direction of ongoing circular movements in 50% of trials.

In Experiments 1 and 2, the quality of the stimulus remained stable and the stimulus-response mapping did not affect Change RT nor accuracy score. Nevertheless, switching visual cues from unambiguous arrows (Experiment 1) to noisy RDM stimulus (Experiment 2) increased the Change RT and decreased the accuracy. In Experiments 3 and 4, lower motion coherence in the second phase resulted in longer Change RT and lower accuracy score. Overall, the results were in accordance with previous studies that RT and accuracy are affected by the quality of visual input (Britten et al., 1992; Pilly and Seitz, 2009; Ramachandran and Anstis, 1983; Roitman and Shadlen, 2002; Szul et al., 2019). Here, continuous movements did not alter this fundamental property.

In Experiments 3 and 4, the maintenance of an ongoing action was affected by a decrease of motion coherence in the second phase. The change in the quality in the visual cue was also reflected in accuracy score (Figures 4.8B and 4.13B). Lower quality of visual inputs introduced more uncertainty, hence the increased hesitation, accidental stopping or momentary changes of direction.

In Experiment 4, the accuracy increased despite the increase in Change RT. Assuming the learning of the task saturated in Experiment 4, participants seemed to improve the maintenance of the stable movement. Summary of the speed of the movement (Figure 4.11) showed that in Experiment 3, participants were slower to regain the speed after the change of the direction under more noisy visual input. This effect disappeared in Experiment 4 (Figure 4.16).

In summary, this chapter extended a conventional perceptual-decision task with continuous responses over a time-scale of several seconds. The new paradigm enables to examine new research questions such as action maintenance and action switch with concurrent decision-making. I observed the expected effects of task difficulty and learning across multiple sessions (Gold and Shadlen, 2007; Ratcliff et al., 2016). Combining current results with Chapter 3, I concluded that continuous movements are valid and robust to indicate perceptual decision outcomes and their changes. In Chapter 5, I implemented this paradigm in MEG to investigate the electrophysiological signatures of continuous movements.

Chapter 5

MEG representations of continuous responses during decision-making

5.1 Introduction

The previous chapter presented a novel paradigm that combined perceptual decisions with continuous circular movements to investigate the dynamics of the action-decision coupling (Experiment 4 in Chapter 4). The perceptual decision task, random-dot motion discrimination, was used to coordinate circular movements (clockwise or anti-clockwise) of a joystick. Participants were asked to initiate, maintain or change continuous circular movements based on the direction of the coherent motion.

In this chapter, the behavioural task (Experiment 4 in Chapter 4) was adapted for concurrent magnetoencephalography (MEG) recording. All the participants who took part the experiments in Chapter 4 were re-recruited for the MEG experiment, and therefore all participants had sufficient training of the experimental procedure before the MEG session.

The MEG experiment aimed to identify electrophysiological signatures sensitive to (1) continuous movement directions and (2) changes in RDM coherence.

I examined three categories of MEG activities: ERFs, multivariate patterns and oscillatory power. Below I outlined rationales of the proposed analyses.

First, several electrophysiological signatures are related to decision-making and action initiation. Early EEG studies highlighted readiness potential (RP) as an ERP component related to motor preparatory activity (Kutas and Donchin, 1980). The RP, an event preceding the negative component, was found to be the strongest when participants were able to prepare their responses in advance, i.e., performing a voluntary movement or having a preparatory cue to indicate subsequent actions. For perceptual decisions, the P300 ERP component in central-frontal electrodes is associated with the evidence accumulation process (Twomey et al., 2015). The current experiment instructed participants to initiate their continuous circular movements with a common upward push (for both clockwise and anticlockwise movements). As demonstrated in Chapter 3, such short, ballistic actions are similar to conventional button presses in terms of behavioural performance as well as underlying cognitive processes. Therefore, I will calculate univariate ERFs evoked by the RDM stimulus in different MEG sensor groups and examine whether the ERFs differed between movement directions (in both first and second phases) and between coherence levels (in the second phase).

Second, although continuous movements were not commonly used in perceptual-decision studies, they have been studied extensively in the field of brain-computer interface (BCI), including drawing (Lv et al., 2010), precise finger movement (Kubánek et al., 2009; Sugata et al., 2012; Antelis et al., 2013), linear joystick movement (Waldert et al., 2008; Robinson et al., 2013; Nasseroleslami et al., 2014), point-to-point reaching (Pistohl et al., 2008; Ball et al., 2009; Bradberry et al., 2009, 2010; Toda et al., 2011; Nakanishi et al., 2013; Yeom et al., 2014) and continuous stable motion (Georgopoulos et al., 2005; Langheim et al., 2006). One common interest of BCI researchers is to decode the intention of movements from electrophysiological data, which is then used to provide feedback or control robotic devices to assist people with impaired motor functions. Indeed, previous research showed that multivariate patterns in electrophysiological signals contain information of movement trajectory (e.g. Georgopoulos et al., 2005; Pistohl et al., 2008; Hajipour Sardouie and Shamsollahi, 2012; Sugata et al., 2012; Antelis et al., 2013), indicating that it is possible to classify patterns of movement directions from MEG signals.

In this Chapter, I will use multivariate pattern analysis (MVPA) to decode task relevant information from sensor-level MEG data, including: movement directions (clockwise vs. anticlockwise), motion coherence (high vs. low in the second phase). Because participants were instructed to maintain steady and continuous circular movements throughout the trial, I will further calculate the temporal generalization pattern in multivariate MEG data. As highlighted in Figure 2.8, different temporal generalization patterns would highlight the temporal structure of underlying mental states. Specifically, I expect an oscillatory temporal generalization pattern for classifying movement directions, due to the periodic nature of circular movement. I also expect a sustained generalization pattern for classifying motion coherence in the early period of the second phase, because a change of motion coherence would affect the decision process until the action is altered (i.e., change of direction) or maintained (i.e., no change of direction) (King and Dehaene, 2014). Furthermore, engagement RT and change RT vary across trials and between participant. I will test whether aligning the MEG data to action onset (instead of stimulus onset) would provide a stronger multivariate pattern of movement direction (Leuthold et al., 2004), because time-domain signals may contains information about the phase (Waldert et al., 2008) as well as the velocity (Fuchs et al., 2000) of an action.

Third, Donner et al. (2009) showed that the MEG signals over sensorimotor areas were predictive of perceptual decision outcomes prior to actual behavioural responses. Moreover, the gamma-band activity was found to be reflecting the stimulus strength in a perceptual decision-making task using RDM (Siegel et al., 2007; Donner et al., 2007). Evidence from the non-human primates invasive electrophysiology confirmed that the beta-band activity indeed reflects action selection (Haegens et al., 2011) and its uncertainty (Tzagarakis et al., 2010) during decision-making. These results suggest a rich frequency-specific information during decision-making and action selection. The beta band power also has been found to reflect the uncertainty in the action selection process. The primary motor cortex activity reflects the dynamics of the decision process prior to response. For example, the deliberation and the subsequent commitment as major components in motor control not the sensory information accumulation are reflected in the local field potential (LFP) activity during the reach task (Thura and Cisek, 2014).

One feature of the current experiment was the active maintenance of an action after its initial engagement. The beta band desynchronisation (see: the MEG section in Chapter 2) is a strong feature of active actions in electrophysiological recordings (Taniguchi et al., 2000; Neuper and Pfurtscheller, 2001). For example, beta-band desynchronisation is elicited during the change of limb position in point-to-point reaching and was stable for the duration of the movement (Grent-'t Jong et al., 2014; Grent-'t Jong et al., 2013), and the origin of this activity has been localised in the motor cortex (Kilner et al., 1999; Taniguchi et al., 2000; Engel and Fries, 2010; Kilavik et al., 2013; Khanna and Carmena, 2017). Early modelling work suggested that beta-band desynchronisation is sensitive to movement velocity but not direction (Fuchs et al., 2000). Hence, in this Chapter, I will estimate the beta-band oscillatory power throughout the trial with the expectation of sustained beta-band desynchronization independent of movement direction.

To sum up, in this Chapter, I will set to test the following hypotheses:

- Behavioural results (RT, accuracy and movement trajectory) from MEG sessions are similar to those from behavioural sessions reported in Experiment 4 in Chapter 4.

- Univariate ERFs differ between movement directions (in the first and second phases) and coherence levels (only in the second phase).

- Significant above-chance (50%) MVPA classification accuracy between movement directions (in the first and second phases) and coherence levels (only in the second phase).

- MVPA temporal generalization patters are different when classifying data aligned to stimulus onset vs. action onset.

- Continuous movements would lead to a sustained beta-band desynchronization throughout the trial, regardless of movement directions.

5.2 Methods

5.2.1 Participants

Sixteen participants (thirteen females and 3 males, age range 19-28, M = 21.88 years, SD = 2.42 years) took part in the study following a briefing, MEG safety instructions, and written informed consent. All the participants were right handed. All the participants had normal or corrected-to-normal vision. None of the participants reported a history of motor impairments or neurological disorders. The study was approved by the Cardiff University School of Psychology Ethics Committee.

5.2.2 Apparatus

The experiment was conducted in a shielded MEG chamber with dimmed light. Stimuli were displayed on a MEG compatible PROPixx projector (VPixx Technologies Inc., Canada) projector with 1920x1080 pixels resolution and 120 Hz refresh rate. A chin rest was used to maintain the viewing distance and position (for more details see: Figure A.2). A MEG-compatible joystick (Current Design Inc., Canada) was used to record movement trajectories at 120 Hz. Similar to Chapters 3 and 4, the joystick handle could move nearly freely with little resistance from its neutral position within the 20% movement radius. Beyond the 20% radius, the resistance during joystick movement was approximately constant. The experiment was written using PsychoPy 1.85.4 library (Peirce, 2008).

5.2.3 Experimental Design and stimuli

The experimental design and stimulus were the same as Experiment 4 in Chapter 4. The stimulus-response mapping was counterbalanced across participants.

5.2.4 MEG data acquisition and pre-processing

Data acquisition

The whole head MEG recording was acquired in a magnetically shielded chamber, using a 275-channel axial gradiometer CTF system (VSM MedTech). Two channels were turned off due to excessive noise. The data were acquired continuously with 1200 Hz sampling rate, low-pass filtered at 300 Hz by a built-in on-line filter. For noise cancellation purposes an on-line 3rd order gradient compensation was applied using 29 reference channels. The data was analysed as synthetic, third order gradiometers (Vrba and Robinson, 2001). Horizontal and vertical electro-oculograms were recorded to monitor blinks and eye movements. The horizontal electrodes were placed on temples, and vertical ones, above and below the eye. To track the head position relative to the MEG sensors, three electromagnetic coils were placed on nasion, left and right pre-auricular area. The position of the coils was tracked continuously during the recording. The head shape with the position of the coils was digitised using a Polhemus FASTRAK (Colchester, Vermont). Participants were seated upright with their heads supported by the chin rest to minimise the head movement.

Data pre-processing

Data was processed using a MNE-Python 0.17.1 library (Gramfort et al., 2013, 2014). Continuous raw data was extracted from 5 s before the first trigger to 5 s after the last trigger. Data were separately high-pass filtered at 0.1 Hz and low-passe filtered at 80 Hz with minimum-phase causal filter using a finite impulse response (FIR) design. The data were then downsampled to 250 Hz to reduce computation load.

To remove the artifacts associated with eye movement and cardiac activity, the independent component analysis (ICA) was applied. The FastICA algorithm (Hyvärinen and Oja, 2000) was used to extract 50 independent components. The components containing eye-movement and cardiac activity were rejected. For the time-domain analysis the data were further low-pass filtered at 40 Hz. Subsequently, the continuous data were divided into epochs of -0.5-4.0 s around the onset of each trial, which encompassed the duration of the entire trial. The epochs were baselined using the -0.2 - 0.0 s period before trial onset. In a separate analysis, the data were divided into epochs of -1.0 - 1.0 s around the onset of the movement in each trial (Engage RT, see Figure 4.1) and around the moment of the adjustment of the action (Change RT). For the frequency domain analysis, data were further band-passed to extract functionally relevant frequency bands: alpha band (8-14 Hz), beta band (14-30 Hz), theta band (4-8 Hz) and low gamma band (30-80 Hz). From each band-passed data, the envelope of the Hilbert transformed signal was obtained. The data at each frequency band were epoched in the same manner as in the time-domain analysis.

5.3 Data analyses and results

As in Chapter 4, Bayesian ANOVA (JASP Team, 2018) was used for analysis of RTs and accuracy scores (Table 4.2). To compare the time courses of movement speed I used permutation tests with cluster-level correction for multiple comparisons (Maris and Oostenveld, 2007).

After artefact rejection, visual inspection of the pre-processed data suggested that continuous arm movements led to noisy recordings in temporal sensors. As a result, univariate analyses were conducted on medial frontal, central, parietal and occipital sensors, which have been shown to contain information of action selection, motor execution and visual processing (e.g. Cisek and Kalaska, 2010; Waldert et al., 2008; Donner et al., 2009). For each sensor group, I conducted time-resolved analyses on ERF time courses and Hilbert power envelops. For each participant, the time-courses were robustly averaged across trials using a trimmed mean (5% of the extreme ends of the distribution were discarded) (Wilcox and Rousselet, 2018). The differences between averaged ERFs were assessed by permutation tests with cluster-level corrections for multiple comparisons at different time points. A lenient cluster formation threshold ($F = 2.0$) was used to obtain an initial set of clusters. From the initial set of clusters, permutation test (5000 permutations) was used to establish statistical significance with a threshold of $p < 0.05$. In all ERF figures, significant clusters were highlighted with a green shade ($p < 0.05 corrected$). Non-significant clusters with p-values $0.05 < p < 0.5$ were highlighted in light grey (e.g. right Central Sensors, Figure 5.17). Due to a lenient threshold used for initial cluster detection, the numbers of clusters that survived the uncorrected threshold were high and thus not reported.

MVPA temporal generalization results were corrected for multiple comparisons using a two-dimensional cluster-based correction approach. Similar to the ERF analysis, a lenient cluster threshold ($F = 2.0$) was used to obtain an initial set of 2D clusters. From the initial set of clusters, permutation tests (5000 permutations) were conducted to find significant clusters with a significant threshold of ($p < 0.05$). Significant clusters were highlighted with a black border on temporal generalisation maps.

5.3.1 Behavioural results

I first examined the behavioural performance (Accuracy, Engage RT in the first phase, and Change RT in the second phase, see Table 4.2 for definitions of behavioural measures). For the first phase of a trial, there was no experimental manipulation on the stimulus quality. As expected, I found no difference between conditions (change in directions and/or change in coherence) in accuracy ($BF_{10} = 4.898 \text{ x } 10^{-4}$, strong evidence, Figure 5.2A) or Engage RT ($BF_{10} = 3.603 \text{ x } 10^{-4}$, strong evidence, Figure 5.1B). There was strong evidence for a main effect in accuracy across experimental runs ($BF_{10} = 1.349 \text{ x } 10^{6}$; see Table 5.3A for post-hoc tests) and a main effect in Engage RT ($BF_{10} = 5.043 \text{ x } 10^{45}$; see Table 5.3B for post-hoc tests). None of the main effects interacted (accuracy - $BF_{10} = 2.138 \text{ x } 10^{-6}$ strong evidence; Engage RT - $BF_{10} = 2.197 \text{ x } 10^{-6}$ strong evidence).

For the second phase of a trial, there was a reduction in coherence (50% of trials) and/or a change in coherent motion direction (50% of trials) (see Figure 4.1, Experiment 4). When the motion direction was changed, the Change RT was affected by the reduction in motion coherence. The participants took longer ($BF_{10} = 59499.859$, strong evidence; Figure 5.1B) and were less accurate ($BF_{10} = 5.342 \text{ x } 10^{97}$, strong evidence; Figure 5.2B) in changing the direction of

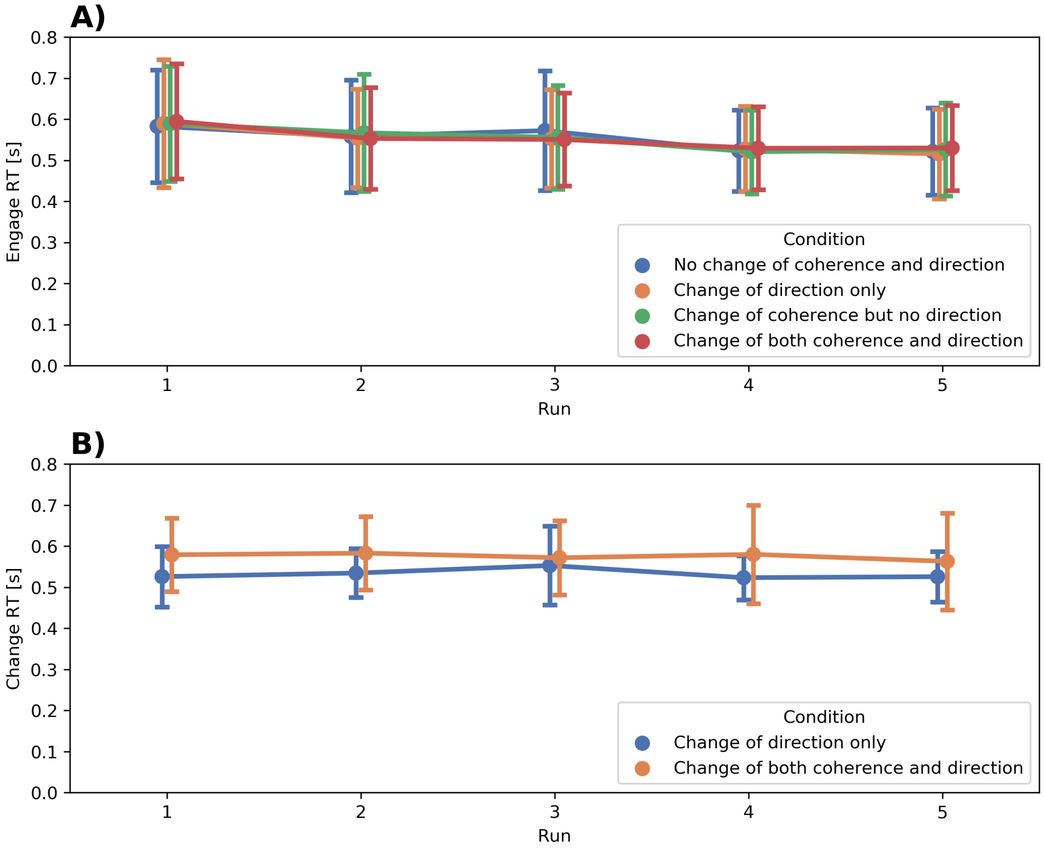

Figure 5.1: Reaction times (see Table 4.2 for the definitions of behavioural measures). (A) Engage RT in each run from the first phase of the trial. (B) Change RT in each run from the second phase of the trial. Data points represent the mean score and bars represent standard deviations. As in Chapter 4, Change RT only reported for trials with a change of motion direction in the second phase.

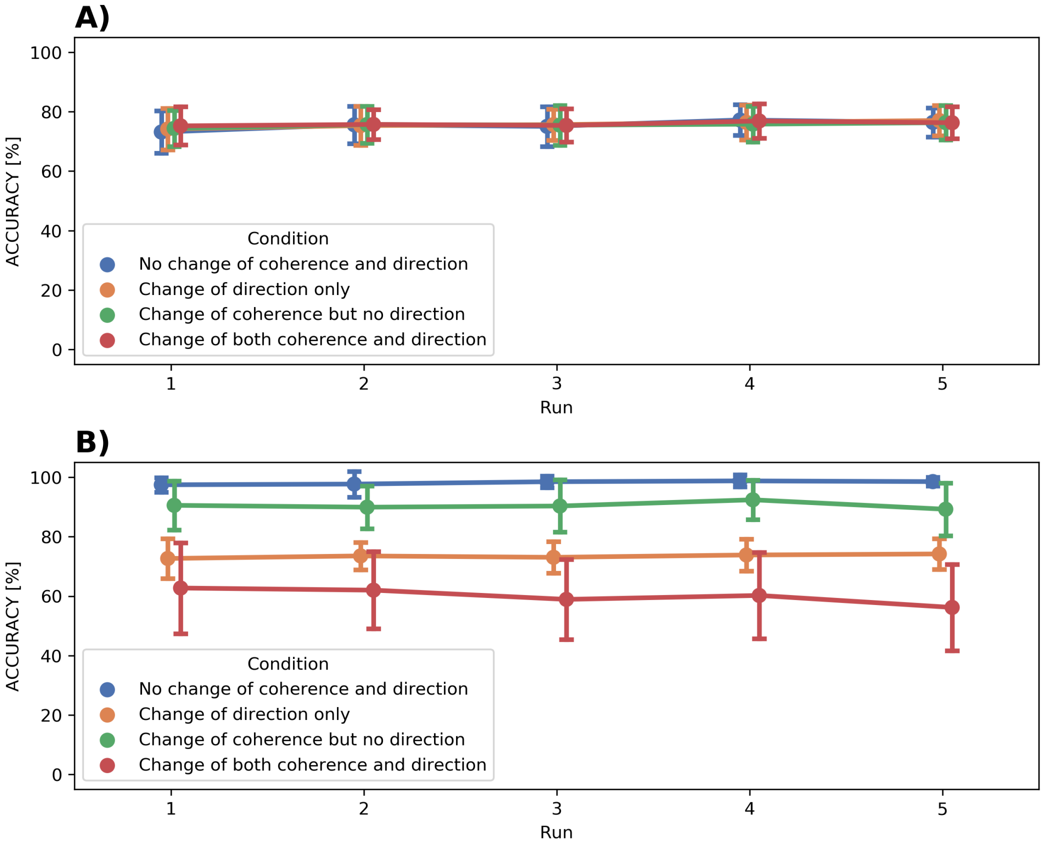

Figure 5.2: Accuracy scores. (A) Accuracy scores in each run from the first phase of the trial. (B) Accuracy scores in each run from the second phase of the trial. Data points represent the mean score and bars represent standard deviations.

A. Accuracy (action engagement)

Run	1	2	3	4	5
1		0.639	0.259	2701.831	2969.783
2			0.016	0.147	0.127
3				0.436	0.383
4					0.014
5					

B. Engage RT (action engagement)

Run	1	2	3	4	5
1		84.033	97.883	2.053 x 10^{17}	3.258 x 10^{17}
2			0.015	2419.536	5064.370
3				2155.933	4511.613
4					0.015
5					

Table 5.3: Posterior odds of post-hoc comparisons of (A) accuracy scores and (B) Engage RT between runs. Cells highlighted in green indicate evidence for the difference in the comparison. Cells highlighted in red indicate evidence against the difference. Cells in white indicate inconclusive evidence.

their circular movements when the motion coherence was reduced, suggesting a sustained sensitivity towards sensory information in the second phase. When the motion direction was not changed, participants were less accurate (BF_{10} = 2.150 x 10^{31}, strong evidence; Figure 5.2B) in maintaining their circular movements under more noisy conditions. Across runs, there was no change in accuracy (BF_{10} = 0.008, strong evidence) or the Change RT (BF_{10} = 4.764 x 10^{-4}, strong evidence). There was an interaction between the change/no-change of the motion coherence and runs on accuracy (BF_{10} = 8.256, moderate evidence), but not on Change RT (BF_{10} = 0.002, strong evidence).

Next, I compared the behavioural measures between the first and second phases. When the second phase had a change of motion direction but not motion coherence, there was no conclusive evidence (BF_{10} = 2.685) that Engage RT (in the first phase) was different to the Change RT (in the second phase). When the change of motion direction and lowered motion coherence occurred in the second phase, there was moderate evidence (BF_{10} = 3.664) that Engage RT and Change RT were different. In both conditions, the change of motion direction led to a decrease in accuracy than that in the first phase

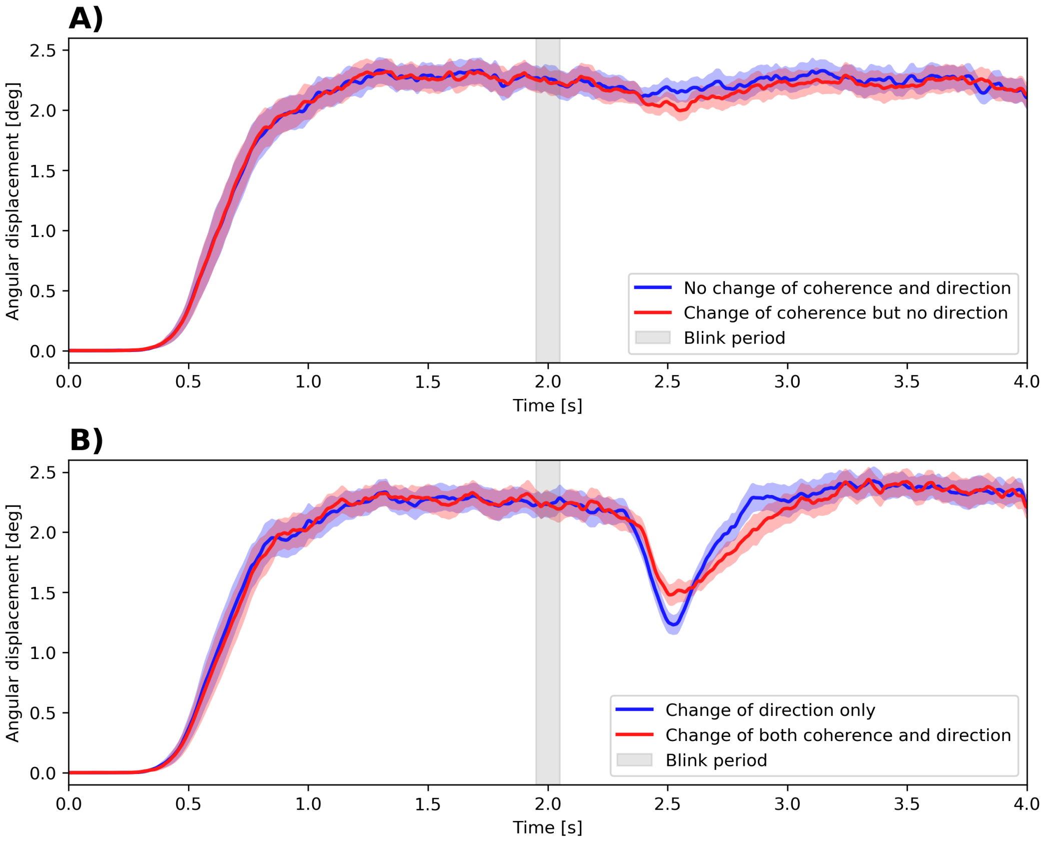

Figure 5.4: Movement speed in trials with (A) and without (B) a change of motion direction in the second phase. Solid lines denote the mean movement speed, and shaded areas denote the standard error of the mean across participants. The grey shading around $t = 2s$ indicates the 100 ms gap between the two phases of the trial.

(change of coherence: BF_{10} = 1.829 x 10^{125}, strong evidence; no change of coherence: BF_{10} = 6.519 x 10^{7}, strong evidence).

The speed of circular movements, as measured by the angular displacement velocity, was not affected by changes in motion coherence (no change of direction trials: Figure 5.4A; change of direction trials: Figure 5.4B). For trials with direction changes, there was no effect of motion coherence in the movement speed when the measure was time-locked to the onset of direction change (Figure 5.5A). The participants achieving the stable motion speed faster in changing the direction of an ongoing action than initiating an action in the first phase (Figure 5.5B). In addition, the participants were decelerating before the change, and accelerating after the direction change at a similar rate,

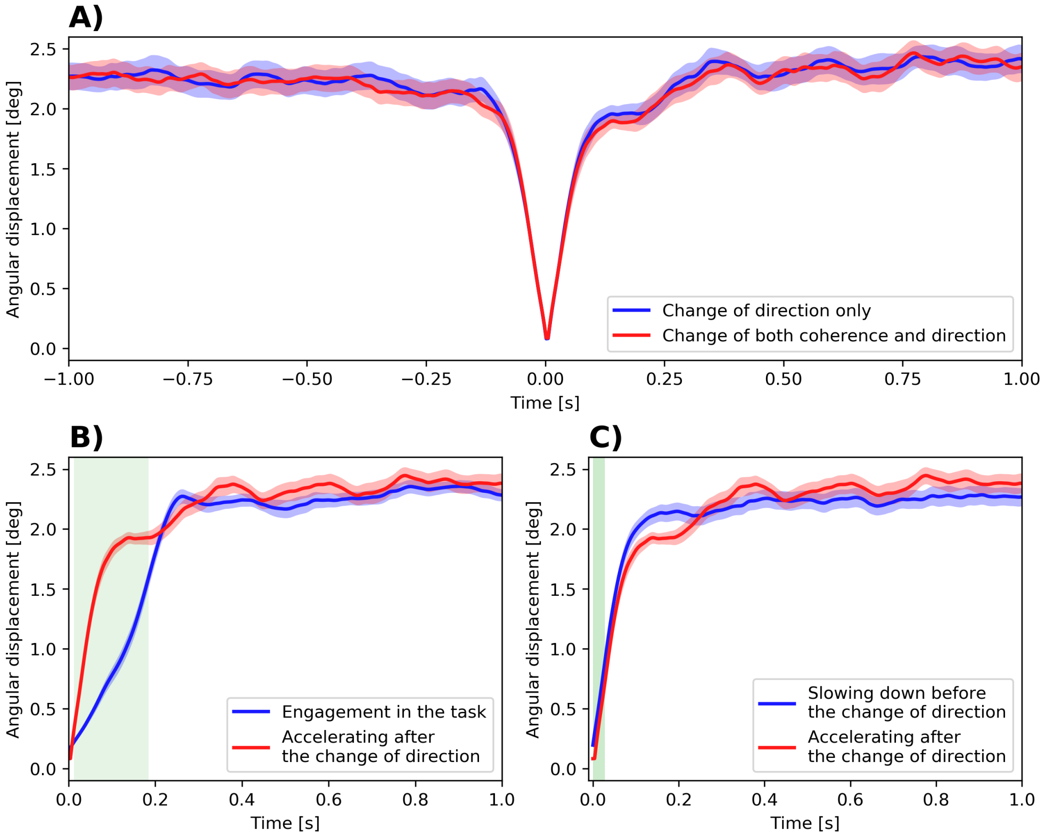

Figure 5.5: Movement speed time-locked to various movement milestones. (A) The time course of movement speed time-locked to Change RT. (B) Movement speed from Engage RT (in the first phase) and Change RT (in the second phase). (C) Movement speed before and after Change RT. Solid lines denote the mean movement speed, and shaded areas denote the standard error of the mean across participants. The differences between conditions are highlighted by green shading (cluster permutation test with cluster-level correction at $p < 0.05$).

except from a short period around the pivotal point of the direction change (Figure 5.5C).

In sum, the behavioural results of the MEG experiment was similar to previous experiments conducted in the behavioural lab (Experiments 3-4 in Chapter 4, confirming the validity of the paradigm in the MEG suite.

5.3.2 MEG results

ERFs

For each participant, the pre-processed MEG data in each condition were averaged using: the movement direction in the first phase (clockwise or anti-clockwise), the presence of direction change in the second phase (change or no change) and the presence of motion coherence change in the second phase (high or low coherence). Figures 5.7 and 5.6 showed the averaged ERFs in four sensor groupings (frontal, central, parietal and occipital), comparing trials with clockwise and anti-clockwise movements. There was no significant difference in ERFs between movement directions. Further tests showed no significant difference in ERFs between trials with high and low motion coherence in the second phase. Therefore, univariate MEG signals were insensitive to the experimental manipulation and the direction of continuous movements.

Time-domain multivariate pattern classification using SVM

I performed two MVPA analyses to evaluate the discriminability of multivariate patterns of MEG activity. The first was binary classifications between clockwise and anti-clockwise movements, separately for the first and second phase of the trial. The second was binary classifications between RDM coherence (high vs. low), separately for trials with and without change in motion direction.

I applied the analysis pipeline outlined in Section 2.3.4. Each analysis included all the MEG sensors. For each classification problem, a 10-fold cross-validation procedure was conducted. In each cross-validation, the data was standardised

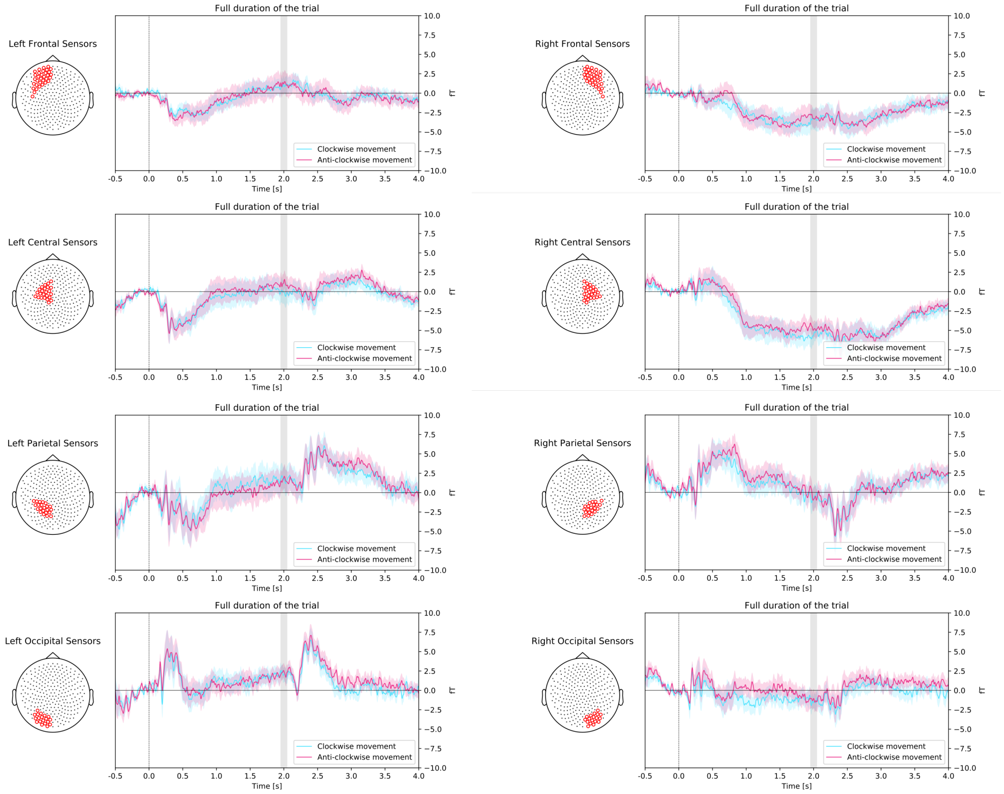

Figure 5.6: ERFs of clockwise vs anticlockwise movements in trials with no change of direction in the second phase. The results were shown separately for each sensor group (frontal, central, parietal and occipital). Solid lines denote the mean movement speed, and shaded areas denote the standard error of the mean across participants. No significant clusters between change and no change of direction conditions were observed at the cluster level $p < 0.05$.

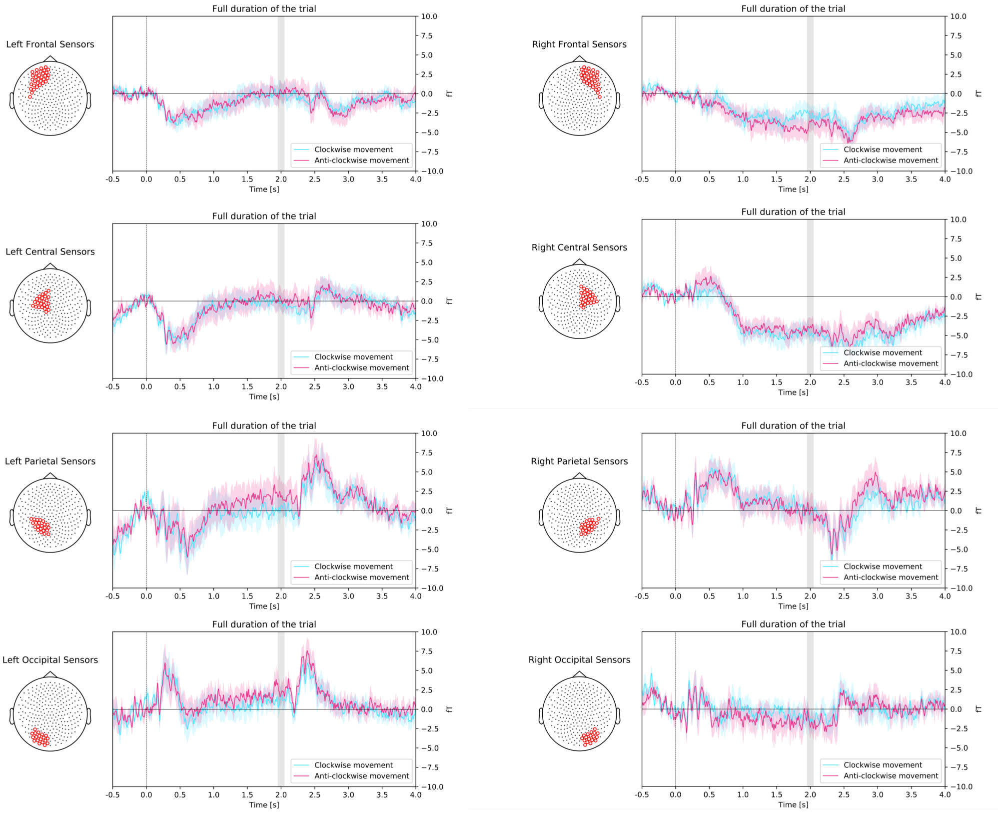

Figure 5.7: ERFs of clockwise vs anticlockwise movements in trials with change of direction in the second phase. The results were shown separately for each sensor group (frontal, central, parietal and occipital). Solid lines denote the mean movement speed, and shaded areas denote the standard error of the mean across participants. No significant clusters between change and no change of direction conditions were observed at the cluster level $p < 0.05$.

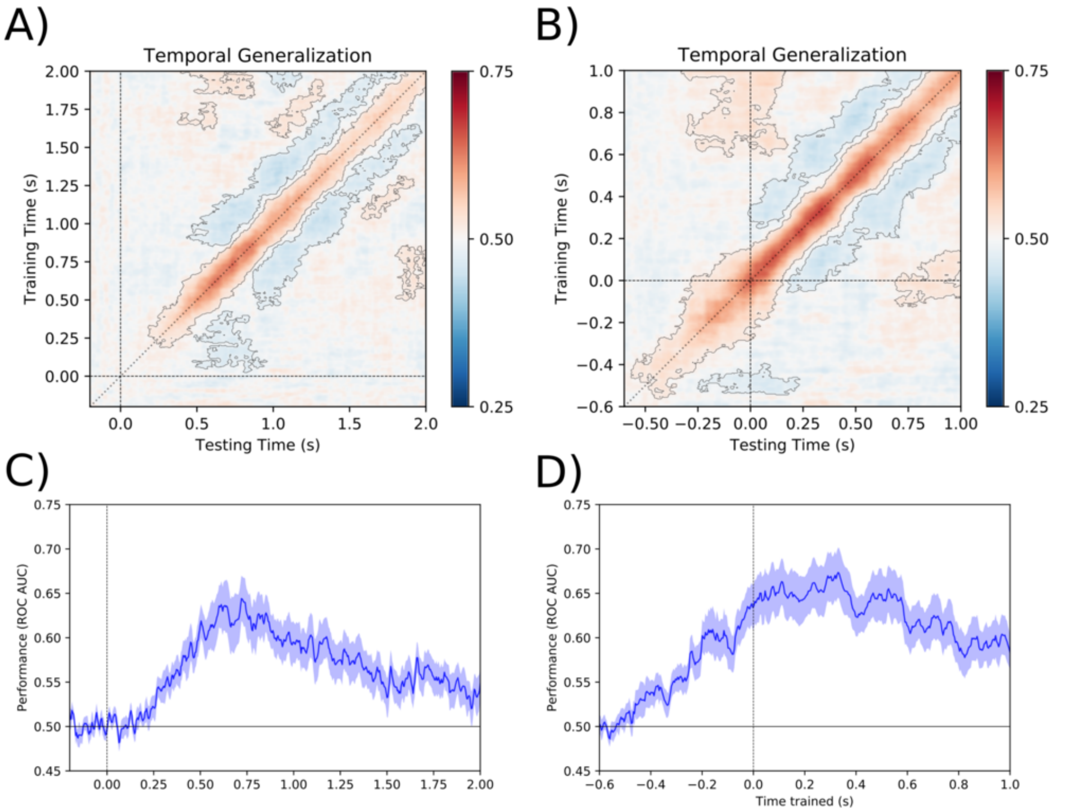

Figure 5.8: MVPA of clockwise vs. anticlockwise movements in the first phase. **A)** and **B)**: Temporal generalisation map of the clockwise vs. anticlockwise movements when the data was time-locked to trial onset (**A**) or Engage RT (**B**). Black outline denotes the clusters with a significant difference from the 50% chance level (one-sample cluster permutation test with cluster-level correction at $p < 0.05$) **C)** and **D)**: Classification performance for the classifier trained on and applied to the data from the same time point. Solid lines denote a mean performance of the classifier. Shaded areas denote the standard error of the mean across participants.

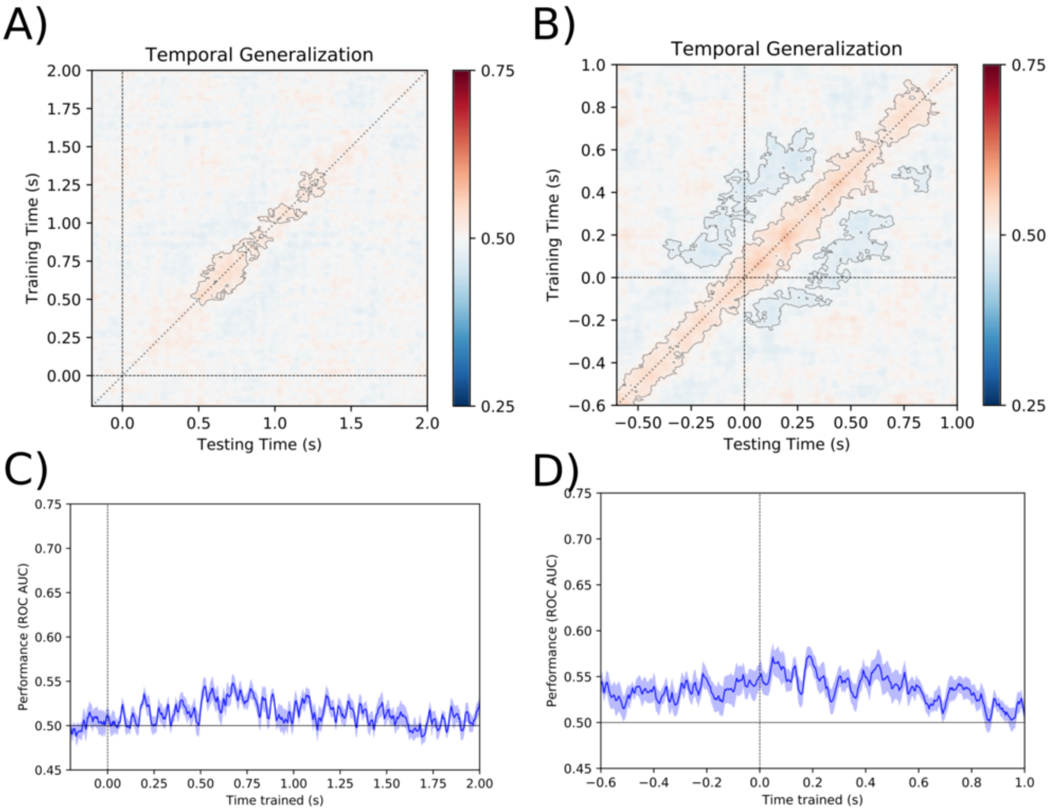

Figure 5.9: MVPA of clockwise vs. anticlockwise movements in the second phase. **A)** and **B)**: Temporal generalisation map of the clockwise vs. anticlockwise movements when the data was time-locked to the onset of the second phase (**A**) or Change RT (**B**). Black outline denotes the clusters with a significant difference from the 50% chance level (one-sample cluster permutation test with cluster-level correction at $p < 0.05$). **C)** and **D)**: Classification performance for the classifier trained on and applied to the data from the same time point. Solid lines denote a mean performance of the classifier. Shaded areas denote the standard error of the mean across participants.

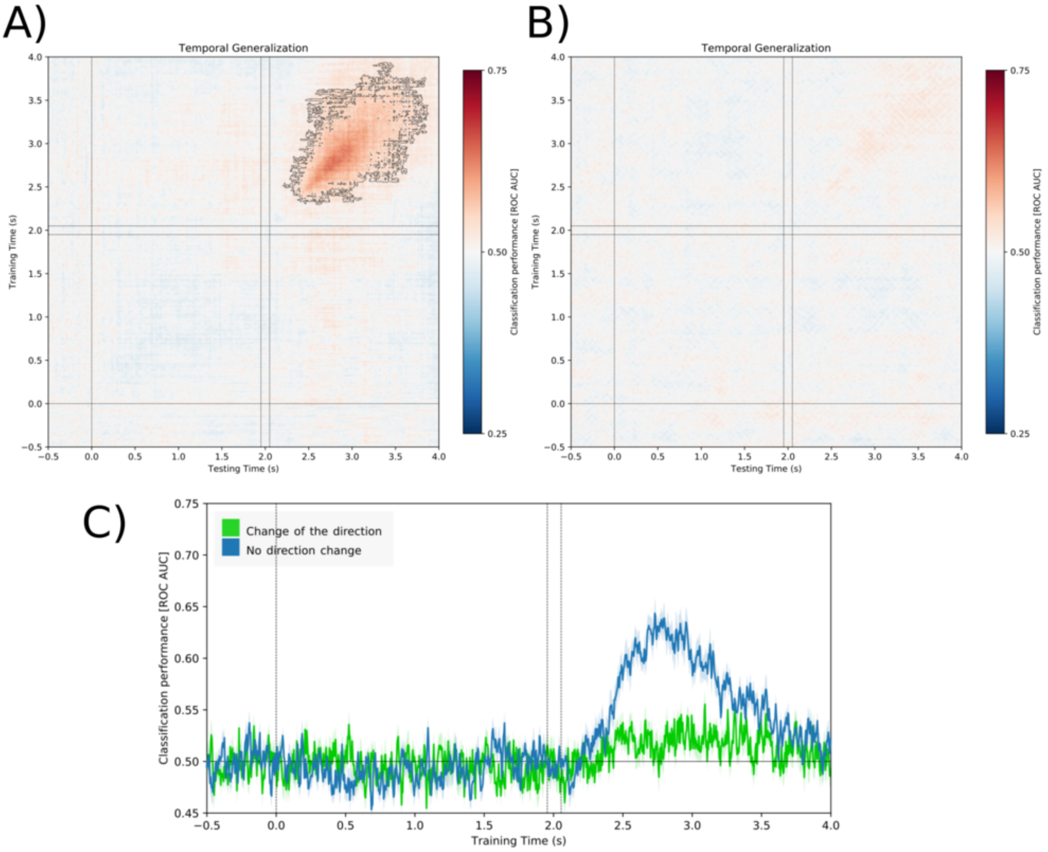

Figure 5.10: MVPA of trials with high vs. low motion coherence presented in the second phase. **A)**: Temporal generalisation performance of the classifier for the trials with no change of the direction in the second phase. **B)**: Temporal generalisation performance of the classifier for the trials with a change of the direction. Black outline denotes the clusters with a significant difference from the 50% chance level (one-sample cluster permutation test with cluster-level correction at $p < 0.05$). **C)**: Performance of the classifier trained on and applied to the data from the same time point. Solid lines denote a mean performance of the classifier. Shaded areas denote the standard error of the mean across participants.

using a robust scaling method. A PCA was conducted on the training set to identify principle components that explained ¿99% of data variance. Both training and test sets were then projected to the reduced space defined by the chosen principle components. A linear support vector classifier (SVC) with LASSO regularisation was used to train and test the multivariate patterns. Furthermore, the temporal generalisation procedure was applied to determine the temporal patterns of the information representations. That is, the SVM classifier was trained on one time point and tested in the data at all time points (King and Dehaene, 2014).

Classification performance was evaluated using the area under the receiver operating characteristic curve (ROC AUC). If $AUC = 0.5$, the classification is uninformative and the classifier cannot separate between the two classes. If $AUC > 0.5$, multivariate patterns contain information to distinguish between the two classes. If $AUC < 0.5$, the classifier is correctly predicting the opposite class (Bradley, 1997).

Figure 5.8 showed the MVPA results and their temporal generalisation pattern of movement directions during the first phase of the trial, when the data was time locked to stimulus onset (panel A) or movement onset (i.e., Figure 5.1B). Panels C and D in Figure 5.8 illustrated the classification performance trained and tested on the same time point (i.e., the values along the diagonal of temporal generalisation plots). The decoding of movement direction was above chance level from 0.25 s after stimulus onset (Figure 5.8A) and 0.5 s before the movement onset (Figures 5.8B). The multivariate patterns sensitive to movement directions had a temporal generalization window of 0.125 s. Beyond this point, the temporal generalization showed a reversed pattern with significant performance below the 50% chance level, possibly due to the periodic nature of circular movements in the current experiment.

During the second phase of the trial, classification of movement directions was significantly above chance 0.5 s after the onset of the second phase (Figure 5.9A and 5.9C), with a temporal generalisation window of 0.125 s. The figure 5.9 shows the results of the classification between clockwise and anti-clockwise movement during the change of the direction. Classifier was able to distinguish the direction of the 0.5 s after the onset of the second phase of the trial with a generalisation of 0.125 s around the diagonal point (Figure 5.9A and 5.9C). When the data was aligned to movement onset or change of movement direction, the classification performance was consistently above chance throughout the second phase of the trial, with a similar temporal generalisation pattern as in the first phase (Figure 5.9 B and 5.9D).

In the second analysis, I trained the classifier to distinguish between the easy vs. difficult trials (i.e., trials with high coherence vs. low coherence in the second phase). In trials with no change of motion direction, classification performance was significantly above chance 0.35 s after the beginning of the second phase (Figures 5.10A and 5.10C), and the temporal generalisation results suggested that the information of motion coherence was maintained across a broad time window. In trials with a change of motion direction, there was no significant classification between motion coherence (Figures 5.10B).

Oscillatory power

The amplitude of Hilbert envelope of each frequency band (Alpha, Beta, Gamma, Theta) was averaged for each condition and baseline corrected to stimulus onset. The relative desynchronization in the Beta band were presented to illustrate the patterns associated with continuous movements (change of direction: Figures 5.11, 5.12; no change of direction: Figures 5.15, 5.16). The strength of the stimulus did not affect the Beta band frequency as well (change of direction: Figures 5.13, 5.14; no change of direction: Figures 5.17, 5.18). There was also no significant difference in oscillatory power in other frequency bands between the direction of the movement and high vs. low motion coherence in the second phase.

5.4 Discussion

The experiment in this chapter was a repetition of Experiment 4 in Chapter 4 with concurrent MEG recording. The goal of the current study was to identify MEG signatures sensitive to movement direction and motion coherence.

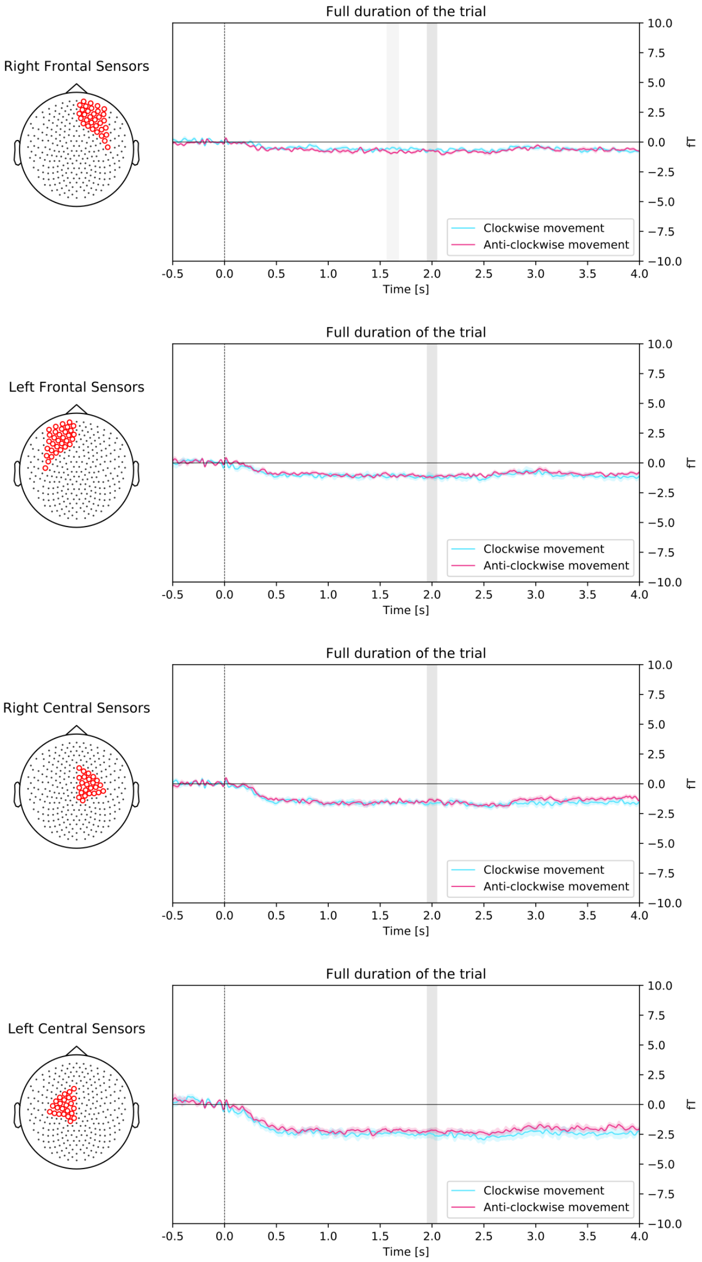

Figure 5.11: Beta frequency band (14-30 Hz) Hilbert envelope of clockwise vs anticlockwise movements in trials with change of direction in the second phase. The results were shown separately for each frontal and central sensor group. Solid lines denote the mean movement speed, and shaded areas denote the standard error of the mean across participants. No significant clusters between clockwise and anticlockwise conditions were observed at the cluster level $p < 0.05$.

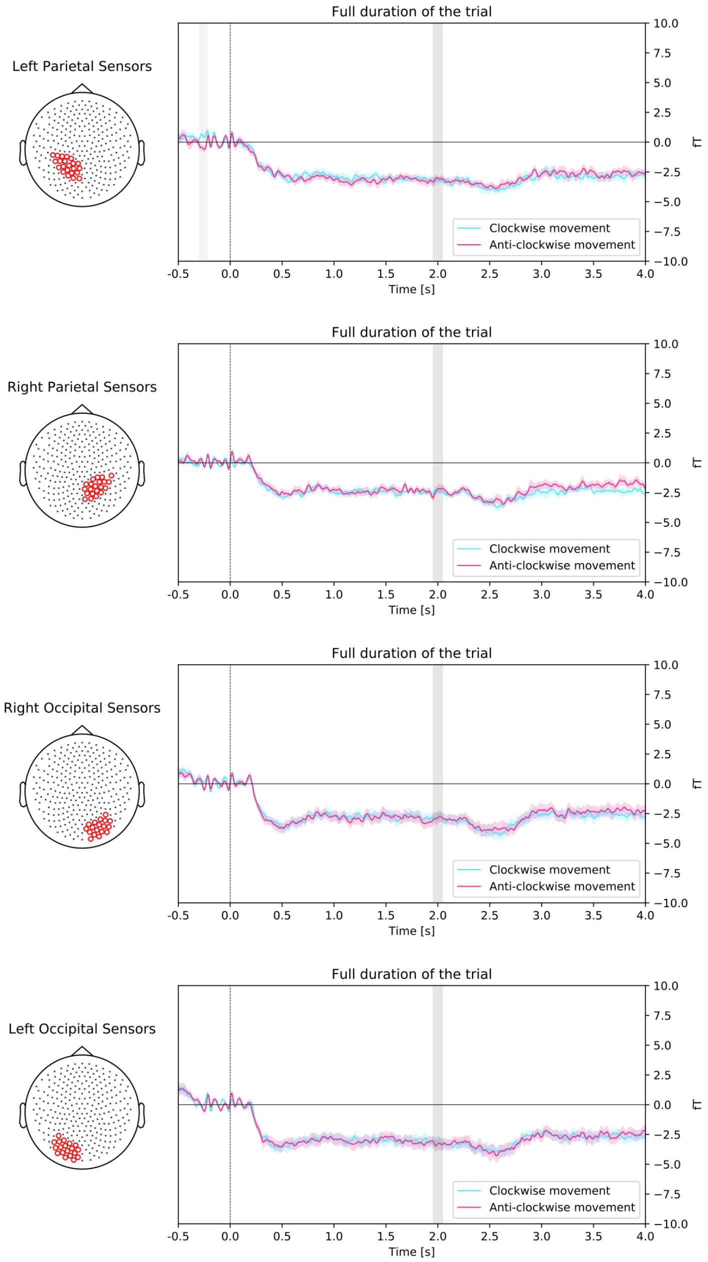

Figure 5.12: Beta frequency band (14-30 Hz) Hilbert envelope of clockwise vs anticlockwise movements in trials with change of direction in the second phase. The results were shown separately for each parietal and occipital sensor group. Solid lines denote the mean movement speed, and shaded areas denote the standard error of the mean across participants. No significant clusters between clockwise and anticlockwise conditions were observed at the cluster level $p < 0.05$.

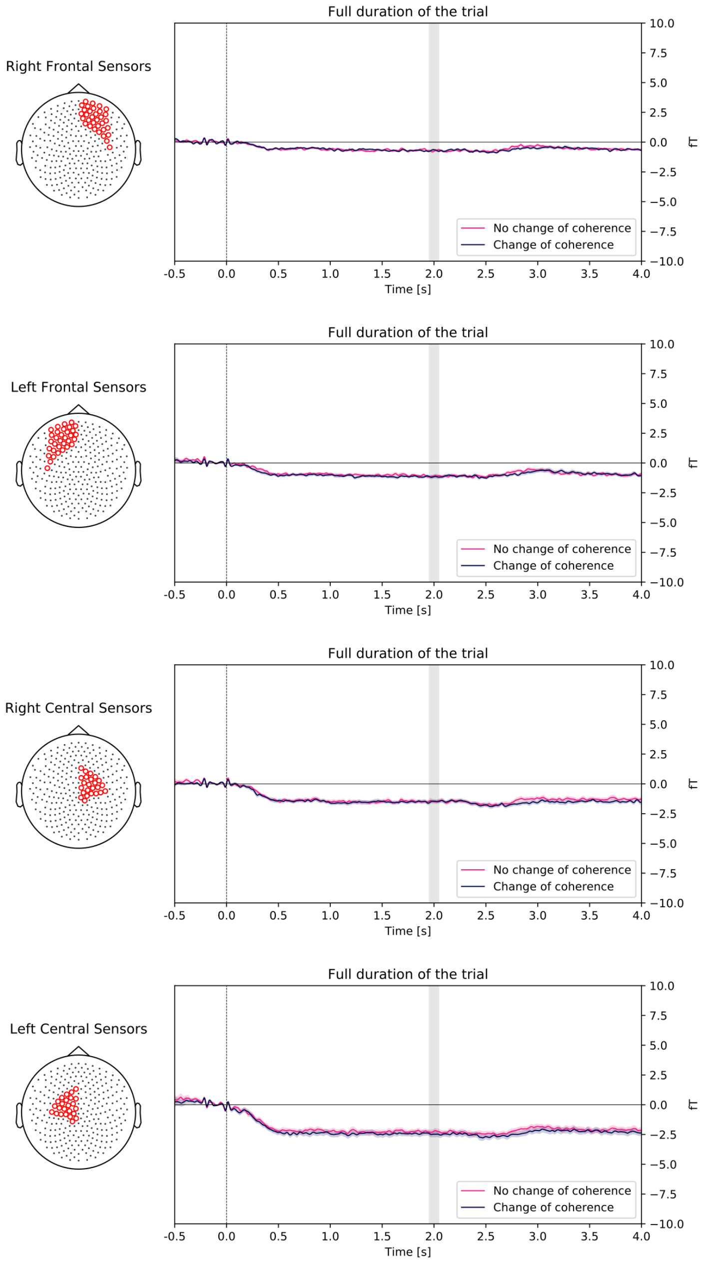

Figure 5.13: Beta frequency band (14-30 Hz) Hilbert envelope of movements in trials with change of direction in the second phase, separately for high or low motion coherence. The results were shown separately for each frontal and central sensor group. Solid lines denote the mean movement speed, and shaded areas denote the standard error of the mean across participants. No significant clusters between change and no change of direction conditions were observed at the cluster level $p < 0.05$.

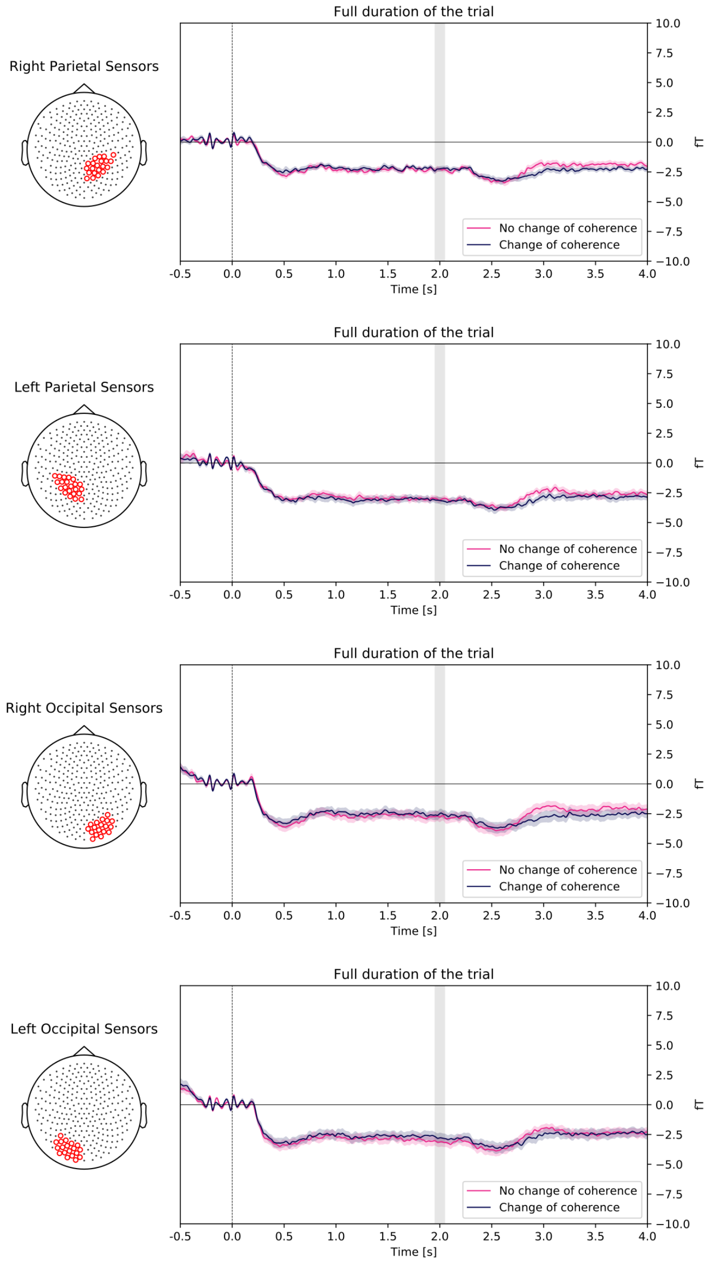

Figure 5.14: Beta frequency band (14-30 Hz) Hilbert envelope of movements in trials with change of direction in the second phase, separately for high or low motion coherence. The results were shown separately for each parietal and occipital sensor group. Solid lines denote the mean movement speed, and shaded areas denote the standard error of the mean across participants. No significant clusters between change and no change of direction conditions were observed at the cluster level $p < 0.05$.

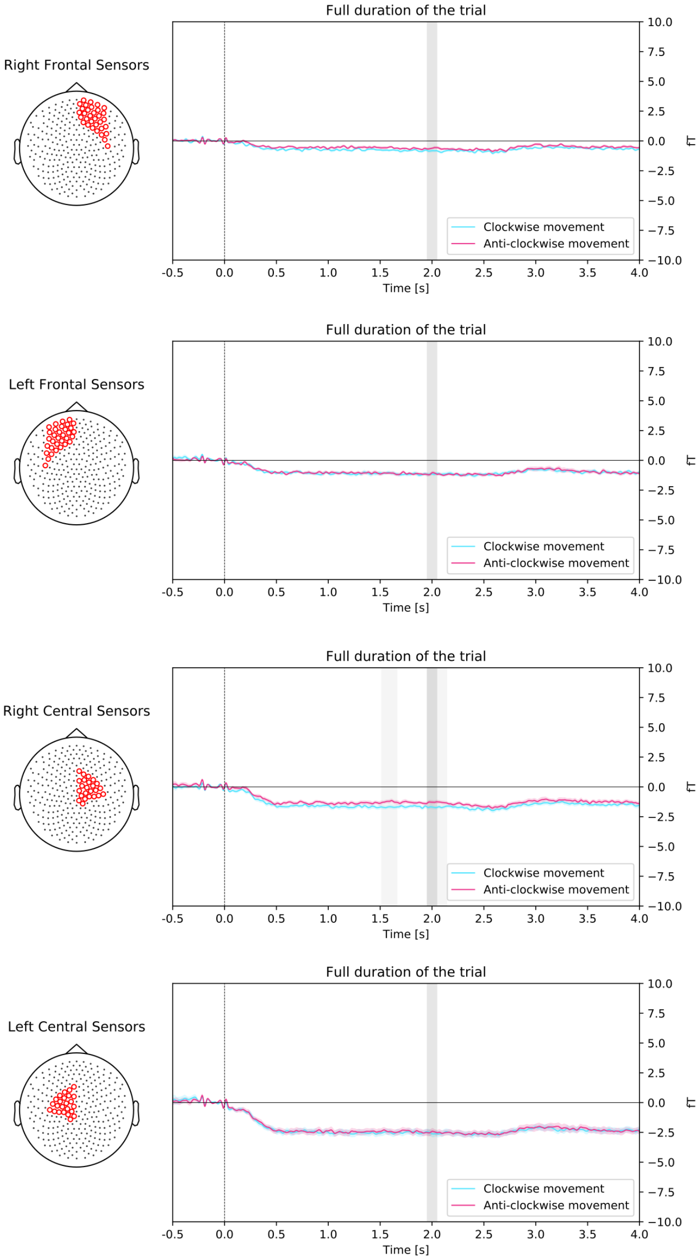

Figure 5.15: Beta frequency band (14-30 Hz) Hilbert envelope of clockwise vs anticlockwise movements in trials with no change of direction in the second phase. The results were shown separately for each frontal and central sensor group. Solid lines denote the mean movement speed, and shaded areas denote the standard error of the mean across participants. No significant clusters between clockwise and anticlockwise conditions were observed at the cluster level $p < 0.05$.

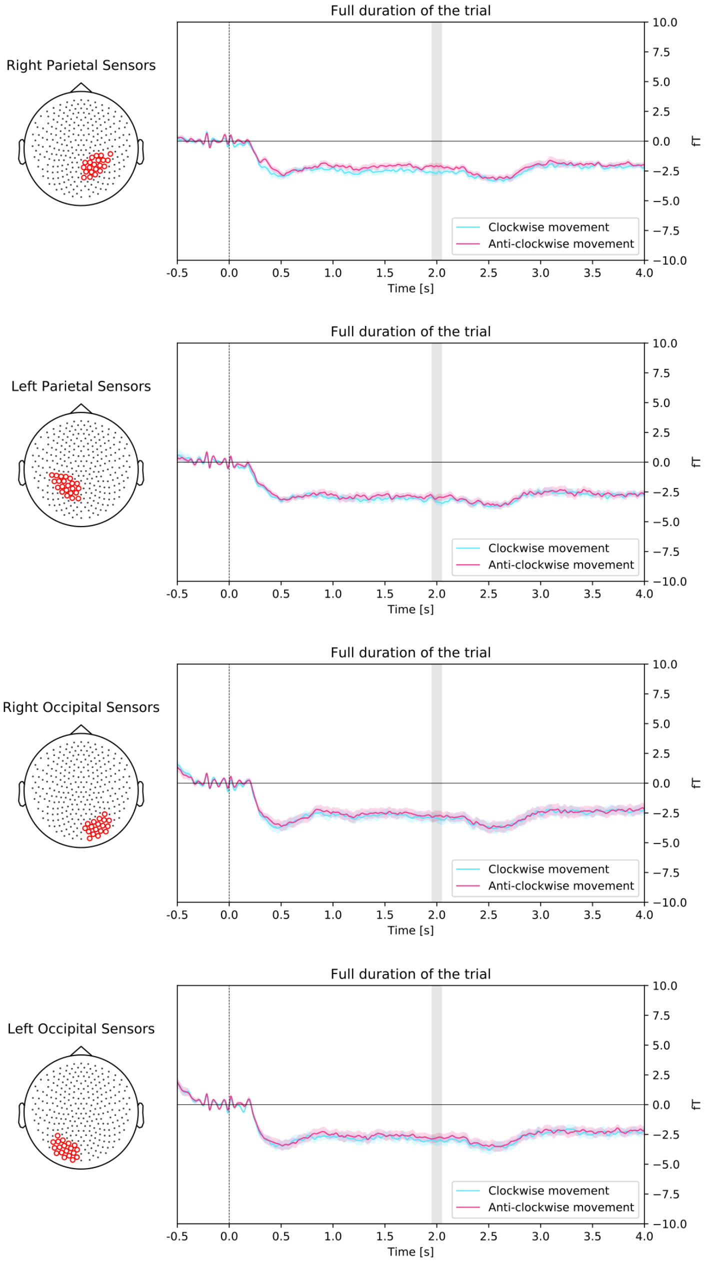

Figure 5.16: Beta frequency band (14-30 Hz) Hilbert envelope of clockwise vs anticlockwise movements in trials with no change of direction in the second phase. The results were shown separately for each parietal and occipital sensor group. Solid lines denote the mean movement speed, and shaded areas denote the standard error of the mean across participants. No significant clusters between clockwise and anticlockwise conditions were observed at the cluster level $p < 0.05$.

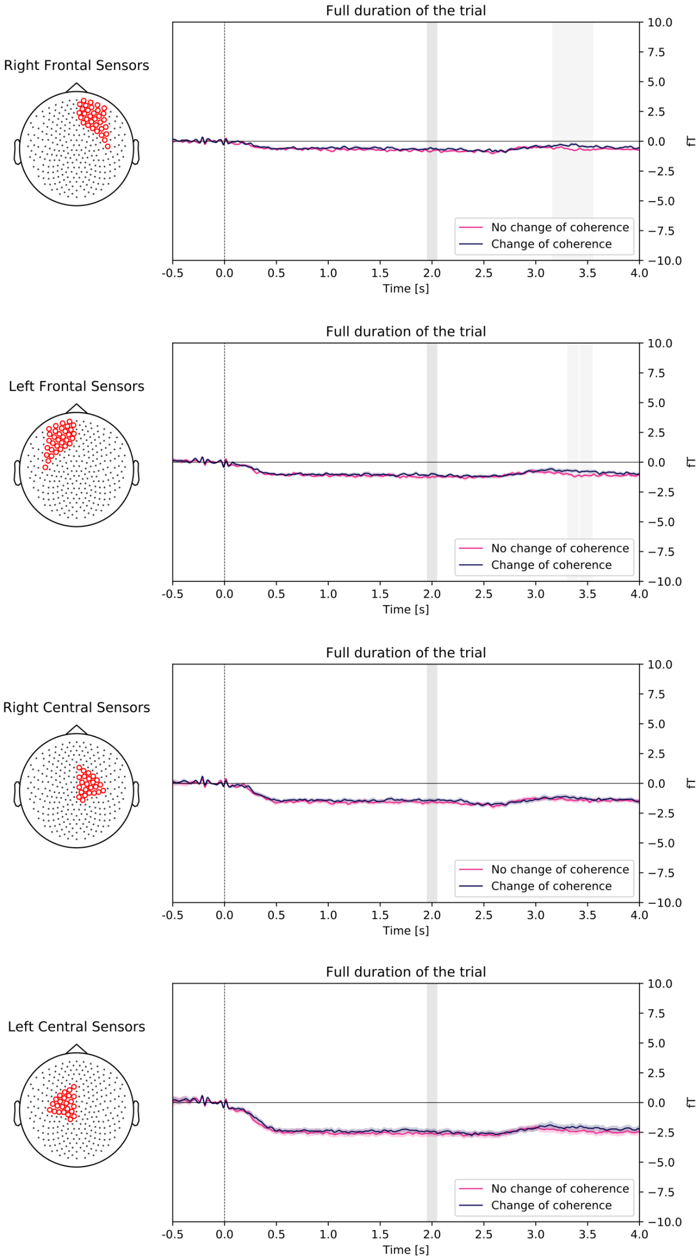

Figure 5.17: Beta frequency band (14-30 Hz) Hilbert envelope of movements in trials with no change of direction in the second phase, separately for high or low motion coherence. The results were shown separately for each frontal and central sensor group. Solid lines denote the mean movement speed, and shaded areas denote the standard error of the mean across participants. No significant clusters between change and no change of direction conditions were observed at the cluster level $p < 0.05$.

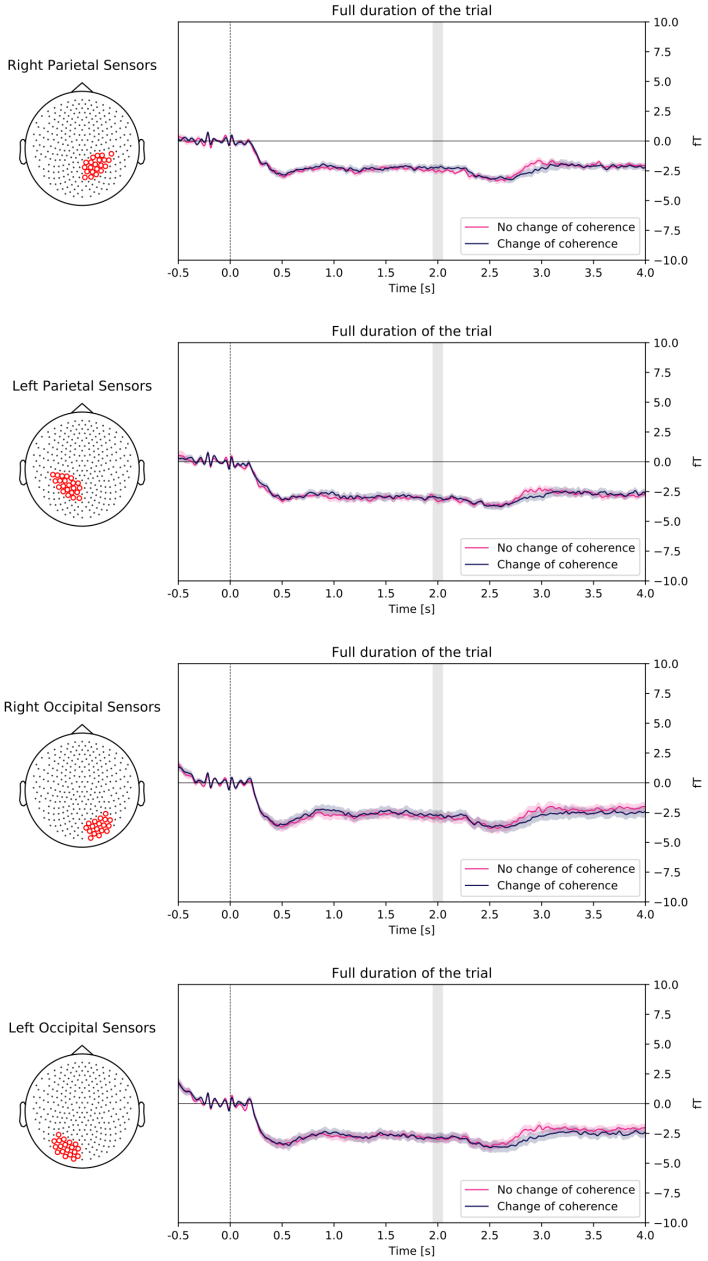

Figure 5.18: Beta frequency band (14-30 Hz) Hilbert envelope of movements in trials with no change of direction in the second phase, separately for high or low motion coherence. The results were shown separately for each parietal and occipital sensor group. Solid lines denote the mean movement speed, and shaded areas denote the standard error of the mean across participants. No significant clusters between change and no change of direction conditions were observed at the cluster level $p < 0.05$.

5.4.1 Behavioural measures

All the participants who took part in experiment described in the current chapter also took part in all the experiments described in the Chapter 4, thus were familiar with the task and procedure.

As in Chapter 5, there was no effect of the experimental conditions on Engage RT or accuracy in the first phase, indicating that the experimental procedure did not introduce any biases in the initial engagement phase of the task.

In the second phase, the experimental manipulation of the stimulus quality (lowering the coherence of RDM stimulus) resulted in increased Change RT and decreased accuracy (Figures 5.1B, 5.2B). However, unlike Experiment 4 in Chapter 4, Change RT and accuracy in the second phase did not vary across runs. Furthermore, when comparing the action engagement (first phase of the trial) and action adjustment (second phase of the trial), there was no conclusive evidence that those two decisions were different in terms of the latency (Engage RT vs. Change RT) when there was no change in motion coherence.

The time courses of movement speed showed that participants further improved their continuous responses to RDM stimulus. Experiment 4 in Chapter 4 showed that motion coherence in the second phase affected the angular speed of the circular joystick movement. This effect was not present in the current experiment (Figures 5.4 and 5.5). Moreover, the difference between the deceleration and acceleration, before and after the change of the direction, was reduced in the current experiment.

We replicated most of the behavioural results in the MEG experiment, indicating the robustness of the paradigm. The small difference in performance between experiments might be due to the change of experimental settings (MEG chamber instead of behavioural lab) and the visual presentation with a lower contrast in MEG sessions (projector instead of the CRT monitor)

5.4.2 MEG signatures

This chapter considered three types of MEG measures: ERFs, oscillatory power in separate sensor groups, and whole-brain multivariate patterns. There was no significant difference between movement directions or between high vs low motion coherence in ERFs or oscillatory power changes. The beta-band power has been related with various stages of movements (Meirovitch et al., 2015; Erbil and Ungan, 2007; Gallivan et al., 2011). Indeed, across all sensor groups (frontal, central, occipital and parietal), the beta-band power decreased throughout the duration of the movement (Figures 5.11, 5.12, 5.15 and 5.16). The stable pattern of beta desynchronisation was observed irrespective of the presence of direction change during the second phase of the trial (Meirovitch et al., 2015; Erbil and Ungan, 2007; Gallivan et al., 2011).

Patterns of movement directions

Previous research on arm kinematics showed that pattern classifications of complex limb movements were possible (e.g. Waldert et al., 2008; Lv et al., 2010; Georgopoulos et al., 2005; Pistohl et al., 2008; Hajipour Sardouie and Shamsollahi, 2012; Sugata et al., 2012; Antelis et al., 2013; Langheim et al., 2006). The current chapter extended these results. MVPA results on clockwise vs. anti-clockwise movements showed that the direction of circular movement can be decoded from MEG activity throughout the trial (Figures 5.8 and 5.9). For the first phase of the trial, the temporal generalisation plots (Figure 5.8A) implied an oscillating/reactivated nature of multivariate patterns of directional information (King and Dehaene, 2014, see also Figure 2.8). The alternating pattern of circular movements when performing clockwise or anti-clockwise movement may correspond to the observed limb kinematics, because the push and pull movement engages the flexor and extensor muscles inversely. The circular movements can elicit an alternating pattern of contracting and relaxing arm's muscle groups that led to the observed pattern of classifier performance (Oliver et al., 2011; Waldert et al., 2008; Ofner et al., 2017; Fuchs et al., 2000).

The theoretical account of the observed temporal generalisation pattern can be a reflection of periodic muscle dynamics (Ofner et al., 2017) was further supported by the MVPA result in the second phase (Figure 5.9). When the MEG data was time-locked to the onset of the second phase, we observed only a narrow window of the temporal generalisation (Figure 5.9A) and low classification performance (Figure 5.9C). When the MEG data was time-locked to the onset of Change RT, the pattern of the temporal generalisation similar to that in the first phase, suggesting the importance of the movement features alignment (Leuthold et al., 2004).

It is worth noting that significant classification of movement direction appeared as early as 0.25 s after stimulus onset (Figure 5.8A) and 0.5 s prior to movement onset (Figure 5.8B). This is consistent with the motor preparatory activity reported in the literature (Thura and Cisek, 2014; Haegens et al., 2011; Masaki et al., 2004) as an indicator of the subsequent choice response (Donner et al., 2009). That is, the multivariate patterns carry information of unimanual and complex movements prior to the initiation of the movement.

Patterns of motion coherence

Because the binary classification between high vs low coherence trials was performed irrespective of the direction of the movement, each class contained balanced trials of the clockwise and the anti-clockwise movement. Therefore, the significant pattern information between motion coherence (Figure 5.10) cannot be readily attributed to the difference of movement direction, but reflected a continuous sensitivity towards sensory inputs independent of continuous movements.

When participants maintained the same movement direction throughout the trial, the SVM classifier was able to distinguish the high from low coherence trials in the second phase (Figure 5.10A and 5.10C). The cluster of significant classification started around 0.5 s from the onset of the second phase, comparable to the mean Change RT (Figure 5.1B), and its temporal generalization results implied a sustained categorisation between high vs low representations.

Interestingly, the same binary classification was not significant in trials with a change of movement direction (Figure 5.10B). According to the affordance competition hypothesis (Cisek and Kalaska, 2010; Wolpert and Landy, 2012, see also Figure 2.4), the decision is essentially an action selection process. In this context, the null MVPA result form the trials with a change of movement direction suggested the quality of sensory inputs did not elicit a stable representation after participants' altered their movement direction, as the sensory information was no longer needed to guide further actions (Cisek and Kalaska, 2010).

5.4.3 Conclusion

This chapter set to examine the electrophysiological signatures of continuous responses to perceptual decisions in a MEG experiment, using an experimental paradigm validated in Chapter 4. The temporal pattern of SVM classifications showed that the MEG representation of circular movements was not abstract and generalisable in time, but possibly linked to the kinematics of arm movements. The phase of the circular movement was an important feature of the signal. During the second phase of the trial, aligning the signal to the movement milestone (Change RT) improved classification performance and temporal generalisation patterns. Moreover, the choice direction of the complex continuous movement can be distinguished up to 0.5 s prior to movement onset. This result linked continuous responses with the previous research on the encoding of action plans of discrete responses (e.g. Thura and Cisek, 2014; Haegens et al., 2011; Masaki et al., 2004; Donner et al., 2009).

Overall, these results supported the use of the continuous movements in perceptual decisions. The responses elicited distinct multivariate MEG patterns that were sensitive to movement characteristics as well as sensory information. In Chapter 6, I capitalised these features to investigate whether continuous movements, when chosen voluntarily, could establish casual expectations of sensory information.

Chapter 6

Continuous action-perception congruency

6.1 Introduction

Chapters 4 and 5 examined how participants performed continuous actions in response to the visual stimulus, and how ongoing actions may affect concurrent perceptual decisions. The previous chapter also observed the temporal MEG patterns that distinguish the direction of continuous movements. In this chapter I built on these results and investigated whether continuous voluntary actions can shape the MEG responses to subsequent visual perception.

6.1.1 Background

Voluntary action and the predictive coding framework

The embodied cognition account outlined in Chapter 2, highlighted the need to consider actions in the context of their interactions with the environment. The voluntary actions, rather than passive sensations, are needed by an intelligent agent to interact with the environment (Clark, 1999, 2013; Shepard, 1984). Here, a voluntary action as opposed to an involuntary act such as a knee-jerk reaction, can be defined as intentional behaviour driven by internal factors (O'Regan and Noë, 2001). The internal factors that guide voluntary actions may include bias, preferences, expected reward, amongst many others (Passingham et al., 2010; Haggard, 2008; Schüür and Haggard, 2011).

The temporal proximity and contingency between an action and its predictive outcome impacts on the subjective acknowledgement of volitional control (e.g., pulling a trigger leads to firing a gun) (Beck et al., 2017). The extent of how voluntary the action is, facilitates the binding between the action and its consequences (Haggard et al., 2002; Moore et al., 2009). The impairments in the perception of action-outcome causality have been associated with psychiatric symptoms in e.g., schizophrenia (Fletcher and Frith, 2009; den Ouden et al., 2012). On the other hand, the prior expectation of an imminent outcome can in turn bias a voluntary behaviour. For example, in a RDM-based perceptual decision task (Summerfield and de Lange, 2014), the behavioural performance was improved by introducing informative cues about the future stimuli.

Therefore, the brain can generate predictions that both influence and are influenced by the voluntary behaviour (Kok et al., 2012, 2019, 2017; Rees and Frith, 1998). In the predictive coding framework (Friston, 2005), the brain constantly generates active inferences (i.e., predictions) based on prior knowledge and compare them with incoming information. The interplay between voluntary actions and active inferences (Friston, 2005) minimises the prediction error, the mismatch between the expectation and the experienced outcome (Bubic et al., 2010; Friston, 2010, 2009).

The oddball paradigm and mismatch negativity

The oddball paradigm is a common experimental design to evaluate the influence of prior expectations during attentional or basic sensory processes. The paradigm involves an manipulation of the relative occurrence probabilities of regular and odd/deviant events (stimuli). The regular stimuli were identical or similar to each other with a higher occurrence probability, which are used to establish the expectations. The odd stimuli are physically distinct from the regular ones and with a lower occurrence probability. The occurrence of an odd stimulus would therefore be perceived as an unexpected event.

In active oddball experiments, participants' attention was directed towards the odd and regular events, for example, when instructed to count the occurrence of odd stimuli. The ERP component P300 (also the N2b) differs between the odd and regular stimuli in active oddball experiments (Polich, 2007; Näätänen et al., 2007). The P300 amplitude is negatively related to the occurrence probability of odd stimuli, and its variability is associated with the subjective evaluation of the frequency of odd stimuli (Sutton et al., 1965; Mars et al., 2008). These results suggested that the P300 component is sensitive to events that violate expectations (Sutton et al., 1965).

In passive oddball experiments, participants' attention was directed away from the stimulus under investigation, for example, when instructed to watch movies during auditory regular and odd stimulus presentation. Contrasting between odd and regular events in passive oddball experiments resulted a fronto-central negative potential at 150–250 ms, namely the mismatch negativity (MMN). The MMN is thought to reflect expectation violation during early sensory processing of physical characteristics (Sams et al., 1983; Näätänen and Gaillard, 1983). The source of MMN can be specific to the sensory modality of the stimulus. For auditory MMN, the main source of MMN is in the primary auditory cortex (Sams et al., 1983; Näätänen and Gaillard, 1983; Näätänen et al., 2007). Visual MMN has its neural source in the V1, and the MMN evoked by tactile stimuli is localised in the somatosensory cortex (Huang et al., 2005; Stefanics et al., 2019, 2014).

In addition to the modality-specific sources, contrasting between odd and regular stimulus also showed a across-modality, wide involvement of the fronto-parietal network, including DLPFC, anterior cingulate cortex and the supramarginal gyrus (Huang et al., 2005). Furthermore, along with changes in the time-domain (Sams et al., 1983; Näätänen and Gaillard, 1983), the oscillatory markers of the odd vs. regular stimulus were found in alpha, delta and theta bands (Ishii et al., 2009).

The predictive coding framework has been used to explain the computational mechanism underlying the results from oddball experiments (Stefanics et al., 2014). Based on the short-term memory trace, frequent presentations of regular stimuli establish an expectation or prediction. The presentation of an odd event would violate this expectation, which give rise to a prediction error during early sensory processing, leading to the observed difference in MEG or EEG signals.

Action-perception congruency

The affordance competition hypothesis (Chapter 2, Cisek and Kalaska (2010)) suggested that action and perception processing can co-exist in parallel (Clark, 1999; Shepard, 1984). A similar proposition came from the common coding theory, suggesting that shared spatial or temporal features between action and perception facilitate information processing. (Prinz, 1997; Hommel et al., 2001).

The influence of actions upon perception has been reported elsewhere. In a binocular rivalry paradigm, when the motion of one rival stimulus was consistent with participants' voluntary hand movements, stable percept of that stimulus were extended (Maruya et al., 2007). More evidence of the impact of action on perception is provided by comparing between discrete and continuous responses (Beets et al., 2010). In a motion discrimination task (clockwise vs. anticlockwise), participants responded with key presses or through continuous rotations of a manipulandum. The percept stabilised only when the action was congruent with the stimulus (i.e., participants were rotating the manipulandum in the same direction as the stimulus), but not when using key presses. Furthermore, when action and perception share the same goal (i.e., direction), action preparation, instead of action itself, is sufficient to bias subsequent perceptual decisions (Wohlschläger, 2000).

6.1.2 The current experiment

This chapter proposed a new action-perception congruency (APC) task (Figure 6.1). It was designed to test a main research question: can voluntarily-initiated, continuous action establish causal expectations of subsequent perception?

The task design has three main ingredients. First, participants were instructed

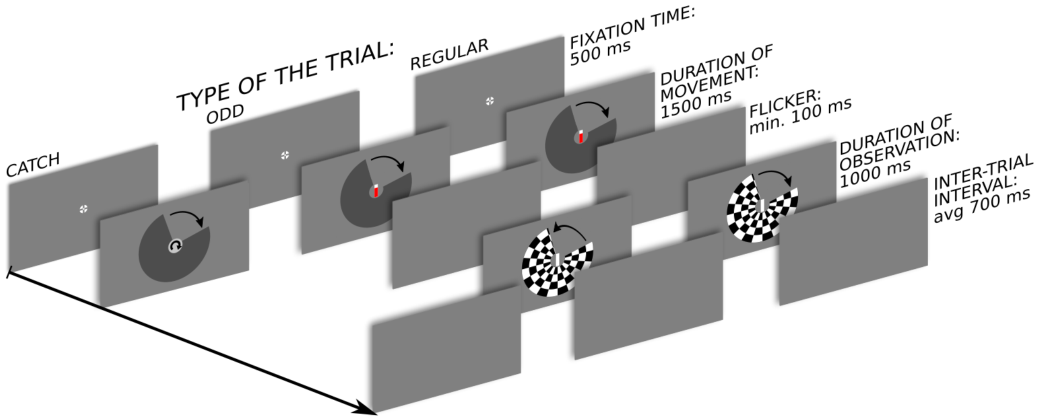

Figure 6.1: The diagram of the action-perception congruency task.

to make a clockwise or anti-clockwise joystick rotation in the first half of a trial, similar to the continuous actions in Chapters 4 and 5. Crucially, The participants can choose the movement direction voluntarily at the beginning of each trial.

Second, the task aimed to establish a causal link between continuous actions and subsequent visual stimulus, with the latter presented in the second half of a trial. During rotation actions, the participants had a full control on the direction and the speed of motion: the circular joystick movement is translated directly to the angular displacement of a wedge shape. After the action and a short delay (100 ms), the participants passively observed the same wedge shape to rotate continually on the screen, and the wedge shape filled with a 8 Hz flickering checkerboard pattern to elicit strong visual evoke responses (Muthukumaraswamy and Singh, 2008). The rotation of the checkerboard pattern started from the same position as the endpoint of participants' voluntary movement, which further facilitates the causal link between the movement and the visual stimulus.

Third, to establish a statistical expectation, in majority of the trials the direction (i.e., clockwise or anti-clockwise) of the checkerboard pattern was congruent with the participants' voluntary movement (regular trials). In a small subset (20%) of pseudo-randomly placed trials, the checkerboard pattern had the opposite (incongruent) rotation direction to the participants' actions (odd trials). As in other oddball experiments, the participants were instructed to count the occurrences of the incongruent perceptual experience.

I set out to test two main lines of hypotheses. First, if participants established an expectation of subsequent visual information on the basis of their voluntary movement direction, I hypothesised a change in MEG univariate activities or multivariate patterns when the expectation was violated in incongruent trials. Both deviance detection (Stefanics et al., 2014; Näätänen et al., 2007; Polich, 2007; Kimura et al., 2009) and sensory templates (Kok et al., 2017) have been found in early sensory cortices. This evidence suggested that the response to the oddball visual stimulus in the APC task could originate from the visual cortex. The common-coding theory (Hommel et al., 2001; Prinz, 1997) suggested that a stimulus causally associated with an action and sharing its spatio-temporal profile may lead to re-activation in the sensorimotor cortices (Hughes and Waszak, 2011). Therefore, in this chapter, the univariate analysis on the congruency effect was focused on two MEG sensor groups: the occipital sensors over the visual cortex and the central sensors over the sensorimotor cortices. For multivariate analyses, all MEG sensors were included in the training and testing procedures, because less relevant data features (i.e., sensors) will be down weighted after the training stage.

In conventional EEG/MEG oddball paradigms (Näätänen et al., 2007; Mars et al., 2008), the congruency effect (i.e., oddball vs. standard stimuli) is commonly characterised by the MMN (e.g. Näätänen et al., 2007) and P300 (e.g, Sutton et al., 1965; Mars et al., 2008) components. The current experiment included a complex chain of events to elicit the congruency effect within a single trial, from a voluntary decision to continuous action, and then to congruent/incongruent continuous visual stimulus. Here, the perceptual congruency originated from continuous actions, a process likely involving multiple cortical networks (Gentili et al., 2011; Gupta and Chen, 2016). As a result, I performed time-resolved univariate and multivariate analyses throughout the time course of a trial, without making an *a priori* assumption of the time window of interest.

Second, I was expecting to replicate the MVPA results in Chapter 5, on the significant classification and temporal generalisation pattern of clockwise vs. anti-clockwise stable movement. However, voluntary and externally triggered actions are associated with distinct brain networks. Voluntary or endogenous actions are associated with networks consisting of the medial prefrontal cortex, preSMA and SMA. It is thought that this medial-frontal network supports self-generated actions and deliberation. In contract, externally cued actions are associated with a lateral network, including the parietal cortex, the motor and premotor cortices (Passingham et al., 2010; Schüür and Haggard, 2011; Haggard, 2008). Therefore, multivariate MEG patterns of continuous action direction in the APC task may be different from those observed in Chapter 5. In addition, I would expect an increase in the gamma-band oscillatory power during the movement period, which has been associated with self-paced movements in previous studies (e.g. Cheyne et al., 2008).

6.2 Methods

6.2.1 Participants

Twenty-four participants (17 females, seven males, age range 18-28, M = 21.25 years, SD = 2.67 years) took part in the study following a briefing and written informed consent. All the participants were right handed. All the participants had normal or corrected-to-normal vision. None of the participants reported a history of motor impairments or neurological disorders. The study was approved by the Cardiff University School of Psychology Ethics Committee.

6.2.2 Apparatus

The joystick data was acquired in the same way as in the Chapter 5.

6.2.3 Experimental Design

Each participant completed the action-perception congruency (APC) task during two sessions of MEG recording on different days. Each session contained 150 trials and each trial consisted of two stages, an action stage and a subse-

Figure 6.2: **Action-Perception Congruency. Movement Phase** The video of the movement phase. Link: https://www.youtube.com/watch?v=jEdheAvNTOk

quent observation stage.

In the action stage, participants rotated a joystick to control the direction of of a low contrast wedge shape (circle with 90° sector removed) (Figure 6.1). After a 500 ms fixation period, the participants initiated circular joystick movements in either clockwise or anti-clockwise direction. The action stage lasted 1000 ms, sufficient for 2 to 4 circles of rotations. The remaining time of the action stage was indicated by a red time bar presented in the middle of the screen. Time bar was shrinking in size proportionally to the elapsed time (i.e., 0 ms - 100%, 1500 ms - 0%). As in Chapters 4-5, to ensure a common starting point of the rotation movement, a trial could proceed only if the joystick was at its neutral position. The participants was instructed to stop continuous movements by the end of the action stage (i.e., before the time bar runs out). To avoid the contamination of the subsequent observation stage, there was a 100 ms gap after action termination or the end of action stage, whichever occurred latter. Moreover, the observation stage of a trial would start only if the joystick was returned to its neutral position.

In the observation stage, participants were presented with a rotating flickering

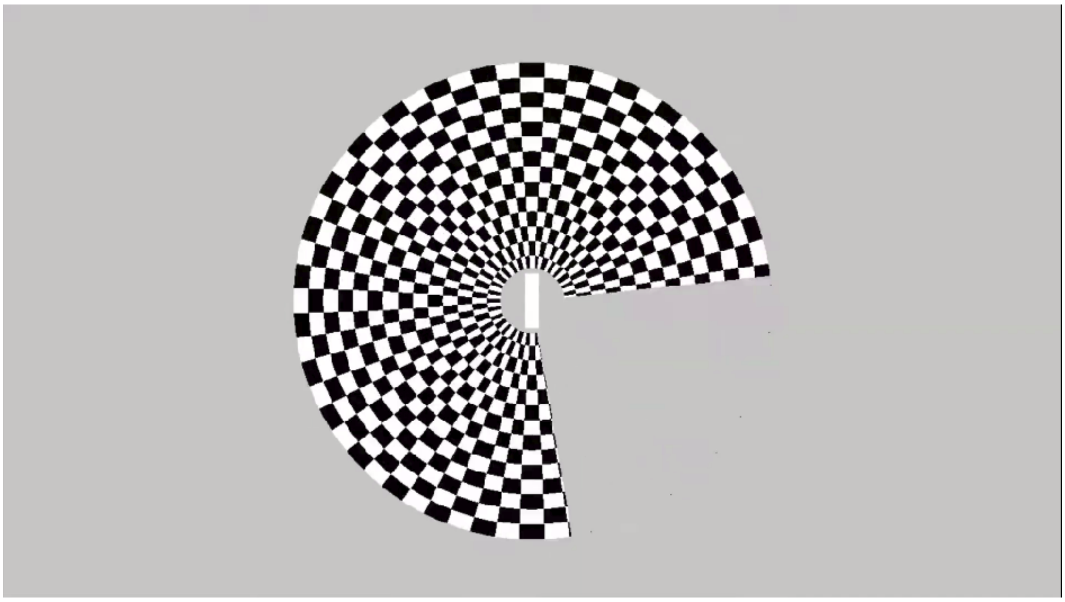

Figure 6.3: **Action-Perception Congruency. Observation Phase** The video of the observation phase. Link: https://www.youtube.com/watch?v=kL3FXCOjSEs

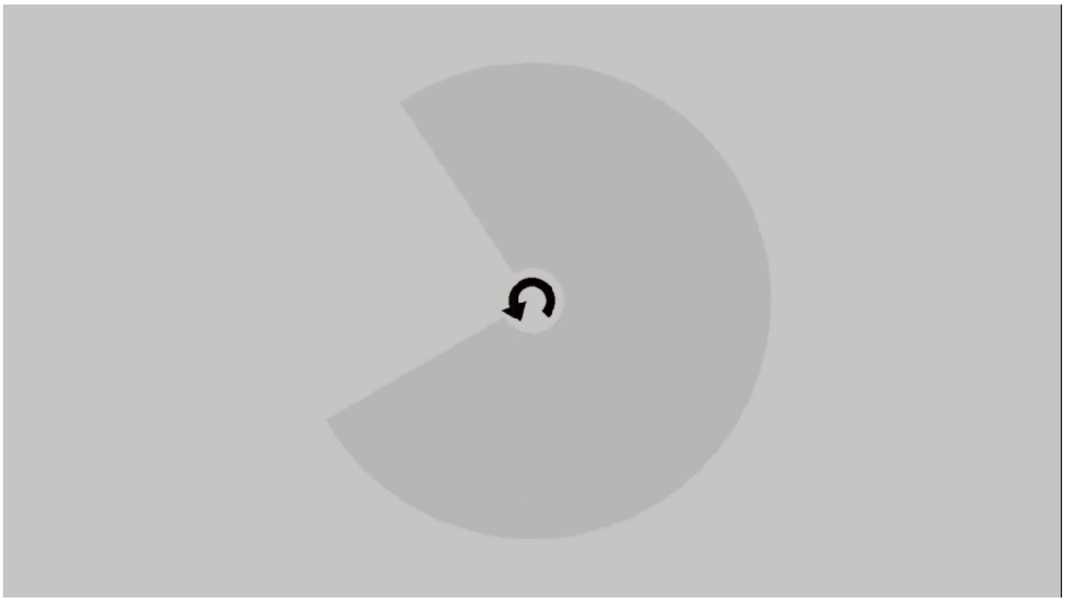

Figure 6.4: **Action-Perception Congruency. Catch Trial** The video of the catch trial. Link: https://www.youtube.com/watch?v=I7Iz48jV24o

checkerboard of the same shape as the low contrast wedge shape in the action stage (for detailed presentation of the stimulus see: Figure 6.2). The visual stimulus lasted for 1500 ms. In a regular trial, the checkerboard shape rotated in the same direction as the voluntary movement (for detailed presentation of the stimulus see: Figure 6.3). In an odd trial, the checkerboard shape rotated in the direction opposite to the movement. Participants were instructed to count the number of trials in which the checkerboard shape moved to the opposite direction of their voluntary movements. The direction of the movement during the action stage was established based on the M score derived from frame-by-frame recording of the circular movement during the action phase of the trial. M denotes the averaged frame-by-frame angular displacement multiplied by the radius (See: Equation 6.1). $M > 0$ indicates a predominantly anti-clockwise movement, and $M < 0$ indicates an anti-clockwise movement.

$$M = \frac{\Sigma_{n=0}^{f}\left(\frac{\Delta\Theta}{\Delta t} r\right)}{n}$$

Equation 6.1: M - movement direction metric, $f - 1$ - number of frames, $\Delta\Theta$ - angle change between two subsequent frames, Δt - time between two frames ($\frac{1}{120} s$), r - radius

The two MEG sessions comprised a total of 20 blocks with 15 trials each, including 73.33% (220/300) regular trials and 20% (60/300) odd trials. The rest 6.67% (20/300) trials were catch trials. In a catch trial, participants were cued by an arrow in the centre of the screen, which specify the direction to rotate the joystick (i.e., they no longer need to make a voluntary choice) and there was no observation stage at the end of the movement (Figure 6.1). Catch trials were used to promote participants to make a fresh voluntary choice at the beginning of each regular or odd trial (Oppenheimer et al., 2009; Nachev et al., 2005) (for detailed presentation of the stimulus see: Figure 6.4). The order of the trials within each block was pseudo-randomly generated, ensuring the odd trial did not occur at the first or the last in a block, and there were no two consecutive odd trials.

6.2.4 Stimuli

In the action stage, the wedge shape had a diameter of 20° visual angle with a 270° arc. The wedge shape was in light gray (29.18% luminance) with a dark gray background (23.07% luminance), resulted in a 1.22 contrast ratio. The average speed of rotation was controlled by the participants (mean = 7.30 rad/s, std = 2.59 rad/s across participants).

In the observation stage, the stimulus was in the same shape as in the action part. The initial position of the shape matched the last position of the shape in the action stage. The speed of rotation of the shape was constant (average speed, 6.28 rad/s) during the 1000 ms of display. The shape was filled with a circular flickering chequerboard pattern. The pattern consisted of XX concentric cycles and XX angular cycles of black and white patches (21 contrast ratio). The chequerboard patterns were alternating the contrasting blocks with 8 Hz frequency to optimise the visual cortex response (e.g. Muthukumaraswamy and Singh, 2008).

6.2.5 MEG data acquisition and pre-processing

Data acquisition

The MEG data was acquired in the same way as in the Chapter 5.

Data pre-processing

The MEG data was pre-processed in the same way as in the Chapter 5. For the time-domain analysis the data were further low-pass filtered at 30 Hz. Subsequently, the continuous data were divided into epochs of -0.7-1.5 s around the onset of the trial and -0.1-1.0 s around the onset of the observation phase. The epoch was initially baselined using the -0.7 - -0.5 s period before the onset of the trial to accommodate for the longer preparatory activity of the voluntary movement. Second baseline was applied separately to the observation phase to avoid differences in the amplitude caused by the post-movement activity from the previous part of the trail. The period between -0.1-0.0 s before the onset of the observation phase was used In a separate analysis, the data were divided into epochs of -1.0-1.0 s around the onset of the movement during the action stage the trial (see Figure 6.1). For the frequency domain analysis, raw data were further band-passed to extract the functionally relevant frequency bands: alpha band (9-14 Hz), beta band (14-30 Hz), theta band (4-7 Hz), low gamma band (30-80 Hz), and a narrow band of frequencies (7-9 Hz) which correspond to the flickering frequency of the stimuli in the observation phase. From each band-passed data the envelope of the Hilbert transformed signal was obtained. The data for each frequency band were divided in the same manner as for the time-domain analysis. From the envelope of the transformed signal, the evoked response has been subtracted.

6.3 Results

6.3.1 Behavioural results

During the action stage of the APC task, participants performed circular movements with a joystick. Four behavioural measures were compared between odd and regular conditions. First, as in previous chapters, the position of the joystick in Cartesian coordinates was transformed into polar coordinates. The movement onset time was calculated as the time when the joystick left the 20% of its maximum movement radius after fixation offset (Szul et al., 2019). Second, the average speed of movements was calculated as the ratio of the total angular displacement and the duration of the action stage (1.5 s). Third, the movement direction in each trial was quantified by the M score (6.1). The absolute value of the M score depended on the relative difference of the movement duration towards the two directions, and the sign of the M score depended on the predominant movement direction during the action stage. $M > 0$ denoted a predominant anti-clockwise movement, and $M < 0$ denoted a predominant clockwise movement. Forth, although the participants were instructed to stop the rotation movement at the end of the 1500 ms action stage, the nature of a continuous action often led to overshoot after the 1500 ms deadline. The duration between the end of the designated action stage (i.e., 1500 ms after fixation offset) and the end of participants' actual movement was measured as the overshoot delay (including a fixed 100 ms delay).

The movement heat map (Figure 6.5) indicated the participants performed most of the circular movements between 40 and 100 % of the joystick's maximum movement range. Since the participants were not aware of the condition prior to the observation stage, one would not expect difference in behavioural measures between regular and odd trials. To validate this prediction, I used a Bayesian and frequentist t-tests (see the Analysis Section in the Chapter 4 for technical details of the analysis). The movement onset time did not differ between the odd and regular conditions (Figure 6.6A; $\mathrm{BF}_{10} = 0.694$, anecdotal evidence; $t(23) = -1.645, p = 0.114$). Similarly, the average movement speed (Figure 6.6B; $\mathrm{BF}_{10} = 0.489$, anecdotal evidence; $t(23) = 1.366, p = 0.185$) and the overshoot delay (Figure 6.6D; $\mathrm{BF}_{10} = 0.290$, anecdotal evidence; $t(23) = -0.817, p = 0.422$) did not differ between the odd and regular trials. Finally, To compare the distributions of the M score pooled across all participants (a trial-by-trial movement direction summary, Figure 6.6C), we used a non-parametric two sample Kolmogorov-Smirnov (KS) test (Pratt and Gibbons, 1981), as the direction distributions were bi-modal. The distribution of the M score did not differ between conditions ($KSstatistic = 0.035, p = 0.117$).

6.3.2 MEG results

Evoked response fields

The pre-processed MEG data was further band-pass filtered between 0.1 and 30 Hz and epoched from -0.6 s (before the fixation onset) to the end of the observation stage. Every epoch contained 0.1 s of baseline period, 0.5 s of fixation duration, 1.5 s of the action stage phase, 0.1 s gap and 1 s of the observation stage (Figure 6.1). The overshoot delay between the end of the action stage and 0.1 s prior to the onset of the action stage was removed (Figure 6.6D). A linear detrending was applied to every epoch with a baseline correction from -0.6 s to -0.5 s. Due to the overly long duration of epochs, a second baseline correction was applied to the data segments of the observation stage, using the averaged activity from the 0.1 s gap prior to the onset of the

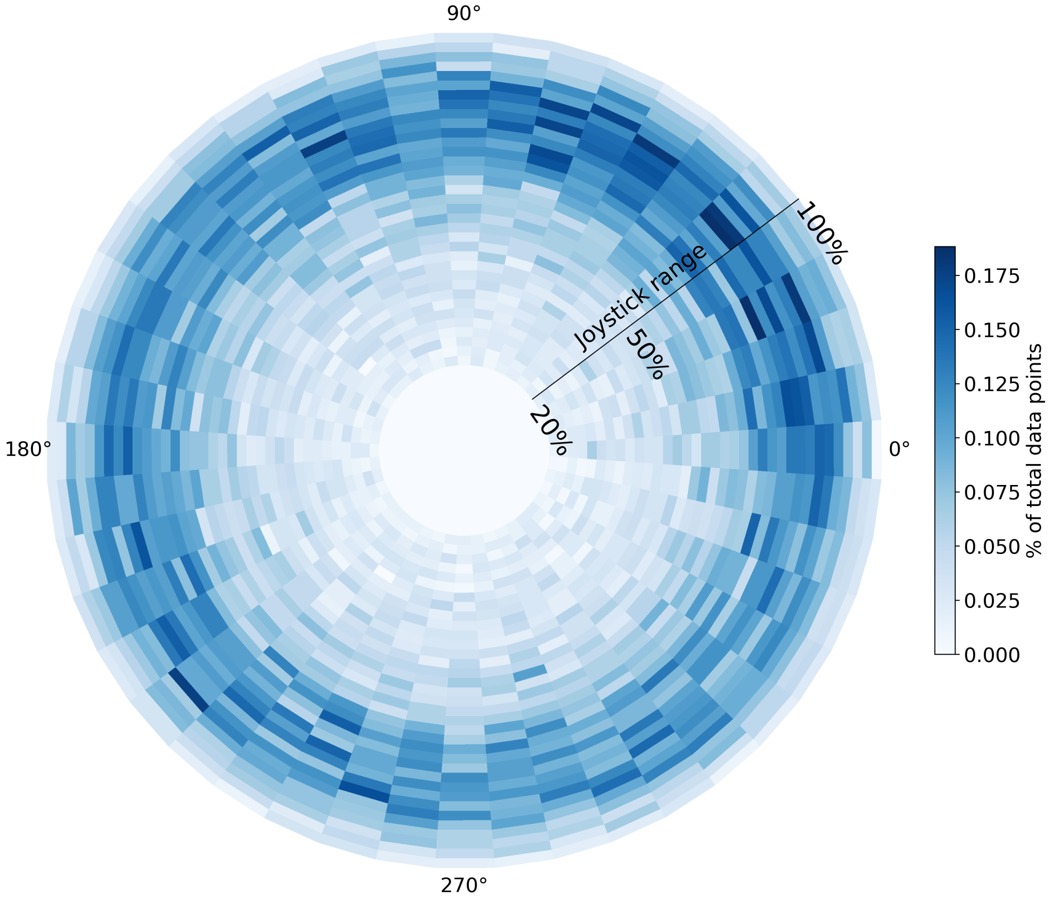

Figure 6.5: JOYSTICK MOVEMENT HEAT MAP. The heat map represents the joystick positions pooled across all the participants from all the trials. The joystick position was initially recorded in Cartesian coordinates and transformed into polar coordinates, which represent circular motion as an angular displacement a distance from the centre of the joystick. The area within 20% of the joystick range was left blank as movements in this area could be due to the lack of resisting force of the joystick.

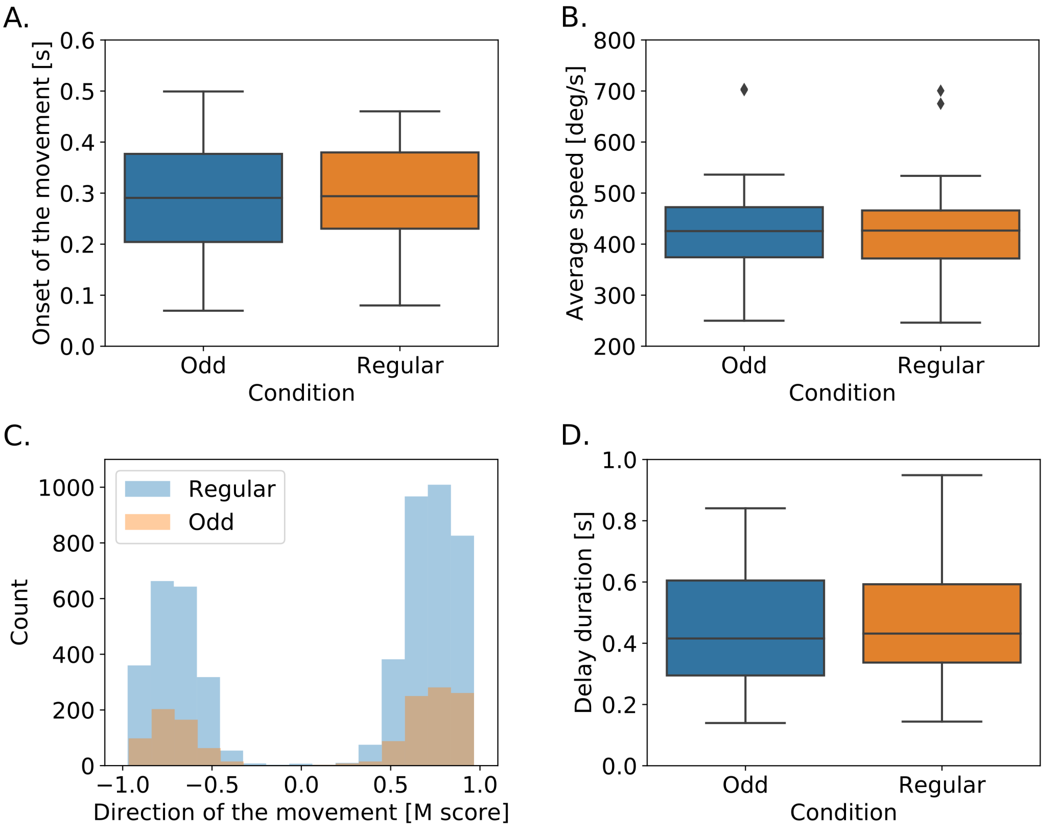

Figure 6.6: SUMMARY OF THE BEHAVIOURAL MEASURES: **A)** Mean movement onset. **B)** The average angular displacement during the action stage. **C)** Distribution of the M scores (Equation 6.1) pooled across all participants, illustrating the predominant direction of rotation movements. **D)** Delay between the end of the action stage and the onset of the observation stage, including a minimum fixed delay of 100 ms. Box and whiskers plots (**A, B, D**), are based on the interquartile range.

action stage. The sensor groupings were based on CTF sensor labels, including right and left occipital sensors (19 each; Figure 6.7) as well as right and left central sensors (30 each; Figure 6.8) close to the sensory-motor cortex.

For each participant, the ERFs from regular and odd trials were averaged separately using a robust average procedure (Wilcox and Rousselet, 2018) (5% of the extreme ends of the distribution were discarded). Trimmed mean provides a reliable estimation of the central tendency for mixed distributions, thus deemed an appropriate way to deal with averaging from uneven amount of samples between odd and regular trials (Leonowicz et al., 2005). Further, the ERFs were averaged across the channels in each sensor grouping. Paired t-test with cluster permutation correction (Maris and Oostenveld, 2007) was used to compare the ERFs between odd and regular conditions (see: Section 5.3 for more detailed description of analysis and reporting of the results). After correction of multiple comparison, both action (Figures 6.7) and observation (Figure 6.8) stages showed no ERF difference in any sensor groupings between the odd and regular conditions.

Oscillatory power during action and observation stages

To calculate the oscillatory power in different frequency bands, the pre-processed MEG data was band-pass filtered into the alpha band (9-14 Hz), beta band (14-30 Hz), theta band (4-7 Hz), low gamma band (30-80 Hz) and a stimulus specific band (7-9 Hz, containing the frequency of flicking checkerboard). The filtered MEG dta was then epoched as in the ERF analysis. In an additional analysis, a new set of 2-second epochs were extracted, which were centred on the onset of the movement in each trial.

For each frequency band, the Hilbert envelop was calculated from each trial, and the envelops were averaged separately for odd and regular conditions Similar to the ERF analysis, paired-test with cluster permutation correction showed no significant difference in oscillatory powers of any sensor groupings between odd and regular trials (Figures 6.9, 6.10 and 6.11).

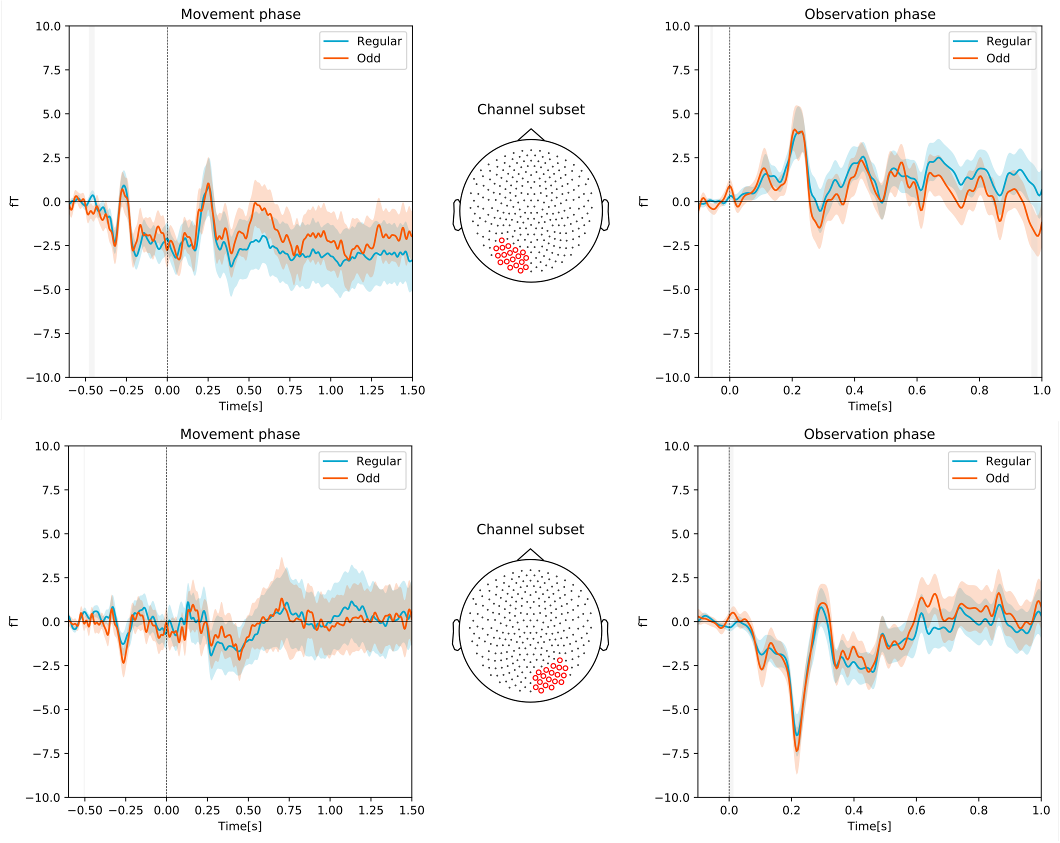

Figure 6.7: The time course of the ERF activity averaged over the set of occipitally located MEG sensors (indicated with red markers on the topography map). The solid line denotes the mean ERF activity, the shaded area denotes a standard error of the mean. We observed no differences in the ERF time course between the incongruent and regular trials in the movement phase as well as in the observation phase.

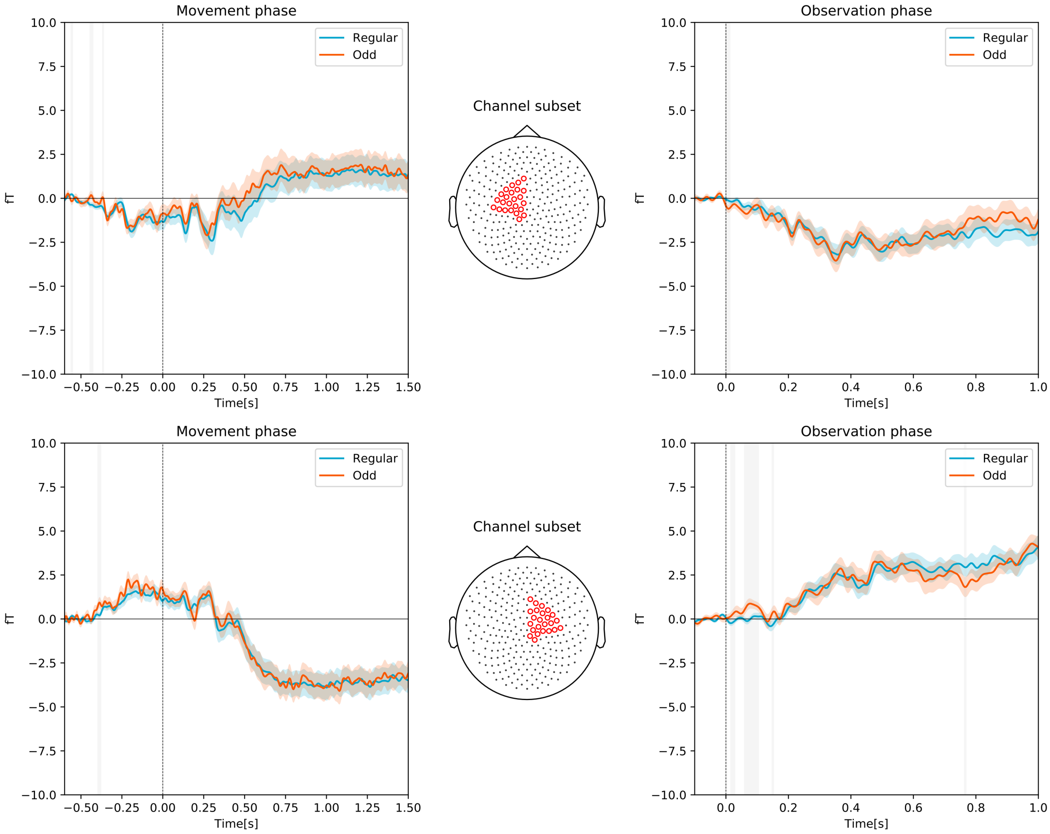

Figure 6.8: The time course of the ERF activity averaged over the set of centrally located MEG sensors (indicated with red markers on the topography map). The solid line denotes the mean ERF activity, the shaded area denotes a standard error of the mean. We observed no differences in the ERF time course between the incongruent and regular trials in the movement phase as well as in the observation phase.

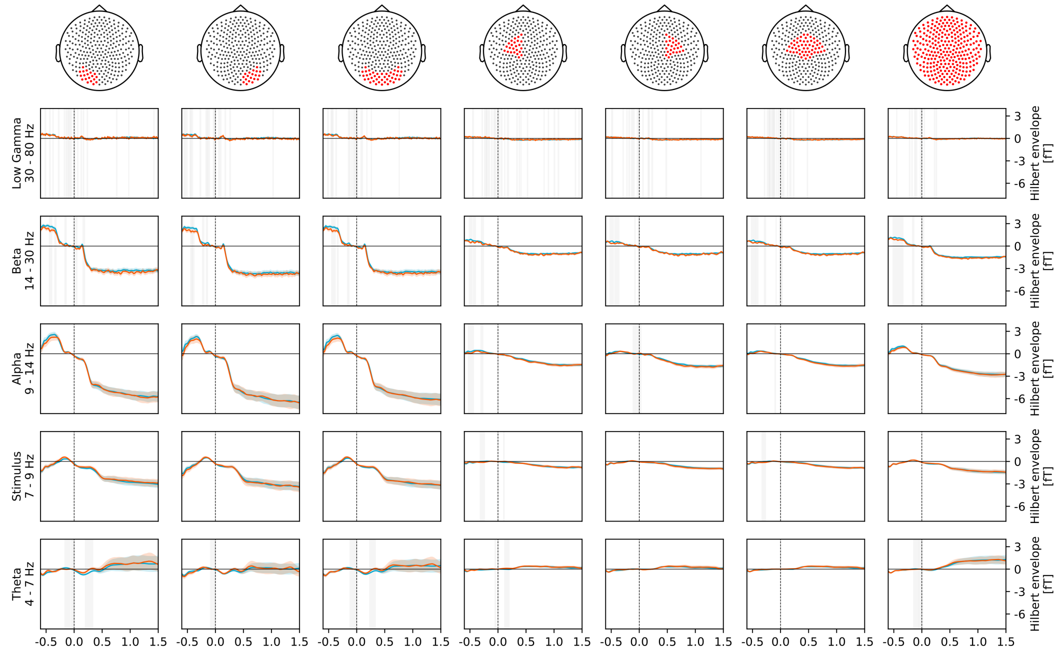

Figure 6.9: The Oscillatory power in the action stage. Figure shows the Hilbert envelope of each frequency band for different sensor groupings. The epochs were aligned to the onset of fixation (Figure 6.1). Solid line denote the mean oscillatory power of odd (orange) and regular (blue) conditions. Shaded areas denote the standard error of the mean across participants.

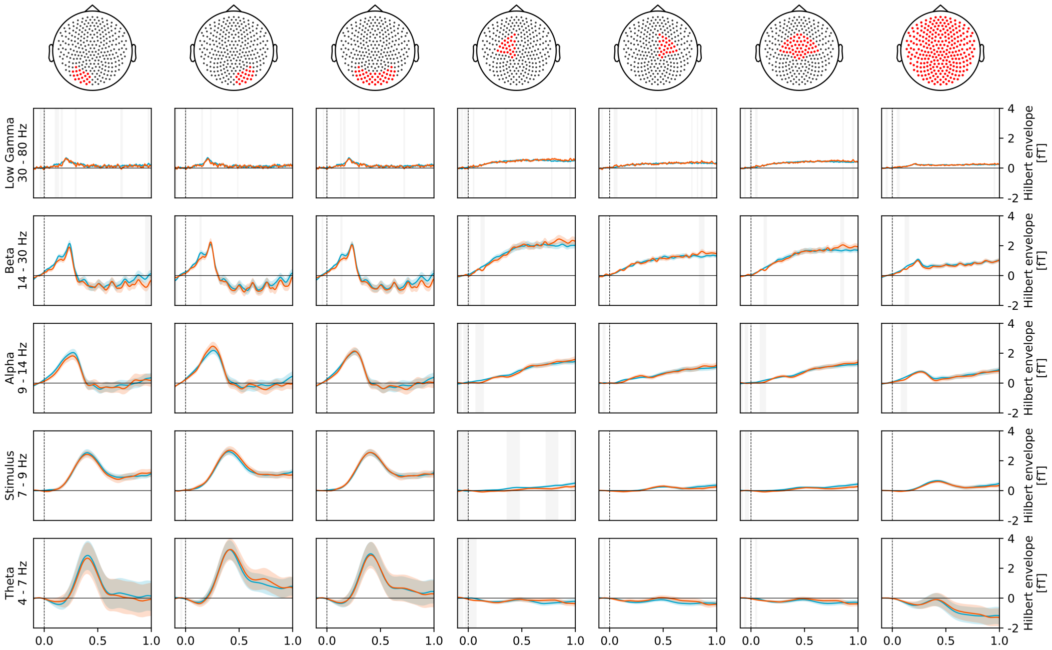

Figure 6.10: The Oscillatory power in the observation stage. Figure shows the Hilbert envelope of each frequency band for different sensor groupings. The epochs were aligned to the onset of the observation stage (Figure 6.1). Solid line denote the mean oscillatory power of odd (orange) and regular (blue) conditions. Shaded areas denote the standard error of the mean across participants.

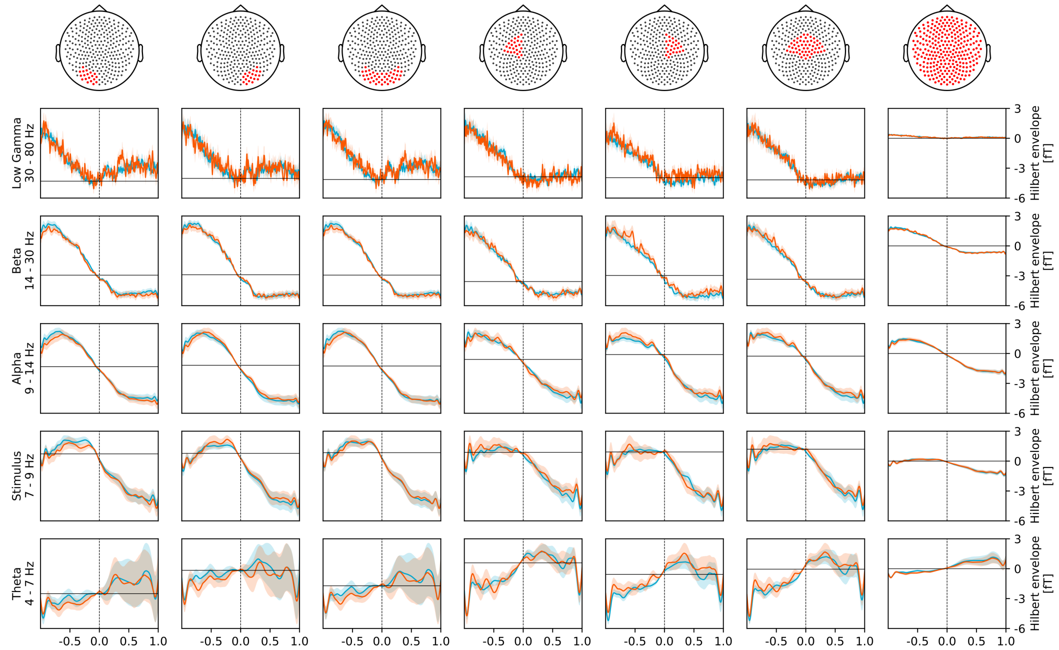

Figure 6.11: The Hilbert envelope of each frequency band for different sensor groupings. The epochs were aligned to the onset of movement (when the joystick left its 20% maximum radius) (Figure 6.1). The colour scheme is the same as in Figure 6.10.

Multivariate pattern analysis (MVPA)

Pre-processed MEG data was band-pass filtered between 0.1 and 30 Hz and epoched as in the ERF analysis. For each participant and each time point of epochs, three analyses were conducted. First, a binary classification between clockwise and anti-clockwise movements, with labels of trials determined by the M score. Second, a binary classification between odd and regular conditions. Third, the MEG data in the action stage was realigned to the movement onset, and the binary classification between clockwise and anti-clockwise movements were conducted.

I applied the analysis pipeline outlined in Section 2.3.4. Each analysis included all the MEG sensors. For each classification problem, a 10-fold cross-validation procedure was conducted. In each cross-validation, the data was standardised using a robust scaling method. A PCA was conducted on the training set to identify principle components that explained ¿99% of data variance. Both training and test sets were then projected to the reduced space defined by the chosen principle components. A linear support vector machine (SVM) classifier with LASSO regularisation was used to train and test the multivariate patterns. Furthermore, the temporal generalisation procedure was applied to determine the temporal patterns of the information representations. That is, the SVM classifier was trained on one time point and tested in the data at all time points (King and Dehaene, 2014).

Classification performance was evaluated using the area under the receiver operating characteristic curve (ROC AUC). If $AUC = 0.5$, the classification is uninformative and the classifier cannot separate between the two classes. If $AUC > 0.5$, multivariate patterns contain information to distinguish between the two classes. If $AUC < 0.5$, the classifier is correctly predicting the opposite class (Bradley, 1997).

The classification of regular vs odd conditions posed a problem of unequal numbers of trials between the two conditions (73.33% regular vs 20% odd). I used under-sampling to randomly select a subset of regular trials to match to the amount of odd trials. This under-sampling was repeated 20 iterations. For each of the 20 iterations,, the same MVPA pipeline was applied to the odd trials and sampled regular trials.

The MVPA analysis resulted in temporal generalisation maps for movement classification (Figure 6.12), congruency classification (Figure 6.13) and movement classification with data aligned to movement onset (Figure 6.14). Classification performance was evaluated with a one-sample t-test against a 50% chance level and spatial clustering permutations to correct for multiple comparisons (Maris and Oostenveld, 2007) which returned. The diagonal values of temporal generalisation maps (Figure 6.15) indicated the classification performance for the classifier trained and tested on data from the same time point.

We observed a significant, above the chance level classification performance for the direction of the movement. Model also managed to appropriately classify the movement coherent with the prior action (Figure 6.12). The ramping up temporal generalisation during the movement phase was observed for the signal aligned to the trial onset. The same signal, temporally aligned to the response onset, yielded a reactivated or oscillatory pattern of generalisation (Figure 6.14). The classification of congruent versus incongruent trials yielded a pattern of significant classification performance during the observation phase (Figure 6.13).

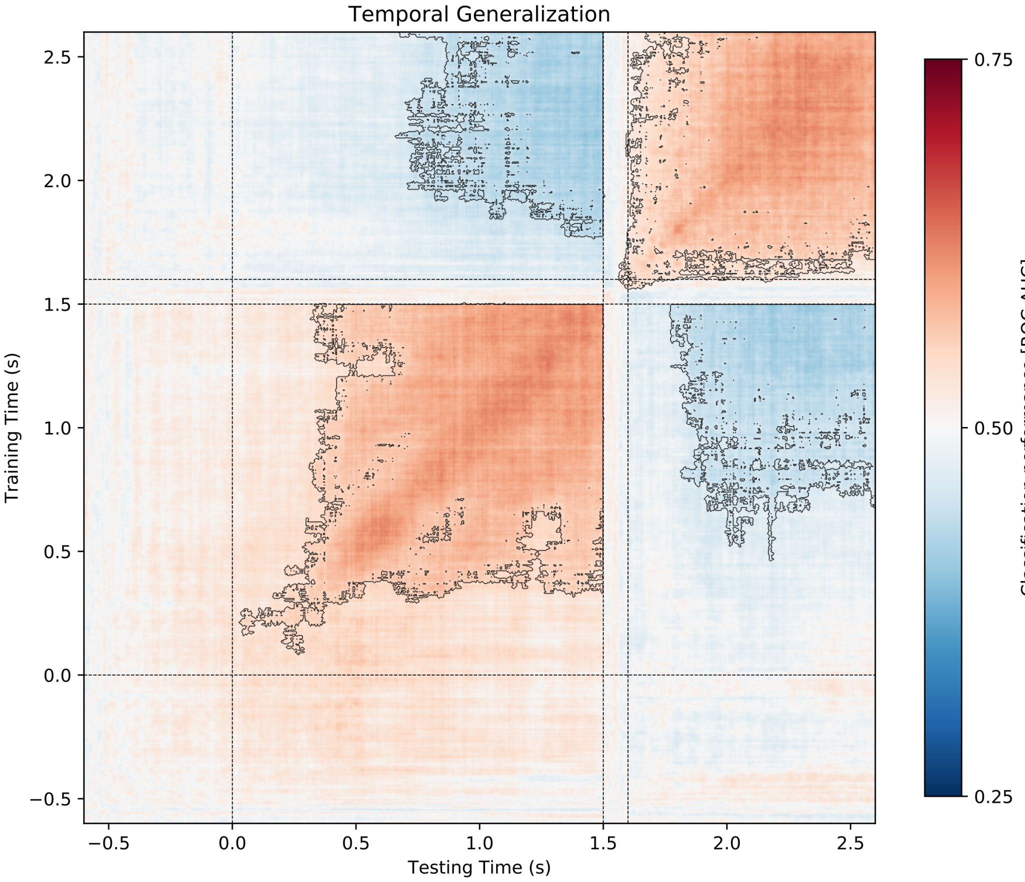

Figure 6.12: Temporal generalisation map of the clockwise vs anticlockwise movement classification. The map includes the action stage aligned to the onset of the trial (0 - 1.5 s) and the observation state (1.6 - 2.6 s). The baselines of the signal were at the beginning of the epoch (-0.6 - -0.5 s) and before the onset of the observation stage (1.5 - 1.6 s). The classification was based on the sign of the M score (see: Equation 6.1). The colourmap indicates the classification performance (ROC AUC). Black outlines denote the clusters of the time that differ ($p < 0.05$) from the chance level (50%).

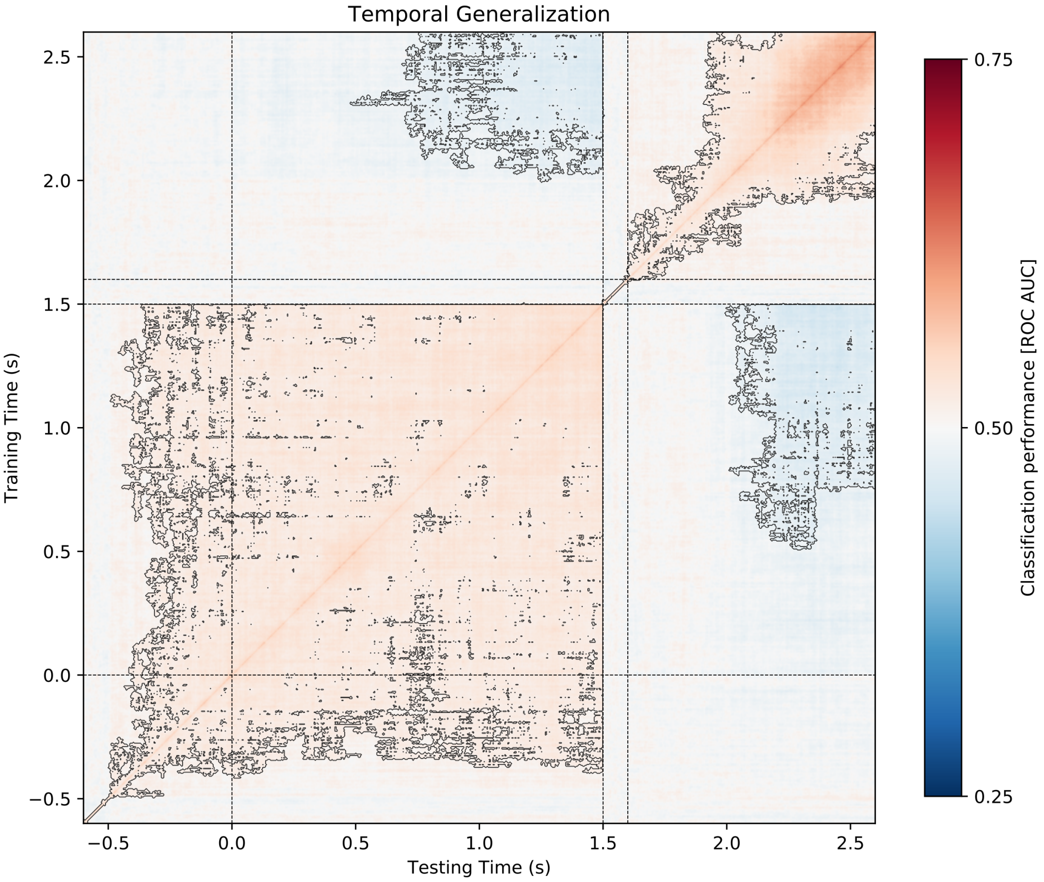

Figure 6.13: Temporal generalisation map of the odd vs regular trials. The classification was based whether the checkerboard motion in the observation stage was incongruent (odd) or congruent (regular) with the movement. The analysis included the full duration of the trial, including a 0.5 s window before the onset of the self-generated movement ($t = 0s$) The colour scheme and epoch timing is the same as in Figure 6.12. The colourmap indicates the classification performance (ROC AUC). Black outlines denote the clusters of the time that differ ($p < 0.05$) from the chance level (50%).

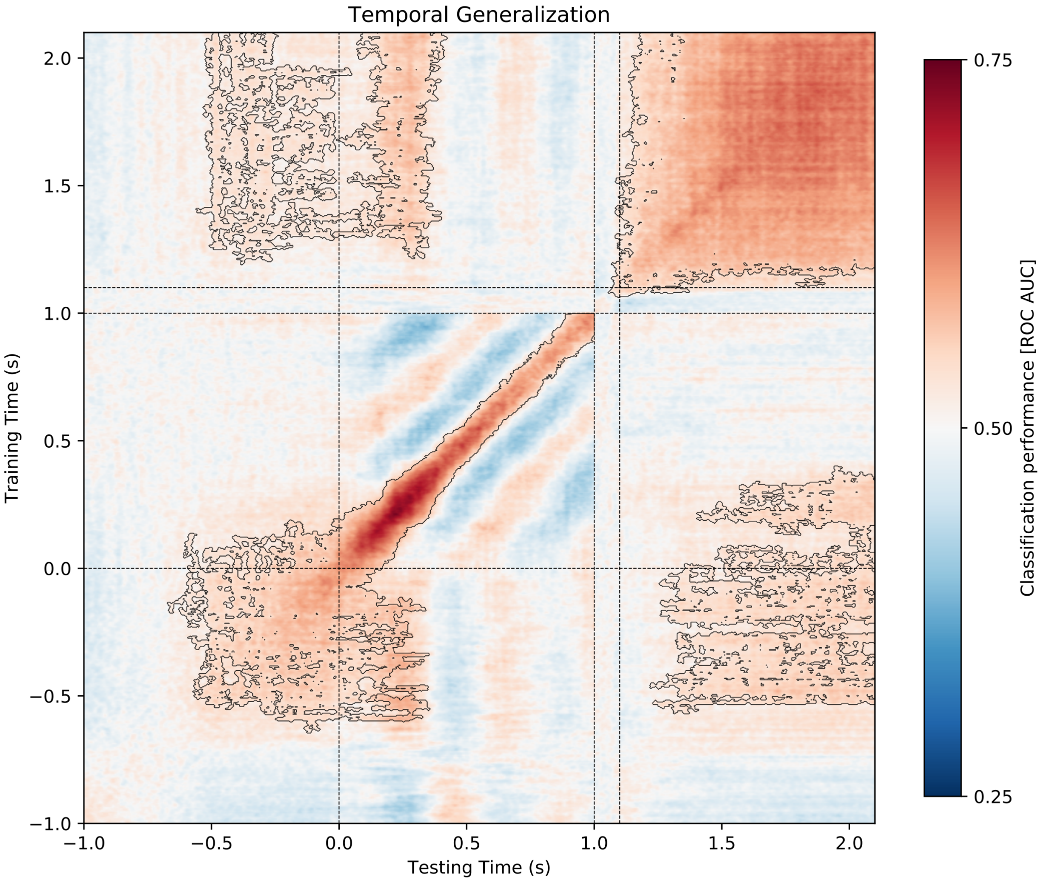

Figure 6.14: Temporal generalisation map of the clockwise vs anticlockwise movement classification. The map includes the action stage aligned to the onset of the movement (-1 - 1 s) and the observation phase (here displayed between 1 and 1.1 s). The baselines of the signal were at the beginning of the epoch (-1 - -0.5 s) and during the blink period before the onset of the observation phase (1.0 - 1.1 s). The classification was based on the sign of the M score (see: Equation 6.1). The colour scheme and epoch timing is the same as in Figure 6.12. The colourmap indicates the classification performance (ROC AUC). Black outlines denote the clusters of the time that differ ($p < 0.05$) from the chance level (50%).

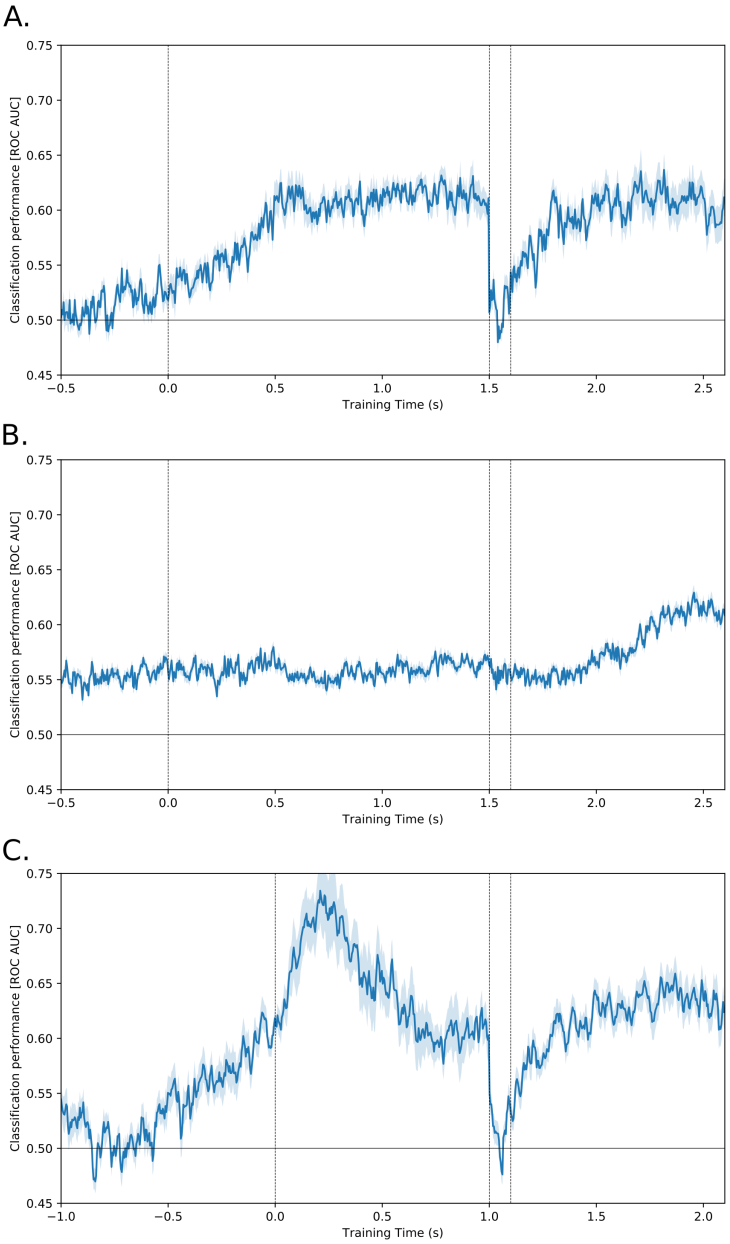

Figure 6.15: Classification performance for the classifier trained on and applied to the data from the same time point. **A)** diagonal of the temporal generalisation map of the clockwise vs anticlockwise movement classification (see: Figure 6.12). **B)** diagonal of the temporal generalisation map of the odd vs regular visual motion classification (see: Figure 6.13). **C)** diagonal of the temporal generalisation map of the clockwise vs anticlockwise movement classification, with movement phase aligned to the movement onset (see: Figure 6.14). Solid lines denote mean performance.Shaded areas denote standard errors of the mean.

6.4 Discussion

In this chapter, I developed the Action-Perception Congruency (APC) task, aiming to establish a causal expectation between voluntary movements in the action stage and subsequent visual stimulus in the observation stage. In regular trials, the motion direction of the visual stimulus was congruent to voluntary movements. In odd trials (20%), the direction of the visual stimulus was opposite to that of voluntary movements. The rare occurrence was designed to violate the expectation of the action-perception causality.

I found no difference in univariate ERF and oscillatory power between odd and regular conditions. MVPA showed that multivariate patterns of MEG activity can be distinguished between odd and regular conditions during the observation stage. These results suggested that continuous movements from voluntary choices elicited representations of action-perception expectations, which can be violated experimentally in the oddball paradigm as in the APC task.

6.4.1 Behavioural measures

The behavioural measures were gathered only during the action stage, which appeared to be the same between congruency conditions from participant's perspective. As expected, there was no conclusive evidence that the congruency conditions affected the onset of the movement (Figure 6.6A), the average movement speed (Figure 6.6B), movement directions (Figure 6.6C), or the delay between action and observation stages (Figure 6.6D).

Moreover, the voluntary movement onset time in the APC task was around 0.3 s, much faster than the onset time in response to the RDM in previous chapters (around 0.6 s, Figure 4.3). This result is in accordance with the evidence from comparison between voluntary and sensory-driven responses: the voluntary movement is faster due to lesser constraints on the preparatory activity (Hughes et al., 2011).

The delay duration between the action and observation stages (Figure 6.6D) was longer than the minimum 0.1 s prescribed in the experimental design

(Figure 6.1). It was caused by the participants failing to stop movements or leaning on the joystick at the end of the action stage. This measure was used to remove the excessive delay in MEG analysis to avoid the contamination of the observation stage by ongoing movements.

6.4.2 ERF and oscillatory power

The P300 component and MMN were associated with deviance detection in oddball tasks (Polich, 2007; Näätänen et al., 2007). In contrast to previous studies (Stefanics et al., 2014; Huang et al., 2005; Knight, 1997; Kimura et al., 2009), the current experiment did not observe any difference between odd and regular conditions in ERFs (Figures 6.7 and 6.8), although there were strong evoked responses in both occipital and central sensors during the observation stage.

The lack of univariate difference between congruency conditions may be due to the design of the APC task, rather than the absence of the deviation detection itself. The MMN depends on the comparison between memory traces of early sensory information and current stimulus during passive observation (Näätänen et al., 2007; Stefanics et al., 2014; Näätänen et al., 2005). Furthermore, short memory traces of visuo-motor information decayed exponentially after 0.5 - 1.5 s (Vaillancourt and Russell, 2002). The duration of the delay between the action and observation stages (Figure 6.6D) may have introduced variability in evoked responses sensitive to expectation violation (Gaspar et al., 2011).

To determine whether the oscillatory power is sensitive to the detection of odd stimuli, I compared Hilbert envelopes between odd and regular conditions and observed no significant difference in any frequency band (Figures 6.9, 6.10 and 6.11). However, I have observed hypothesised oscillatory power patterns. During the action stage (Figure 6.9), beta-band power increased prior to the action stage, followed by stable desynchronisation during the movement, and the beta-band desynchronisation is more prominent when the signal was aligned to movement onset (Figure 6.11). During the observation stage (Figure 6.10), beta-band rebound was observed after movements. In the frequency range encompassing the flickering frequency of the checkerboard stimulus (8 Hz), there was a strong increase in the oscillatory power at 7-9 Hz during the observation stage. Consistent with previous studies (Muthukumaraswamy, 2014), there was also an increase in the low-gamma oscillatory power during the presentation of the 8 Hz flickering stimulus.

The lack of univariate difference between congruency conditions may be due to the design of the APC task, rather than the absence of the deviation detection itself, as supported by the multivariate results. The MMN depends on the comparison between memory traces of early sensory information and current stimulus during passive observation (Näätänen et al., 2007; Stefanics et al., 2014; Näätänen et al., 2005). The current study is departed from classical oddball tasks in several aspects. First, instead of establishing a representation of regular events via consecutive and repetitive stimuli (e.g., continuous tones), the APC task elicited congruency or incongruency on a trial-by-trial basis. Second, the MMN is commonly established in a passive paradigm, in which participants do not need to attend to the stimulus, and standard and deviant events have a similar spatiotemporal structure but differ in simple sensory features (e.g., frequency, pitch or duration in auditory MMN). In contrast, the APC task established an expectation of movement direction by combining voluntary choice and continuous movements, with the latter coupled with concurrent visual feedback to elicit a strong action-outcome causality, which is a hallmark of healthy prefrontal function (O'Callaghan et al., 2019). As a result, successful deviant detection in the APC task likely involves conflict monitoring across time (from movement to observation phases) and top-down predictions between modalities (from action to visual perception). These novel features afforded by the APC task make it a good candidate paradigm to investigate the interplay between decision, expectation and outcome in future research. Furthermore, short memory traces of visuo-motor information decayed exponentially after 0.5 - 1.5 s (Vaillancourt and Russell, 2002). The duration of the delay between the action and observation stages (Figure 6.6D) may have introduced variability in evoked responses sensitive to expectation violation (Gaspar et al., 2011), which contributes to the absence of the congruency effect in ERF.

6.4.3 Multivariate analysis results

MVPA with temporal generalisation showed that MEG activities contained multivariate information of odd vs regular events (Figure 6.13). In the observation stage, the signal evolved from an early narrow generalisation window to a wider window of generalisation (ca. 400-500 ms after the stimulus onset), much later than the P300 component in other active oddball experiments. This pattern of temporal generalisation can be interpreted as a gradual formation of information from fragmented (chained) to a stable (sustained) one (see Figure2.8) (King and Dehaene, 2014), leading to a categorical representation of odd vs. regular events. Although the temporal generalisation results provided new insights into the evolution of information representation within a trial (King and Dehaene, 2014; Grootswagers et al., 2016; Hebart and Baker, 2018), it is working noting the limitation of MVPA results, which lacked interpretations of the signal that led to significant classification (Hebart and Baker, 2018).

The classification between clockwise and anticlockwise movements showed a ramping up pattern towards a stable representation (Figure 6.12), replicating the MVPA results in Chapter 5. When the MEG data was aligned to movement onset, significant classification occurred prior to movement with sustained representation (Figure 6.14), suggesting categorical action plans for different movement directions. After movement onsets, the representation of movement direction switched to a reactivated and interleaving pattern (see: Figure 2.8), probably relating to the recurrent characteristic of circular movements (see: Chapter 4). The temporal generalisation pattern before the movement was different than the one underlying the actual movement. It can be interpreted as the evidence that movement direction predictive activity has a more abstract character than the actual movement that it leads to (Passingham et al., 2010). Comparing the ramping up temporal pattern between the sensory-driven (Figure 5.8) and voluntary movement (Figure 6.14) showed a different temporal extent. It further supports the conclusions drawn from the behavioural data. Not only the onset of the movement occurred faster, but the temporal pattern of the preparatory activity was visibly distinct (Hughes et al., 2011).

The classification of clockwise vs. anticlockwise movements was significant during the fixation period, before the onset of continuous movements (-0.5 s to 0 in Figure 6.14). This result is expected if participants had made and held their voluntary choices on movement direction during the fixation period. Previous studies showed that, before execution, task sets and action plans were actively maintained in the frontoparietal (Zhang et al., 2013) and medial prefrontal networks (Haynes and Rees, 2006), consistent with the results in the current experiment. Surprisingly, the classification of the odd vs regular trials (Figure 6.13) was also significant during the fixation and movement periods. This result could not be explained by the active encoding of congruent vs. incongruent events, because the visual stimulus and task instruction were the same between the two conditions up until the observation phase. Unlike the ERF analyses, MVPA was performed on individual trials with no robust averaging across trials. Therefore, it is likely that the classifier used here exhibited a bias between the two conditions due to their unequal sample sizes (e.g., the classification accuracy was at a steady level of 55% before the observation phase, Figure 6.15), an issue needs to be examined in more detail in future studies.

6.4.4 Conclusion

In the current chapter, the APC task was used to associate continuous movements from voluntary choices with expectations of subsequent visual perception, and this expectation was violated in a small subset of trials. I observed multivariate representation, but not univariate activity, that was sensitive to the contrast of odd vs. regular events (Polich, 2007; Näätänen et al., 2007; Knight, 1997; Stefanics et al., 2014; Kimura et al., 2009). I have discussed possible future works to improve the design and analysis that may result in a more sensitive paradigm for examining action-perception congruency.

Chapter 7

Discussion

This chapter summarised the contents of the thesis in Section 7.1. I further discussed limitations and possible future work in Section 7.2, which may provide a broader understanding of continuous sensory-motor transformations.

7.1 Summary of contributions

This thesis began with a review of theoretical and experimental foundations in Chapter 2. The decision-making process was formalised as a statistical inference problem, based on which the classical Drift-diffusion model (DDM) of decision-making was introduced. In the context of DDM, I reviewed commonly observed factors affecting behavioural performance in decision-making, such as speed-accuracy trade-off, quality of the sensory evidence, number of alternatives and contextual influences. Next, I reviewed the seminal research on signatures of decision-making obtained from invasive electrophysiological recordings as well as non-invasive neuroimaging. Following that, I reviewed adopting continuous response measures as a way to expand the scope of the methodology to understand the decision-making process.

The use of the joystick as a response device allows for a better understanding of perception, motor control and contextual factors such as expectation that collectively drive sensorimotor transformation. The studies presented in this thesis established the joystick as an valid response device in rapid decision-making (Chapter 3), extended a classical perceptual decision paradigm with continuous motor outputs (Chapters 4 and 5) and highlighted its potential in examining expectancy violation elicited by continuous actions (Chapter 6). These new results challenge the conventional sequential sampling account of actions as merely decision outcomes, highlighting a reciprocal influence of decision-making and action. Below I summarise main contributions of the thesis.

Comparing joystick movements to key presses

Chapter 3 investigated to what extent a change of response modality affects behavioural performance and underlying decision processes, by comparing button presses with joystick movements. Across four directions and two levels of perceptual difficulty, participants were instructed to decide the direction of coherent motion of the RDM stimulus, either with a button press or a ballistic joystick movement. I compared raw behavioural measures (RT and accuracy) and parameters of the DDM between response modalities. I found that the initial stage of the joystick trajectory was comparable to a button press in terms of behavioural performance and underlying cognitive processes. The decision process was affected only by the stimulus strength, but additional measures derived from joystick trajectories were also affected by ergonomic factors (e.g., movement direction). These results established that the joystick is a valid instrument for decision-making research. Importantly, compared with key presses, the additional complexity and continuity associated with joystick movements did not affect raw behavioural measures such as accuracy and RT, as well as underlying decision-making processes.

Chapter 3 laid foundation for the following experiments, establishing a common ground between the widely used key press and joystick trajectories. The ergonomic limitations has been taken into account when designing experiments presented in Chapters 4-6. For example, the initial engagement in a continuous movement was made uniform across conditions and across stimulus-response mapping to enable a reliable comparison. To my best knowledge, the research described in the Chapter 3 is the first study compared explicitly response modalities in perceptual decision-making.

Integrating continuous circular movements with perceptual decisions

Chapter 4 developed an experimental paradigm that integrates continuous movements and perceptual decisions. Participants performed continuous circular movements (clockwise or anti-clockwise) to indicate the coherent direction of RDM stimulus and its changes within a trial. Participants initiated movements based on visual information and maintained the chosen action unless the visual information indicated to change to the opposite movement direction. The possible change of movement direction created a unique state in which an alternative action plan had to be selected while performing another action. This allowed to investigate how ongoing actions may affected subsequent decisions. Through a series of four experiments, I observed consistent results that participants had longer RT, lower accuracy and slower movement speed when changing or maintaining movement directions in the presence of more noisy sensory information.

Chapter 4 established an experimental design that utilised continuous movements as a response measure. Participants used a circular movement (clockwise and anti-clockwise) to indicate the direction of non-stationary visual cues. This design mimics scenarios in real-life decision making and would be difficult to implement with discrete key press. Participants engaged in circular movements based on the visual cue and maintained their chosen action until the visual cue changed in the second half of the trial or until the end of the trial. Having a circular movement as a response introduced three stages: a phase of action engagement in the absence of prior movements, a period of action maintenance and a possible action change.

The change of action created a unique state in which an alternative action plan had to be selected while performing the other action. It allowed to investigate how prior action affected the subsequent decision process. In the initial experiment, participants performed a direction discrimination based on a very clear cue (an arrow), which had 50% chance to change direction in the middle of the trial. Participants were able to perform the task well. Participants were able to engage in action, and adjust it according to the change of the visual cue.

In the next experiment, the RDM was introduced as the visual cue to guide circular movements. Participants were still able to engage in, and adjust the movement based on the noisy and ambiguous visual stimulus. When the RDM stimulus changed with a lower coherence in the second phase (in Experiment 3 and 4), as expected, participants were slower and less accurate in changing to a new direction and maintaining the ongoing action. I observed the movement velocity being affected by the quality of the visual cue. Participants were slower in recovering the speed of movement from the direction change when using a noisy cue. Also, when maintaining the action under noisy conditions, participants were more likely to slow down or stop making their movement less accurate. Throughout the experiments 3 and 4, I observed the improvement in behavioural performance which led to reduction of the effects observed in the movement velocity, and behavioural performance. Overall, the participants were able to perform a task without any problems. The experimental manipulation in stimulus strength elicited the changes in the expected direction.

These behavioural results supported continuous circular movement as a valid and sensitive to experimental manipulations approach to respond in a perception-decision task. I have shown that complex continuous response conjoined with a simple, widely used perceptual decision task could still elicit a predictable pattern of the behavioural results. The latency between the onset of the stimulus change and the moment in which the action is adjusted is affected by the stimulus strength. This effect has been observed not only in latency but also in measures derived from the joystick trajectory. However, what I also observed is that, repetitive training extinguished the effects found in the motor response, while the experimental manipulation still robustly modulated the accuracy and RT. These observations highlighted the flexibility of human motor function. When learning to perform a simple motor task, the motor output reached optimum after a few sessions as shown in the Chapter 4 and to certain extent in Chapter 5.

Chapter 5 conducted the same experiment in MEG. The univariate analysis of ERF and oscillatory power did not show any difference between experimental conditions (movement direction or stimulus strength). MVPA showed that the direction of the movement can be decoded up to 0.5 s prior to the onset of the movement. This results extended previous findings on the encoding of action plans in the cortex (Donner et al., 2009) by showing that complex actions (e.g., circular movements) also have distinct cortical representations.

During continuous movements, the temporal generalisation pattern of MVPA results showed that, instead of an abstract and generalisable representation of clockwise and anti-clockwise actions, continuous circular movements elicited periodic multivariate patterns. Furthermore, for high vs. low motion coherence, I observed significant MVPA results only in trials without a change of motion direction. Because a change of motion direction led to a change of movement direction, it is possible that switching an ongoing action to the opposite direction masks the necessity to monitor the sensor information, although further work is needed to validate this hypothesis.

Moreover, the MVPA was only able to distinguish the stimulus strength for the trials when participants maintained the action throughout the trial. This result may reflect the lack of action commitment when maintaining a previous action plan, and necessity of representing the stimulus for the error monitoring purposes. The commitment to switching the action removes the necessity to monitor the performance, especially when the participants were well trained in the task.

Chapter 5 showed that a continuous periodic movement can be utilised in decision-making studies with neuroimaging. It provides a detectable movement pattern and an opportunity to adopt the design for a wide range of the studies. The experiment presented in Chapter 6, is an example of such design. Using circular movements, participants controlled the rotation of a shape presented on the screen. The main difference between the Experiment presented in the Chapter 5 is that participants performed a self paced voluntary action with an on-line feedback about the movement. As with Chapter 5, the MVPA was used to extract the temporal representations of the experimental conditions.

Establishing sensory expectations with continuous actions

Chapter 5 showed that a continuous periodic movement can be utilised in decision-making studies with neuroimaging. It provides a detectable movement pattern and an opportunity to adopt the design for a wide range of the studies. The Action-Perception Congruency (APC) task in Chapter 6, is an example of such design.

Chapter 6 developed the APC task. The goal was to establish a causal expectation between voluntary movement in the action stage and subsequent visual stimulus in the observation stage. In congruent trials, the motion direction of the visual stimulus was the same as voluntary movements. In the incongruent trials (20%), the direction of the visual stimulus was opposite to that of voluntary movement. The rare occurrence of incongruent trials was designed to violate the expectation of the action-perception causality. I found no difference in univariate ERF and oscillatory power between congruent and incongruent conditions. However, MVPA showed that multivariate patterns of MEG activity can be distinguished between congruent and incongruent conditions during the observation stage. These results suggested that continuous movements from voluntary choices indeed elicited the action-perception expectations.

Comparing the results between Chapter 6, and the one presented in Chapter 5, one can observe the patterns differentiating the sensory driven and voluntary, free choice. Primarily, the temporal generalisation pattern prior to the engagement in the action. In the sensory driven task, the pattern was resembling the one found later, a reactivated/oscillating pattern of the circular movement of the joystick. When the participants were asked to perform a free choice, the pattern of activity resembled a single state, ramping up, quite distinct to a common across the experiments pattern of the stable circular movement (King and Dehaene, 2014).

What results of those experiments showed us, is that the continuous response allowed to easily distinguish a voluntary responses from a sensory driven in the preparatory stage. What I managed to show, once the action plan is executed, whether it is the voluntary choice or the stimulus driven discrimination, subsequent action is similar. The continuous movement allowed to establish a unique pattern of the temporal generalisation that can be used in future studies on volition and free choice.

7.2 Limitations and future directions

The applications of joystick and other devices

Chapter 3 showed that a key press and the initial engagement in a joystick movement were similar in terms of behavioural performance and underlying cognitive processes. Here, I only used a joystick to record movement trajectories, which is commonly used and widely available in behavioural testing labs. However, there are many other devices capable for recording continuous responses, such as computer mouse (e.g. Koop and Johnson, 2011), optic motion sensor (e.g. Chapman et al., 2010) and robotic arms (Abrams et al., 1990; Archambault et al., 2009; Berg et al., 2016; Burk et al., 2014; Resulaj et al., 2009). Below I briefly outline relevant research using those alternative devices.

An even more widely available device that can be used to record continuous responses is a computer mouse, which has been used in decision-making research (Koop and Johnson, 2011; Freeman, 2018). The widespread use of the digital pointing devices allows them to be used in both lab-based and online experiments. The main difference between joystick and mouse is the range of movement and affordance. The limited range in joystick is more suitable for precise movements and repetitive/periodic trajectories. Most joysticks are self-centred without external force, and the resistance of their internal springs is approximately stable within the maximum movement range. These features allow a joystick well suited for experiments requiring a fixed starting position (Oliver et al., 2011). In contrast, a computer mouse cannot offer the same level of repeatability of the movement qualities such as a fixed starting point or a consistent range of movements, leading to less control to limb and hand positions. There are also practical considerations towards data collection and analysis from mouse tracking. A standard mouse driver returns the cursor position on the screen. The transition between the physical movement of the mouse and the displacement of the cursor is affected by factors like the mouse resolution, the quality of the surface and screen resolution. Although those factors can be amended in a controlled experimental environment, they are difficult to control in online experiments, in which participants use different computers. To sum up, although both joystick (Chapter 3) and computer mouse (Hehman et al., 2015) can offer continuous movement recordings, there are technique and practical challenges for mouse tracking.

On the other spectrum of affordability and availability are complex robotic arms like vBOT (Howard et al., 2009). Using computer controlled electric motors, the experimenter can not only locate the position of the arm, but also apply the resistive forces to participants. This type of setup has been used to study sensorimotor control, haptic perception (Wolpert and Flanagan, 2010) and decision-making (Gallivan et al., 2016). The limitations are the high equipment cost and complexity in operation and programming. It is also worth noting that the most robotic arms cannot be used during fMRI (due to ferromagnetic parts of the device) or MEG (due to electromagnetic fields generated by electric motors) recordings.

Bridging the gap between widely available devices and specialised robotic arms is a myriad of strategies used to record continuous movements in decision-making and motor control research. For example, touchscreens and tablets are used to mimic button presses and additionally track finger movements (e.g. Anguera et al., 2013; Gallivan et al., 2011). They allow to extend the functionality and flexibility of experimental design, i.e. dynamically adjusting decision alternatives (Gallivan et al., 2015; Gallivan and Chapman, 2014). The advent of touchscreen smartphones opens a new avenue to record continuous finger movements, offering an exciting possibility to large-scale online testing. Technically, a touch interface has comparable qualities as a computer mouse in terms of digitising movements.

Beyond simple finger and arm movements, full body movements can be digitised and tracked using continuous 3D motion capture. Cameras record the movement of markers (e.g., inferred tracers) attached on body, which is then transformed to body movements in 3D. The quality and precision of the recording depend on cameras' resolution and framerate, and improvements in quality come with increased costs. One advantage of motion capture is that movements are no longer constrained, enabling experiments in a realistic setting (Gallivan et al., 2015; Chapman et al., 2010; Gallivan and Chapman, 2014).

Limitations

There are several issues requiring further consideration. First, the experiment described in the Chapter 3 offered a comprehensive comparison between key presses and joystick movements, but it is yet to be validated whether measures from other devices mentioned above are consistent with discrete responses. I also offered a practical solution to measure RT from joystick movement comparable to that from key presses, taking into account the small resistive forces near the joystick's neural position, which potentially can be extrapolated to other devices.

Second, the DDM required the behavioural data to be presented as binary choices (Ratcliff and McKoon, 2008). To meet this constraint, I simplified our four-choice task data into correct and incorrect decisions, and incorrect responses contained errors towards three different directions from the correct motion direction. Our modelling results provided a good fit to the observed data. It would be useful to extend the analysis using other models that are designed for decision problems with multiple alternatives (Brown and Heathcote, 2008; Usher and McClelland, 2001; Wong and Wang, 2006; Bogacz et al., 2007; Zhang and Bogacz, 2009). A hierarchical Bayesian implementation of those more complex models can be useful especially when using the joystick as a response instrument affords higher flexibility in experimental design.

Third, I instructed participants to make directional movements in the joystick session, which allows for intra-individual comparisons between response modalities. Motion trajectories suggested that the participants mainly made ballistic actions towards one of the four cardinal directions (Figure 3.5A). One could explore the further potential of continuous responses in behavioural tasks, such as in response to the change of mind (Berg et al., 2016; Burk et al., 2014; Resulaj et al., 2009) or external distractions (Gallivan and Chapman, 2014). Furthermore, the description of the joystick trajectory measures was limited to the physical direction of the movement and the experimental conditions. However, I observed a modest effect of the experimental conditions on action velocity. It is possible that a joystick trajectory can contain more information beyond the response time and accuracy. It has been shown that a joystick trajectory can be used to associate the confidence with the change of mind (Berg et al., 2016). It would be useful to explore the movement velocities with regard to the post-decision confidence judgements (You and Wang, 2013). The brain stimulation biased action selection competition affected the confidence judgements in the correct responses (Fleming et al., 2015). Moreover, the cost of action also affects the decision process, biasing it towards a lower cost option (Marcos et al., 2015; Hagura et al., 2017). The simple keyboard press, a linear joystick response and circular joystick movement require different physical effort to complete the response. Thus, it is reasonable to examine whether physical effort can influence the action selection process and in turn affect the post-decision confidence rating (Fleming et al., 2015; Yeung and Summerfield, 2012; Moran et al., 2015).

Fourth, the novelty of the task in Chapters 4-5 also posed a limitation. Many previous studies used a continuously measured response but with a discrete movement (Burk et al., 2014; Resulaj et al., 2009; Acerbi et al., 2017; Berg et al., 2016). Some other studies focused on continuous movements, but not explicitly manipulating sensory inputs (Howard et al., 2011; Huys et al., 2008; Torre and Balasubramaniam, 2009). To the best of my knowledge, there is currently no extensive research with a task design similar to that in Chapters 4-5, which combined continuous movements with continuous visual inputs during perceptual decisions. Therefore, it was difficult to predict participants' performance and their training progress. As a result, it was difficult to distinguish between the training effects on perceptual decisions and that on action execution. Interestingly, the stimulus strength affected the movement velocity in the second phase of the trial in Experiment 3, however this effect was diminished in Experiment 4. It might be due to repetitive training of simple movement, which leads to automatic responses that are less susceptible to changes in the environment (Shmuelof et al., 2012).

Finally, in Chapter 4, the change of motion coherence in the second phase elicited different multivariate patterns. The experiment did not vary the motion coherence in the first phase of the trial. This design aimed to minimize the number of conditions due to a time constraint and participants' fatigue during MEG recording. Future studies could manipulate motion coherence also in the first phase, which allows to dissociate the influence of ongoing actions (Pape and Siegel, 2016; Pape et al., 2017) and visual perception on the MEG signatures of subsequent decisions.

Further directions

The results presented in the Chapter 6 suggested that the APC task elicited evoked responses and oscillatory power changes during voluntary action and subsequent perception. However, these responses were not modulated by expectation violations, prohibiting further applications of the APC task as traditional oddball tasks, e.g. manipulating the probability of the odd stimuli (Polich, 2007). Nevertheless, further works are need with more complex statistical models and refined experimental design. One could employ a multivariate General Linear Model for data analysis, which are able to account for signal and timing variability across trials. For example, It can incorporate trial-by-trial covariates such as the expected occurrence probability of an odd stimulus or the delay between action and observation stages (Warbrick et al., 2009; Ouyang et al., 2015). Increasing the involvement of the participants in the task may improve deviance detection and the related MEG markers (Polich, 2007). One possible solution would be to require participants to detect the presence of incongruent stimulus in each trial (Hughes and Waszak, 2011; Hughes et al., 2011; Desantis et al., 2014) with monetary rewards (Pfabigan et al., 2014).

The trajectory recording from the experiments in Chapters 5 and 6 offer a great opportunity to examine further the electrophysiological signals underlying continuous movement under different context (Kilavik et al., 2013; Todorov and Jordan, 2002; Todorov, 2004). In Chapter 6, participants performed a voluntarily chosen movement with visual feedback of the movement. In Chapter 5, although the movement patterns were the same (circular movement), the movement direction was determined by sensory stimulus. I observed different multivariate patterns of the preparatory activity prior to the movement onset under these two contexts but common patterns during stable movements. Future work is needed to relate the preparatory activity, and the movement trajectory itself to the source localised MEG signal (Baillet, 2017). A search-light procedure could be used to systematically map the classifier performance of multivariate patterns across the brain (Kriegeskorte et al., 2006). Moreover, patterns of activity during stable movement may offer an insight into the nature of the motor control of continuous movement. It may be possible to obtain the signatures of the motor control process (Kilavik et al., 2013; Todorov and Jordan, 2002; Todorov, 2004).

Continuous movements would expand the scope of decision-making research beyond what is possible with conventional experiments with key presses. Two theoretical accounts support this promise. First, during continuous movements, motor control can be framed as an instance of the statistical decision theory (Wolpert and Landy, 2012), which integrates action selection with prior information (e.g. experience, expectations), environmental cues and cost functions (e.g., a trade-off between movement variability and effort). Second, the affordance competition hypothesis (Cisek and Kalaska, 2010, see also Section 2.2.1) posits that when continuous movements are visually guided, they influence both the feed-forward and feed-back stream of information. Continuous movements could therefore be used to interact with various environmental factors (Standage et al., 2011; Doya, 2008), which, according to the urgency-gating model (Cisek et al., 2009; Thura and Cisek, 2017; Thura et al., 2014), could modulate the environmental dependent urgency signal, and in turn influence perceptual processing (Chapman et al., 2010; Gallivan et al., 2015, 2016; Gallivan and Chapman, 2014) and motor planning (Plamondon and Alimi, 1997; Wobbrock et al., 2008).

Guided by the those theoretical promises, one ambitious attempt to capitalise further the potential of continuous movement measures would be to envisage a continuous action-perception-action paradigm, extending from common trial-based experiments to examine how contextual factors affect decision-making and motor control (Doya, 2008). Figure 7.1A showed a schematic of such a proposal, in which visual inputs shape action selection by combining available pathways and the time to execution. Here, continuous movements are constantly affected by response urgency, movement precision prior experience (e.g. the trajectory of previous responses may bias future actions) and ongoing evidence (e.g. the visible path informs the action plan). Dependent measures (Figure 7.1B) such as joystick trajectories (how precise the path is traced by

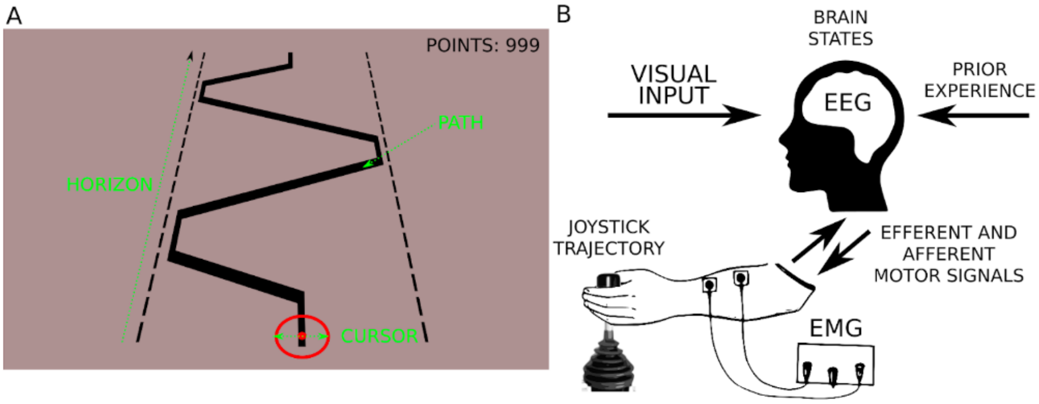

Figure 7.1: A continuous joystick task with various environmental pressures. **A)** Schematic of the experiment. The path refers to a continuous stream of visual information that guides action selection. The cursor is controlled by the participant using left- or rightward joystick movements, which contains a central point indicating the actual position of the joystick and an outer ring indicating the bounds for the precision of the movement to be considered "on the path". Participants earn game points from their accuracy on the task, with penalties for not following the path and rewards for being precise in following the path. Speed of the path: how fast participants will be required to follow the path, this will introduce the time pressure and challenge the movement precision; Horizon controls how much information is available in advance for participants to plan their actions. **B)** Dependent measures. Movement trajectory can be measured by a joystick. EMG activity can be recorded from the forearm (forearm flexor-extensor tension balance) with concurrent EEG activity.

the cursor), brain states (measured by the EEG) and effector states (measured by EMG) could then be measured concurrently to inform an action-selection model.

Finally, paradigms with continuous sensorimotor transformation (e.g., Chapter 4) could be useful for investigating action inhibition. Conventional inhibition paradigms such as the stop-signal task require participants to abort an immediate action following a stopping cue (Logan et al., 1984; de Jong et al., 1990). Successful inhibition of a pending action involves monitoring of the stopping cue and the ability to alter one's responses (Verbruggen and Logan, 2008). It has been suggested that keypress-based tasks (as used in most stop-signal and go/no-go tasks) and continuous tasks measure the same inhibition process (Morein-Zamir et al., 2004), which is in accordance with results in Chapter 3.

Therefore, results in Chapter 4 have the potential to be examined in a similar context. For example, in both Chapters 4 and 5, I observed a slowing of movement in the second phase of the trial, when the direction of the visual motion maintained, and this slowing effect sustained throughout several sessions of intensive training. These results suggest that ongoing actions are attenuated at the presence of new sensory information, possible as a preparatory mechanism for optimal motor control. Future research can compare MEG signatures between overt action inhibition and action attenuation observed in this thesis.

7.3 Summary

In conclusion, the results presented in this thesis contributed to the field of decision-making and offered a novel methodological approach. I validated the joystick as a response instrument for decision-making experiments. Furthermore, I capitalised the continuous recording of joystick trajectories in two novel paradigms: one focusing on continuous actions in response to perceptual decisions, and the other focusing on statistical violations of action-perception congruency. Behavioural and MEG results indicated a close, continuous and mutual influence between perception and action, which calls for new research on the continuity of human cognition across different domains.

Appendix A

Technical considerations regarding the use of joystick.

There are several technical issues to be considered when using joysticks for continuous response measures. First, continuous movements with forearms are often accompanied with head movements (especially with large circular movements used in Chapter 3), which affect the viewing distance. To minimise this effect, a chin rest was used in all behavioural experiments (see Figure A.1 for the experimental setup). Second, when used with concurrent MEG recording, the joystick needs to be MEG-compatible, i.e., containing no moving metal parts that could interfere with the magnetic field in the shielded room. To minimise further muscle artifacts in MEG recording, in all MEG experiments, participants were seated comfortably and a MEG-compatible chin-rest was used to limit head movements (see Figure A.2 for the setup of MEG experiments).

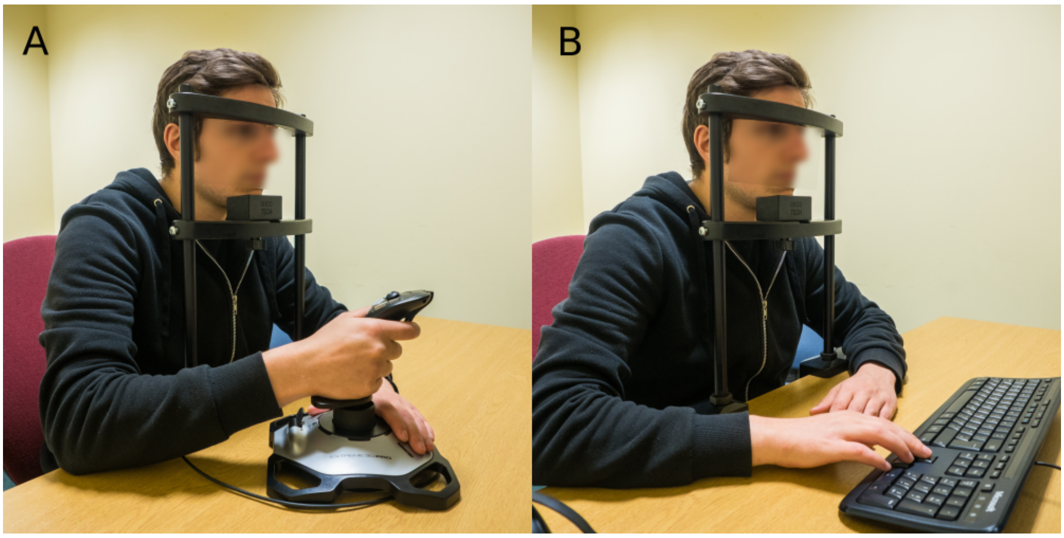

Figure A.1: **The experimental setup and joystick positioning.** Each participant was seated in front of the screen. Distance from the screen and head position were maintained using a chin rest. The seating height was adjusted to the most comfortable position, and the joystick was positioned to the right of the participant **(A)**. The exact position of the device was adjusted to the most comfortable position. Participants were asked to hold the base of the joystick while responding. The keyboard was placed parallel to the screen to ensure that the arrow directions corresponded to the direction of the motion of the visual stimuli **(B)**.

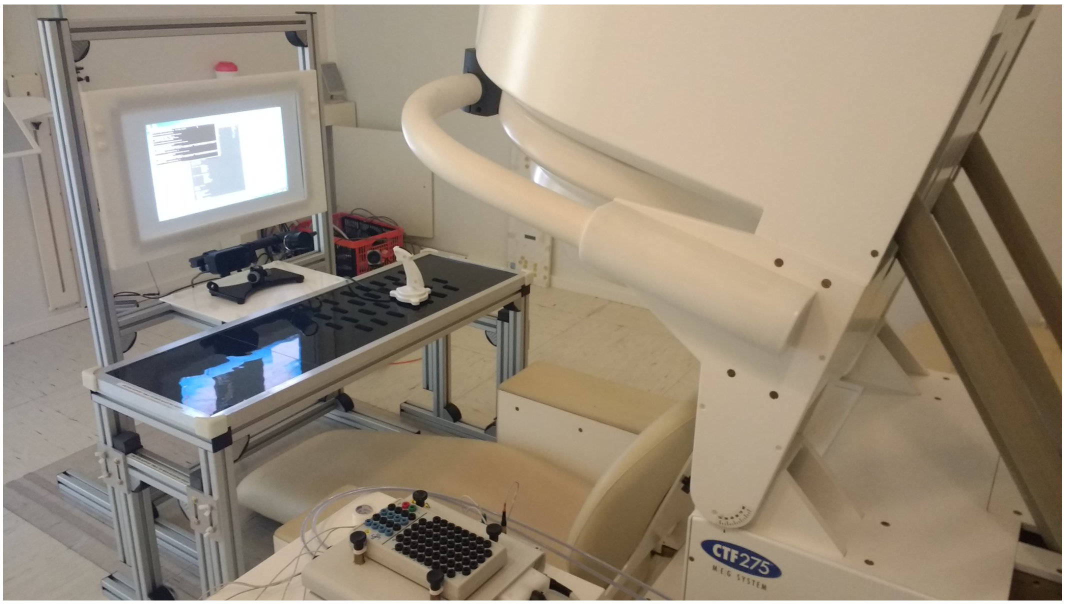

Figure A.2: **The experimental setup for the MEG.** Each participant was seated in the MEG chamber. The seating position was adjusted to fit the MEG helmet. Additionally, the head was fixed using a chin rest, and pillows between the participant's body and the arms of the seat (both items were not pictured). The table was slid over the seat, and the height was adjusted at an appropriate level. The MEG-compatible joystick was then attached to the table using velcros in a comfortable position. The visual stimuli were displayed on a projector screen, with an eye-tracker camera underneath.

Bibliography

Abrams, R. A., Meyer, D. E., and Kornblum, S. (1990). Eye-hand coordination: Oculomotor control in rapid aimed limb movements. *Journal of Experimental Psychology: Human Perception and Performance*, 16(2):248–267.

Acerbi, L., Vijayakumar, S., and Wolpert, D. M. (2017). Target Uncertainty Mediates Sensorimotor Error Correction. *PLOS ONE*, 12(1):e0170466.

Aine, C. J. (2010). Highlights of 40 Years of SQUID-Based Brain Research and Clinical Applications. In Supek, S. and Sušac, A., editors, *17th International Conference on Biomagnetism Advances in Biomagnetism – Biomag2010*, IFMBE Proceedings, pages 9–34. Springer Berlin Heidelberg.

Albantakis, L. and Deco, G. (2009). The encoding of alternatives in multiple-choice decision making. *Proceedings of the National Academy of Sciences*, 106(25):10308–10313.

Altemeier, L. E., Abbott, R. D., and Berninger, V. W. (2008). Executive functions for reading and writing in typical literacy development and dyslexia. *Journal of Clinical and Experimental Neuropsychology*, 30(5):588–606. Publisher: Routledge _eprint: https://doi.org/10.1080/13803390701562818.

Amzica, F. and Steriade, M. (1998). Electrophysiological correlates of sleep delta waves. *Electroencephalography and Clinical Neurophysiology*, 107(2):69–83.

Anguera, J. A., Bernard, J. A., Jaeggi, S. M., Buschkuehl, M., Benson, B. L., Jennett, S., Humfleet, J., and Reuter-lorenz, P. (2013). The effects of working memory resource depletion and training on Sensorimotor Adaptation. 228(1):107–115.

Antelis, J. M., Montesano, L., Ramos-Murguialday, A., Birbaumer, N., and Minguez, J. (2013). On the Usage of Linear Regression Models to Reconstruct Limb Kinematics from Low Frequency EEG Signals. *PLoS ONE*, 8(4):e61976.

Archambault, P. S., Caminiti, R., and Battaglia-Mayer, A. (2009). Cortical Mechanisms for Online Control of Hand Movement Trajectory: The Role of the Posterior Parietal Cortex. *Cerebral Cortex*, 19(12):2848–2864.

Ayaz, A., Saleem, A., Schölvinck, M., and Carandini, M. (2013). Locomotion Controls Spatial Integration in Mouse Visual Cortex. *Current Biology*, 23(10):890–894.

Baillet, S. (2017). Magnetoencephalography for brain electrophysiology and imaging. *Nature Neuroscience*, 20(3):327–339.

Baillet, S., Mosher, J. C., and Leahy, R. M. (2001). Electromagnetic brain mapping. *IEEE Signal Processing Magazine*, 18(6):14–30.

Ball, T., Schulze-Bonhage, A., Aertsen, A., and Mehring, C. (2009). Differential representation of arm movement direction in relation to cortical anatomy and function. *Journal of Neural Engineering*, 6(1):016006.

Barr, D. J. (2013). Random effects structure for testing interactions in linear mixed-effects models. *Frontiers in Psychology*, 4. Publisher: Frontiers.

Battaglia, P. W. and Schrater, P. R. (2007). Humans Trade Off Viewing Time and Movement Duration to Improve Visuomotor Accuracy in a Fast Reaching Task. *Journal of Neuroscience*, 27(26):6984–6994.

Bayarri, M. J. and Berger, J. O. (2004). The Interplay of Bayesian and Frequentist Analysis. *Statistical Science*, 19(1):58–80.

Beck, B., Di Costa, S., and Haggard, P. (2017). Having control over the external world increases the implicit sense of agency. *Cognition*, 162:54–60.

Beersma, B., Hollenbeck, J. R., Humphrey, S. E., Moon, H., Conlon, D. E., and Ilgen, D. R. (2003). COOPERATION, COMPETITION, AND TEAM PERFORMANCE: TOWARD A CONTINGENCY APPROACH. *Academy of Management Journal*, 46(5):572–590.

Beets, I. A. M., Hart, B. M. t., Rösler, F., Henriques, D. Y. P., Einhäuser, W., and Fiehler, K. (2010). Online action-to-perception transfer: Only percept-dependent action affects perception. *Vision Research*, 50(24):2633–2641.

Berg, R. v. d., Anandalingam, K., Zylberberg, A., Kiani, R., Shadlen, M. N., and Wolpert, D. M. (2016). A common mechanism underlies changes of mind about decisions and confidence. *eLife*, 5:e12192.

Bernat, E. M., Malone, S. M., Williams, W. J., Patrick, C. J., and Iacono, W. G. (2007). Decomposing delta, theta, and alpha time–frequency ERP activity from a visual oddball task using PCA. *International Journal of Psychophysiology*, 64(1):62–74.

Binder, J. R., Liebenthal, E., Possing, E. T., Medler, D. A., and Ward, B. D. (2004). Neural correlates of sensory and decision processes in auditory object identification. *Nature Neuroscience*, 7(3):295–301.

Bland, B. H. (1986). The physiology and pharmacology of hippocampal formation theta rhythms. *Progress in Neurobiology*, 26(1):1–54.

Bland, B. H. and Oddie, S. D. (2001). Theta band oscillation and synchrony in the hippocampal formation and associated structures: the case for its role in sensorimotor integration. *Behavioural Brain Research*, 127(1):119–136.

Bogacz, R., Brown, E., Moehlis, J., Holmes, P., and Cohen, J. D. (2006). The physics of optimal decision making: A formal analysis of models of performance in two-alternative forced-choice tasks. *Psychological Review*, 113(4):700–765.

Bogacz, R., Usher, M., Zhang, J., and McClelland, J. L. (2007). Extending a biologically inspired model of choice: multi-alternatives, nonlinearity and value-based multidimensional choice. *Philosophical Transactions of the Royal Society of London B: Biological Sciences*, 362(1485):1655–1670.

Bogacz, R., Wagenmakers, E.-J., Forstmann, B. U., and Nieuwenhuis, S. (2010). The neural basis of the speed–accuracy tradeoff. *Trends in Neurosciences*, 33(1):10–16.

Bollimunta, A., Chen, Y., Schroeder, C. E., and Ding, M. (2008). Neuronal Mechanisms of Cortical Alpha Oscillations in Awake-Behaving Macaques. *Journal of Neuroscience*, 28(40):9976–9988.

Bompas, A., Hedge, C., and Sumner, P. (2017). Speeded saccadic and manual visuo-motor decisions: Distinct processes but same principles. *Cognitive Psychology*, 94:26–52.

Bonnefond, M. and Jensen, O. (2013). The role of gamma and alpha oscillations for blocking out distraction. *Communicative & Integrative Biology*, 6(1):e22702. Publisher: Taylor & Francis _eprint: https://doi.org/10.4161/cib.22702.

Bonnefond, M. and Jensen, O. (2015). Gamma Activity Coupled to Alpha Phase as a Mechanism for Top-Down Controlled Gating. *PLoS ONE*, 10(6).

Bradberry, T. J., Gentili, R. J., and Contreras-Vidal, J. L. (2010). Reconstructing Three-Dimensional Hand Movements from Noninvasive Electroencephalographic Signals. *The Journal of Neuroscience*, 30(9):3432–3437.

Bradberry, T. J., Rong, F., and Contreras-Vidal, J. L. (2009). Decoding center-out hand velocity from MEG signals during visuomotor adaptation. *NeuroImage*, 47(4):1691–1700.

Bradley, A. P. (1997). The Use of the Area Under the ROC Curve in the Evaluation of Machine Learning Algorithms. *Pattern Recogn.*, 30(7):1145–1159.

Braun, A., Urai, A. E., and Donner, T. H. (2018). Adaptive History Biases Result from Confidence-Weighted Accumulation of past Choices. *Journal of Neuroscience*, 38(10):2418–2429.

Brinkman, L., Stolk, A., Marshall, T. R., Esterer, S., Sharp, P., Dijkerman, H. C., Lange, F. P. d., and Toni, I. (2016). Independent Causal Contributions of Alpha- and Beta-Band Oscillations during Movement Selection. *Journal of Neuroscience*, 36(33):8726–8733.

Britten, K. H., Newsome, W. T., Shadlen, M. N., Celebrini, S., and Movshon, J. A. (1996). A relationship between behavioral choice and the visual responses of neurons in macaque MT. *Visual Neuroscience*, 13(1):87–100.

Britten, K. H., Shadlen, M. N., Newsome, W. T., and Movshon, J. A. (1992). The analysis of visual motion: a comparison of neuronal and psychophysical performance. *The Journal of Neuroscience*, 12(12):4745–4765.

Bronfman, Z. Z., Brezis, N., Moran, R., Tsetsos, K., Donner, T., and Usher, M. (2015). Decisions reduce sensitivity to subsequent information. *Proc. R. Soc. B*, 282(1810):20150228.

Brookes, M. J., Woolrich, M., Luckhoo, H., Price, D., Hale, J. R., Stephenson, M. C., Barnes, G. R., Smith, S. M., and Morris, P. G. (2011). Investigating the electrophysiological basis of resting state networks using magnetoencephalography. *Proceedings of the National Academy of Sciences*, 108(40):16783–16788.

Brown, S. D. and Heathcote, A. (2008). The simplest complete model of choice response time: Linear ballistic accumulation. *Cognitive Psychology*, 57(3):153–178.

Brunton, B. W., Botvinick, M. M., and Brody, C. D. (2013). Rats and Humans Can Optimally Accumulate Evidence for Decision-Making. *Science*, 340(6128):95–98.

Bubic, A., Von Cramon, D. Y., and Schubotz, R. I. (2010). Prediction, cognition and the brain. *Frontiers in Human Neuroscience*, 4.

Budd, T. W. and Michie, P. T. (1994). Facilitation of the N1 peak of the auditory ERP at short stimulus intervals. *Neuroreport: An International Journal for the Rapid Communication of Research in Neuroscience*, 5(18):2513–2516.

Buhl, H. U. (2011). From Revolution to Participation: Social Media and the Democratic Decision-Making Process. *Business & Information Systems Engineering*, 3(4):195–198.

Burk, D., Ingram, J. N., Franklin, D. W., Shadlen, M. N., and Wolpert, D. M. (2014). Motor Effort Alters Changes of Mind in Sensorimotor Decision Making. *PLOS ONE*, 9(3):e92681.

Burra, N., Baker, S., and George, N. (2017). Processing of gaze direction within the N170/M170 time window: A combined EEG/MEG study. *Neuropsychologia*, 100:207–219.

Busemeyer, J. R. and Townsend, J. T. (1993). Decision field theory: A dynamic-cognitive approach to decision making in an uncertain environment. *Psychological Review*, 100(3):432–459.

Buzsáki, G. and Draguhn, A. (2004). Neuronal Oscillations in Cortical Networks. *Science*, 304(5679):1926–1929.

Buzsáki, G. and Wang, X.-J. (2012). Mechanisms of Gamma Oscillations. *Annual Review of Neuroscience*, 35(1):203–225.

Candès, E. J. (2006). Compressive sampling. In *Proceedings oh the International Congress of Mathematicians: Madrid, August 22-30,2006 : invited lectures, Vol. 3, 2006, ISBN 978-3-03719-022-7, págs. 1433-1452*, pages 1433–1452.

Canolty, R. T. and Knight, R. T. (2010). The functional role of cross-frequency coupling. *Trends in Cognitive Sciences*, 14(11):506–515.

Carandini, M. and Churchland, A. K. (2013). Probing perceptual decisions in rodents. *Nature Neuroscience*, 16(7):824–831.

Chapman, C. S., Gallivan, J. P., Wood, D. K., Milne, J. L., Culham, J. C., and Goodale, M. A. (2010). Reaching for the unknown: Multiple target encoding and real-time decision-making in a rapid reach task. *Cognition*, 116(2):168–176.

Cheyne, D., Bells, S., Ferrari, P., Gaetz, W., and Bostan, A. C. (2008). Self-paced movements induce high-frequency gamma oscillations in primary motor cortex. *NeuroImage*, 42(1):332–342.

Chittka, L., Skorupski, P., and Raine, N. E. (2009). Speed–accuracy tradeoffs in animal decision making. *Trends in Ecology & Evolution*, 24(7):400–407.

Churchland, A. K., Kiani, R., and Shadlen, M. N. (2008). Decision-making with multiple alternatives. *Nature neuroscience*, 11(6):693–702.

Cisek, P. (2005). Neural representations of motor plans, desired trajectories, and controlled objects. *Cognitive Processing*, 6(1):15–24.

Cisek, P. (2007). Cortical mechanisms of action selection: the affordance competition hypothesis. *Philosophical Transactions of the Royal Society of London B: Biological Sciences*, 362(1485):1585–1599.

Cisek, P. (2012). Making decisions through a distributed consensus. *Current Opinion in Neurobiology*, 22(6):927–936.

Cisek, P. and Kalaska, J. F. (2010). Neural Mechanisms for Interacting with a World Full of Action Choices. *Annual Review of Neuroscience*, 33(1):269–298.

Cisek, P., Puskas, G. A., and El-Murr, S. (2009). Decisions in Changing Conditions: The Urgency-Gating Model. *The Journal of Neuroscience*, 29(37):11560–11571.

Clark, A. (1999). An embodied cognitive science? *Trends in Cognitive Sciences*, 3(9):345–351.

Clark, A. (2013). Whatever next? Predictive brains, situated agents, and the future of cognitive science. *Behavioral and Brain Sciences*, 36(3):181–204.

Coenen, A., Fine, E., and Zayachkivska, O. (2014). Adolf Beck: A Forgotten Pioneer in Electroencephalography. *Journal of the History of the Neurosciences*, 23(3):276–286.

Cowles, M. K. and Carlin, B. P. (1996). Markov Chain Monte Carlo Convergence Diagnostics: A Comparative Review. *Journal of the American Statistical Association*, 91(434):883–904.

Crease, R. P. (1991). Images of conflict: MEG vs. EEG. *Science*, 253(5018):374–375.

Cruikshank, L. C., Singhal, A., Hueppelsheuser, M., and Caplan, J. B. (2012). Theta oscillations reflect a putative neural mechanism for human sensorimotor integration. *Journal of Neurophysiology*, 107(1):65–77.

Csaszar, F. A. and Eggers, J. P. (2013). Organizational Decision Making: An Information Aggregation View. *Management Science*, 59(10):2257–2277.

Cunillera, T., Fuentemilla, L., Periañez, J., Marco-Pallarès, J., Krämer, U. M., Càmara, E., Münte, T. F., and Rodríguez-Fornells, A. (2012). Brain oscillatory activity associated with task switching and feedback processing. *Cognitive, Affective, & Behavioral Neuroscience*, 12(1):16–33.

da Silva, F. H. L. (2010). Electrophysiological basis of MEG signals. In *MEG: An introduction to methods*, pages 1–23. Oxford University Press, New York, NY, US.

Dang-Vu, T. T., Schabus, M., Desseilles, M., Albouy, G., Boly, M., Darsaud, A., Gais, S., Rauchs, G., Sterpenich, V., Vandewalle, G., Carrier, J., Moonen, G., Balteau, E., Degueldre, C., Luxen, A., Phillips, C., and Maquet, P. (2008). Spontaneous neural activity during human slow wave sleep. *Proceedings of the National Academy of Sciences*, 105(39):15160–15165.

Darvas, F., Pantazis, D., Kucukaltun-Yildirim, E., and Leahy, R. M. (2004). Mapping human brain function with MEG and EEG: methods and validation. *NeuroImage*, 23:S289–S299.

da Silva, F. L. (2013). EEG and MEG: Relevance to Neuroscience. *Neuron*, 80(5):1112–1128.

De Dreu, C. K. W., Nijstad, B. A., and van Knippenberg, D. (2008). Motivated Information Processing in Group Judgment and Decision Making. *Personality and Social Psychology Review*, 12(1):22–49.

de Jong, R., Coles, M. G. H., Logan, G. D., and Gratton, G. (1990). In search of the point of no return: The control of response processes. *Journal of Experimental Psychology: Human Perception and Performance*, 16(1):164–182.

de Lange, F. P. and Fritsche, M. (2017). Perceptual Decision-Making: Picking the Low-Hanging Fruit? *Trends in Cognitive Sciences*, 21(5):306–307.

den Ouden, H. E. M., Kok, P., and de Lange, F. P. (2012). How Prediction Errors Shape Perception, Attention, and Motivation. *Frontiers in Psychology*, 3.

Desantis, A., Roussel, C., and Waszak, F. (2014). The temporal dynamics of the perceptual consequences of action-effect prediction. *Cognition*, 132(3):243–250.

Devine, D. J., Clayton, L. D., Dunford, B. B., Seying, R., and Pryce, J. (2001). Jury decision making: 45 years of empirical research on deliberating groups. *Psychology, Public Policy, and Law*, 7(3):622–727.

Dietz, V. (2003). Spinal cord pattern generators for locomotion. *Clinical Neurophysiology*, 114(8):1379–1389.

Dillon, D. G., Wiecki, T., Pechtel, P., Webb, C., Goer, F., Murray, L., Trivedi, M., Fava, M., McGrath, P. J., Weissman, M., Parsey, R., Kurian, B., Adams, P., Carmody, T., Weyandt, S., Shores-Wilson, K., Toups, M., McInnis, M., Oquendo, M. A., Cusin, C., Deldin, P., Bruder, G., and Pizzagalli, D. A. (2015). A computational analysis of flanker interference in depression. *Psychological Medicine*, 45(11):2333–2344. Publisher: Cambridge University Press.

Ding, L. and Gold, J. I. (2012). Neural Correlates of Perceptual Decision Making before, during, and after Decision Commitment in Monkey Frontal Eye Field. *Cerebral Cortex*, 22(5):1052–1067.

Ditterich, J. (2010). A comparison between mechanisms of multi-alternative perceptual decision making: ability to explain human behavior, predictions for neurophysiology, and relationship with decision theory. *Decision Neuroscience*, 4:184.

Donders, F. C. (1969). On the speed of mental processes. *Acta Psychologica*, 30:412–431.

Donner, T. H., Siegel, M., Fries, P., and Engel, A. K. (2009). Buildup of Choice-Predictive Activity in Human Motor Cortex during Perceptual Decision Making. *Current Biology*, 19(18):1581–1585.

Donner, T. H., Siegel, M., Oostenveld, R., Fries, P., Bauer, M., and Engel, A. K. (2007). Population Activity in the Human Dorsal Pathway Predicts the Accuracy of Visual Motion Detection. *Journal of Neurophysiology*, 98(1):345–359.

Doya, K. (2008). Modulators of decision making. *Nature Neuroscience*, 11(4):410–416.

Drew, T., Prentice, S., and Schepens, B. (2004). Cortical and brainstem control of locomotion. In *Progress in Brain Research*, volume 143 of *Brain Mechanisms for the Integration of Posture and Movement*, pages 251–261. Elsevier.

Driel, J. v., Olivers, C. N. L., and Fahrenfort, J. J. (2019). High-pass filtering artifacts in multivariate classification of neural time series data. *bioRxiv*, page 530220.

Dubner, R. and Zeki, S. M. (1971). Response properties and receptive fields of cells in an anatomically defined region of the superior temporal sulcus in the monkey. *Brain Research*, 35(2):528–532.

Eckhoff, P., Holmes, P., Law, C., Connolly, P. M., and Gold, J. (2008). On diffusion processes with variable drift rates as models for decision making during learning. *New journal of physics*, 10(015006):015006 –1–015006 –27.

Engel, A. K. and Fries, P. (2010). Beta-band oscillations—signalling the status quo? *Current Opinion in Neurobiology*, 20(2):156–165.

Engel, A. K., Maye, A., Kurthen, M., and König, P. (2013). Where's the action? The pragmatic turn in cognitive science. *Trends in Cognitive Sciences*, 17(5):202–209.

Erbil, N. and Ungan, P. (2007). Changes in the alpha and beta amplitudes of the central EEG during the onset, continuation, and offset of long-duration repetitive hand movements. *Brain Research*, 1169:44–56.

Ergen, M., Marbach, S., Brand, A., Başar-Eroğlu, C., and Demiralp, T. (2008). P3 and delta band responses in visual oddball paradigm in schizophrenia. *Neuroscience Letters*, 440(3):304–308.

Euston, D. R., Tatsuno, M., and McNaughton, B. L. (2007). Fast-Forward Playback of Recent Memory Sequences in Prefrontal Cortex During Sleep. *Science*, 318(5853):1147–1150.

Fine, I. and Jacobs, R. A. (2002). Comparing perceptual learning across tasks: A review. *Journal of Vision*, 2(2):5–5.

Fischer, J. and Whitney, D. (2014). Serial dependence in visual perception. *Nature Neuroscience*, 17(5):738–743.

Fleming, S. M., Maniscalco, B., Ko, Y., Amendi, N., Ro, T., and Lau, H. (2015). Action-Specific Disruption of Perceptual Confidence. *Psychological Science*, 26(1):89–98.

Fletcher, P. C. and Frith, C. D. (2009). Perceiving is believing: a Bayesian approach to explaining the positive symptoms of schizophrenia. *Nature Reviews Neuroscience*, 10(1):48–58.

Fontanesi, L., Gluth, S., Spektor, M. S., and Rieskamp, J. (2019). A reinforcement learning diffusion decision model for value-based decisions. *Psychonomic Bulletin & Review*.

Forstmann, B., Ratcliff, R., and Wagenmakers, E.-J. (2016). Sequential Sampling Models in Cognitive Neuroscience: Advantages, Applications, and Extensions. *Annual Review of Psychology*, 67(1):641–666.

Forstmann, B. U., Anwander, A., Schafer, A., Neumann, J., Brown, S., Wagenmakers, E.-J., Bogacz, R., and Turner, R. (2010a). Cortico-striatal connections predict control over speed and accuracy in perceptual decision making. *Proceedings of the National Academy of Sciences*, 107(36):15916–15920.

Forstmann, B. U., Brown, S., Dutilh, G., Neumann, J., and Wagenmakers, E.-J. (2010b). The neural substrate of prior information in perceptual decision making: a model-based analysis. *Frontiers in Human Neuroscience*, 4:40.

Forstmann, B. U., Dutilh, G., Brown, S., Neumann, J., Cramon, D. Y. v., Ridderinkhof, K. R., and Wagenmakers, E.-J. (2008). Striatum and pre-SMA facilitate decision-making under time pressure. *Proceedings of the National Academy of Sciences*, 105(45):17538–17542.

Foxe, J. J. and Snyder, A. C. (2011). The Role of Alpha-Band Brain Oscillations as a Sensory Suppression Mechanism during Selective Attention. *Frontiers in Psychology*, 2.

Fredericksen, R., Verstraten, F., and Van De Grind, W. (1994). Temporal integration of random dot apparent motion information in human central vision. *Vision Research*, 34(4):461–476.

Freeman, J. B. (2018). Doing Psychological Science by Hand. *Current Directions in Psychological Science*, 27(5):315–323.

Freeman, J. B. and Ambady, N. (2010). MouseTracker: Software for studying real-time mental processing using a computer mouse-tracking method. *Behavior Research Methods*, 42(1):226–241.

Freeman, J. B., Dale, R., and Farmer, T. A. (2011). Hand in Motion Reveals Mind in Motion. *Frontiers in Psychology*, 2.

Friedman, D. and Johnson, R. (2000). Event-related potential (ERP) studies of memory encoding and retrieval: A selective review. *Microscopy Research and Technique*, 51(1):6–28.

Frisby, J. P. and Clatworthy, J. L. (1975). Learning to See Complex Random-Dot Stereograms. *Perception*, 4(2):173–178.

Friston, K. (2005). A theory of cortical responses. *Philosophical Transactions of the Royal Society B: Biological Sciences*, 360(1456):815–836.

Friston, K. (2009). The free-energy principle: a rough guide to the brain? *Trends in Cognitive Sciences*, 13(7):293–301.

Friston, K. (2010). The free-energy principle: a unified brain theory? *Nature Reviews Neuroscience*, 11(2):127–138.

Fründ, I., Wichmann, F. A., and Macke, J. H. (2014). Quantifying the effect of intertrial dependence on perceptual decisions. *Journal of Vision*, 14(7):9–9.

Fuchs, A., Jirsa, V. K., and Kelso, J. A. S. (2000). Theory of the Relation between Human Brain Activity (MEG) and Hand Movements. *NeuroImage*, 11(5):359–369.

Gaetz, W. and Cheyne, D. (2006). Localization of sensorimotor cortical rhythms induced by tactile stimulation using spatially filtered MEG. *NeuroImage*, 30(3):899–908.

Gallivan, J. P., Barton, K. S., Chapman, C. S., Wolpert, D. M., and Randall Flanagan, J. (2015). Action plan co-optimization reveals the parallel encoding of competing reach movements. *Nature Communications*, 6:7428.

Gallivan, J. P. and Chapman, C. S. (2014). Three-dimensional reach trajectories as a probe of real-time decision-making between multiple competing targets. *Frontiers in Neuroscience*, 8.

Gallivan, J. P., Logan, L., Wolpert, D. M., and Flanagan, J. R. (2016). Parallel specification of competing sensorimotor control policies for alternative action options. *Nature Neuroscience*, 19(2):320–326.

Gallivan, J. P., McLean, D. A., Valyear, K. F., Pettypiece, C. E., and Culham, J. C. (2011). Decoding Action Intentions from Preparatory Brain Activity in Human Parieto-Frontal Networks. *Journal of Neuroscience*, 31(26):9599–9610.

Gamerman, D. and Lopes, H. F. (2006). *Markov chain Monte Carlo stochastic simulation for Bayesian inference.* Taylor & Francis, Boca Raton. OCLC: 1066429593.

Gaspar, C. M., Rousselet, G. A., and Pernet, C. R. (2011). Reliability of ERP and single-trial analyses. *NeuroImage*, 58(2):620–629.

Gelman, A., Carlin, J. B., Stern, H. S., Dunson, D. B., Vehtari, A., and Rubin, D. B. (2014). *Bayesian data analysis.*

Gentili, R. J., Bradberry, T. J., Oh, H., Hatfield, B. D., and Vidal, J. L. C. (2011). Cerebral cortical dynamics during visuomotor transformation: Adaptation to a cognitive-motor executive challenge. *Psychophysiology*, 48(6):813–824. _eprint: https://onlinelibrary.wiley.com/doi/pdf/10.1111/j.1469-8986.2010.01143.x.

Georgopoulos, A. P., Langheim, F. J. P., Leuthold, A. C., and Merkle, A. N. (2005). Magnetoencephalographic signals predict movement trajectory in space. *Experimental Brain Research*, 167(1):132–135.

Gilley, P. M., Sharma, A., Dorman, M., Finley, C. C., Panch, A. S., and Martin, K. (2006). Minimization of cochlear implant stimulus artifact in cortical auditory evoked potentials. *Clinical Neurophysiology*, 117(8):1772–1782.

Gillman, H. (2001). What's Law Got to Do with It? Judicial Behavioralists Test the "Legal Model" of Judicial Decision Making. *Law & Social Inquiry*, 26(2):465–504.

Gold, J. I. and Shadlen, M. N. (2000). Representation of a perceptual decision in developing oculomotor commands. *Nature*, 404(6776):390.

Gold, J. I. and Shadlen, M. N. (2007). The neural basis of decision making. *Annual review of neuroscience*, 30:535–74.

Goldman, R. I., Stern, J. M., Engel, J., and Cohen, M. S. (2002). Simultaneous EEG and fMRI of the alpha rhythm. *Neuroreport*, 13(18):2487–2492.

Gomez, P., Ratcliff, R., and Childers, R. (2015). Pointing, looking at, and pressing keys: A diffusion model account of response modality. *Journal of Experimental Psychology: Human Perception and Performance*, 41(6):1515–1523.

Gomez, P., Ratcliff, R., and Perea, M. (2007). A model of the go/no-go task. *Journal of Experimental Psychology: General*, 136(3):389–413. Place: US Publisher: American Psychological Association.

Gonzalez-Moreno, A., Aurtenetxe, S., Lopez-Garcia, M.-E., del Pozo, F., Maestu, F., and Nevado, A. (2014). Signal-to-noise ratio of the MEG signal after preprocessing. *Journal of Neuroscience Methods*, 222:56–61.

Grabot, L., Kononowicz, T. W., Tour, T. D. l., Gramfort, A., Doyère, V., and Wassenhove, V. v. (2019). The Strength of Alpha–Beta Oscillatory Coupling Predicts Motor Timing Precision. *Journal of Neuroscience*, 39(17):3277–3291.

Gramfort, A., Luessi, M., Larson, E., Engemann, D. A., Strohmeier, D., Brodbeck, C., Goj, R., Jas, M., Brooks, T., Parkkonen, L., and Hämäläinen, M. (2013). MEG and EEG data analysis with MNE-Python. *Frontiers in Neuroscience*, 7.

Gramfort, A., Luessi, M., Larson, E., Engemann, D. A., Strohmeier, D., Brodbeck, C., Parkkonen, L., and Hämäläinen, M. S. (2014). MNE software for processing MEG and EEG data. *NeuroImage*, 86:446–460.

Grent-'t Jong, T., Oostenveld, R., Jensen, O., Medendorp, W. P., and Praamstra, P. (2013). Oscillatory dynamics of response competition in human sensorimotor cortex. *NeuroImage*, 83:27–34.

Grent-'t Jong, T., Oostenveld, R., Jensen, O., Medendorp, W. P., and Praamstra, P. (2014). Competitive interactions in sensorimotor cortex: oscillations express separation between alternative movement targets. *Journal of Neurophysiology*, 112(2):224–232.

Grootswagers, T., Wardle, S. G., and Carlson, T. A. (2016). Decoding Dynamic Brain Patterns from Evoked Responses: A Tutorial on Multivariate Pattern Analysis Applied to Time Series Neuroimaging Data. *Journal of Cognitive Neuroscience*, 29(4):677–697.

Gross, J., Baillet, S., Barnes, G. R., Henson, R. N., Hillebrand, A., Jensen, O., Jerbi, K., Litvak, V., Maess, B., Oostenveld, R., Parkkonen, L., Taylor, J. R., van Wassenhove, V., Wibral, M., and Schoffelen, J.-M. (2013). Good practice for conducting and reporting MEG research. *NeuroImage*, 65:349–363.

Guiard, Y. (1997). Fitts' law in the discrete vs. cyclical paradigm. *Human Movement Science*, 16(1):97–131.

Gupta, D. S. and Chen, L. (2016). Brain oscillations in perception, timing and action. *Current Opinion in Behavioral Sciences*, 8:161–166.

Haas, L. F. (2003). Hans Berger (1873–1941), Richard Caton (1842–1926), and electroencephalography. *Journal of Neurology, Neurosurgery & Psychiatry*, 74(1):9–9. Publisher: BMJ Publishing Group Ltd Section: Neurological stamp.

Haegens, S., Nácher, V., Hernández, A., Luna, R., Jensen, O., and Romo, R. (2011). Beta oscillations in the monkey sensorimotor network reflect somatosensory decision making. *Proceedings of the National Academy of Sciences*, 108(26):10708–10713.

Haggard, P. (2008). Human volition: towards a neuroscience of will. *Nature Reviews Neuroscience*, 9(12):934–946.

Haggard, P., Clark, S., and Kalogeras, J. (2002). Voluntary action and conscious awareness. *Nature Neuroscience*, 5(4):382–385.

Hagura, N., Haggard, P., and Diedrichsen, J. (2017). Perceptual decisions are biased by the cost to act. *Elife*, 6:e18422.

Hajipour Sardouie, S. and Shamsollahi, M. B. (2012). Selection of efficient features for discrimination of hand movements from MEG using a BCI competition IV data set. *Neuroprosthetics*, 6:42.

Hamel-Thibault, A., Thénault, F., Whittingstall, K., and Bernier, P.-M. (2018). Delta-Band Oscillations in Motor Regions Predict Hand Selection for Reaching. *Cerebral Cortex*, 28(2):574–584.

Hamidi, M., Slagter, H. A., Tononi, G., and Postle, B. R. (2009). Repetitive Transcranial Magnetic Stimulation Affects behavior by Biasing Endogenous Cortical Oscillations. *Frontiers in Integrative Neuroscience*, 3.

Hancock, P. A. and Newell, K. M. (1985). The Movement Speed-Accuracy Relationship in Space-Time. In Heuer, H., Kleinbeck, U., and Schmidt, K.-H., editors, *Motor Behavior*, pages 153–188. Springer Berlin Heidelberg, Berlin, Heidelberg.

Hanks, T., Kiani, R., and Shadlen, M. N. (2014). A neural mechanism of speed-accuracy tradeoff in macaque area LIP. *eLife*, 3:e02260.

Hanks, T. D., Ditterich, J., and Shadlen, M. N. (2006). Microstimulation of macaque area LIP affects decision-making in a motion discrimination task. *Nature Neuroscience*, 9(5):682–689. Number: 5 Publisher: Nature Publishing Group.

Hanks, T. D., Kopec, C. D., Brunton, B. W., Duan, C. A., Erlich, J. C., and Brody, C. D. (2015). Distinct relationships of parietal and prefrontal cortices to evidence accumulation. *Nature*, 520(7546):220–223.

Hari, R., Parkkonen, L., and Nangini, C. (2010). The brain in time: insights from neuromagnetic recordings. *Annals of the New York Academy of Sciences*, 1191(1):89–109.

Hari, R. and Salmelin, R. (2012). Magnetoencephalography: From SQUIDs to neuroscience: Neuroimage 20th Anniversary Special Edition. *NeuroImage*, 61(2):386–396.

Harper, J., Malone, S. M., and Bernat, E. M. (2014). Theta and delta band activity explain N2 and P3 ERP component activity in a go/no-go task. *Clinical Neurophysiology*, 125(1):124–132.

Hartley, T., Lever, C., Burgess, N., and O'Keefe, J. (2014). Space in the brain: how the hippocampal formation supports spatial cognition. *Phil. Trans. R. Soc. B*, 369(1635):20120510.

Hastie, T., Tibshirani, R., and Friedman, J. H. (2009). *The elements of statistical learning: data mining, inference, and prediction*. Springer series in statistics. Springer, New York, NY, 2nd ed edition.

Haxby, J. V. (2012). Multivariate pattern analysis of fMRI: The early beginnings. *Neuroimage*, 62(2):852–855.

Haxby, J. V., Gobbini, M. I., Furey, M. L., Ishai, A., Schouten, J. L., and Pietrini, P. (2001). Distributed and Overlapping Representations of Faces and Objects in Ventral Temporal Cortex. *Science*, 293(5539):2425–2430.

Haynes, J.-D. and Rees, G. (2006). Decoding mental states from brain activity in humans. *Nature Reviews Neuroscience*, 7(7):523–534.

Hebart, M. N. and Baker, C. I. (2018). Deconstructing multivariate decoding for the study of brain function. *NeuroImage*, 180:4–18.

Heekeren, H. R., Marrett, S., Bandettini, P. A., and Ungerleider, L. G. (2004). A general mechanism for perceptual decision-making in the human brain. *Nature*, 431(7010):859–862.

Heekeren, H. R., Marrett, S., Ruff, D. A., Bandettini, P. A., and Ungerleider, L. G. (2006). Involvement of human left dorsolateral prefrontal cortex in perceptual decision making is independent of response modality. *Proceedings of the National Academy of Sciences*, 103(26):10023–10028.

Heekeren, H. R., Marrett, S., and Ungerleider, L. G. (2008). The neural systems that mediate human perceptual decision making. *Nature Reviews Neuroscience*, 9(6):467–479.

Hehman, E., Stolier, R. M., and Freeman, J. B. (2015). Advanced mouse-tracking analytic techniques for enhancing psychological science. *Group Processes & Intergroup Relations*, 18(3):384–401.

Heise, M. (2002). The Past, Present, and Future of Empirical Legal Scholarship: Judicial Decision Making and the New Empiricism Symposium: Empirical and Experimental Methods in Law. *University of Illinois Law Review*, 2002:819–850.

Heitz, R. and Schall, J. (2012). Neural Mechanisms of Speed-Accuracy Trade-off. *Neuron*, 76(3):616–628.

Heitz, R. P. (2014). The speed-accuracy tradeoff: history, physiology, methodology, and behavior. *Frontiers in Neuroscience*, 8.

Herzog, M. H. and Fahle, M. (1997). The role of feedback in learning a vernier discrimination task. *Vision Research*, 37(15):2133–2141.

Hillebrand, A. and Barnes, G. R. (2002). A Quantitative Assessment of the Sensitivity of Whole-Head MEG to Activity in the Adult Human Cortex. *NeuroImage*, 16(3, Part A):638–650.

Ho, T. C., Brown, S., and Serences, J. T. (2009). Domain General Mechanisms of Perceptual Decision Making in Human Cortex. *Journal of Neuroscience*, 29(27):8675–8687.

Hoenig, H., Daalmans, G., Folberth, W., Reichenberger, H., Schneider, S., and Seifert, H. (1989). Biomagnetic multichannel system with integrated SQUIDs and first order gradiometers operating in a shielded room. *Cryogenics*, 29(8):809–813.

Hogan, N. and Sternad, D. (2007). On rhythmic and discrete movements: reflections, definitions and implications for motor control. *Experimental Brain Research*, 181(1):13–30.

Hommel, B., Müsseler, J., Aschersleben, G., and Prinz, W. (2001). The Theory of Event Coding (TEC): A framework for perception and action planning. *Behavioral and Brain Sciences*, 24(5):849–878.

Honey, C., Thesen, T., Donner, T., Silbert, L., Carlson, C., Devinsky, O., Doyle, W., Rubin, N., Heeger, D., and Hasson, U. (2012). Slow Cortical Dynamics and the Accumulation of Information over Long Timescales. *Neuron*, 76(2):423–434.

Hopf, J.-M., Luck, S. J., Girelli, M., Hagner, T., Mangun, G. R., Scheich, H., and Heinze, H.-J. (2000). Neural Sources of Focused Attention in Visual Search. *Cerebral Cortex*, 10(12):1233–1241.

Howard, I. S., Ingram, J. N., and Wolpert, D. M. (2009). A modular planar robotic manipulandum with end-point torque control. *Journal of Neuroscience Methods*, 181(2):199–211.

Howard, I. S., Ingram, J. N., and Wolpert, D. M. (2011). Separate representations of dynamics in rhythmic and discrete movements: evidence from motor learning. *Journal of Neurophysiology*, 105(4):1722–1731.

Hsiao, F.-J., Wu, Z.-A., Ho, L.-T., and Lin, Y.-Y. (2009). Theta oscillation during auditory change detection: An MEG study. *Biological Psychology*, 81(1):58–66.

Huang, M.-X., Lee, R. R., Miller, G. A., Thoma, R. J., Hanlon, F. M., Paulson, K. M., Martin, K., Harrington, D. L., Weisend, M. P., Edgar, J. C., and Canive, J. M. (2005). A parietal–frontal network studied by somatosensory oddball MEG responses, and its cross-modal consistency. *NeuroImage*, 28(1):99–114.

Hughes, G., Schütz-Bosbach, S., and Waszak, F. (2011). One Action System or Two? Evidence for Common Central Preparatory Mechanisms in Voluntary and Stimulus-Driven Actions. *Journal of Neuroscience*, 31(46):16692–16699.

Hughes, G. and Waszak, F. (2011). ERP correlates of action effect prediction and visual sensory attenuation in voluntary action. *NeuroImage*, 56(3):1632–1640.

Huk, A. C. and Shadlen, M. N. (2005). Neural Activity in Macaque Parietal Cortex Reflects Temporal Integration of Visual Motion Signals during Perceptual Decision Making. *Journal of Neuroscience*, 25(45):10420–10436.

Huys, R., Studenka, B. E., Rheaume, N. L., Zelaznik, H. N., and Jirsa, V. K. (2008). Distinct Timing Mechanisms Produce Discrete and Continuous Movements. *PLoS Computational Biology*, 4(4):e1000061.

Hyvärinen, A. and Oja, E. (2000). Independent component analysis: algorithms and applications. *Neural Networks*, 13(4-5):411–430.

Händel, B. and Haarmeier, T. (2009). Cross-frequency coupling of brain oscillations indicates the success in visual motion discrimination. *NeuroImage*, 45(3):1040–1046.

Ishii, R., Canuet, L., Herdman, A., Gunji, A., Iwase, M., Takahashi, H., Nakahachi, T., Hirata, M., Robinson, S. E., Pantev, C., and Takeda, M. (2009). Cortical oscillatory power changes during auditory oddball task revealed by spatially filtered magnetoencephalography. *Clinical Neurophysiology*, 120(3):497–504.

Ivanoff, J., Branning, P., and Marois, R. (2008). fMRI Evidence for a Dual Process Account of the Speed-Accuracy Tradeoff in Decision-Making. *PLOS ONE*, 3(7):e2635.

JASP Team (2018). *JASP (Version 0.8.6).*

Jensen, O., Kaiser, J., and Lachaux, J.-P. (2007). Human gamma-frequency oscillations associated with attention and memory. *Trends in Neurosciences*, 30(7):317–324.

Jensen, O. and Mazaheri, A. (2010). Shaping Functional Architecture by Oscillatory Alpha Activity: Gating by Inhibition. *Frontiers in Human Neuroscience*, 4.

John-Saaltink, E. S., Kok, P., Lau, H. C., and Lange, F. P. d. (2016). Serial Dependence in Perceptual Decisions Is Reflected in Activity Patterns in Primary Visual Cortex. *Journal of Neuroscience*, 36(23):6186–6192.

Jung, T.-P., Humphries, C., Lee, T.-W., Makeig, S., McKeown, M. J., Iragui, V., and Sejnowski, T. J. (1998). Extended ICA Removes Artifacts from Electroencephalographic Recordings. In Jordan, M. I., Kearns, M. J., and Solla, S. A., editors, *Advances in Neural Information Processing Systems 10*, pages 894–900. MIT Press.

Kahol, K., Smith, M., Brandenberger, J., Ashby, A., and Ferrara, J. J. (2011). Impact of Fatigue on Neurophysiologic Measures of Surgical Residents. *Journal of the American College of Surgeons*, 213(1):29–34.

Kaiser, J., Hertrich, I., Ackermann, H., and Lutzenberger, W. (2006). Gamma-band activity over early sensory areas predicts detection of changes in audiovisual speech stimuli. *NeuroImage*, 30(4):1376–1382.

Kamitani, Y. and Tong, F. (2006). Decoding Seen and Attended Motion Directions from Activity in the Human Visual Cortex. *Current Biology*, 16(11):1096–1102.

Karahan, E., Costigan, A. G., Graham, K. S., Lawrence, A. D., and Zhang, J. (2019). Cognitive and white-matter compartment models revealed the contribution of microstructural variability along sensorimotor tracts to simple reaction time. *Journal of Neuroscience*, in press.

Kebbe, H. and Vinter, A. (2013). How Culture, Age, and Manual Dominance Affect Directionality in Drawing Side View Objects. *Journal of Cross-Cultural Psychology*, 44(1):160–172.

Keinrath, C., Wriessnegger, S., Müller-Putz, G. R., and Pfurtscheller, G. (2006). Post-movement beta synchronization after kinesthetic illusion, active and passive movements. *International Journal of Psychophysiology*, 62(2):321–327.

Kelly, S. P. and O'Connell, R. G. (2015). The neural processes underlying perceptual decision making in humans: Recent progress and future directions. *Journal of Physiology-Paris*, 109(1-3):27–37.

Keuken, M. C., Müller-Axt, C., Langner, R., Eickhoff, S. B., Forstmann, B. U., and Neumann, J. (2014). Brain networks of perceptual decision-making: an fMRI ALE meta-analysis. *Frontiers in Human Neuroscience*, 8.

Kew, J. J. M., Goldstein, L. H., Leigh, P. N., Abrahams, S., Cosgrave, N., Passingham, R. E., Frackowiak, R. S. J., and Brooks, D. J. (1993). The relationship between abnormalities of cognitive function and cerebral activation in amyotrophic lateral sclerosisA neuropsychological and positron emission tomography study. *Brain*, 116(6):1399–1423.

Khanna, P. and Carmena, J. M. (2017). Beta band oscillations in motor cortex reflect neural population signals that delay movement onset. *eLife*, 6:e24573.

Kilavik, B. E., Zaepffel, M., Brovelli, A., MacKay, W. A., and Riehle, A. (2013). The ups and downs of beta oscillations in sensorimotor cortex. *Experimental Neurology*, 245:15–26.

Kilner, J. M., Baker, S. N., Salenius, S., Jousmäki, V., Hari, R., and Lemon, R. N. (1999). Task-dependent modulation of 15-30 Hz coherence between rectified EMGs from human hand and forearm muscles. *The Journal of Physiology*, 516(2):559–570.

Kim, J.-N. and Shadlen, M. N. (1999). Neural correlates of a decision in the dorsolateral prefrontal cortex of the macaque. *Nature Neuroscience*, 2(2):176.

Kimura, M., Katayama, J., Ohira, H., and Schröger, E. (2009). Visual mismatch negativity: New evidence from the equiprobable paradigm. *Psychophysiology*, 46(2):402–409.

King, J.-R. and Dehaene, S. (2014). Characterizing the dynamics of mental representations: the temporal generalization method. *Trends in Cognitive Sciences*, 18(4):203–210.

Klimesch, W. (1999). EEG alpha and theta oscillations reflect cognitive and memory performance: a review and analysis. *Brain Research Reviews*, 29(2):169–195.

Klimesch, W. (2012). Alpha-band oscillations, attention, and controlled access to stored information. *Trends in Cognitive Sciences*, 16(12):606–617.

Klimesch, W., Sauseng, P., and Hanslmayr, S. (2007). EEG alpha oscillations: The inhibition–timing hypothesis. *Brain Research Reviews*, 53(1):63–88.

Knight, R. T. (1997). Distributed Cortical Network for Visual Attention. *Journal of Cognitive Neuroscience*, 9(1):75–91.

Knyazev, G. G. (2012). EEG delta oscillations as a correlate of basic homeostatic and motivational processes. *Neuroscience & Biobehavioral Reviews*, 36(1):677–695.

Kok, P., Jehee, J. M., and de Lange, F. (2012). Less Is More: Expectation Sharpens Representations in the Primary Visual Cortex. *Neuron*, 75(2):265–270.

Kok, P., Mostert, P., and Lange, F. P. d. (2017). Prior expectations induce prestimulus sensory templates. *Proceedings of the National Academy of Sciences*, 114(39):10473–10478.

Kok, P., Rait, L. I., and Turk-Browne, N. B. (2019). Content-based dissociation of hippocampal involvement in prediction. *bioRxiv*, page 568303.

Koop, G. J. and Johnson, J. G. (2011). Response dynamics: A new window on the decision process. *Judgment and Decision Making*, 6(8):750.

Kramer, A. F., Larish, J. L., Weber, T. A., and Bardell, L. (1999). Training for executive control: Task coordination strategies and aging. In *Attention and performance XVII: Cognitive regulation of performance: Interaction of theory and application*, Attention and performance, pages 617–652. The MIT Press, Cambridge, MA, US.

Kriegeskorte, N. and Douglas, P. K. (2018). Cognitive computational neuroscience. *Nature Neuroscience*, 21(9):1148.

Kriegeskorte, N., Goebel, R., and Bandettini, P. (2006). Information-based functional brain mapping. *Proceedings of the National Academy of Sciences*, 103(10):3863–3868.

Krueger, L. E. (1989). Reconciling Fechner and Stevens: Toward a unified psychophysical law. *Behavioral and Brain Sciences*, 12(2):251–267.

Kruschke, J. K. (2013). Bayesian estimation supersedes the t test. *Journal of Experimental Psychology: General*, 142(2):573–603.

Kruschke, J. K. (2015). *Doing Bayesian data analysis: a tutorial with R, JAGS, and stan*. Academic Press, Boston, 2e [edition] edition.

Kruschke, J. K. and Liddell, T. M. (2018). The Bayesian New Statistics: Hypothesis testing, estimation, meta-analysis, and power analysis from a Bayesian perspective. *Psychonomic Bulletin & Review*, 25(1):178–206.

Kubánek, J., Miller, K. J., Ojemann, J. G., Wolpaw, J. R., and Schalk, G. (2009). Decoding flexion of individual fingers using electrocorticographic signals in humans. *Journal of Neural Engineering*, 6(6):066001.

Kutas, M. and Donchin, E. (1980). Preparation to respond as manifested by movement-related brain potentials. *Brain Research*, 202(1):95–115.

Langheim, F. J. P., Merkle, A. N., Leuthold, A. C., Lewis, S. M., and Georgopoulos, A. P. (2006). Dipole analysis of magnetoencephalographic data during continuous shape copying. *Experimental Brain Research*, 170(4):513–521.

Lappin, J. S. and Bell, H. H. (1976). The detection of coherence in moving random-dot patterns. *Vision Research*, 16(2):161–168.

Larsen, R. J. and Marx, M. L. (2012). *An introduction to mathematical statistics and its applications*. Prentice Hall, Boston. OCLC: 502674159.

Larsen, T. and Bogacz, R. (2010). Initiation and termination of integration in a decision process. *Neural Networks*, 23(3):322–333.

Laxmisan, A., Hakimzada, F., Sayan, O. R., Green, R. A., Zhang, J., and Patel, V. L. (2007). The multitasking clinician: Decision-making and cognitive demand during and after team handoffs in emergency care. *International Journal of Medical Informatics*, 76(11):801–811.

Leonowicz, Z., Karvanen, J., and Shishkin, S. L. (2005). Trimmed estimators for robust averaging of event-related potentials. *Journal of Neuroscience Methods*, 142(1):17–26.

Lerche, V. and Voss, A. (2016). Model Complexity in Diffusion Modeling: Benefits of Making the Model More Parsimonious. *Frontiers in Psychology*, 7. Publisher: Frontiers.

Leuthold, H., Sommer, W., and Ulrich, R. (2004). Preparing for Action: Inferences from CNV and LRP. *Journal of Psychophysiology*, 18(2/3):77–88.

Lewis-Peacock, J. A. and Postle, B. R. (2012). Decoding the internal focus of attention. *Neuropsychologia*, 50(4):470–478.

Limousin, P., Greene, J., Pollak, P., Rothwell, J., Benabid, A.-L., and Frackowiak, R. (1997). Changes in cerebral activity pattern due to subthalamic nucleus or internal pallidum stimulation in Parkinson's disease. *Annals of Neurology*, 42(3):283–291.

Lindley, D. V. (1965). *Introduction to probability and statistics from a Bayesian point of view, Part 2, Inference.* OCLC: 992848123.

Litvak, V., Mattout, J., Kiebel, S., Phillips, C., Henson, R., Kilner, J., Barnes, G., Oostenveld, R., Daunizeau, J., Flandin, G., Penny, W., and Friston, K. (2011). *EEG and MEG Data Analysis in SPM8.* Publication Title: Computational Intelligence and Neuroscience Type: Research article.

Liu, T. and Pleskac, T. J. (2011). Neural correlates of evidence accumulation in a perceptual decision task. *Journal of Neurophysiology*, 106(5):2383–2398.

Logan, G. D., Cowan, W. B., and Davis, K. A. (1984). On the ability to inhibit simple and choice reaction time responses: A model and a method. *Journal of Experimental Psychology: Human Perception and Performance*, 10(2):276–291.

Lu, H., Zuo, Y., Gu, H., Waltz, J. A., Zhan, W., Scholl, C. A., Rea, W., Yang, Y., and Stein, E. A. (2007). Synchronized delta oscillations correlate with the resting-state functional MRI signal. *Proceedings of the National Academy of Sciences*, 104(46):18265–18269.

Luce, R. D. (1986). *Response Times: Their Role in Inferring Elementary Mental Organization.* Oxford Psychology Series. Oxford University Press, Oxford, New York.

Lv, J., Li, Y., and Gu, Z. (2010). Decoding hand movement velocity from electroencephalogram signals during a drawing task. *BioMedical Engineering OnLine*, 9:64.

Maanen, L. v., Grasman, R. P. P. P., Forstmann, B. U., Keuken, M. C., Brown, S. D., and Wagenmakers, E.-J. (2012). Similarity and number of alternatives in the random-dot motion paradigm. *Attention, Perception, & Psychophysics*, 74(4):739–753.

Magnuson, J. S. (2005). Moving hand reveals dynamics of thought. *Proceedings of the National Academy of Sciences*, 102(29):9995–9996.

Malmivuo, J. (2012). Comparison of the Properties of EEG and MEG in Detecting the Electric Activity of the Brain. *Brain Topography*, 25(1):1–19.

Marcos, E., Cos, I., Girard, B., and Verschure, P. F. M. J. (2015). Motor Cost Influences Perceptual Decisions. *PLOS ONE*, 10(12):e0144841.

Marder, E. and Bucher, D. (2001). Central pattern generators and the control of rhythmic movements. *Current Biology*, 11(23):R986–R996.

Maris, E. and Oostenveld, R. (2007). Nonparametric statistical testing of EEG- and MEG-data. *Journal of Neuroscience Methods*, 164(1):177–190.

Marr, D. and Poggio, T. (1976). From Understanding Computation to Understanding Neural Circuitry.

Marr, D., Poggio, T., and Brenner Sydney (1979). A computational theory of human stereo vision. *Proceedings of the Royal Society of London. Series B. Biological Sciences*, 204(1156):301–328.

Mars, R. B., Debener, S., Gladwin, T. E., Harrison, L. M., Haggard, P., Rothwell, J. C., and Bestmann, S. (2008). Trial-by-Trial Fluctuations in the Event-Related Electroencephalogram Reflect Dynamic Changes in the Degree of Surprise. *Journal of Neuroscience*, 28(47):12539–12545.

Maruya, K., Yang, E., and Blake, R. (2007). Voluntary action influences visual competition. *Psychological Science*, 18(12):1090–1098.

Masaki, H., Wild-wall, N., Sangals, J., and Sommer, W. (2004). The functional locus of the lateralized readiness potential. *Psychophysiology*, 41(2):220–230.

Mascord, D. J. and Heath, R. A. (1992). Behavioral and physiological indices of fatigue in a visual tracking task. *Journal of Safety Research*, 23(1):19–25.

Mathewson, K. E., Gratton, G., Fabiani, M., Beck, D. M., and Ro, T. (2009). To See or Not to See: Prestimulus Phase Predicts Visual Awareness. *Journal of Neuroscience*, 29(9):2725–2732.

McClamrock, R. (1991). Marr's three levels: A re-evaluation. *Minds and Machines*, 1(2):185–196.

McMillen, T. and Behseta, S. (2009). On the Effects of Signal Acuity in a Multi-Alternative Model of Decision Making. *Neural Computation*, 22(2):539–580.

Meirovitch, Y., Harris, H., Dayan, E., Arieli, A., and Flash, T. (2015). Alpha and Beta Band Event-Related Desynchronization Reflects Kinematic Regularities. *Journal of Neuroscience*, 35(4):1627–1637.

Melloni, L., Molina, C., Pena, M., Torres, D., Singer, W., and Rodriguez, E. (2007). Synchronization of Neural Activity across Cortical Areas Correlates with Conscious Perception. *Journal of Neuroscience*, 27(11):2858–2865.

Moher, J. and Song, J.-H. (2014). Perceptual decision processes flexibly adapt to avoid change-of-mind motor costs. *Journal of Vision*, 14(8):1–1.

Moore, J. W., Lagnado, D., Deal, D. C., and Haggard, P. (2009). Feelings of control: contingency determines experience of action. *Cognition*, 110(2):279–283.

Moran, R., Teodorescu, A. R., and Usher, M. (2015). Post choice information integration as a causal determinant of confidence: Novel data and a computational account. *Cognitive Psychology*, 78:99–147.

Morein-Zamir, S., Nagelkerke, P., Chua, R., Franks, I., and Kingstone, A. (2004). Inhibiting prepared and ongoing responses: Is there more than one kind of stopping? *Psychonomic Bulletin & Review*, 11(6):1034–1040.

Morrell, M. E. (2005). Deliberation, Democratic Decision-Making and Internal Political Efficacy. *Political Behavior*, 27(1):49–69.

Mulder, M. J., Keuken, M. C., Maanen, L., Boekel, W., Forstmann, B. U., and Wagenmakers, E.-J. (2013). The speed and accuracy of perceptual decisions in a random-tone pitch task. *Attention, Perception, & Psychophysics*, 75(5):1048–1058.

Mulder, M. J., van Maanen, L., and Forstmann, B. U. (2014). Perceptual decision neurosciences – A model-based review. *Neuroscience*, 277:872–884.

Murakami, S. and Okada, Y. (2006). Contributions of principal neocortical neurons to magnetoencephalography and electroencephalography signals. *The Journal of Physiology*, 575(3):925–936.

Muthukumaraswamy, S. D. (2010). Functional Properties of Human Primary Motor Cortex Gamma Oscillations. *Journal of Neurophysiology*, 104(5):2873–2885.

Muthukumaraswamy, S. D. (2014). The use of magnetoencephalography in the study of psychopharmacology (pharmaco-MEG). *Journal of Psychopharmacology*, 28(9):815–829.

Muthukumaraswamy, S. D. and Singh, K. D. (2008). Spatiotemporal frequency tuning of BOLD and gamma band MEG responses compared in primary visual cortex. *NeuroImage*, 40(4):1552–1560.

Nachev, P., Rees, G., Parton, A., Kennard, C., and Husain, M. (2005). Volition and Conflict in Human Medial Frontal Cortex. *Current Biology*, 15(2):122–128.

Nakagawa, K., Aokage, Y., Fukuri, T., Kawahara, Y., Hashizume, A., Kurisu, K., and Yuge, L. (2011). Neuromagnetic beta oscillation changes during motor imagery and motor execution of skilled movements:. *NeuroReport*, 22(5):217–222.

Nakanishi, Y., Yanagisawa, T., Shin, D., Fukuma, R., Chen, C., Kambara, H., Yoshimura, N., Hirata, M., Yoshimine, T., and Koike, Y. (2013). Prediction of Three-Dimensional Arm Trajectories Based on ECoG Signals Recorded from Human Sensorimotor Cortex. *PLOS ONE*, 8(8):e72085.

Nakasatp, N., Levesque, M. F., Barth, D. S., Baumgartner, C., Rogers, R. L., and Sutherling, W. W. (1994). Comparisons of MEG, EEG, and ECoG source localization in neocortical partial epilepsy in humans. *Electroencephalography and Clinical Neurophysiology*, 91(3):171–178.

Nasseroleslami, B., Lakany, H., and Conway, B. A. (2014). EEG signatures of arm isometric exertions in preparation, planning and execution. *NeuroImage*, 90:1–14.

Neuper, C. and Pfurtscheller, G. (2001). Evidence for distinct beta resonance frequencies in human EEG related to specific sensorimotor cortical areas. *Clinical Neurophysiology*, 112(11):2084–2097.

Newell, K. (1980). The Speed-Accuracy Paradox in Movement Control: Errors of Time and space. In *Advances in Psychology*, volume 1, pages 501–510. Elsevier.

Newsome, W. T., Britten, K. H., and Movshon, J. a. (1989). Neuronal correlates of a perceptual decision. *Nature*.

Newsome, W. T. and Pare, E. B. (1988). A selective impairment of motion perception following lesions of the middle temporal visual area (MT). *The Journal of Neuroscience*, 8(6):2201–2211.

Nácher, V., Ledberg, A., Deco, G., and Romo, R. (2013). Coherent delta-band oscillations between cortical areas correlate with decision making. *Proceedings of the National Academy of Sciences*, 110(37):15085–15090.

Näätänen, R. and Gaillard, A. W. K. (1983). The Orienting Reflex and the N2 Deflection of the Event-Related Potential (ERP). In Gaillard, A. W. K. and Ritter, W., editors, *Advances in Psychology*, volume 10 of *Tutorials in Event Related Potential Research: Endogenous Components*, pages 119–141. North-Holland.

Näätänen, R., Jacobsen, T., and Winkler, I. (2005). Memory-based or afferent processes in mismatch negativity (MMN): A review of the evidence. *Psychophysiology*, 42(1):25–32.

Näätänen, R., Paavilainen, P., Rinne, T., and Alho, K. (2007). The mismatch negativity (MMN) in basic research of central auditory processing: A review. *Clinical Neurophysiology*, 118(12):2544–2590.

O'Connell, R. G., Dockree, P. M., and Kelly, S. P. (2012). A supramodal accumulation-to-bound signal that determines perceptual decisions in humans. *Nature Neuroscience*, 15(12):1729–1735.

Oddie, S. D. and Bland, B. H. (1998). Hippocampal Formation Theta Activity and Movement Selection. *Neuroscience & Biobehavioral Reviews*, 22(2):221–231.

Ofner, P., Schwarz, A., Pereira, J., and Müller-Putz, G. R. (2017). Upper limb movements can be decoded from the time-domain of low-frequency EEG. *PLOS ONE*, 12(8):e0182578.

O'Hora, D., Dale, R., Piiroinen, P. T., and Connolly, F. (2013). Local dynamics in decision making: The evolution of preference within and across decisions. *Scientific Reports*, 3(1).

Oliver, M. L., Northey, G. W., Murphy, T. A., MacLean, A., and Sexsmith, J. R. (2011). Joystick stiffness, movement speed and direction effects on upper limb muscular loading. *Occupational Ergonomics*, 10(4):175–187.

Oostenveld, R., Fries, P., Maris, E., and Schoffelen, J.-M. (2011). FieldTrip: Open Source Software for Advanced Analysis of MEG, EEG, and Invasive Electrophysiological Data. *Intell. Neuroscience*, 2011:1:1–1:9.

Oppenheimer, D. M., Meyvis, T., and Davidenko, N. (2009). Instructional manipulation checks: Detecting satisficing to increase statistical power. *Journal of Experimental Social Psychology*, 45(4):867–872.

O'Regan, J. K. and Noë, A. (2001). A sensorimotor account of vision and visual consciousness. *Behavioral and Brain Sciences*, 24(5):939–973.

Osipova, D., Hermes, D., and Jensen, O. (2008). Gamma Power Is Phase-Locked to Posterior Alpha Activity. *PLOS ONE*, 3(12):e3990.

Ossmy, O., Moran, R., Pfeffer, T., Tsetsos, K., Usher, M., and Donner, T. (2013). The Timescale of Perceptual Evidence Integration Can Be Adapted to the Environment. *Current Biology*, 23(11):981–986.

Ouyang, G., Sommer, W., and Zhou, C. (2015). Updating and validating a new framework for restoring and analyzing latency-variable ERP components from single trials with residue iteration decomposition (RIDE). *Psychophysiology*, 52(6):839–856.

O'Callaghan, C., Vaghi, M. M., Brummerloh, B., Cardinal, R. N., and Robbins, T. W. (2019). Impaired awareness of action-outcome contingency and causality during healthy ageing and following ventromedial prefrontal cortex lesions. *Neuropsychologia*, 128:282–289.

O'Connell, R. G., Shadlen, M. N., Wong-Lin, K., and Kelly, S. P. (2018). Bridging Neural and Computational Viewpoints on Perceptual Decision-Making. *Trends in Neurosciences*, 41(11):838–852.

Padoa-Schioppa, C. (2011). Neurobiology of Economic Choice: A Good-Based Model. *Annual Review of Neuroscience*, 34(1):333–359.

Palmer, J., Huk, A. C., and Shadlen, M. N. (2005). The effect of stimulus strength on the speed and accuracy of a perceptual decision. *Journal of Vision*, 5(5):1–1.

Pape, A.-A., Noury, N., and Siegel, M. (2017). Motor actions influence subsequent sensorimotor decisions. *Scientific Reports*, 7(1):15913.

Pape, A.-A. and Siegel, M. (2016). Motor cortex activity predicts response alternation during sensorimotor decisions. *Nature Communications*, 7:13098.

Parkkonen, L. (2010). Instrumentation and Data Processing. In *MEG: An introduction to methods*, pages 1–23. Oxford University Press, New York, NY, US.

Paré, M. and Wurtz, R. H. (1997). Monkey posterior parietal cortex neurons antidromically activated from superior colliculus. *Journal of Neurophysiology*, 78(6):3493–3497.

Passingham, R. E., Bengtsson, S. L., and Lau, H. C. (2010). Medial frontal cortex: from self-generated action to reflection on one's own performance. *Trends in Cognitive Sciences*, 14(1):16–21.

Peirce, J. W. (2008). Generating stimuli for neuroscience using PsychoPy. *Frontiers in Neuroinformatics*, 2.

Perkins, T. J. and Swain, P. S. (2009). Strategies for cellular decision-making. *Molecular Systems Biology*, 5(1):326.

Pfabigan, D. M., Seidel, E.-M., Sladky, R., Hahn, A., Paul, K., Grahl, A., Küblböck, M., Kraus, C., Hummer, A., Kranz, G. S., Windischberger, C., Lanzenberger, R., and Lamm, C. (2014). P300 amplitude variation is related to ventral striatum BOLD response during gain and loss anticipation: An EEG and fMRI experiment. *NeuroImage*, 96:12–21.

Pfurtscheller, G. (1992). Event-related synchronization (ERS): an electrophysiological correlate of cortical areas at rest. *Electroencephalography and Clinical Neurophysiology*, 83(1):62–69.

Pfurtscheller, G., Graimann, B., Huggins, J. E., Levine, S. P., and Schuh, L. A. (2003). Spatiotemporal patterns of beta desynchronization and gamma synchronization in corticographic data during self-paced movement. *Clinical Neurophysiology*, 114(7):1226–1236.

Pfurtscheller, G. and Lopes da Silva, F. H. (1999). Event-related EEG/MEG synchronization and desynchronization: basic principles. *Clinical Neurophysiology*, 110(11):1842–1857.

Pfurtscheller, G., Stancák, A., and Neuper, C. (1996). Event-related synchronization (ERS) in the alpha band — an electrophysiological correlate of cortical idling: A review. *International Journal of Psychophysiology*, 24(1):39–46.

Philiastides, M. G., Ratcliff, R., and Sajda, P. (2006). Neural Representation of Task Difficulty and Decision Making during Perceptual Categorization: A Timing Diagram. *The Journal of Neuroscience*, 26(35):8965–8975.

Philiastides, M. G. and Sajda, P. (2006). Temporal Characterization of the Neural Correlates of Perceptual Decision Making in the Human Brain. *Cerebral Cortex*, 16(4):509–518.

Philiastides, M. G. and Sajda, P. (2007). EEG-Informed fMRI Reveals Spatiotemporal Characteristics of Perceptual Decision Making. *Journal of Neuroscience*, 27(48):13082–13091.

Picazio, S., Veniero, D., Ponzo, V., Caltagirone, C., Gross, J., Thut, G., and Koch, G. (2014). Prefrontal Control over Motor Cortex Cycles at Beta Frequency during Movement Inhibition. *Current Biology*, 24(24):2940–2945.

Pilly, P. K. and Seitz, A. R. (2009). What a difference a parameter makes: A psychophysical comparison of random dot motion algorithms. *Vision Research*, 49(13):1599–1612.

Pistohl, T., Ball, T., Schulze-Bonhage, A., Aertsen, A., and Mehring, C. (2008). Prediction of arm movement trajectories from ECoG-recordings in humans. *Journal of Neuroscience Methods*, 167(1):105–114.

Plamondon, R. and Alimi, A. M. (1997). Speed/accuracy trade-offs in target-directed movements. *Behavioral and Brain Sciences*, 20(2):279–303.

Pleger, B., Ruff, C. C., Blankenburg, F., Bestmann, S., Wiech, K., Stephan, K. E., Capilla, A., Friston, K. J., and Dolan, R. J. (2006). Neural Coding of Tactile Decisions in the Human Prefrontal Cortex. *Journal of Neuroscience*, 26(48):12596–12601.

Poldrack, R. A., Baker, C. I., Durnez, J., Gorgolewski, K. J., Matthews, P. M., Munafò, M. R., Nichols, T. E., Poline, J.-B., Vul, E., and Yarkoni, T. (2017). Scanning the horizon: towards transparent and reproducible neuroimaging research. *Nature Reviews Neuroscience*, 18(2):115–126.

Polich, J. (2007). Updating P300: An integrative theory of P3a and P3b. *Clinical Neurophysiology*, 118(10):2128–2148.

Pratt, J. W. and Gibbons, J. D. (1981). Kolmogorov-Smirnov Two-Sample Tests. In *Concepts of Nonparametric Theory*, pages 318–344. Springer New York, New York, NY.

Prinz, W. (1997). Perception and Action Planning. *European Journal of Cognitive Psychology*, 9(2):129–154.

Rae, B., Heathcote, A., Donkin, C., Averell, L., and Brown, S. (2014a). The hare and the tortoise: Emphasizing speed can change the evidence used to make decisions. *Journal of Experimental Psychology: Learning, Memory, and Cognition*, 40(5):1226–1243.

Rae, C. L., Hughes, L. E., Weaver, C., Anderson, M. C., and Rowe, J. B. (2014b). Selection and stopping in voluntary action: A meta-analysis and combined fMRI study. *NeuroImage*, 86:381–391.

Ramachandran, V. and Anstis, S. (1983). Displacement thresholds for coherent apparent motion in random dot-patterns. *Vision Research*, 23(12):1719–1724.

Rammsayer, T. and Ulrich, R. (2001). Counting models of temporal discrimination. *Psychonomic Bulletin & Review*, 8(2):270–277.

Rasch, B., Büchel, C., Gais, S., and Born, J. (2007). Odor Cues During Slow-Wave Sleep Prompt Declarative Memory Consolidation. *Science*, 315(5817):1426–1429.

Ratcliff, R. (1978). A theory of memory retrieval. *Psychol. Rev*, 85(2):59–108.

Ratcliff, R. (1979). Group reaction time distributions and an analysis of distribution statistics. *Psychological bulletin*, 86(3):446.

Ratcliff, R. (1981). A theory of order relations in perceptual matching. *Psychological Review*, 88(6):552–572.

Ratcliff, R. (1985). Theoretical interpretations of the speed and accuracy of positive and negative responses. *Psychological Review*, 92(2):212–225.

Ratcliff, R. (1988). Continuous versus discrete information processing: Modeling accumulation of partial information. *Psychological Review*, 95(2):238–255.

Ratcliff, R. (2002). A diffusion model account of response time and accuracy in a brightness discrimination task: Fitting real data and failing to fit fake but plausible data. *Psychonomic Bulletin & Review*, 9(2):278–291.

Ratcliff, R. and Childers, R. (2015). Individual differences and fitting methods for the two-choice diffusion model of decision making. *Decision*, 2(4):237–279.

Ratcliff, R. and McKoon, G. (2008). The diffusion decision model: theory and data for two-choice decision tasks. *Neural computation*, 20(4):873–922.

Ratcliff, R., Philiastides, M. G., and Sajda, P. (2009). Quality of evidence for perceptual decision making is indexed by trial-to-trial variability of the EEG. *Proceedings of the National Academy of Sciences*, 106(16):6539–6544.

Ratcliff, R. and Rouder, J. N. (1998). Modeling Response Times for Two-Choice Decisions. *Psychological Science*, 9(5):347–356.

Ratcliff, R. and Smith, P. L. (2004). A Comparison of Sequential Sampling Models for Two-Choice Reaction Time. *Psychological Review*, 111(2):333–367.

Ratcliff, R., Smith, P. L., Brown, S. D., and McKoon, G. (2016). Diffusion Decision Model: Current Issues and History. *Trends in Cognitive Sciences*, 0(0).

Ratcliff, R., Thapar, A., and McKoon, G. (2006). Aging, Practice, and Perceptual Tasks: A Diffusion Model Analysis. *Psychology and aging*, 21(2):353–371.

Rees, G. and Frith, C. D. (1998). How do we select perceptions and actions? Human brain imaging studies. *Philosophical Transactions of the Royal Society B: Biological Sciences*, 353(1373):1283–1293.

Reid, C. R., Garnier, S., Beekman, M., and Latty, T. (2015). Information integration and multiattribute decision making in non-neuronal organisms. *Animal Behaviour*, 100:44–50.

Reid, C. R., MacDonald Hannelore, Mann Richard P., Marshall James A. R., Latty Tanya, and Garnier Simon (2016). Decision-making without a brain: how an amoeboid organism solves the two-armed bandit. *Journal of The Royal Society Interface*, 13(119):20160030.

Ress, D. and Heeger, D. J. (2003). Neuronal correlates of perception in early visual cortex. *Nature Neuroscience*, 6(4):414–420.

Resulaj, A., Kiani, R., Wolpert, D. M., and Shadlen, M. N. (2009). Changes of mind in decision-making. *Nature*, 461(7261):263–266.

Robinson, N., Guan, C., Vinod, A. P., Ang, K. K., and Tee, K. P. (2013). Multi-class EEG classification of voluntary hand movement directions. *Journal of Neural Engineering*, 10(5):056018.

Roelfsema, P. R., van Ooyen, A., and Watanabe, T. (2010). Perceptual learning rules based on reinforcers and attention. *Trends in Cognitive Sciences*, 14(2):64–71.

Roenker, D. L., Cissell, G. M., Ball, K. K., Wadley, V. G., and Edwards, J. D. (2003). Speed-of-Processing and Driving Simulator Training Result in Improved Driving Performance. *Human Factors*, 45(2):218–233.

Roitman, J. D. and Shadlen, M. N. (2002). Response of Neurons in the Lateral Intraparietal Area during a Combined Visual Discrimination Reaction Time Task. *The Journal of Neuroscience*, 22(21):9475–9489.

Román, A., El Fathi, A., and Santiago, J. (2013). Spatial biases in understanding descriptions of static scenes: the role of reading and writing direction. *Memory & Cognition*, 41(4):588–599.

Rouder, J. N., Speckman, P. L., Sun, D., Morey, R. D., and Iverson, G. (2009). Bayesian t tests for accepting and rejecting the null hypothesis. *Psychonomic Bulletin & Review*, 16(2):225–237.

Salzman, C. D. and Newsome, W. T. (1994). Neural mechanisms for forming a perceptual decision. *Science*, 264(5156):231–237.

Sams, M., Alho, K., and Näätänen, R. (1983). Sequential effects on the ERP in discriminating two stimuli. *Biological Psychology*, 17(1):41–58.

Sasada, S., Tazoe, T., Nakajima, T., Zehr, E. P., and Komiyama, T. (2010). Effects of Leg Pedaling on Early Latency Cutaneous Reflexes in Upper Limb Muscles. *Journal of Neurophysiology*, 104(1):210–217.

Sauseng, P. and Klimesch, W. (2008). What does phase information of oscillatory brain activity tell us about cognitive processes? *Neuroscience & Biobehavioral Reviews*, 32(5):1001–1013.

Savoie, F.-A., Hamel, R., Lacroix, A., Thénault, F., Whittingstall, K., and Bernier, P.-M. (2019). Luring the Motor System: Impact of Performance-Contingent Incentives on Pre-Movement Beta-Band Activity and Motor Performance. *Journal of Neuroscience*, 39(15):2903–2914.

Schouten, J. and Bekker, J. (1967). Reaction time and accuracy. *Acta Psychologica*, 27:143–153.

Schriver, A. T., Morrow, D. G., Wickens, C. D., and Talleur, D. A. (2008). Expertise Differences in Attentional Strategies Related to Pilot Decision Making. *Human Factors*, 50(6):864–878.

Schüür, F. and Haggard, P. (2011). What are self-generated actions? *Consciousness and Cognition*, 20(4):1697–1704.

Scott, S. H. (2004). Optimal feedback control and the neural basis of volitional motor control. *Nature Reviews Neuroscience*, 5(7):532–546.

Scott, S. H., Cluff, T., Lowrey, C. R., and Takei, T. (2015). Feedback control during voluntary motor actions. *Current Opinion in Neurobiology*, 33:85–94.

Seitz, A. R., Sr, J. E. N., Holloway, S. R., and Watanabe, T. (2006). Perceptual Learning of Motion Leads to Faster Flicker Perception. *PLOS ONE*, 1(1):e28.

Sejnowski, T. J. and Paulsen, O. (2006). Network Oscillations: Emerging Computational Principles. *Journal of Neuroscience*, 26(6):1673–1676.

Selen, L. P. J., Shadlen, M. N., and Wolpert, D. M. (2012). Deliberation in the Motor System: Reflex Gains Track Evolving Evidence Leading to a Decision. *Journal of Neuroscience*, 32(7):2276–2286.

Shadlen, M. and Kiani, R. (2013). Decision Making as a Window on Cognition. *Neuron*, 80(3):791–806.

Shadlen, M. N., Britten, K. H., Newsome, W. T., and Movshon, J. A. (1996). A computational analysis of the relationship between neuronal and behavioral responses to visual motion. *Journal of Neuroscience*, 16(4):1486–1510.

Shadlen, M. N. and Newsome, W. T. (1996). Motion perception: seeing and deciding. *Proceedings of the National Academy of Sciences*, 93(2):628–633.

Shadlen, M. N. and Newsome, W. T. (2001). Neural Basis of a Perceptual Decision in the Parietal Cortex (Area LIP) of the Rhesus Monkey. *Journal of Neurophysiology*, 86(4):1916–1936.

Shepard, R. N. (1984). Ecological Constraints on Internal Representation: Resonant Kinematics of Perceiving, Imagining, Thinking, and Dreaming. *Psychological Review*, 91(4):417–447.

Shiu, L.-P. and Pashler, H. (1992). Improvement in line orientation discrimination is retinally local but dependent on cognitive set. *Perception & Psychophysics*, 52(5):582–588.

Shmuelof, L., Krakauer, J. W., and Mazzoni, P. (2012). How is a motor skill learned? Change and invariance at the levels of task success and trajectory control. *Journal of Neurophysiology*, 108(2):578–594.

Siegel, M., Donner, T. H., Oostenveld, R., Fries, P., and Engel, A. K. (2007). High-Frequency Activity in Human Visual Cortex Is Modulated by Visual Motion Strength. *Cerebral Cortex*, 17(3):732–741.

Sigrist, R., Rauter, G., Riener, R., and Wolf, P. (2013). Augmented visual, auditory, haptic, and multimodal feedback in motor learning: A review. *Psychonomic Bulletin & Review*, 20(1):21–53.

Singh, K. D. (2006). Magnetoencephalography. In Senior, C., Russell, T., and Gazzaniga, M. S., editors, *Methods in mind*, Cognitive neuroscience. MIT Press, Cambridge, Mass. OCLC: ocm62134829.

Siéroff, E., Dahmen, R., and Fagard, J. (2012). Mechanisms of attention in reading parafoveal words: A cross-linguistic study in children. *Neuropsychology*, 26(3):334–346. Place: US Publisher: American Psychological Association.

Smith, P. L. (1995). Psychophysically principled models of visual simple reaction time. *Psychological Review*, 102(3):567–593.

Smith, P. L. and Ratcliff, R. (2004). Psychology and neurobiology of simple decisions. *Trends in Neurosciences*, 27(3):161–168.

Smits-Engelsman, B., Swinnen, S., and Duysens, J. (2006). The advantage of cyclic over discrete movements remains evident following changes in load and amplitude. *Neuroscience Letters*, 396(1):28–32.

Snyder, A. C. and Foxe, J. J. (2010). Anticipatory Attentional Suppression of Visual Features Indexed by Oscillatory Alpha-Band Power Increases:A High-Density Electrical Mapping Study. *Journal of Neuroscience*, 30(11):4024–4032.

Song, J.-H. and Nakayama, K. (2009). Hidden cognitive states revealed in choice reaching tasks. *Trends in Cognitive Sciences*, 13(8):360–366.

Souman, J. L., Freeman, T. C. A., Eikmeier, V., and Ernst, M. O. (2010). Humans do not have direct access to retinal flow during walking. *Journal of Vision*, 10(11):14–14.

Spaak, E., de Lange, F. P., and Jensen, O. (2014). Local Entrainment of Alpha Oscillations by Visual Stimuli Causes Cyclic Modulation of Perception. *Journal of Neuroscience*, 34(10):3536–3544.

Spivey, M. J. and Dale, R. (2004). On the continuity of mind: Toward a dynamical account of cognition. *Psychology of learning and motivation*, 45:87–142.

Spivey, M. J. and Dale, R. (2006). Continuous dynamics in real-time cognition. *Current Directions in Psychological Science*, 15(5):207–211.

Spivey, M. J., Grosjean, M., and Knoblich, G. (2005). Continuous attraction toward phonological competitors. *Proceedings of the National Academy of Sciences of the United States of America*, 102(29):10393–10398.

Standage, D., You, H., Wang, D.-H., and Dorris, M. C. (2011). Gain Modulation by an Urgency Signal Controls the Speed–Accuracy Trade-Off in a

Network Model of a Cortical Decision Circuit. *Frontiers in Computational Neuroscience*, 5.

Starns, J. J. and Ratcliff, R. (2014). Validating the unequal-variance assumption in recognition memory using response time distributions instead of ROC functions: A diffusion model analysis. *Journal of Memory and Language*, 70:36–52.

Stefanics, G., Kremláček, J., and Czigler, I. (2014). Visual mismatch negativity: a predictive coding view. *Frontiers in Human Neuroscience*, 8.

Stefanics, G., Stephan, K. E., and Heinzle, J. (2019). Feature-specific prediction errors for visual mismatch. *NeuroImage*.

Sternberg, S. (1969). The discovery of processing stages: Extensions of Donders' method. *Acta Psychologica*, 30:276–315.

Stillman, P. E., Medvedev, D., and Ferguson, M. J. (2017). Resisting Temptation: Tracking How Self-Control Conflicts Are Successfully Resolved in Real Time. *Psychological Science*, 28(9):1240–1258.

Strafella, A. P., Dagher, A., and Sadikot, A. F. (2003). Cerebral blood flow changes induced by subthalamic stimulation in Parkinson's disease. *Neurology*, 60(6):1039–1042.

Sugata, H., Goto, T., Hirata, M., Yanagisawa, T., Shayne, M., Matsushita, K., Yoshimine, T., and Yorifuji, S. (2012). Neural decoding of unilateral upper limb movements using single trial MEG signals. *Brain Research*, 1468:29–37.

Summerfield, C. and de Lange, F. P. (2014). Expectation in perceptual decision making: neural and computational mechanisms. *Nature Reviews Neuroscience*, 15(11):745–756.

Sutton, S., Braren, M., Zubin, J., and John, E. R. (1965). Evoked-Potential Correlates of Stimulus Uncertainty. *Science*, 150(3700):1187–1188.

Szul, M. J., Bompas, A., Sumner, P., and Zhang, J. (2019). The validity and consistency of continuous joystick response in perceptual decision-making. *Behavior Research Methods*.

Tadel, F., Baillet, S., Mosher, J. C., Pantazis, D., and Leahy, R. M. (2011). Brainstorm: A User-friendly Application for MEG/EEG Analysis. *Intell. Neuroscience*, 2011:8:1–8:13.

Taguchi, M. (2010). Cultural Differences in Drawing Movements between Right-Handed Japanese and German Participants. *Psychological Reports*, 107(1):329–335.

Taguchi, M. and Noma, Y. (2005). Relationship between Directionality and Orientation in Drawings by Young Children and Adults. *Perceptual and Motor Skills*, 101(1):90–94. Publisher: SAGE Publications Inc.

Tan, H., Wade, C., and Brown, P. (2016). Post-Movement Beta Activity in Sensorimotor Cortex Indexes Confidence in the Estimations from Internal Models. *Journal of Neuroscience*, 36(5):1516–1528.

Taniguchi, M., Kato, A., Fujita, N., Hirata, M., Tanaka, H., Kihara, T., Ninomiya, H., Hirabuki, N., Nakamura, H., Robinson, S. E., Cheyne, D., and Yoshimine, T. (2000). Movement-Related Desynchronization of the Cerebral Cortex Studied with Spatially Filtered Magnetoencephalography. *NeuroImage*, 12(3):298–306.

Tanner, D., Norton, J. J. S., Morgan-Short, K., and Luck, S. J. (2016). On high-pass filter artifacts (they're real) and baseline correction (it's a good idea) in ERP/ERMF analysis. *Journal of Neuroscience Methods*, 266:166–170.

Tassinari, H., Hudson, T. E., and Landy, M. S. (2006). Combining Priors and Noisy Visual Cues in a Rapid Pointing Task. *The Journal of Neuroscience*, 26(40):10154–10163.

Taylor, M. J. (2002). Non-spatial attentional effects on P1. *Clinical Neurophysiology*, 113(12):1903–1908.

Thaler, L., Schütz, A. C., Goodale, M. A., and Gegenfurtner, K. R. (2013). What is the best fixation target ? The effect of target shape on stability of fixational eye movements. *Vision Research*, 76:31–42.

Thura, D. and Cisek, P. (2014). Deliberation and Commitment in the Premotor and Primary Motor Cortex during Dynamic Decision Making. *Neuron*, 81(6):1401–1416.

Thura, D. and Cisek, P. (2017). The Basal Ganglia Do Not Select Reach Targets but Control the Urgency of Commitment. *Neuron*.

Thura, D., Cos, I., Trung, J., and Cisek, P. (2014). Context-Dependent Urgency Influences Speed–Accuracy Trade-Offs in Decision-Making and Movement Execution. *The Journal of Neuroscience*, 34(49):16442–16454.

Thut, G., Nietzel, A., Brandt, S. A., and Pascual-Leone, A. (2006). Alpha-Band Electroencephalographic Activity over Occipital Cortex Indexes Visuospatial Attention Bias and Predicts Visual Target Detection. *Journal of Neuroscience*, 26(37):9494–9502. Publisher: Society for Neuroscience Section: Articles.

Toda, A., Imamizu, H., Kawato, M., and Sato, M.-a. (2011). Reconstruction of two-dimensional movement trajectories from selected magnetoencephalography cortical currents by combined sparse Bayesian methods. *NeuroImage*, 54(2):892–905.

Todorov, E. (2004). Optimality principles in sensorimotor control. *Nature Neuroscience*, 7(9):907–915.

Todorov, E. and Jordan, M. I. (2002). Optimal feedback control as a theory of motor coordination. *Nature Neuroscience*, 5(11):1226–1235.

Torre, K. and Balasubramaniam, R. (2009). Two different processes for sensorimotor synchronization in continuous and discontinuous rhythmic movements. *Experimental Brain Research*, 199(2):157–166.

Tort, A. B. L., Kramer, M. A., Thorn, C., Gibson, D. J., Kubota, Y., Graybiel, A. M., and Kopell, N. J. (2008). Dynamic cross-frequency couplings of local field potential oscillations in rat striatum and hippocampus during performance of a T-maze task. *Proceedings of the National Academy of Sciences*, 105(51):20517–20522.

Tosoni, A., Galati, G., Romani, G. L., and Corbetta, M. (2008). Sensory-motor mechanisms in human parietal cortex underlie arbitrary visual decisions. *Nature Neuroscience*, 11(12):1446–1453.

Trommershäuser, J., Maloney, L. T., and Landy, M. S. (2008). Decision making, movement planning and statistical decision theory. *Trends in Cognitive Sciences*, 12(8):291–297.

Tsetsos, K., Usher, M., and McClelland, J. L. (2011). Testing Multi-Alternative Decision Models with Non-Stationary Evidence. *Frontiers in Neuroscience*, 5.

Twomey, D. M., Murphy, P. R., Kelly, S. P., and O'Connell, R. G. (2015). The classic P300 encodes a build-to-threshold decision variable. *European Journal of Neuroscience*, 42(1):1636–1643. _eprint: https://onlinelibrary.wiley.com/doi/pdf/10.1111/ejn.12936.

Tzagarakis, C., Ince, N. F., Leuthold, A. C., and Pellizzer, G. (2010). Beta-Band Activity during Motor Planning Reflects Response Uncertainty. *Journal of Neuroscience*, 30(34):11270–11277.

Tzagarakis, C., West, S., and Pellizzer, G. (2015). Brain oscillatory activity during motor preparation: effect of directional uncertainty on beta, but not alpha, frequency band. *Frontiers in Neuroscience*, 9.

Uhlhaas, P., Pipa, G., Lima, B., Melloni, L., Neuenschwander, S., Nikolić, D., and Singer, W. (2009). Neural synchrony in cortical networks: history, concept and current status. *Frontiers in Integrative Neuroscience*, 3.

Urai, A. E., Braun, A., and Donner, T. H. (2017). Pupil-linked arousal is driven by decision uncertainty and alters serial choice bias. *Nature Communications*, 8:14637.

Urai, A. E., Gee, J. W. d., Tsetsos, K., and Donner, T. H. (2018). Choice history biases subsequent evidence accumulation. *bioRxiv*, page 251595.

Usher, M. and McClelland, J. L. (2001). The time course of perceptual choice: The leaky, competing accumulator model. *Psychological Review*, 108(3):550–592.

Vaillancourt, D. E. and Russell, D. M. (2002). Temporal capacity of short-term visuomotor memory in continuous force production. *Experimental Brain Research*, 145(3):275–285.

Van Petten, C. and Luka, B. J. (2012). Prediction during language comprehension: Benefits, costs, and ERP components. *International Journal of Psychophysiology*, 83(2):176–190.

van Veen, V., Krug, M. K., and Carter, C. S. (2008). The Neural and Computational Basis of Controlled Speed-Accuracy Tradeoff during Task Performance. *Journal of Cognitive Neuroscience*, 20(11):1952–1965.

van Vugt, M. K., Sederberg, P. B., and Kahana, M. J. (2007). Comparison of spectral analysis methods for characterizing brain oscillations. *Journal of Neuroscience Methods*, 162(1-2):49–63.

Vandekerckhove, J., Tuerlinckx, F., and Lee, M. D. (2011). Hierarchical diffusion models for two-choice response times. *Psychological Methods*, 16(1):44–62.

Verbruggen, F. and Logan, G. D. (2008). Response inhibition in the stop-signal paradigm. *Trends in Cognitive Sciences*, 12(11):418–424.

Virtanen, J., Ahveninen, J., Ilmoniemi, R. J., Näätänen, R., and Pekkonen, E. (1998). Replicability of MEG and EEG measures of the auditory N1/N1m-response. *Electroencephalography and Clinical Neurophysiology/Evoked Potentials Section*, 108(3):291–298.

Voss, A., Rothermund, K., and Voss, J. (2004). Interpreting the parameters of the diffusion model: An empirical validation. *Memory & Cognition*, 32(7):1206–1220.

Voss, A., Voss, J., and Lerche, V. (2015). Assessing cognitive processes with diffusion model analyses: a tutorial based on fast-dm-30. *Frontiers in Psychology*, 6. Publisher: Frontiers.

Vrba, J. (2002). Magnetoencephalography: the art of finding a needle in a haystack. *Physica C: Superconductivity*, 368(1):1–9.

Vrba, J. and Robinson, S. E. (2001). Signal Processing in Magnetoencephalography. *Methods*, 25(2):249–271.

Vugt, V., Karlijn, M., Simen, P., Nystrom, L. E., Holmes, P., and Cohen, J. D. (2012). EEG Oscillations Reveal Neural Correlates of Evidence Accumulation. *Frontiers in Neuroscience*, 6.

Wagenmakers, E.-J. (2009). Methodological and empirical developments for the Ratcliff diffusion model of response times and accuracy. *European Journal of Cognitive Psychology*, 21(5):641–671.

Wagenmakers, E.-J., Lee, M., Lodewyckx, T., and Iverson, G. J. (2008a). Bayesian versus frequentist inference. In *Bayesian evaluation of informative hypotheses*, pages 181–207. Springer.

Wagenmakers, E.-J., Ratcliff, R., Gomez, P., and McKoon, G. (2008b). A Diffusion Model Account of Criterion Shifts in the Lexical Decision Task. *Journal of memory and language*, 58(1):140–159.

Wagner, J., Makeig, S., Gola, M., Neuper, C., and Müller-Putz, G. (2016). Distinct Beta Band Oscillatory Networks Subserving Motor and Cognitive Control during Gait Adaptation. *Journal of Neuroscience*, 36(7):2212–2226.

Waldert, S., Preissl, H., Demandt, E., Braun, C., Birbaumer, N., Aertsen, A., and Mehring, C. (2008). Hand Movement Direction Decoded from MEG and EEG. *Journal of Neuroscience*, 28(4):1000–1008.

Wang, X.-J. (2008). Decision Making in Recurrent Neuronal Circuits. *Neuron*, 60(2):215–234.

Warbrick, T., Mobascher, A., Brinkmeyer, J., Musso, F., Richter, N., Stoecker, T., Fink, G. R., Shah, N. J., and Winterer, G. (2009). Single-trial P3 amplitude and latency informed event-related fMRI models yield different BOLD response patterns to a target detection task. *NeuroImage*, 47(4):1532–1544.

Wascher, E., Hoffmann, S., Sänger, J., and Grosjean, M. (2009). Visuospatial processing and the N1 component of the ERP. *Psychophysiology*, 46(6):1270–1277.

Watamaniuk, S. N., Sekuler, R., and Williams, D. W. (1989). Direction perception in complex dynamic displays: The integration of direction information. *Vision Research*, 29(1):47–59.

Wessel, K., Verleger, R., Nazarenus, D., Vieregge, P., and Kömpf, D. (1994). Movement-related cortical potentials preceding sequential and goal-directed finger and arm movements in patients with cerebellar atrophy. *Electroencephalography and Clinical Neurophysiology/Evoked Potentials Section*, 92(4):331–341.

White, C. N., Ratcliff, R., Vasey, M. W., and McKoon, G. (2010). Using diffusion models to understand clinical disorders. *Journal of Mathematical Psychology*, 54(1):39–52.

Wickelgren, W. A. (1977). Speed-accuracy tradeoff and information processing dynamics. *Acta Psychologica*, 41(1):67–85.

Wiecki, T. V., Sofer, I., and Frank, M. J. (2013). HDDM: Hierarchical Bayesian estimation of the Drift-Diffusion Model in Python. *Frontiers in Neuroinformatics*, 7.

Wilcox, R. R. and Rousselet, G. A. (2018). A Guide to Robust Statistical Methods in Neuroscience. *Current Protocols in Neuroscience*, 82(1):8.42.1–8.42.30. _eprint: https://currentprotocols.onlinelibrary.wiley.com/doi/pdf/10.1002/cpns.41.

Williams, M. A., Dang, S., and Kanwisher, N. G. (2007). Only some spatial patterns of fMRI response are read out in task performance. *Nature Neuroscience*, 10(6):685–686.

Wobbrock, J. O., Cutrell, E., Harada, S., and MacKenzie, I. S. (2008). An error model for pointing based on Fitts' law. In *Proceeding of the twenty-sixth annual CHI conference on Human factors in computing systems - CHI '08*, page 1613, Florence, Italy. ACM Press.

Wohlschläger, A. (2000). Visual motion priming by invisible actions. *Vision Research*, 40(8):925–930.

Wolpert, D. M. and Flanagan, J. R. (2010). Q&A: Robotics as a tool to understand the brain. *BMC Biology*, 8(1):92.

Wolpert, D. M. and Landy, M. S. (2012). Motor control is decision-making. *Current Opinion in Neurobiology*, 22(6):996–1003.

Wong, K.-F., Huk, A. C., Shadlen, M. N., and Wang, X.-J. (2007). Neural circuit dynamics underlying accumulation of time-varying evidence during perceptual decision making. *Frontiers in Computational Neuroscience*, 1:6.

Wong, K.-F. and Wang, X.-J. (2006). A Recurrent Network Mechanism of Time Integration in Perceptual Decisions. *The Journal of Neuroscience*, 26(4):1314–1328.

Wulff, P., Ponomarenko, A. A., Bartos, M., Korotkova, T. M., Fuchs, E. C., Bähner, F., Both, M., Tort, A. B. L., Kopell, N. J., Wisden, W., and Monyer, H. (2009). Hippocampal theta rhythm and its coupling with gamma oscillations require fast inhibition onto parvalbumin-positive interneurons. *Proceedings of the National Academy of Sciences*, 106(9):3561–3566.

Yeom, H. G., Hong, W., Kang, D.-Y., Chung, C. K., Kim, J. S., and Kim, S.-P. (2014). A Study on Decoding Models for the Reconstruction of Hand Trajectories from the Human Magnetoencephalography. *BioMed Research International*, 2014:e176857.

Yeung, N. and Summerfield, C. (2012). Metacognition in human decision-making: confidence and error monitoring. *Philosophical Transactions of the Royal Society B: Biological Sciences*, 367(1594):1310–1321.

You, H. and Wang, D.-H. (2013). Dynamics of Multiple-Choice Decision Making. *Neural Computation*, 25(8):2108–2145.

Zhang, J. (2012). The effects of evidence bounds on decision-making: theoretical and empirical developments. *Cognitive Science*, 3:263.

Zhang, J. and Bogacz, R. (2009). Optimal Decision Making on the Basis of Evidence Represented in Spike Trains. *Neural Computation*, 22(5):1113–1148.

Zhang, J., Hughes, L. E., and Rowe, J. B. (2012). Selection and inhibition mechanisms for human voluntary action decisions. *NeuroImage*, 63(1):392–402.

Zhang, J., Kriegeskorte, N., Carlin, J. D., and Rowe, J. B. (2013). Choosing the Rules: Distinct and Overlapping Frontoparietal Representations of Task Rules for Perceptual Decisions. *Journal of Neuroscience*, 33(29):11852–11862.

Zhang, J., Rittman, T., Nombela, C., Fois, A., Coyle-Gilchrist, I., Barker, R. A., Hughes, L. E., and Rowe, J. B. (2016). Different decision deficits impair response inhibition in progressive supranuclear palsy and Parkinson's disease. *Brain*, 139(1):161–173.

Zhang, J. and Rowe, J. B. (2014). Dissociable mechanisms of speed-accuracy tradeoff during visual perceptual learning are revealed by a hierarchical drift-diffusion model. *Frontiers in Neuroscience*, 8.

Zhang, M. (2020). The use and limitations of null-model-based hypothesis testing. *Biology & Philosophy*, 35(2):31.

Zuo, X.-N., Kelly, C., Adelstein, J. S., Klein, D. F., Castellanos, F. X., and Milham, M. P. (2010). Reliable intrinsic connectivity networks: Test–retest evaluation using ICA and dual regression approach. *NeuroImage*, 49(3):2163–2177.